Publishers' page

Publishers' page

Publishers' page

Publishers' page

To my parents

Preface

It is known that the balance between nonlinearity and dispersion may result in an appearance of localized long bell-shaped strain waves of permanent form (solitary waves or solitons) which may propagate and transfer energy over the long distance along. Starting with the first documented water surface solitary wave observation, made by J.Scott Russell yet in 1834, solitons in fluids were observed and generated many times. It was the most surprising fact, however, that despite of almost similar description of stresses in fluids and solids, bulk longitudinal strain solitary waves have not been observed in nonlinearly elastic wave guides.

One of reason of the lack of the results on nonlinear wave in solids is that the complete description of a three-dimensional (3-D) nonlinear continuum is a difficult problem. That is why initial 3-D problems are usually reduced to the one-dimensional (1-D) form in order to clarify the simplest but qualitatively new *analytical* solutions. Certainly the cylindrical elastic rod seems to be a suitable real-life 1-D wave guide. Recently, the theory has been developed to account for long longitudinal strain solitary waves propagating in a free lateral surface elastic rod with permanent cross section. The nonlinearity, caused by both the finite stress values and elastic material properties, and the dispersion resulting from the finite transverse size of the rod, when in balance allow the propagation of the bulk strain solitary waves. Motivated by analytical theoretical predictions, there has been successful experimental generation of strain solitary waves in a polystyrene free lateral surface rod using the holographic interferometry. Hence it was proven that bulk long localized nonlinear strain waves of permanent form really exist.

However, presence of a dissipation (accumulation) destroys the balance between nonlinearity and dispersion, and nonlinear strain wave in the rod

may attenuate or amplify. One possibility occurs when the radius of the rod varies. Dissipative (active) effects may be caused by internal features of the elastic material, hence, an irreversible part should be included into the stress tensor in addition to the reversible one depending only upon the density of the Helmholtz energy. Dissipation (accumulation) may also come in an elastic wave guide through phenomena occurring at its lateral surface. Among the volume sources of dissipation/accumulation one can mention a microstructure, point moving defects, thermal effects. When dissipation and activation act together there may be another balance resulted in a formation of a bell-shaped wave with the amplitude and the velocity prescribed by the condition of the dissipative/active balance. Hence the wave is selected. Note that there exist another kind of nonlinear wave of a permanent shape sustained either by a balance between nonlinearity and dissipation or by a balance between nonlinearity, dispersion and dissipation. This wave has the form of a shock and is often called kink-shaped wave or simply kink.

The amplification of the waves (i.e., growth of the amplitude) may cause the appearance of plasticity zones or microcracks in a wave guide. This is of importance for an assessment of durability of elastic materials and structures, methods of non-destructive testing, determination of the physical properties of elastic materials, particularly, polymeric solids, and ceramics. Bulk waves provide better suited detection requirements than surface strain waves in setting up a valuable non-destructive test for pipelines.

Inclusion of dissipation (accumulation) yields nonlinear dispersive- dissipative governing equations that are nonintegrable as a rule. Hence, only particular, usually travelling wave, solutions may be obtained analytically. Certainly, these solutions require specific initial conditions. Moreover, they usually have no free parameters, and additional relationships between the equation coefficients are required for the existence of the solutions. That is why the obtaining of the exact solutions is often considered as useless by many authors preferring to apply numerical methods only.

I would like to achieve two tasks in this monograph. First, it is planned to provide the sequential analytical consideration of the strain waves amplification/attenuation and selection in solids, mainly in an elastic rod. It may be of interest for those working in the field of solid mechanics. Another task is to demonstrate the use of even particular analytical solutions for the description of unsteady nonlinear wave processes. It may attract the attention of the specialists in various fields since the structure of the governing equations is rather universal. The content is essentially based on the author previous research. However, many works were done in a collaboration. The

author thanks a lot Profs. G.V. Dreiden, I.L. Kliakhandler, G.A. Maugin, F. Pastrone, D.F. Parker, A.M. Samsonov, M.G. Velarde; Mr. V.V. Gursky and Mrs. I.V. Semenova for a long time fruitful collaboration. The book preparation has been supported by the INTAS grant 99-0167 and by the RFBR under Grant 2000-01-00482.

I dedicate this book to my parents. They always believe in my efforts and expected this book more than whoever it may be.

Saint-Petersburg, December, 2002 A.V. Porubov

Contents

Chapter 1

Basic concepts

This chapter is focused on some features of nonlinear waves to be used further in the book. Linear waves are accounted for the linear equations, they have infinitesimal amplitude. Nonlinear waves are described by nonlinear equations. In contrast to the linear waves, an amplitude, a velocity and a wave number of the nonlinear waves are connected to one another. More general information about nonlinear waves may be found in numerous special books, like Ablowitz and Segur (1981); Bhatnagar (1979); Calogero and Degasperis (1982); Newell (1985); Sachdev (1987); Whitham (1974) etc.

The governing equations for the nonlinear strain waves to be considered are nonitegrable by the inverse scattering transform method, and only particular exact solutions may be obtained. Of special interest are the single travelling wave solutions that keep their shapes on propagation. This is a result of the balances between various factors affecting the wave behaviour. There are two main types of the nonlinear travelling solitary waves which could propagate keeping its shape, bell-shaped and kink-shaped solitary waves. The bell-shaped solitary wave usually appears as a result of a balance between nonlinearity and dispersion. The kink-shaped wave may be sustained by different balances, one possibility occurs when nonlinearity is balanced by dissipation (or accumulation) , another case corresponds to the simultaneous balance between dispersion, nonlinearity and dissipation (or accumulation). The single travelling wave solution requires specific initial conditions. However, one can show that these solutions account for the final quasistationary part of an arbitrary initial pulse evolution. This unsteady process may be described analytically for the integrable equations or numerically for others. We illustrate all mentioned above further in this Chapter.

1.1 Single nonlinear waves of permanent shape

1.1.1 *Monotonic bell-shaped solitary waves*

The simplest celebrated model equation containing nonlinear and dispersive terms is the well-known Korteweg- de Vries (KdV) equation Korteweg and de Vries (1895),

$$u_t + 2b\,u\,u_x + d\,u_{xxx} = 0, \tag{1.1}$$

whose exact one-parameter single solitary wave solution is

$$u = 6\frac{d}{b}k^2\cosh^{-2}k(x - 4dk^2t). \tag{1.2}$$

The wave amplitude $A = 6dk^2/b$ and the velocity $V = 4dk^2$ depend upon the wave number k which is a free parameter. One can call the solution (1.2) travelling solitary wave one since it depends upon the phase variable $\theta = x - Vt$ only, and monotonic solitary wave since it decays monotonically when $|\theta| \to \infty$. Typical shape of the wave is shown in Fig. 1.1 where one can see also that the wave is symmetric with respect to its maximum.

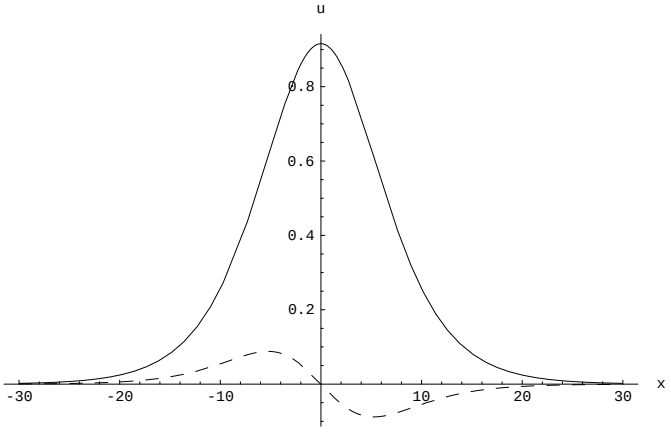

Fig. 1.1 Monotonic solitary wave (solid line) and its first derivative (dashed line)

Sometimes there is a need for the inclusion of higher- order derivative (dispersion) or nonlinear terms into Eq.(1.1). A particular case arises for water waves when surface tension suppresses coefficient d Hunter and Scheurle (1988) and fifth-order dispersion u_{5x} is added in Eq.(1.1). Also higher- order derivative terms model weak nonlocality Engelbrecht

and Braun (1998), provide an improvement of bad dispersive properties Christov *et. al* (1996); Maugin and Muschik (1994), account for a continuum limit of discrete models with far neighbour interactions Kosevich and Savotchenko (1999), to say nothing of dissipative (active) generalizations. An example of the inclusion of higher- order nonlinearity is the Sawada-Kotera equation Sawada and Kotera (1974).

Hence, the following nonlinear equation may be considered:

$$u_t + 2b\,u\,u_x + 3c\,u^2 u_x + r\,u\,u_{xxx} + s\,u_x\,u_{xx} + d\,u_{3x} + f\;u_{5x} = 0, \quad (1.3)$$

We get from Eq.(1.3) a fifth-order (in space derivatives) KdV equation Hunter and Scheurle (1988) when $c = r = s = 0$. This equation was studied in many papers, see, e.g., Karpman (1993); Karpman (1998); Karpman and Vanden-Broeck (1995); Kawahara (1972); Kawahara and Takaoka (1988); Benilov *et. al* (1993); Grimshaw *et. al* (1994). When, in addition $d = 0$, the resulting equation models the LC ladder electrical transmittion lines. Its solutions were obtained in Nagashima and Kuwahara (1981); Kano and Nakayama (1981). A special integrable case corresponds to the Sawada-Kotera equation with $b = d = 0$, $c = -r = -s/2 = 10$, $f = 1$ Sawada and Kotera (1974). Its solitary wave solutions may be found in Parkes and Duffy (1996), see also references therein.

Equation (1.3) is obviously nonintegrable by the Inverse Scattering Transform method, and only particular exact solutions may be obtained. Let us consider an exact solution vanishing at infinity. In case of the fifth-order KdV equation it has the form Kano and Nakayama (1981):

$$u = \frac{210d}{13b} k^2 \cosh^{-4} k(x - Vt), \quad (1.4)$$

with $k^2 = -d/(52f)$. Hence the width of the wave is prescribed by the dispersion coefficients d and f which should be of opposite sign. For the wave velocity we have $V = 144dk^2/13 = -36d^2/(169f)$. Hence, simultaneous triggering of the signs of b, d and f results in changing only the wave propagation direction.

In the general case the exact solitary- wave solution has a form similar to the KdV soliton (1.2),

$$u = A \cosh^{-2} k(x - Vt). \quad (1.5)$$

Important particular cases are:

(i) In presence of only cubic nonlinear term, $r = s = 0$, we get the solution with fixed parameters,

$$A = 2\sqrt{-\frac{30f}{c}}k^2, V = 4k^2(2b\sqrt{-\frac{30f}{c}} - 5d - 116f\,k^2),\ k^2 = \frac{b\sqrt{-30f/c} - 3d}{60f}. \tag{1.6}$$

In this case the existence of solution vanishing at infinity is provided by the linear fifth order term $f\,u_{5x}$. Indeed at $f = 0$ we get from Eq.(1.3) the Gardner equation whose solution is Grimshaw *et. al* (1999):

$$u = \frac{A_1}{\cosh m(x - Vt) + B_1}, \tag{1.7}$$

where

$$A_1 = \frac{3\sqrt{2}d\,m^2}{\sqrt{2b^2 + 9cd\,m^2}},\ B_1 = \frac{\sqrt{2}b}{\sqrt{2b^2 + 9cd\,m^2}},\ V = dm^2. \tag{1.8}$$

An important feature of the solution is the existence of the finite limiting amplitude when B is large Slyunyaev and Pelinovsky (1999). However, at nonzero f a substitution of Eq.(1.7) into Eq.(1.3) yields $B_1 = 1$, $\cosh\, m(x - Vt) + 1 = 2\cosh^2 m(x - Vt)/2$, and we get the solution (1.5), (1.6) with $m = 2k$.

(ii) When only quadratic higher- order term $r\,uu_{xxx}$ is taken into account, $c = s = 0$, the fixed parameters of the solution (1.5) are

$$A = \frac{30fk^2}{r}, V = \frac{2(50b^2f^2 + 5bdfr - 3d^2r^2)}{25f\,r^2}, k^2 = \frac{5bf - dr}{10fr}. \tag{1.9}$$

Note that the solution exists at $d = 0$.

(iii) In case $c = r = 0$ the parameter k is free but an additional restriction on the equation coefficients holds,

$$A = \frac{60fk^2}{s}, V = 4k^2(d + 4f\,k^2), 10b\,f = d\,s. \tag{1.10}$$

One can see that s may be excluded from the amplitude expression using the third formula from (1.10). Then the amplitude coincides with that of the KdV soliton (1.2). We also see that the wave velocity consists of two parts, $V_1 = 4dk^2$ and $V_2 = 16fk^4$, the first of which being exactly the KdV soliton velocity. Let us rewrite the ODE reduction of the equation (1.3) in the form ($' = \partial/\partial\theta$, $\theta = x - Vt$):

$$b\,u^2 + d\,u'' - V_1 u + \frac{s}{2}\,u'^2 + f\,u'''' - V_2\,u = 0.$$

One can check that the solution (1.5), (1.10) satisfies separately

$$\begin{aligned} b\,u^2 + d\,u'' - V_1 u = 0, \\ \frac{s}{2}\,u'^2 + f\,u'''' - V_2\,u = 0, \end{aligned} \tag{1.11}$$

where the first of these equations is the ODE reduction of the KdV equation (1.1) having a one-parameter solitary- wave solution.
(iv) Higher order nonlinear terms may support the existence of solitary-wave solutions even in absence of the linear dispersion terms. Higher- order nonlinear terms provide bounded localized solutions at $d = 0$ in contrast to the case $c = r = s = d = 0$ Kano and Nakayama (1981). The parameters of the solution (1.5) are

$$A = \frac{120fk^4}{b + 2k^2(r+s)}, V = 16fk^4,$$

while k satisfies the equation

$$4[30cf - r(r+s)]k^4 + 2bsk^2 + b^2 = 0.$$

Thanks to the higher order terms the solitary- wave solution may exist even in the absence of the KdV's nonlinear term, $b = 0$, provided that the restriction $30cf - r(r+s) = 0$ is satisfied. Then k may be a free parameter.

When $f = 0$ we have

$$A = \frac{3cd - 2b(2r+s)}{c(r+s)},\ V = \frac{2d[3cd - 2b(2r+s)]}{(r+s)(2r+s)},\ k^2 = \frac{3cd - 2b(2r+s)}{2(r+s)(2r+s)}.$$

There is no exact solution vanishing at infinity in the case $d = f = 0$. Instead the solution in the form of a solitary wave on an "pedestal" may be obtained as

$$u = A\cosh^{-2} k(x - Vt) + B, \tag{1.12}$$

with

$$A = \frac{2k^2(2r+s)}{c}, B = -\frac{(2r+s)[b + 2k^2(r+s)]}{3c(r+s)},$$

$$V = \frac{s(2r+s)[4k^4(r+s)^2 - b^2]}{3c(r+s)^2}.$$

Even equations with dissipation may possess bell-shaped solitary wave solution. In particular, it was recently found Garazo and Velarde (1991);

Rednikov *et. al* (1995) that appropriately heating a shallow horizontal liquid layer long free surface waves $u(x,t)$ can be excited whose evolution is governed by a dissipation-modified Korteweg- de Vries (DMKdV) equation

$$u_t + 2\alpha_1\, u\, u_x + \widetilde{\alpha}_2\, u_{xx} + \alpha_3\, u_{xxx} + \widetilde{\alpha}_4\, u_{xxxx} + \widetilde{\alpha}_5\, (u\, u_x)_x = 0. \qquad (1.13)$$

The coefficients in Eq.(1.13) depend upon parameters characterizing the liquid (Prandtl number etc.), temperature gradient across the layer, and its depth. The exact travelling bell-shaped solitary wave solution have been obtained in the form (1.12) Lou *et. al* (1991); Porubov (1993) with

$$A = 12\, \widetilde{\alpha}_4\, k^2 / \widetilde{\alpha}_5,\ B = -(\widetilde{\alpha}_2 + 4\, \widetilde{\alpha}_4\, k^2) / \widetilde{\alpha}_5,$$

$$V = -2\alpha_1\, \widetilde{\alpha}_2 \,/\, \widetilde{\alpha}_5, \alpha_3 = 2\alpha_1\, \widetilde{\alpha}_4 \,/\, \widetilde{\alpha}_5\ . \qquad (1.14)$$

The meaning of the last expression in (1.14) is similar to that in case $c = r = 0$ for Eq.(1.3). Indeed, when the relationships for V and α_3 hold, the ODE reduction Eq.(1.13) may be rewritten as

$$(\widetilde{\alpha}_2\, \frac{\partial}{\partial\theta} + \frac{2\alpha_1\, \widetilde{\alpha}_2}{\widetilde{\alpha}_5}) \left(u_\theta + \frac{\widetilde{\alpha}_4}{\widetilde{\alpha}_2} u_{\theta\theta\theta} + \frac{\widetilde{\alpha}_5}{2\, \widetilde{\alpha}_2} (u^2)_\theta \right) = 0, \qquad (1.15)$$

The restrictions on the equation coefficients do not necessary provide an evidence of the KdV ODE reduction like Eqs.(1.11), (1.15). Particular case corresponds to the Kawahara equation (Eq.(1.13) with $\widetilde{\alpha}_5 = 0$) whose exact solution is Kudryashov (1988):

$$u = \frac{15\alpha_3^3}{128\alpha_1\, \widetilde{\alpha}_4^2} \cosh^{-2}(\frac{\alpha_3}{8\, \widetilde{\alpha}_4}\theta)(1 - \tanh(\frac{\alpha_3}{8\, \widetilde{\alpha}_4}\theta)), \qquad (1.16)$$

where $V = 5\alpha_3^3$, $\widetilde{\alpha}_2 = \alpha_3^2/(16\, \widetilde{\alpha}_4)$.

All solutions (1.4), (1.5), (1.7) account for monotonic and symmetric solitary waves. Despite difference in their functional form they have one and the same shape shown in Fig. 1.1. In contrast to them exact solitary wave solution (1.16) of the Kawahara equation is monotonic but asymmetric, see Fig. 1.2.

1.1.2 *Oscillatory bell-shaped solitary waves*

The solitary wave does not decay necessarily in a monotonic manner. Thus Kawahara (1972) studied decay at infinity of the wave solution of the fifth-

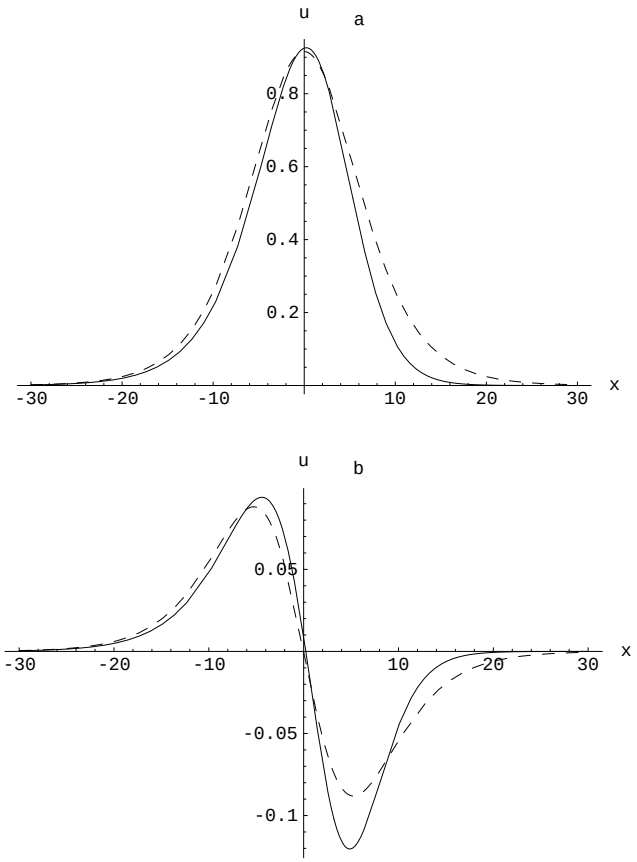

Fig. 1.2 Symmetric (solid line) vs asymmetric monotonic solitary wave (dashed line). a) profiles; b)their first derivatives.

order KdV equation using linearized equation analysis phase analysis. It was found that the wave decays monotonically or oscillatory depending upon the parameter ε, which is proportional (in our notations) to d and is inverse proportional by the product of f and the wave velocity. The same technique has been used in Karpman (2001) when nonlinear term in the fifth-order KdV equation is of the form $u^p\, u_x$. The oscillatory solitary-wave solution is shown in Fig. 1.3. The profile of the first derivative with respect to the phase variable reveals its symmetric nature.

Eq.(1.3) does not possess exact oscillatory solitary wave solution. How-

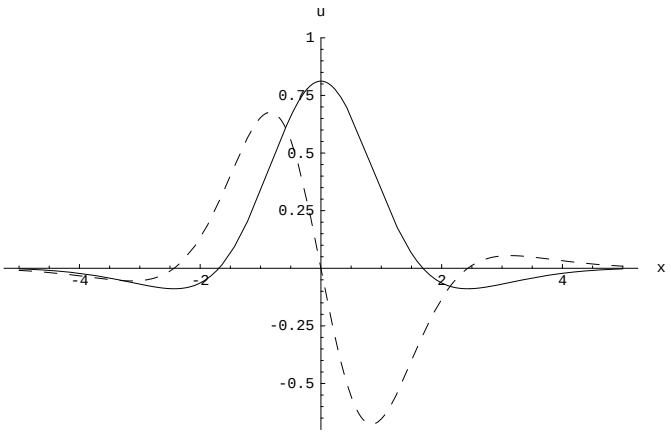

Fig. 1.3 Oscillatory solitary wave (solid line) and its first derivative (dashed line)

ever, it may be described asymptotically. Certainly the fifth-order KdV equation is often considered as a perturbed KdV equation. First the asymptotic solution is obtained which consists of the KdV solitary wave solution and a small perturbation that oscillates but does not vanish at infinity or a non-local solution Benilov *et. al* (1993); Hunter and Scheurle (1988); Karpman (1993); Karpman (1998). Let us consider the fifth- order derivative term and higher- order nonlinear terms as small perturbations assuming $f = \delta F$, $r = \delta R$, $s = \delta S$, $c = \delta C$, $\delta << 1$. The asymptotic solution $u = u(\theta)$, $\theta = x - Vt$, is sought in the form

$$u = u_0(\theta) + \delta\, u_1(\theta) + ..., \tag{1.17}$$

with $u_i \to 0$ at $|\theta| \to \infty$. In the leading order we get the KdV equation (1.1) for the function u_0 whose travelling solitary wave solution is (1.2). In the next order an inhomogeneous linear equation results for u_1,

$$2b\,(u_0u_1)_\theta + d\,u_{1,\theta\theta\theta} - 4dk^2\,u_{1,\theta} = -F\,u_{0,\theta\theta\theta\theta\theta} - 3C\,u_0^2u_{0,\theta} - R\,u_0u_{0,\theta\theta\theta} -$$

$$S\,u_{0,\theta}u_{0,\theta\theta}. \tag{1.18}$$

Its solution vanishing at infinity is

$$u_1 = (\frac{3C}{4b} + \frac{5bF}{2d^2} - \frac{2R+S}{4d})\,u_0^2 + (\frac{S}{b} + \frac{4R}{b} - \frac{14F}{d} - \frac{9Cd}{b^2})k^2\,u_0 - \frac{2k^2F}{d}\theta\,u_{0,\theta}. \tag{1.19}$$

The shape of the solution $u = u_0(\theta) + \delta\, u_1(\theta)$ depends upon the values of the coefficients of Eq.(1.3). It may account for an oscillatory solitary wave solution first obtained numerically in Kawahara (1972), see Fig. 1.3. In the case of the fifth-order KdV equation, this profile exists at positive d and f, what corresponds to the Case IV in Kawahara (1972).

Finally, there exist nonlinear equations having exact travelling wave solutions in the form of an oscillatory solitary wave. In particular, an equation

$$u_t + a\, u_x + 2b\, u\, u_x + 3c\, u^2 u_x + d\, u_{3x} + f\ u_{5x} + g\, u_{7x} = 0, \tag{1.20}$$

possesses the exact solution

$$u = \sqrt{\frac{35g}{c}} k^3 \cosh^{-1} k(x - Vt) \left(24 \cosh^{-2} k(x - Vt) - \frac{288}{17} \right),$$

where $b = 0$, $k^2 = 17f/(581g)$, $V = a + 102825k^6 g/289$. The equation coefficients should be connected by $d\, g = 37.405\, f^2$.

Oscillatory solitary waves of permanent shape arise also in dissipative problems, however, usually they are asymmetric and may be found only numerically.

1.1.3 *Kink-shaped waves*

The celebrated Burgers' equation Burgers (1948) is the simplest equation that models the balance between nonlinearity and dissipation,

$$u_t + 2b\, u\, u_x + g\, u_{xx} = 0, \tag{1.21}$$

In particular, it possesses the exact travelling solution of permanent form,

$$u \ = \ A\, m\, \tanh(m\, \theta) + B, \tag{1.22}$$

where

$$A = \frac{g}{b},\ B = \frac{V}{2b},\ m - free.$$

If the boundary conditions are

$$u \to h_1 \text{ at } \theta \to \infty,\ u \to h_2 \text{ at } \theta \to -\infty, \tag{1.23}$$

then

$$m = \frac{(h_1 - h_2)b}{2g},\ V = b(h_1 + h_2).$$

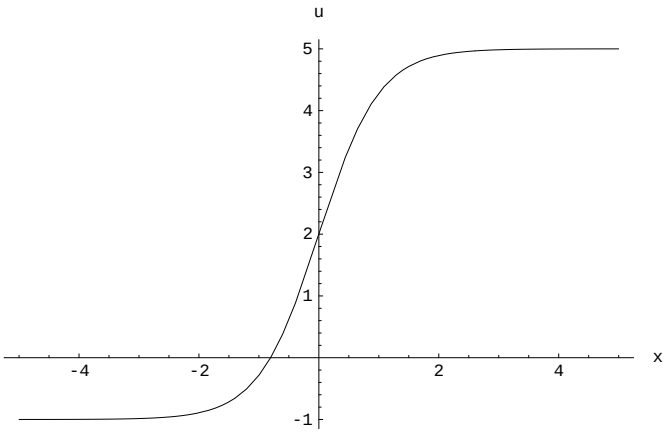

Fig. 1.4 Burgers' kink-shaped wave

The shape of the solution (1.22), called kink, is shown in Fig. 1.4. Kinks may arise also due to the balance between nonlinearity, dispersion and dissipation like in the case of the Korteweg-de Vries-Burgers equation (KdVB),

$$u_t + 2b\,u\,u_x + g\,u_{xx} + du_{xxx} = 0, \tag{1.24}$$

whose exact solution was obtained independently by many authors Vlieg-Hultsman and Halford (1991)

$$u \ = \ A\ \tanh(m\,\theta)sech^2(m\,\theta) + 2A\ \tanh(m\,\theta) + C, \tag{1.25}$$

with

$$A = \frac{6g^2}{50Vd},\ \ C = \frac{V}{2b},\ m = \frac{g}{10d}.$$

It follows from the boundary conditions (1.23) that

$$h_+ - h_- = 2B,\ V = b(h_+ + h_-),$$

and the solution exists under

$$h_+^2 - h_-^2 = \frac{12g^2}{25bd}.$$

Equations without dissipative terms may also possess the kink-shaped solutions. Thus the modified Korteweg-de Vries equation (MKdV),

$$u_t + 3c\,u^2\,u_x + du_{xxx} = 0, \tag{1.26}$$

has an exact solution

$$u = \sqrt{-\frac{2d}{c}}m\ \tanh(m\,\theta), \tag{1.27}$$

where $V = -dm^2$. Note that the MKdV equation has both the bell-shaped and the kink-shaped solutions. Dissipative equation may possess the same property. In particular, the DMKdV equation (1.13) has exact kink-shaped solution Lou *et. al* (1991); Porubov (1993)

$$u \ = \ C + \frac{36\ \widetilde{\alpha}_4}{\widetilde{\alpha}_5} m\ \cosh^{-2}(\sqrt{-3m}\,\theta) +$$

$$\frac{12(\alpha_3\ \widetilde{\alpha}_5\ -2\alpha_1\ \widetilde{\alpha}_4)}{5\ \widetilde{\alpha}_5}\ \sqrt{-3m}\tanh(\sqrt{-3m}\,\theta), \tag{1.28}$$

where

$$C = \frac{12\ \widetilde{\alpha}_4}{\widetilde{\alpha}_5}m - \frac{\widetilde{\alpha}_2}{\widetilde{\alpha}_5} + \frac{2\alpha_1(\alpha_3\ \widetilde{\alpha}_5\ -2\alpha_1\ \widetilde{\alpha}_4)}{5\ \widetilde{\alpha}_5^3} + \frac{(\alpha_3\ \widetilde{\alpha}_5\ -2\alpha_1\ \widetilde{\alpha}_4)^2}{25\ \widetilde{\alpha}_4\widetilde{\alpha}_5^3},$$

$$V = 2\alpha_1 C + \frac{24\alpha_1\ \widetilde{\alpha}_4}{\widetilde{\alpha}_5}m,$$

while m is a free parameter if $\alpha_3 = 12\alpha_1\ \widetilde{\alpha}_4\ /\ \widetilde{\alpha}_5$ or

$$m = -\frac{(\alpha_3\ \widetilde{\alpha}_5\ -2\alpha_1\ \widetilde{\alpha}_4)^2}{300\ \widetilde{\alpha}_4^2\widetilde{\alpha}_5^2}.$$

The shapes of the kink solutions (1.25), (1.27) are similar to that shown in Fig. 1.4, while the kink (1.28) may have also different profile shown by solid and dashed lines in Fig. 1.5.

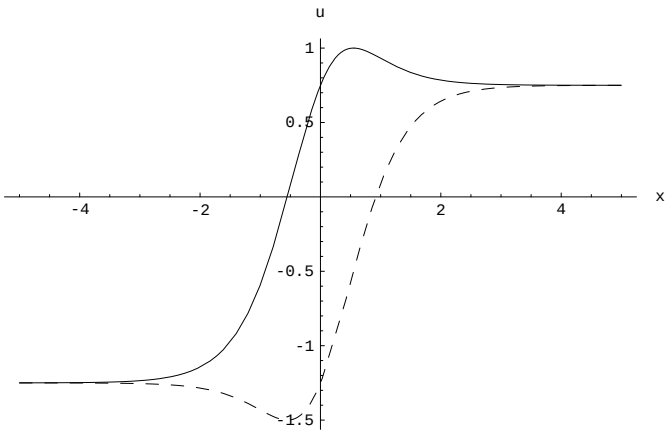

Fig. 1.5 Kink-shaped waves with a "hat"

1.1.4 *Periodic nonlinear waves*

Usually single bell-shaped solitary wave solutions are the particular cases of more general periodic solutions. Thus Korteweg and de Vries (1895) found the periodic solution of the KdV equation (1.1),

$$u = 6\frac{d}{b}k^2\left(1 - \kappa^2 + \frac{E}{K} + \kappa^2 cn^2(k\theta, \kappa)\right) \tag{1.29}$$

where K and E are the complete elliptic integrals of the first and the second kind respectively , κ is the modulus of the Jacobian elliptic function Bateman and Erdelyi (1953-54); Byrd and Friedman (1954); Newille (1951). They called Eq.(1.29) the *cnoidal* wave solution since it is expressed through the Jacobi elliptic function cn . Cnoidal wave is not a linear superposition of the bell-shaped solitary waves. It tends to the single solitary wave solution (1.2) at $\kappa \to 1$ as shown in the right column in Fig. 1.6 [1]. Exact periodic and bell-shaped solitary wave solutions correspond in the same manner in case of the generalized 5th-order KdV equation (1.3) and the DMKdV equation (1.13).

Although many equations, like Burgers', BKdV and DMKdV equations have not exact bounded periodic solutions that transform into the kink-shaped ones, there exist exceptions. Thus the MKdV periodic solution

[1] Reprinted with permission from Elsevier Science

Ablowitz and Segur (1981)

$$u = \sqrt{-\frac{2d}{c}}\, m\, sn(m\,\theta, \kappa), \tag{1.30}$$

transforms into the kink solution (1.27) at $\kappa \to 1$. Another example is a dissipative nonlinear equation

$$u_t + 2bu\, u_x + 3c\, u^2\, u_x + du_{xxx} + f(u^2)_{xx} + gu_{xx} = 0, \tag{1.31}$$

This evolution equation represents an analog of the hyperbolic equation to be derived further in Sec. 5.3. Its bounded periodic solution Porubov (1996) is

$$u = \frac{m}{\sqrt{-c}}\, \frac{cn(m\,\theta,\, \kappa)\, sn(m\,\theta,\, \kappa)\, dn(m\,\theta,\, \kappa)}{C_1 + cn^2(m\,\theta,\, \kappa)} - \frac{b}{3c}. \tag{1.32}$$

with

$$C_1 = \frac{1 - 2\kappa^2 + \sqrt{\kappa^4 - \kappa^2 + 1}}{3\kappa^2},\; m^2 = \frac{3g^2 - V}{4\sqrt{\kappa^4 - \kappa^2 + 1}},$$

and the following restrictions on the coefficients:

$$f = -\frac{1}{2}\sqrt{-c},\; b = 3g\sqrt{-c}.$$

The periodic wave solution (1.32) has a functional form different from both the KdV cnoidal wave and the MKdV bounded periodic solution. When $\kappa = 1$ we have $C_1 = 0$, and the solution (1.31) tends to the kink-shaped solution (1.27) as it is shown in the left column in Fig. 1.6 in comparison with the transformation of the KdV cnoidal wave solution to the bell-shaped solitary wave.

1.2 Formation of nonlinear waves of permanent shape from an arbitrary input

All solutions presented in previous section require specific initial conditions. In practice more important is to know how an arbitrary finite amplitude input evolves. Analytical solutions of unsteady problems may be obtained if governing nonlinear equations are integrable Ablowitz and Segur (1981); Bhatnagar (1979); Calogero and Degasperis (1982); Dodd *et. al* (1982); Newell (1985), otherwise only numerical solutions are available. Often initial input transforms into the stable quasistationary wave structures of

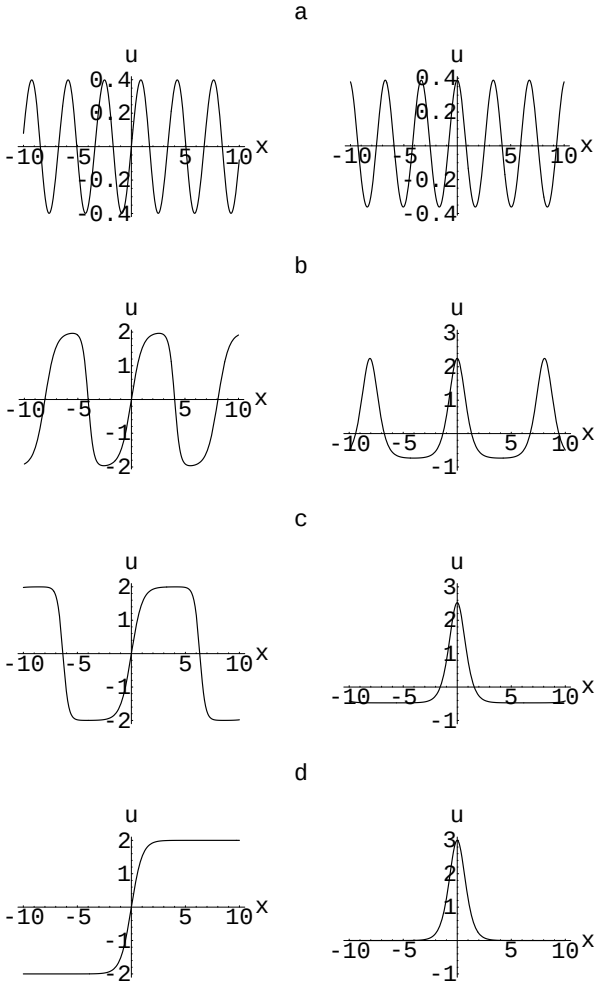

Fig. 1.6 Comparison of the periodic solution (1.32) (left column) and the KdV cnoidal wave (1.29)(right column) for different values of the Jacobi modulus: (a)$\kappa^2 = 0.25$, (b) $\kappa^2 = 0.995$, (c)$\kappa^2 = 0.99995$, (d)$\kappa^2 = 1$. After Porubov and Velarde (2002).

permanent form which may be described by the analytical solutions. Also the analysis gives the conditions when the formation of them is possible. In this section we illustrate it using some instructive examples.

1.2.1 *Bell-shaped solitary wave formation from an initial localized pulse*

The fifth-order KdV was extensively studied numerically. The oscillatory travelling solitary- wave solutions were found in Boyd (1991); Nagashima and Kuwahara (1981). The evolution of the initial monotonic solitary wave into radiating or oscillatory solitary waves was simulated in Benilov *et. al* (1993); Karpman and Vanden-Broeck (1995). In a series of papers Salupere *et. al* (1997); Salupere *et. al* (2001) the solitary wave formation from a periodic input was studied for an equation similar to Eq.(1.3). We shall study the evolution of a *localized* initial pulse. Previously, localized pulse evolution into an oscillatory solitary wave was considered in Nagashima and Kuwahara (1981) for the equation $u_t + u\,u_x - \gamma^2\ u_{5x} = 0$. Below we consider the formation of solitary waves in the systems governed by Eq.(1.3). Following Porubov *et. al* (2002) we use two methods for computations, finite-difference and pseudo-spectral, see Sec. 2.3.2. Below only those results are shown that were obtained using both numerical methods. We have tried various shapes of the initial localized pulses, rectangular, Gaussian distribution etc.

Influence of the fifth-order dispersive term. First the 5th-order KdV equation was studied. Since the role of the fifth-order derivative term is of interest the coefficients b and d in Eq.(1.3) were fixed for all computations, $b = 1$, $d = 0.5$. We found that the rectangular initial pulse splits into a sequence of solitary waves when the coefficients of dispersive terms, d and f, are of opposite sign. For both coefficients positive the initial rectangular profile is dispersed without formation of any localized waves. The dependence upon the sign of the ratio d/f is in agreement with the exact solitary- wave solution (1.4) and the analysis of the dispersion relation Karpman (1993). However, more smooth Gaussian initial profiles provide the appearance of solitary waves even for positive coefficients when f is rather small, e.g., $f = 0.01$.

The next result we have obtained is the dependence of the number of solitary waves upon the value of f when $d/f < 0$.

Shown in Fig. 1.7 is the formation of the train of solitary waves from a Gaussian initial pulse in the KdV case, $f = 0$.

Figs. 1.8-1.10 demonstrate the decrease of the solitary waves for $f = -1, -10, -50$ respectively. Both the amplitude and the velocity decrease with the increase of the absolute value of f in qualitative agreement with the exact solution (1.4).The ratio between the amplitude and the velocity

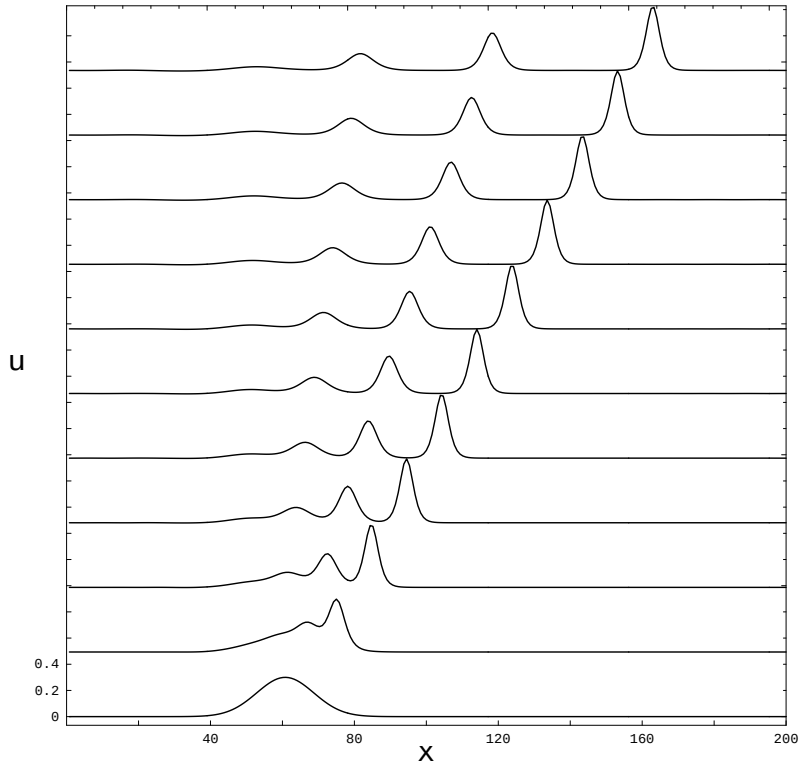

Fig. 1.7 Evolution of the initial Gaussian profile in the KdV case, $f = 0$.

of each solitary wave in Fig. 1.7 is equal to 1.5 just as for the KdV soliton (1.2) . This ratio (and the amplitude) decreases with the decrease of f, from 1.43 at $f = -1$ to 1.33 at $f = -50$. A similar tendency is revealed by the phase analysis of *single* travelling wave solutions, cf. Fig. 2 in Kawahara (1972). The ratio for the 5th- order KdV exact solution (1.4) is 1.46, the amplitude and the velocity for given b and d are $-105/(1352f)$, $-9/(169f)$, respectively. Only at small $f = -0.1 \div -0.15$ are the numerical results for the leading solitary wave in quantitative agreement with the exact solution (1.4). More important is that the decrease of f affects the solitary- wave transformation from monotonic KdV solitons (1.2) to the oscillatory solitary waves. For convenience the last stages from Figs. 1.7-1.10 are collected in Fig. 1.11. In case $f = -1$, Fig. 1.11(B), the higher leading solitary wave

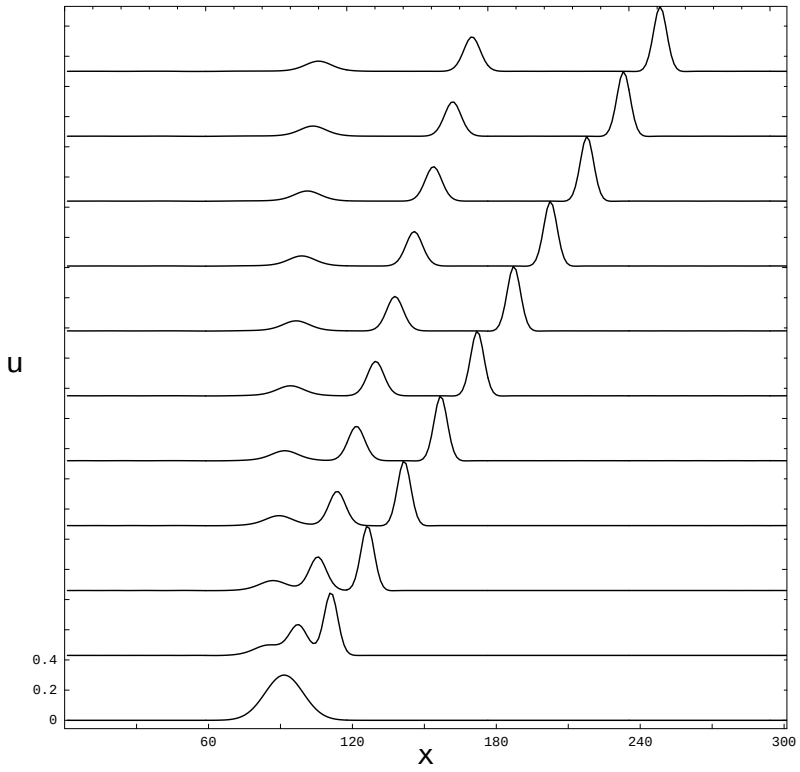

Fig. 1.8 Evolution of the initial Gaussian profile in the 5th-order KdV case, $f = -1$.

is oscillatory while other solitary waves remain monotonic, then the transformation occurs also for the second solitary wave, Fig. 1.11(C) . Alternate transformation of the solitary waves confirms the dependence of the kind of solitary wave upon the value of the product of f and the wave amplitude (hence, its velocity) found in Kawahara (1972).

Finally, we have found that simultaneous triggering of the signs of b, d, f doesn't affect the shapes of the solitary waves. They simply evolve to the opposite direction according to the analysis of the exact solution (1.4).

Influence of the cubic nonlinearity. Now we add cubic nonlinearity, $c \neq 0$, while $r = s = 0$. The analytical solutions predict an action of the cubic nonlinear term depends upon the sign of c. Also the solution is sensitive to the ratio between nonlinear terms contributions, b/c, and the

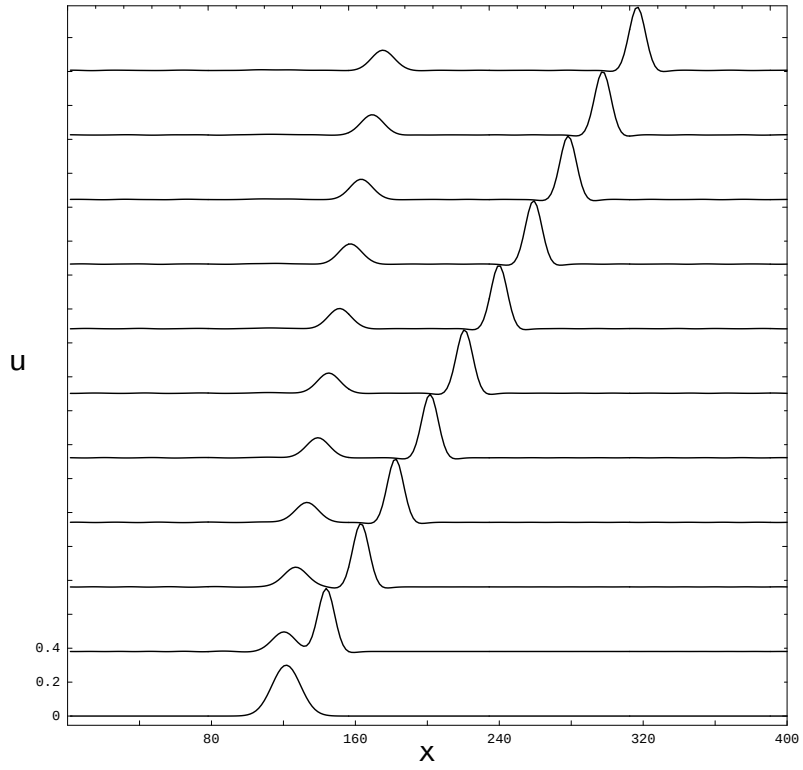

Fig. 1.9 Evolution of the initial Gaussian profile in the 5th-order KdV case, $f = -10$.

value of the amplitude of an initial pulse. Indeed we have found that at $b = 1$, $c = 1$, $d = 0.5$, $f = -1$ the train of solitary waves arises only from positive initial pulse with amplitude equal to 0.5 while a negative one is dispersed. Dependence of the amplitude on the sign of b is very typical for the exact solutions of the equation with quadratic nonlinearity, see (1.2), (1.4). However, at smaller b, $b = 0.2$ or $b = -0.2$, the formation of solitary waves no longer depends upon the sign of the initial pulse amplitude. A similar tendency is observed when the initial amplitude becomes close to 1 or higher when predominant cubic nonlinearity excludes an influence of the quadratic one on the sign of the wave amplitude like in the exact solution (1.5), (1.6).

At the same time, the stage of forthcoming evolution of already gen-

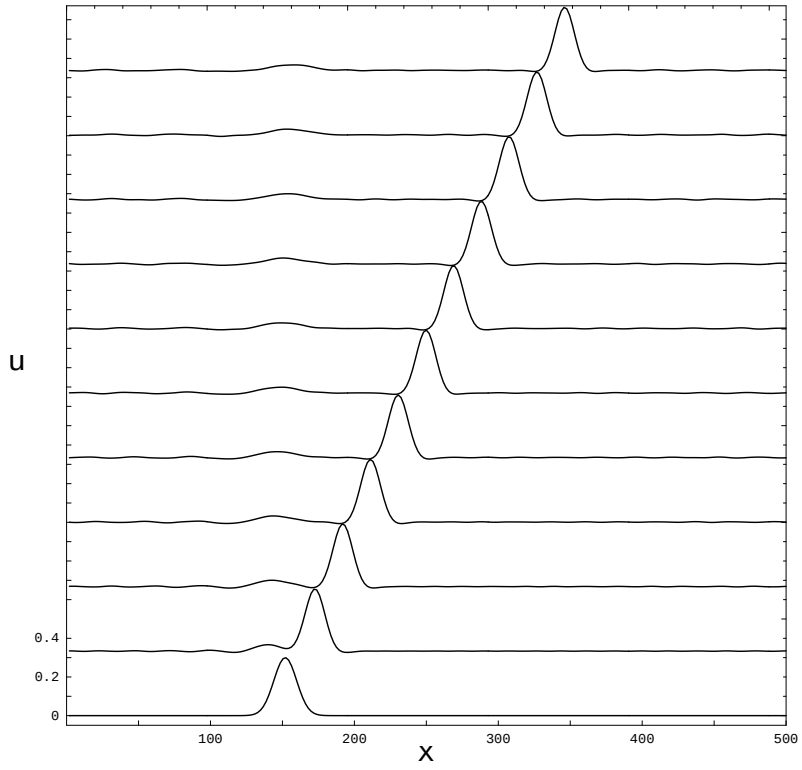

Fig. 1.10 Evolution of the initial Gaussian profile in the 5th-order KdV case, $f = -50$.

erated solitary waves is not so sensitive to the value of b, while other analytical restrictions on the coefficients become more important. Besides the condition $d/f < 0$ following from the *linear* analysis Karpman (1993); Kawahara (1972), there is $f/c < 0$ resulted from the *nonlinear* exact solution (1.5), (1.6). Moreover, at small f one can anticipate an evidence of the condition $d/c > 0$ given by Eq.(1.8).

When $c > 0$, $f < 0$ all above mentioned inequalities are satisfied. The number of solitary waves generated from the initial localized pulse increases with the increase of the value of c and fixed values of $d = 0.5$, $f = -1$ and also $b = 1$ or $b = 0.2$. The velocity of the waves increases also, the width (proportional to $1/k$) decreases, while the amplitude remains practically one and the same. We also observed the alternate transformation of the solitary

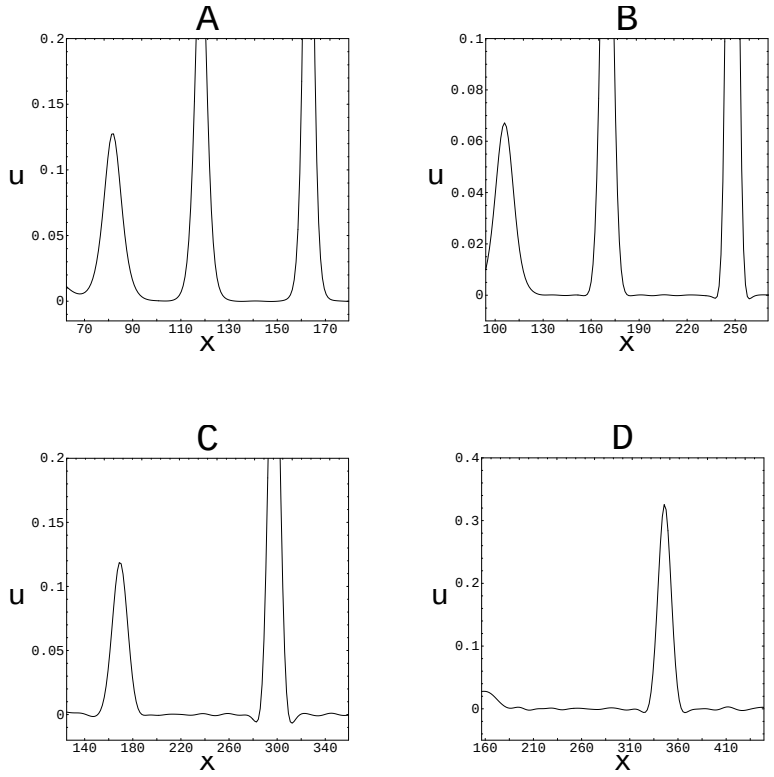

Fig. 1.11 Transformation of the kind of solitary waves in the 5th-order KdV case. (A) $f = 0$, (B) $f = -1$, (C) $f = -10$, (D) $f = -50$.

waves from monotonic to oscillatory when c increases for both values of b. Independence of the amplitude of c doesn't follow from the exact solution (1.6) as well as from the asymptotic solution. The third formula in (1.6) predicts growth of positive values of k^2 only for $b = 0.2$ giving negative values for $b = 1$. However, let us express k through the amplitude A and substitute it into the expression for the velocity V. Then one can exhibit for both values of b the similarity of the variation of the velocity with respect to c with that obtained in numerics.

As found in previous subsection, the decrease of the negative f values affects the decrease in the number of solitary waves. Assume $b = 1$, $d = 0.5$, we have tried simultaneous variations of c and f in order to sustain one

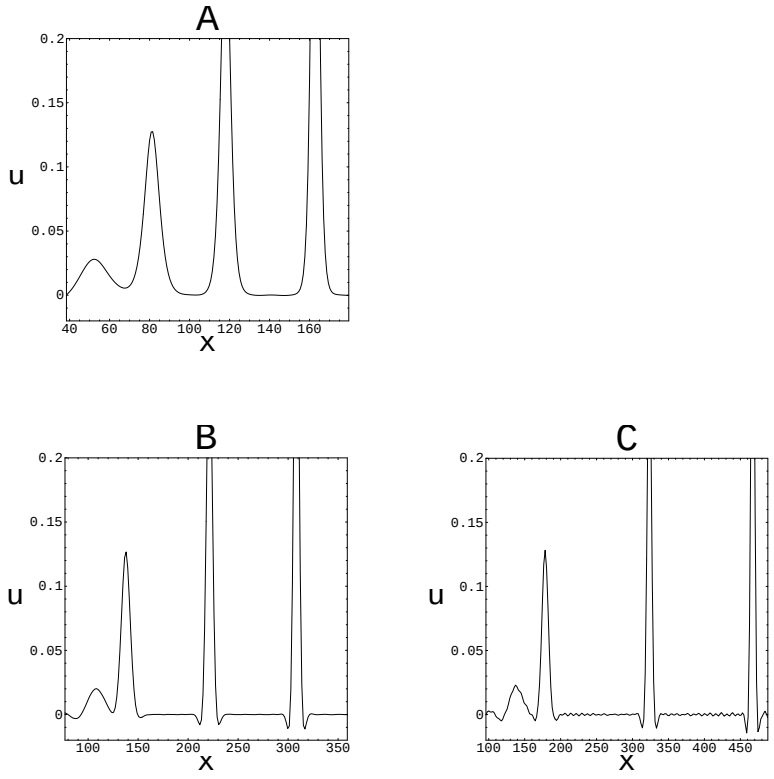

Fig. 1.12 Conservation of the number of solitary wave thanks to the simultaneous presence of cubic nonlinearity and fifth-order derivative term. (A) $c = 0$, $f = 0$, (B) $c = 15$, $f = -10$, (C) $c = 75$, $f = -50$.

and the same number, see Fig. 1.12. We see that the wave amplitude keeps its value from Fig. 1.12(A) to Fig. 1.12(C) while the velocity growths. This confirms that the amplitude depends upon the ratio f/c but velocity is proportional to f. The kind of solitary wave alters from monotonic Fig. 1.12(A) to oscillatory Fig. 1.12(B, C).

At $c < 0$, $d > 0$, $f > 0$ only one inequality, $f/c < 0$, is satisfied, and solitary wave formation is observed only for small f , otherwise the initial pulse is dispersed in this case. On the contrary small absolute values of c provides the solitary waves formation at $c < 0$, $d > 0$, $f < 0$. When both c and f are positive no solitary waves appear.

Influence of nonlinearities s $\mathbf{u}_x\mathbf{u}_{xx}$ and r $\mathbf{uu}_{xxx}$. Suppose $c = r = 0$

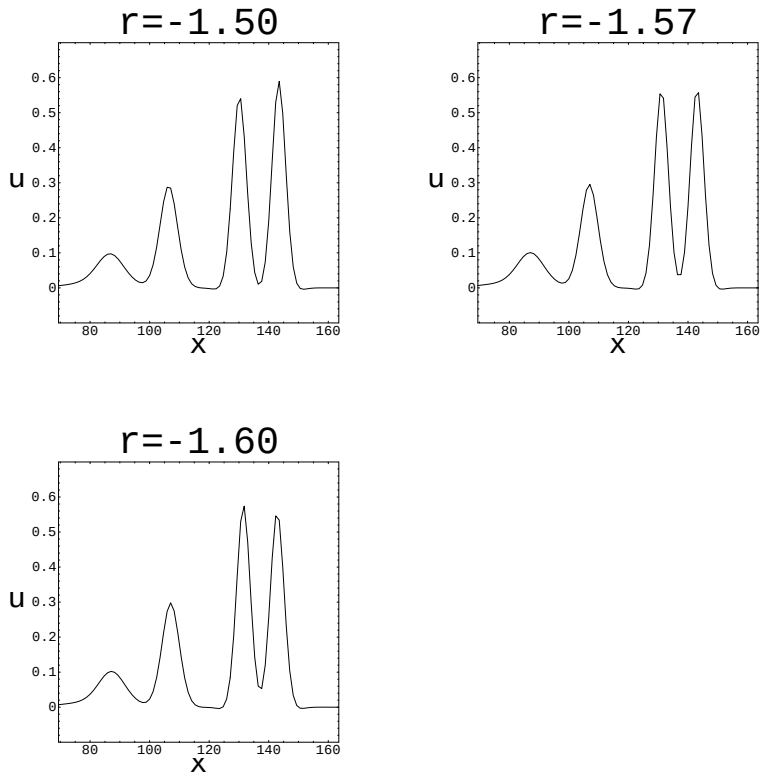

Fig. 1.13 Equalization of the first and the second solitary waves and subsequent exceeding of the second wave due to the alteration of the negative values of the coefficient r.

and vary s at fixed b, d and f, that we choose $b = 1$, $d = 0.5$, $f = -1$. It is found that the amount of solitary waves and its transition from monotonic to oscillatory don't depend upon the value of s. The wave amplitude decreases with the increase of s while the velocity keeps its value. Wave behavior is not sensitive to the sign of s. The condition for the solitary wave formation $d/f < 0$ remains valid.

The fact the velocity doesn't depend upon s is in agreement with the exact solution. Certainly, solitary waves exist outside the restriction from (1.10). We also used numerical values of the amplitude to define k and then V using (1.10). A comparison of the velocities with those obtained numerically demonstrates the more agreement the less is the value of b.

Asymptotic solution (1.17), (1.19) also predicts the decrease of amplitude at permanent velocity. Indeed, we get that $u_{\max} = u_0(0)+\delta u_1(0) = 6dk^2/b(1+k^2[f/d - s/(2b)])$. At coefficient values we used the value of $u_{\max}$ decreases with the increase of s (s is not large in the asymptotic solution), while the exact solution predicts the same behavior only for positive values of s.

When $s = c = 0$ the behavior of the solution differs from the previous one. Having the same values for b, d, f we obtain that increase of positive values of r yields a decrease in the velocity and an increase in the amplitude of the solitary waves. The number of solitary waves decreases. However, at negative values of r we found that at the initial stage of the splitting of the Gaussian profile the amplitude of the second solitary wave becomes equal to that of the first one at $r = -1.57$, see Fig. 1.13. At lesser r second solitary wave becomes higher, and two solitary waves form a two-humps localized structure shown in Fig. 1.14.

It is no longer quasistationary since amplitudes of the humps vary in time. It looks like an interaction of two solitary waves when the second higher solitary wave surpasses the first one, then it becomes lower, and the process repeats. Decreasing r we achieve formation of a three-humps localized structure shown in Fig. 1.15. Its evolution is similar to those presented in Fig. 1.14. Finally, only multi-humps localized structure arises from an initial pulse as shown in Fig. 1.16. The localized multi-humps structures in Figs. 1.14-1.16 keep their width, while their shapes vary in time.

Certainly, unsteady multi-humps localized structures are not governed by the ODE reduction of Eq.(1.3) and, hence cannot be explained either by the phase portraits analysis or by the exact travelling wave solution (1.5), (1.9). Moreover, at negative values of f the exact solution doesn't predict propagation to the right of the solitary wave with positive amplitude.

Absence of linear dispersive terms. We have found an exact solitary wave solution that may be supported by higher -order nonlinear terms even without linear dispersive terms, at $d = 0$ or $f = 0$. Numerical simulations show that there are no solitary waves at both zero d and f. Some solutions from previous subsections keep their features at $d = 0$, in particular, this relates to the case $r \neq 0$. At the same time cubic nonlinearity at $d = r = s = 0$ supports two-humps localized waves for $c > 0$. At negative c the wave picture is similar to those at $d \neq 0$. No stable solitary waves propagate in absence of only the fifth-derivative term, $d \neq 0$, $f = 0$ with the exception of the Gardner equation case where Slyunyaev and Pelinovsky (1999) found generation of the limiting amplitude solitons.

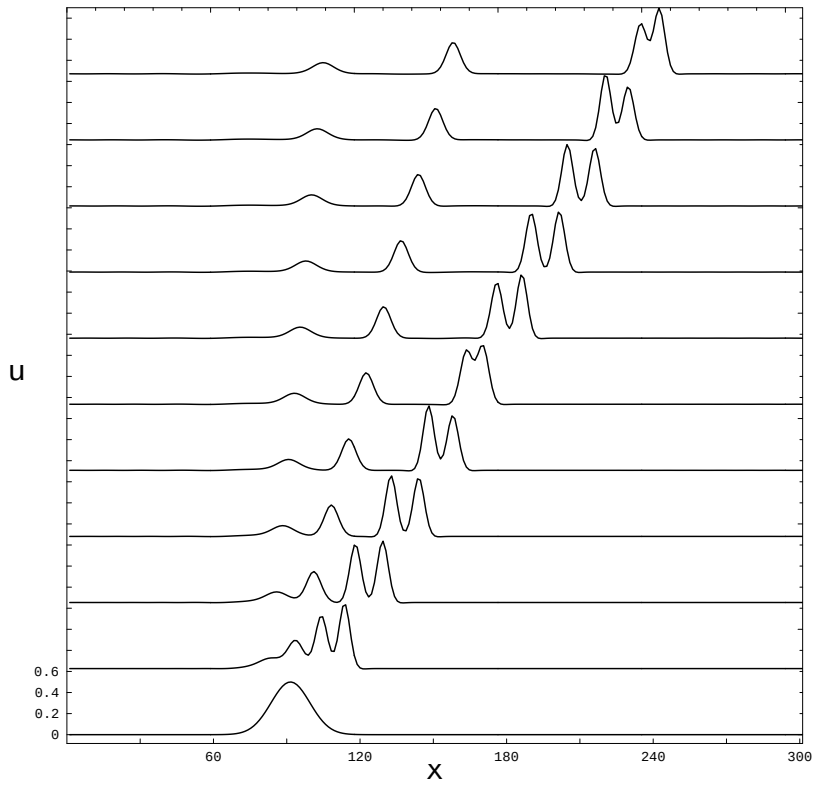

Fig. 1.14 Two-humps solitary wave formation at $r = -1.6$.

To sum up, both higher order nonlinear and dispersive terms affect the formation of localized nonlinear waves their shape and their parameters. Thus, the number of solitary waves and the transition from monotonic to oscillatory wave are under responsibility of both 5th- order linear dispersive term, cubic nonlinearity and higher- order quadratic nonlinearity $r\,u\,u_{xxx}$. More important is the formation of an unsteady but localized multi-humps wave structure thanks to $r\,u\,u_{xxx}$ and cubic nonlinearity at $d = 0$. The sign of the coefficient b of the KdV quadratic nonlinear term is important for choosing the sign of the input amplitude. At the same time the nonlinearity $s\,u_x u_{xx}$ doesn't affect the formation and behavior of solitary waves.

Certainly, the shapes of the resulting solitary waves are not obviously governed by the exact and asymptotic travelling wave solutions. Some

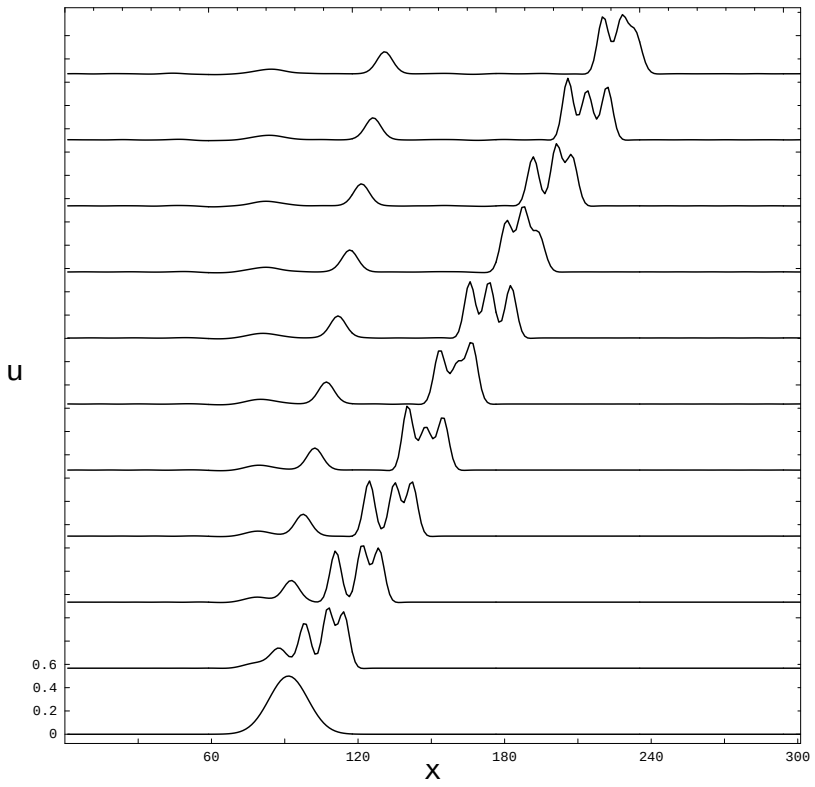

Fig. 1.15 Three-humps solitary wave formation at $r = -3.2$.

other features of numerical solutions, like the dependence of the number of solitary waves upon the values of the equation coefficients or a transition from monotonic wave to an oscillatory one, are not predicted by analytical solutions. However, the combinations of equation coefficients required for the existence of solitary wave are realized in numerics. Also numerical wave amplitude and velocity relate like in the analysis. Evidence of all these predictions even qualitatively is very important for a justification of the numerical results.

Formation of the bell-shaped solitary waves in presence of dissipation or an energy influx will be considered further in the book.

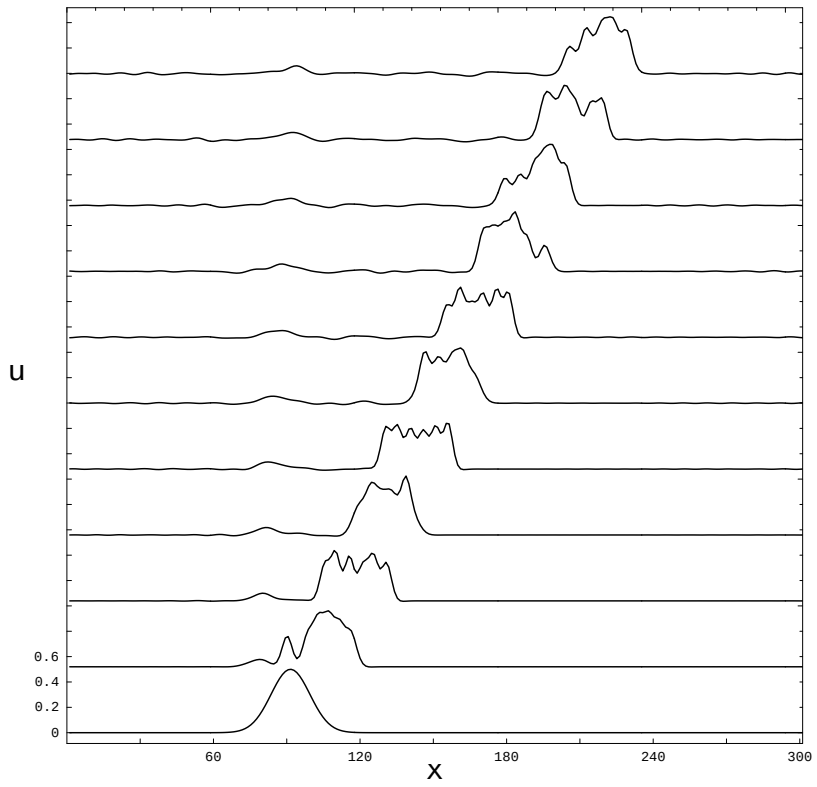

Fig. 1.16 No solitary waves other than multi-humps one at $r = -12$.

1.2.2 *Kink-shaped and periodic waves formation*

The formation of the kink-shaped waves was studied considering the evolution of the Taylor shock from discontinuous (step) initial conditions under the governance of the Burgers equation Sachdev (1987); Whitham (1974). It was found the appearance in due time the steady state kink solution (1.22). A quasihyperbolic analog of the Burgers equation was studied in Alexeyev (1999) where it was found that kink may be formed from suitable initial conditions. The Korteweg-de Vries-Burgers equation (1.24) also extensively studied but mainly in the direction of generation of the triangle profiles and oscillating wave packets Berezin (1987), see also references therein. Of special interest is the formation of the kinks with a

"hat" shown in Fig. 1.5. One possibility will be considered in Sec. 5.3.

Usually periodic waves are generated in finite domains from a harmonic input. Thus the KdV cnoidal waves (1.29) are realized numerically and in experiments in a paper by Bridges (1986), also Kawahara (1983) obtained numerically periodic wave structures in a system governed by Eq.(1.13) with $\widetilde{\alpha}_5 = 0$, while at nonzero coefficient similar results were found in Rednikov *et. al* (1995). Note that harmonic input in the finite domains is used also for the study of the bell-shaped solitary waves interactions where no periodic wave structure of permanent shape arises Salupere *et. al* (1994); Salupere *et. al* (1997); Salupere *et. al* (2001).

1.3 Amplification, attenuation and selection of nonlinear waves

As already noted the bell-shaped solitary wave is sustained by a balance between nonlinearity and dispersion. What happens with the wave when dissipation/accumulation destroys this balance? It was shown in Sec. 1.1 that the bell-shaped wave may exist even in presence of dissipation but under strong restrictions on the equation coefficients. Assume the influence of dissipation/ accumulation is weak and is characterized by a small parameter $\varepsilon << 1$. It turns out that an asymptotic solution may be found in this case whose leading order part is defined as a solitary wave with slowly varying parameters. Depending on the problem either slow time, $T = \varepsilon t$, or slow coordinate, $X = \varepsilon x$, may be used.

In the former case the solitary wave solution is

$$u(\theta, T) = A(T)\cosh^{-2}(k(T)\theta), \tag{1.33}$$

where $\theta_x = 1$, $\theta_t = -V(T)$. In the latter case we have

$$u(\theta, X) = A(X)\cosh^{-2}(k(X)\theta), \tag{1.34}$$

where $\theta_x = P(X)$, $\theta_t = -1$. Next order solutions give us the functional form of the dependence of the wave parameters upon the slow variable. Derivation of the asymptotic solution will be described in Sec. 2.2. Now only general features of the wave behaviour are considered. When $A(T)$ increases in time $k(T)$ usually increases also, hence the width of the wave inverse proportional to $k(T)$, decreases. This is an *amplification* of the solitary wave. On the contrary, we have an *attenuation* of the solitary wave when its

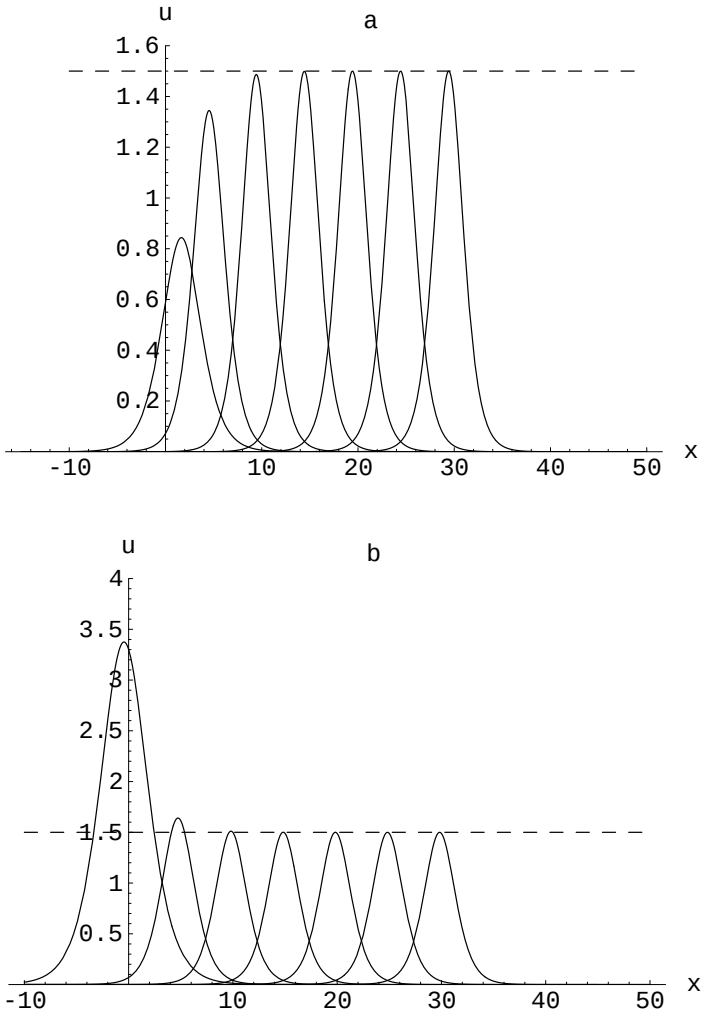

Fig. 1.17 Temporal evolution of an initial solitary wave resulting in a selection: a) from below, b) from above.

amplitude decreases while its width increases. Sometimes it happens that the increase/decrease of $A(T)$ takes place not up to infinity/zero but to the finite value A^*. Usually this value is defined by the governing equation coefficients, hence, by the physical parameters of the problem. To put

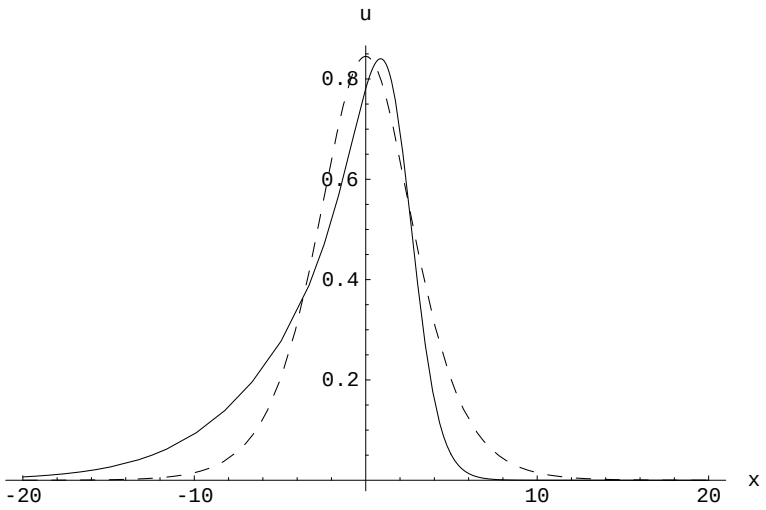

Fig. 1.18 Solitary wave (1.33) (dashed line) vs solitary wave (1.34) (solid line).

this another way, the parameters of the resulted steady wave are *selected*. Selection provided by an amplification of an initial wave, will be called selection from below, see Fig. 1.17(a), while selection from above happens as a result of an attenuation of an initial wave, see Fig. 1.17(b).

Shown in Fig. 1.18 is the profile of the wave (1.34) in comparison with the symmetric solitary wave solution (1.33) at $t = 0$. One can see that the wave (1.34) is asymmetric with respect to its core (or maximum). However, only initial stages of the temporal evolution of (1.34) differs from that of Eq.(1.33). As follows from Fig. 1.19, the final stage of the selection both from below and above, is the symmetric bell-shaped solitary wave like shown in the last stages in Fig. 1.17.

The amplification/attenuation of the kink may be described asymptotically and numerically Sachdev (1987), it will be shown in Sec. 5.3. Cnoidal wave evolution may be accounted for an asymptotic solution similar to that of the bell-shaped solitary waves Rednikov *et. al* (1995); Svendsen and Buhr-Hansen (1978).

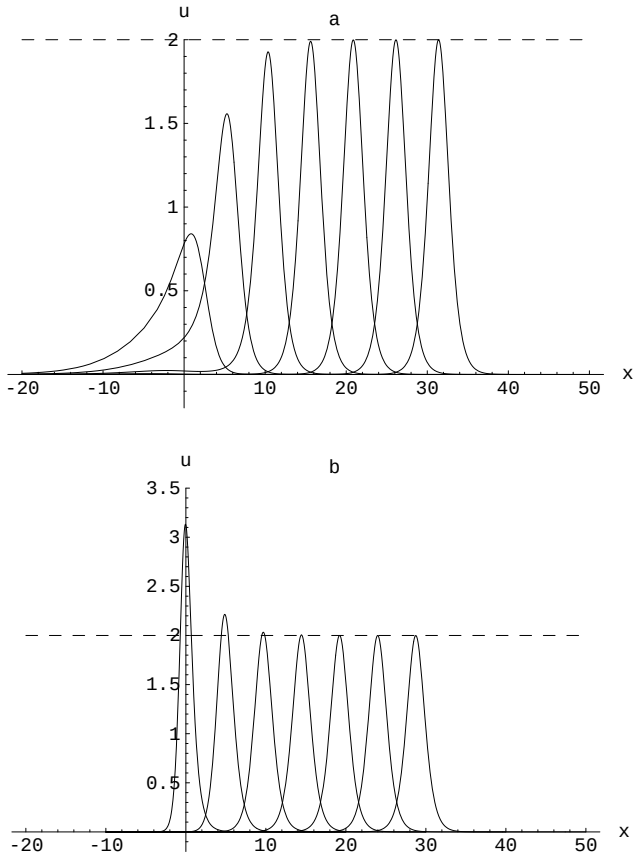

Fig. 1.19 Selection of the asymmetric monotonic solitary wave: a) from below, b) from above.

Chapter 2

Mathematical tools for the governing equations analysis

As a rule governing equations for nonlinear strain waves are nonitegrable by the inverse scattering transform method, and only particular analytical solutions may be obtained. Hence the study of real physical processes requires a combined analytico-numerical approach. The aim of this chapter is to describe methods to be used in this book. The choice of the analytical and numerical procedures is based on an experience of the author and does not claim a completeness.

2.1 Exact solutions

2.1.1 *Direct methods and elliptic functions*

Most of the mathematical work in the realm of nonlinear phenomena refers to integrable equations and their exact solutions, particularly, periodic. Among the recently developed general methods the algebrogeometrical approach may be used in an efficient way to find such solutions. Not only the numerical realization and graphical representation of the solution is provided by this method but also multi phase quasiperiodic solutions as well as purely periodic ones may be represented using the algebrogeometrical approach as illustrated in Belokolos *et. al* (1994). When we are interested in a self-similar solution of a partial differential equation one can use well developed theory of the solutions of ordinary differential equations, see, e.g., Ince (1964). Exact solutions of nonlinear nonintegrable partial differential equations are obtained usually using various direct methods. The significant point in direct methods is to build in advance the appropriate functional form of the solution (ansatz) of the equation studied. For example, the usage of ansatz in the form

of a hyperbolic tangent (tanh) power series resulted in finding of new exact travelling wave solutions (see, e.g., Korpel and Banerjee (1984); Parkes and Duffy (1996) and references therein). The choice of tanh is caused by the fact that any derivatives of tanh may be expressed as a polynomial with respect to the tanh itself. Then the equation studied becomes polynomial of the tanh after substituting the ansatz, and solution parameters are obtained from the algebraic equations appearing after equating to zero coefficients at each order of tanh . One would like to apply the same procedure to find more general periodic solutions. First of all another appropriate "basic" function is required instead of the tanh . For this purpose various elliptic functions were proposed recently, the most popular were theta functions (see, e.g.,Chow (1995), Nakamura (1979)), Jacobian elliptic functions (see, e.g.,Kostov and Uzunov (1992); Parker and Tsoy (1999)) and the Weierstrass elliptic function Kascheev (1990); Porubov (1993); Porubov (1996); Porubov and Parker (2002); Samsonov (1995); Samsonov (2001). In principle, periodical solutions could be obtained in terms of any of these functions. The efficient choice is caused by the simplest procedure of the ansatz construction and the least complicated algebra for determining solution parameters. It is well known that theta functions may be included in the Hirota bilinear method in order to get N-periodical solutions Nakamura (1979). However most of dissipative equations cannot be transformed to the bilinear form. At the same time single travelling wave solution derivation looks very complicated even for non-dissipative equations Chow (1995), Nakamura (1979). Moreover we have to deal with *four* theta functions that results in additional difficulties for the ansatz construction. Explicit periodic travelling wave solutions may be found for many nonintegrable equations and systems by using an ansatz in terms of $\wp$, with appropriate forms for the ansatz suggested by information about the poles of the solution. When compared to the use of theta functions or Jacobi elliptic functions, a prime advantage of using the function $\wp$ is that the algebra is drastically simplified. The ansatz for the solution involves only *one* Weierstrass function $\wp(\zeta, g_2, g_3)$, instead of *four* theta functions or *three* Jacobi elliptic functions $cn(\zeta,\ k)$, $sn(\zeta,\ k)$ and $dn(\zeta,\ k)$. Another advantage is that two apparently distinct solutions are readily recognized as equivalent. In order to see it let us first give some properties of the Weierstrass elliptic function $\wp$ to be used below. According to its definition Whittaker and Watson (1927), the Weierstrass function is analytical in the complex plane other than in the points where

it has double poles. The governing equation for the function $\wp$ is:

$$\{\wp'(\zeta)\}^2 = 4\wp^3 - g_2\wp - g_3 \tag{2.1}$$

where g_2 and g_3 are constant parameters. Remarkable features of the function $\wp$ are that all of its derivatives can be written by means of itself, and that any *elliptic function* f may be expressed using $\wp$ it and its first derivative as Whittaker and Watson (1927)

$$f = A(\wp) + B(\wp)\wp', \tag{2.2}$$

where A and B are rational functions with respect to $\wp$. Depending on the ratio between g_2 and g_3 the Weierstrass function may be bounded or unbounded inside the domain under study. The bounded periodic solutions are more conveniently expressed by writing them in terms of the Jacobi elliptic functions *cn*, *sn* and *dn* which are bounded on the real axis. For this purpose the relation between the Weierstrass function and the Jacobian functions is used as a special case of (2.2). Indeed, the familiar link is obtained in Whittaker and Watson (1927) but using the singular function sn^{-2},

$$\wp(\zeta,\ g_2,\ g_3) \ = \ e_3 + (e_1 - e_3)sn^{-2}(\sqrt{e_1 - e_3}\zeta, k). \tag{2.3}$$

However, following the method introduced in Whittaker and Watson (1927) one can check that the following formula is valid:

$$\wp(\zeta,\ g_2,\ g_3) \ = \ e_2 - (e_2 - e_3)cn^2(\sqrt{e_1 - e_3}\zeta, k), \tag{2.4}$$

connecting the Weierstrass function with the Jacobi function *cn*, regular along the real axes. Here $k = \sqrt{(e_2 - e_3)/(e_1 - e_3)}$ is the modulus of the Jacobian elliptic function, while $\tau = e_m$ ($m = 1, 2, 3$, $e_3 \ \leq \ e_2 \ \leq \ e_1$) are the real roots of the cubic equation

$$4\tau^3 - g_2\tau - g_3 = 0. \tag{2.5}$$

Expressing these results in terms of an appropriate choice of parameters, the wave number $\kappa = \sqrt{e_1 - e_3}$ and the Jacobian elliptic modulus k, we have

$$e_3 = -\frac{1+k^2}{3}\kappa^2, \quad e_2 = \frac{2k^2-1}{3}\kappa^2, \quad e_1 = \frac{2-k^2}{3}\kappa^2,$$

$$g_2 = \frac{8}{3}\kappa^4(1-k^2+k^4),\ g_3 = \frac{4}{27}\kappa^6(k^2+1)(2-k^2)(1-2k^2). \qquad (2.6)$$

The localized both the bells-shaped and the kink-shaped solitary wave solutions appear in the limit $k \to 1$ of the Jacobi elliptic functions.

Now consider an instructive example Porubov and Parker (2002). In Parker and Tsoy (1999), solutions were sought in terms of powers and products of Jacobi functions and thereby two solutions were obtained

$$z_1 = \ e_2 - (e_2 - e_3)\, cn^2(\sqrt{e_1 - e_3}\zeta,\ k), \qquad (2.7)$$

$$z_2 = \frac{\hat{r}^2 m^2}{2} sn^2(\hat{r}\zeta, m) \pm \frac{\hat{r}^2 m}{2} cn(\hat{r}\zeta, m) dn(\hat{r}\zeta, m) - \frac{\hat{r}^2(1+m^2)}{12}, \qquad (2.8)$$

which appear different. Obviously, the solution (2.7) is a representation of the Weierstrass function (2.3). However, one can check by direct substitution that the solution (2.8) also satisfies equation (2.1) when the parameters $\hat{r}$ and m are defined as solutions to

$$\frac{\hat{r}^4}{12}(1+14m^2+m^4) = g_2\,,\ \frac{\hat{r}^6}{216}(1-33m^2-33m^4+m^6) = g_3. \qquad (2.9)$$

Therefore z_2 is also a solution satisfying the same governing equation (2.1) defining the Weierstrass function. The two expressions (2.7) and (2.8) are essentially equivalent solutions, provided that $(\hat{r}, m)$ are appropriately related to (r, k). Accordingly, working with $\wp$ reveals links between seemingly distinct forms of solution.

It is to be noted that the first Weierstrass function derivative $\wp'$ cannot be expressed as a *polynomial* of the Weierstrass function itself Whittaker and Watson (1927), and we have to equate zero separately coefficients at each order of $\wp$ and at products of $\wp'$ and corresponding orders of $\wp$ Kascheev (1990); Porubov (1993); Porubov (1996); Samsonov (1995); Samsonov (2001). Therefore we really deal with two functions, and it is unlikely to get the solution using the ansatz proposed in the form of power series with respect both of the $\wp$ and $\wp'$ as it was done for the tanh. Another idea may be used, based on the singular point analysis of the possible solution and the well known fact that the Weierstrass function $\wp$ has the second order poleWhittaker and Watson (1927). In order to check the poles of a solution we shall use the WTK method Weiss *et. al* (1983) looking for the solution in the form of Laurént- type series about the singular manifold. It will be explained in details in Sec. 2.1.2.

The exact solutions obtained in this manner, usually belong to the class of travelling wave solutions which require special initial conditions. In case of the solitary wave solution the initial condition should be have the shape of the solitary wave itself. Moreover, travelling wave solutions for the dissipative equations usually have not free parameters, and additional relationships on the equation coefficients are required for the existence of the solutions Porubov (1993); Porubov (1996); Porubov and Velarde (1999); Porubov and Parker (1999); Porubov and Parker (2002); Samsonov (1995); Samsonov (2001).

2.1.2 *Painlevé analysis*

Recently it was developed the theory of nonlinear ordinary differential equations whose solutions have not movable singularities, other than poles. Then the theory has been extended to partial differential equations. Usually these equations are called "equations with the Painlevé property". The achievements of the theory may be found in Cariello and Tabor (1989); Conte (1989); Conte *et. al* (1993); Levi and Winternitz (1992); Newell *et. al* (1987); Weiss *et. al* (1983). Here we concentrate on the one aspect of the theory-the singular manifold method or WTC method for partial differential equations Newell *et. al* (1987); Weiss *et. al* (1983). Let $\varphi(x,t) = 0$ is the "singular" or "pole" manifold on which a solution $u(x,t)$ is singular. The main idea of the WTC is to demonstrate that the expansion

$$u(x,t) = \frac{1}{\varphi^{\alpha}} \sum_{j=0}^{\infty} q_j(x,t)\varphi^j \tag{2.10}$$

is single valued. This requires (i) α is an integer, (ii) φ is analytic in x and t and (iii) the equations for the coefficients q_j have self-consistent solutions. When all these conditions are satisfied the equation under study has the Laurént property. Also it is necessary to assume that neither φ_x nor φ_t vanish on $\varphi(x,t) = 0$. Let us illustrate how the methods works on an example of the KdV equation (1.1). Following Newell *et. al* (1987); Weiss *et. al* (1983) we assume $b = 3$, $d = 1$. Substituting the ansatz (2.10) into Eq.(1.1) one can find $\alpha = 2$ and $q_0 = -2\varphi_x^2$. Recursion relations for the q_j are

$$(j+1)(j-4)(j-6)q_j = F(\varphi_t, \varphi_x, ..., q_k; k < j). \tag{2.11}$$

The values of j, $j = -1$, 4 and 6 are called resonances. At each such

resonance the right-hand side of Eq.(2.11) vanishes thus ensuring the indeterminancy of the corresponding q_j. Moreover, the expansion (2.10) may be truncated at $O(\varphi^0)$. As a result we obtain using Eq.(2.11) an auto-Bäcklund transformation for the solution of Eq.(1.1),

$$u(x,t) = 2\frac{\partial}{\partial x^2}\log\varphi + q_2,$$

where q_2 satisfies the KdV equation. Also the Lax pair for the KdV equation follows from the solution of Eq.(2.11) Newell *et. al* (1987); Weiss *et. al* (1983).

However, the Lax pair cannot be obtained for nonitegrable equations as opposed to a truncated expansion that carries an information about possible pole orders of a solution. Using this information the anzats for the solution may be proposed, in particular, in terms of the Weierstrass elliptic function $\wp$ and $\wp'$. Substituting the proposed form of the solution into the equation under study and equating to zero coefficients at each order of $\wp$ and at products of $\wp'$ and corresponding orders of $\wp$ one can get the algebraic equations on the solution parameters, the phase velocity and the Weierstrass function parameters g_2, g_3. Certainly this procedure is of phenomenological kind but it allows to obtain the solutions of nonitegrable nonlinear equations in an explicit form. Some examples are presented below.

2.1.3 *Single travelling wave solutions*

First we consider exact solutions of DMKdV Eq.(1.13) obtained in Porubov (1993). It was found there the following auto-Bäcklund transformation for the solution $u(x,t)$

$$u = \frac{12\,\widetilde{\alpha}_4}{\widetilde{\alpha}_5}(\log\varphi)_{xx} + \frac{12}{5\,\widetilde{\alpha}_5}(\alpha_3 - \frac{2\alpha_1\,\widetilde{\alpha}_4}{\widetilde{\alpha}_5})(\log\varphi)_x + \widetilde{u}, \tag{2.12}$$

where $\widetilde{u}\,(x,t)$ satisfies Eq.(1.13). Concerning only tavelling wave solutions, one can reduce Eq.(1.13) to the third-order ODE of the form:

$$\widetilde{\alpha}_4\,u''' + \alpha_3\,u'' + \widetilde{\alpha}_2\,u' + \widetilde{\alpha}_5\,u\,u' + \alpha_1\,u^2 - V\,u + P = 0, \tag{2.13}$$

where $P = const$, prime denotes differentiation with respect to θ, $\theta = x - Vt$. Based on Eq.(2.12) possible solution may contain simple and second-order poles that may be modelled in terms of $\wp$ as Porubov (1993):

$$u = A\wp + \frac{B\wp'}{\wp + C} + D. \tag{2.14}$$

Substituting Eq.(2.14) into Eq.(2.13) one can derive a system of algebraic equations in A, B, C, D, phase velocity V and Weierstrass function parameters g_2, g_3:

$$(g_2C - g_3 - 4C^3)B = 0,\ (12C^2 - g_2)B = 0,$$

$$P = VD + 8\alpha_1 B^2 C - \alpha_1 D^2 - \alpha_3 g_2 A/2 - 2\,\widetilde{\alpha}_2\, BC + 12\,\widetilde{\alpha}_4\, BC^2 - \widetilde{\alpha_5}\,(2ABC^2 + g_2 AB/2 - 2BCD),$$

$$2\alpha_1(2B^2 + AD) - VA + 2\,\widetilde{\alpha}_2\, B + 2\,\widetilde{\alpha_5}\,(BD - ABC) = 0,$$
$$\alpha_1 A^2 + 6\alpha_3 A + 12\,\widetilde{\alpha}_4\, B + 6\,\widetilde{\alpha_5}\, AB = 0,$$

$$B(2\alpha_1(D - AC) - V) = 0,\ A(12\,\widetilde{\alpha}_4 + \widetilde{\alpha_5}\, A) = 0,$$

$$2\alpha_1 AB + 2\alpha_3 B + \widetilde{\alpha}_2\, A + \widetilde{\alpha_5}\,(AD + 2\,\widetilde{\alpha_5}\, B^2) = 0.$$

The solutions of these equations are:

(i) when g_2, g_3 are free parameters and $\alpha_3 = 2\alpha_1\,\widetilde{\alpha}_4\,/\,\widetilde{\alpha_5}$;

$$A = -\frac{12\,\widetilde{\alpha}_4}{\widetilde{\alpha_5}},\ B = 0,\ D = -\frac{\widetilde{\alpha}_2}{\widetilde{\alpha_5}},\ V = -\frac{2\alpha_1\,\widetilde{\alpha}_2}{\widetilde{\alpha_5}}.$$

(ii) when either

$$C = -\frac{1}{300\,\widetilde{\alpha_4}^{\,2}}(\alpha_3 - \frac{2\alpha_1\,\widetilde{\alpha}_4}{\widetilde{\alpha_5}})^2,$$

or $\alpha_3 = 12\alpha_1\,\widetilde{\alpha}_4\,/\,\widetilde{\alpha_5}$, C is a free parameter

$$A = -\frac{12\,\widetilde{\alpha}_4}{\widetilde{\alpha_5}},\ B = -\frac{6}{5\,\widetilde{\alpha_5}}(\alpha_3 - \frac{2\alpha_1\,\widetilde{\alpha}_4}{\widetilde{\alpha_5}}),$$
$$D = -\frac{\widetilde{\alpha}_2}{\widetilde{\alpha_5}} + \frac{2\alpha_1}{\widetilde{\alpha_5}^{\,2}}(\alpha_3 - \frac{2\alpha_1\,\widetilde{\alpha}_4}{\widetilde{\alpha_5}}) + \frac{1}{25\,\widetilde{\alpha}_4\widetilde{\alpha_5}}(\alpha_3 - \frac{2\alpha_1\,\widetilde{\alpha}_4}{\widetilde{\alpha_5}})^2,$$
$$V = \frac{24\alpha_1\,\widetilde{\alpha}_4}{\widetilde{\alpha_5}}C - \frac{2\alpha_1\,\widetilde{\alpha}_2}{\widetilde{\alpha_5}} + \frac{4\alpha_1^2}{\widetilde{\alpha_5}^{\,2}}(\alpha_3 - \frac{2\alpha_1\,\widetilde{\alpha}_4}{\widetilde{\alpha_5}}) +$$
$$\frac{2\alpha_1}{25\,\widetilde{\alpha}_4\widetilde{\alpha_5}}(\alpha_3 - \frac{2\alpha_1\,\widetilde{\alpha}_4}{\widetilde{\alpha_5}})^2,\ g_2 = 12C^2,\ g_3 = 8C^3.$$

Using (2.4) the solution (2.14) with parameters defined by (i) may describe a particular bounded cnoidal wave, propagating with fixed phase velocity, of the form:

$$u = \frac{12\ \widetilde{\alpha}_4}{\widetilde{\alpha}_5} k^2 \kappa^2 c n^2(k\theta, \kappa) - \frac{\widetilde{\alpha}_2}{\widetilde{\alpha}_5} - \frac{4\ \widetilde{\alpha}_4}{\widetilde{\alpha}_5} k^2 (2\kappa^2 - 1) \tag{2.15}$$

where k is a free parameter. When the Jacobian elliptic functions modulus $\kappa \to 1$ the solution (2.15) transforms to the solitary wave solution (1.12). The solution (2.14) with parameters defined by (ii) accounts for a bounded kink-shaped solution (1.28). When C is a free parameter, kink propagates with any phase velocity value.

Besides bounded solutions (2.15) and (1.28), the solution (2.14) also describes unbounded ones in the form of localized and periodic discontinuities. Finally it is to be noted that the functional form (2.14) in terms of the Weierstrass function is not unique. One can see that there exist at least one more solution of the form:

$$u = -\frac{12}{25\ \widetilde{\alpha}_4 \widetilde{\alpha}_5} (\alpha_3 - \frac{2\alpha_1\ \widetilde{\alpha}_4}{\widetilde{\alpha}_5})^2 \exp(2y) \wp(\exp(y) + G, 0, g_3),$$

where

$$y = \exp(\gamma\theta),\ \gamma = -\frac{1}{5\ \widetilde{\alpha}_4} (\alpha_3 - \frac{2\alpha_1\ \widetilde{\alpha}_4}{\widetilde{\alpha}_5}),$$

G and g_3 are free parameters. This solution allows to describe only the bounded kink-shaped wave (1.28). At the same time it accounts for a new periodically discontinious solution.

In previous Chapter the bounded periodic solution (1.32) of the equation (1.31) was considered. When studying travelling wave solutions, i.e. solutions depending only on the phase variable $\theta = x - Vt$, this equation may be transformed into the O.D.E., which results in the following equation after integrating once with respect to θ:

$$d\eta''' + g\eta'' - V\eta' + b(\eta^2)' + f(\eta^2)'' + c(\eta^3)' = N. \tag{2.16}$$

Further we follow the results obtained in Porubov (1996). The transformation is obtained here using the WTK method of the form

$$u = \frac{f \pm \sqrt{f^2 - 2cd}}{c} (\log\varphi)' + \widetilde{u}. \tag{2.17}$$

Therefore possible solution should contain first order pole. The Weierstrass elliptic function $\wp$ possesses second order pole, and we shall propose three solution forms. The first of them is

$$u \;=\; \frac{A\wp'}{\wp + C} + B. \tag{2.18}$$

In order to find the solution parameters the formula (2.18) is substituted into the Eq.(2.16). Then equating to zero coefficients at each order of $\wp+C$ and $\wp'$ one can derive the algebraic equations on A, B, C, phase velocity V and the Weierstrass function parameters g_2, g_3:

$$\begin{aligned}
(\wp + C)^{-4} &: (g_2C - g_3 - 4C^3)^2(6Af - 3A^2c - 6d) \;=\; 0,\\
(\wp + C)^{-3} &: (g_2C - g_3 - 4C^3)(12C^2 - g_2)(14Af - 9A^2c - 12d) = 0,\\
(\wp + C)^{-2} &: 4(g_2C - g_3 - 4C^3)(2bB - V + 48ACf + 3c(12A^2C -\\
&\qquad B^2) - 48Cd) - 3(12C^2 - g_2)^2(2f - 2Ac - d) \;=\; 0,\\
(\wp + C)^{-1} &: 4(g_2C - g_3 - 4C^3)(10f - 4f + 3Ac + 6d) - (12C^2 -\\
&\qquad g_2)(2Bb - V + 24ACf + 3(B^2 - 12A^2C)c - 12Ad) = 0,\\
\wp^0 &: 4(12C^2 - g_2)qA^2 = N,\\
(\wp + C) &: 2Bb - V + 24ACf + 6(B^2 - 12A^2C)c - 12Cd = 0,\\
(\wp + C)^2 &: 2Af + d + 2A^2c = 0,\\
\wp'(\wp + C)^{-3} &: (g_2C - g_3 - 4C^3)(g + 2Bf - Ab - 3ABc) = 0,\\
\wp'(\wp + C)^{-2} &: (12C^2 - g_2)(2Ab - g - 2Bf + 6ABc) = 0,\\
\wp' &: 2Ab + g + 2Bf + 6ABc = 0.
\end{aligned}$$

Three solutions of algebraic equations are obtained. The first appears when

$$12C^2 - g_2 = 0, \quad g_2C - g_3 - 4C^3 = 0.$$

In this case two of three roots e_i of Eq.(2.5) are equal to one another, and no periodical solution exists. Then the solution (2.18) will have the form of localized discontinuity under positive C values. When the parameter C is negative we get $\kappa \;=\; 1$, and the bounded kink-shaped solitary wave solution follows from Eq.(2.18):

$$u \;=\; \gamma \tanh(m\theta) + u_0. \tag{2.19}$$

For the wave amplitude γ two formulaes are valid

$$\gamma \;=\; A_1 m, \; A_1 \;=\; (f + (f - 2cd)^{1/2})/(6c),$$

$$\gamma \;=\; A_2 m,\; A_2 \;=\; (f-(f-2cd)^{1/2})/(6c).$$

Then for u_0 we have

$$u_0 = \frac{2bA_j - g}{2(3cA_j + f)},\; j = 1, 2,$$

and phase velocities $V_1,\; V_2$ are

$$V_1 = 2u_{01}b + 6c(u_{01}^2 + 4A_1^2m^2) - 4m^2(2fA_1 - d),$$

$$V_2 = 2u_{02}b + 6c(u_{02}^2 + 4A_2^2m^2) - 4m^2(2fA_2 - d),$$

while $m^2 \;= -3C \;=\; 3e_1$ is a free parameter.

The second solution corresponds to the situation when

$$g_2C - g_3 - 4C^3 = 0, \quad 12C^2 - g_2 \neq 0. \tag{2.20}$$

In this case the solution may exist under additional conditions on the equation coefficients $f \;=\; g \;=\; 0$, that results in absence of the dissipative terms in Eq.(2.16). Hence it becomes now the O.D.E. reduction of the Gardner equation. The bounded cnoidal wave solution arises when $C \;= -e_1$ and has the form

$$u \;=\; \pm\sqrt{-\frac{2d}{c}}\kappa^2 m\frac{cn(m\theta,\kappa)sn(m\theta,\kappa)}{dn(m\theta,\kappa)} - \frac{b}{3c}, \tag{2.21}$$

where $m^2 \;=\; e_1 - e_3$. It governs the travelling cnoidal wave, propagating with the phase velocity $V \;= -b^2/(3c) - 6e_1d.$ that transforms into the kink-shaped soluiton (2.19) when $\kappa \;=\; 1$.

Finally, the third solution arises when

$$12C^2 - g_2 = 0, \quad g_2C - g_3 - 4C^3 \;\neq\; 0.$$

In this case the bounded cnoidal wave solution (1.32) holds. When $\kappa \;=\; 1$ we have $C^* = 0$, and it transforms into the kink-shaped solution (2.19), see Fig. 1.6.

Now we shall consider the second possible solution's form in terms of the Weierstrass elliptic function $\wp$:

$$\eta = \sqrt{A\wp + B}. \tag{2.22}$$

Substitution Eq.(2.22) into the Eq.(2.16) allows us to conclude that solution may now exist only when $f \;=\; g \;=\; 0$. Then one can get the algebraic

equations for the solution parameters equating to zero coefficients at the terms $\wp' \wp^k$, $k = 0 \div 3$, and $(A\wp + B)^{5/2}$:

$$\begin{aligned}
\wp' \wp^3 &: cA + 2d = 0 \\
\wp' \wp^2 &: 9cAB - VA + +15dB = 0 \\
\wp' \wp &: 9cAB - 2VA + +12dB = 0 \\
\wp' &: 12cB^3 - 4VB^2 + dA(Bg_2 - Ag_3) = 0 \\
(A\wp + B)^{5/2} &: N = 0
\end{aligned}$$

One can obtain the following solution of these equations:

$$A = -\frac{2d}{c},\ B = \frac{2de_i}{c},\ i = 1 \div 3, V = -\frac{1}{2}cB,$$

where e_i are the real roots of Eq. (2.5). We again deal with the O.D.E. reduction of the Gardner equation, however now one can obtain its another bounded solutions. Thus for $d/fc > 0$ we find cnoidal wave solutions of the form:
(I) for $B = 2de_2/c$

$$u = \sqrt{\frac{2d}{c}}\ m\ \kappa\ cn(m\theta, \kappa), \tag{2.23}$$

where $m^2 = e_1 - e_3$ and for the phase velocity we have $V = dm^2(2\kappa^2 - 1)$.
(II) for $B = 2de_1/c$ we obtain

$$u = \sqrt{\frac{2d}{c}}\ m\ \kappa\ dn(m\theta, \kappa), \tag{2.24}$$

Solution (2.24) represents cnoidal wave propagating with the phase velocity $V = dm^2(2 - \kappa^2)$. It is to be noted that at $\kappa = 1$ both the solutions (2.23) and (2.24) transform to the bell-shaped solitary wave

$$u = \sqrt{\frac{2d}{c}}\ m\ ch^{-1}(m\theta, \kappa),$$

propagating with the velocity $V = dm^2$.

When $d/c > 0$ the bounded solution appears from (2.22) if $B = 2de_3/c$ and has the form

$$u = \sqrt{\frac{2d}{c}}\ m\ \kappa\ sn(m\theta, \kappa), \tag{2.25}$$

For the phase velocity we find $V = -dm^2(1+\kappa^2)$. In contrast to solutions (2.23), (2.24) the solution (2.25) transforms to the kink-shaped solution (2.19) when $\kappa = 1$.

Finally one can construct the third possible solution in terms of the Weierstrass elliptic function $\wp$ depending now on new independent variable $y = \exp(k\theta)$. Changing variable in auto-Bäcklund transformation (2.17) one can see that the following solution may be proposed:

$$u = A\frac{y\wp'_y}{\wp + C} + B, \tag{2.26}$$

Substituting it into Eq.(2.16) one can find that solution may exist under $f = 0$. Therefore we now deal with the O.D.E. reduction of the Gardner equation with linear dissipation. The solution of the form (2.26) for the last equation was already obtained previously in Samsonov (1995). It was found that this solution may correspond either to discontinuous periodical solution or to the bounded kink-shaped solution of the form similar to the solution (2.19).

2.1.4 *Exact solutions of more complicated form*

The procedure of the obtaining exact solutions is based on the reduction to the ODE, hence only travelling wave solutions may be found. However, sometimes this procedure is applied to obtain only the part of a solution, and more complicated profiles are decsribed. Consider some examples. Recently the coupled nonlinear Schrödinger equations (CNLS)

$$\begin{aligned} iW_t + sW_{xx} + (\eta WW^* + \sigma UU^*)W = 0, \\ i\rho U_t + rU_{xx} + (\eta^{-1}UU^* + \sigma WW^*)U = 0, \end{aligned} \tag{2.27}$$

with $r, s = \pm 1$; ρ, σ, η real, have attracted considerable interest because of their role in governing various physical wave-guiding systems. These equations are not generally integrable by the inverse scattering transform method, except in cases of high symmetry (e.g. $\rho = 1, \eta = \sigma = \pm 1$). The machinery of the Weierstrass function is applied in the search for travelling wave solutions of equations (2.27) in the form

$$W = w(\zeta)\, e^{i\zeta}, \qquad U = u(\zeta)\, e^{i\phi}, \tag{2.28}$$

where $\theta = x - c\,t, \zeta = \zeta(\theta, t)$, $\phi = \phi(\theta, t)$, with u, w, ζ and ϕ real. Substitution (2.28) into equations (2.27) allows to separate the real and imaginary

parts. The solutions for u and w are sought in the form

$$w = \sqrt{F\wp^2 + A\wp + B}, \qquad u = \sqrt{G\wp^2 + D\wp + E}, \tag{2.29}$$

while for ζ and ϕ we have

$$\begin{aligned} \zeta &= \tfrac{1}{2} s\, c\, \theta - s\, C_1 \int \frac{d\theta}{w^2} + \zeta_0(t)\,, \\ \phi &= \tfrac{1}{2} r\, c\, \rho\, \theta - r\, C_2 \int \frac{d\theta}{u^2} + \phi_0(t)\,, \end{aligned} \tag{2.30}$$

where C_i $(i = 1, 2)$ are free parameters. The most notable difference from previous solutions is the dependence of the "frequency" and "phase" on w and u, when $C_i \neq 0$. This introduces significant features into the profiles of the real and imaginary parts of W and of U. Thus, we find for W of the form:

$$W = w\ \exp\ \imath\, Y, \tag{2.31}$$

where w is defined by Porubov and Parker (1999)

$$w = \sqrt{A\left\{\frac{2k^2-1}{3}\kappa^2 - k^2\kappa^2 cn^2(\kappa\theta,\, k) + B/A\right\}}, \tag{2.32}$$

while for the phase function Y we have

$$Y = \frac{cs\theta}{2} - \frac{sC_1\Pi[\varphi,\, n,\, k]}{\kappa\, A(H_1 - e_3)} + (\gamma + \frac{c^2 s}{4})t, \tag{2.33}$$

$\Pi[\varphi,\, n,\, k]$ is the elliptic integral of the third kind, $\varphi = \arcsin(sn(\kappa\theta))$, $n = -\kappa^2 k^2/(B/A + e_3)$ and C_1 is defined by

$$A = \frac{2(\sigma\, r\, \eta - s)}{\eta(1-\sigma^2)}\,, C_1^2 = \frac{A^2}{4}\left\{4\left(\frac{B}{A}\right)^3 - g_2\,\frac{B}{A} + g_3\right\}, \tag{2.34}$$

$$\gamma = \frac{\sigma(E\, A - B\, D) - 3s\, B}{A}, D = \frac{2(s\,\sigma - r\,\eta)}{1-\sigma^2}\,,$$

where B, E, g_2 and g_3 are free parameters. The shape of the wave (2.31) depends strongly on the values of the parameters κ, k and H_1. An example of the behavior of $Re\, W$ is shown in Fig.2.1(a) for the case $H_1 \in [e_2, e_3]$, $c \sim \kappa$ and at $t = 0$. We get an interesting wave, consisting of the carrier wave slightly modulated and with superposed periodic disturbances. Therefore,

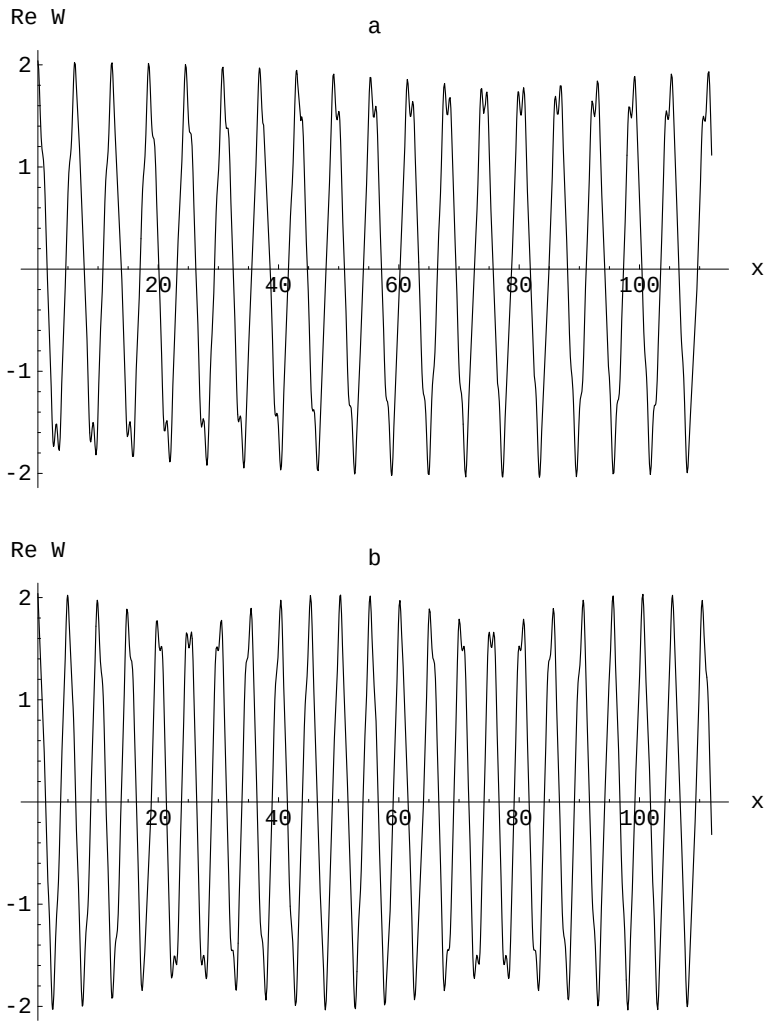

Fig. 2.1 Exact solutions of the CNLS. a) profile with moving disturbances; b) almost envelope wave solution.

the wave shape is not determined solely by the amplitude wave shape. When c considerably exceeds the wave number κ we get the profile closer to the usual envelope wave solution, see Fig. 2.1(b).

Another interesting profiles correspond to the exact solutions of the

complex Ginzburg-Landau equation, CGLE,

$$\imath\, u_t + p\, u_{xx} + q\, |u|^2\, u = \imath\, \gamma\, u \tag{2.35}$$

where the constant coefficients are $p = p_r + \imath\ p_i$, $q = q_r + \imath\, q_i$, with $p_j,\ q_j \neq 0$, $(u, p, q) \in \mathbf{C}$, $\gamma \in \mathbf{R}$. The subscripts t and x denote temporal and spatial derivatives, respectively. This equation appears in the description of a large variety of physical phenomena, e.g., in nonlinear optics, non-equilibrium pattern formation, lasers, superconductivity etc. Like in case of CNLS equations, first of all, we decompose the solution $u(x,t)$ in its amplitude, y, and phase, θ, both real,

$$u = y(\zeta)\, e^{\imath\theta}, \tag{2.36}$$

where $\zeta = x - c\, t$, $\theta = \theta(\zeta, t)$. Substituting (2.36) into (2.35) and equating to zero the real and imaginary parts one obtains two coupled equations for the functions y and $z \equiv \theta_\zeta$. Then periodic and pulse solutions of the CGLE may be found Porubov and Velarde (1999). The first derivative of the real part of the periodic solution with respect to x, $v = (Re\, u)_x$, is

$$v = \frac{Z}{y} \sin\left(\theta + \arcsin(\frac{y\ y_x}{Z})\right), \tag{2.37}$$

with

$$y = \sqrt{\frac{2q_r}{p_r}\left\{k_1^2 \mathrm{dn}^2(k_1\zeta,\, \kappa) - \delta_1^2\right\}},\ Z = \sqrt{y^2 y_x^2 + C^2}. \tag{2.38}$$

When $C = 0$, the zeroes of the first derivative (2.37) are defined by the zeroes of the function y_x and correspond to the zeroes of the Jacobi functions cn and sn. Their positions do not change in time, and for u we have harmonic temporal oscillations of the spatially periodic state defined by the amplitude parts of the solutions (2.36). However, the situation changes dramatically when $C \neq 0$. In this case Z never vanishes, and the zeroes of the first derivative are defined by the zeroes of the sin function only, whose position vary in time. A typical situation is shown in Fig. 2.2. Fig. 2.2(a) shows a structure with four spatially repeated parts. During half of the time period the shapes of these parts vary, and we get in Fig. 2.2(d) a profile which is practically the mirror image to Fig. 2.2(a). Qualitatively this evolution does not depend upon the value of the modulus κ of Jacobi functions.

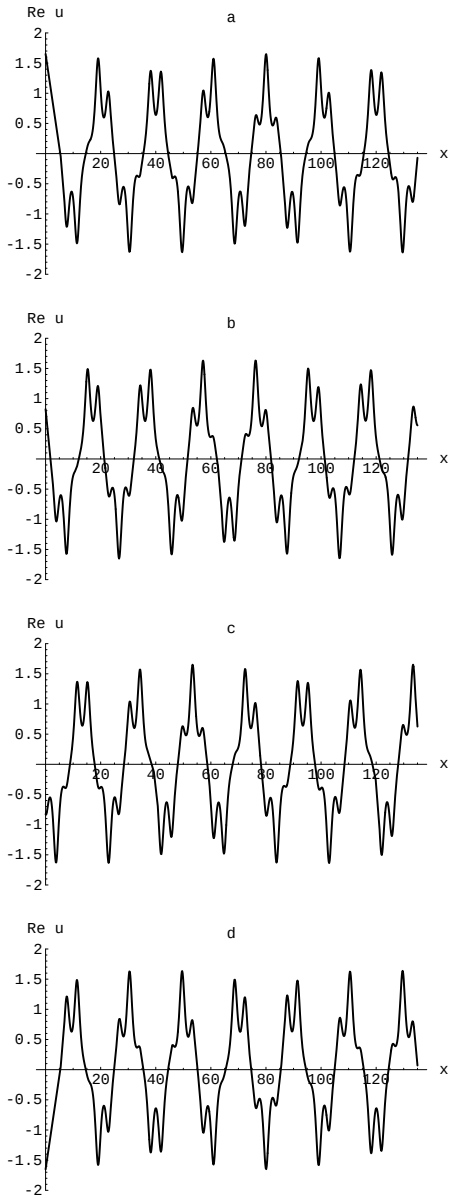

Fig. 2.2 Evolution of the periodic solution (2.36) $Re\, u$ *vs* x for times $t = m\, p_i \pi/(3 p_r \gamma)$, $0 < m < 3$ with $k = 0.9$, $\delta_1 = 0.5$. a)$m = 0$, b)$m = 1$, c)$m = 2$, d)$m = 3$.

Consider now the pulse solution Porubov and Velarde (1999),

$$u = \sqrt{\frac{6Al_1}{l_2}}\, k\, \cosh^{-1}(k\zeta)\, \exp \imath\theta, \tag{2.39}$$

with

$$\kappa^2 = -\frac{\gamma}{2(p_i + 4A\, p_r - 4A^2 p_i)},\ l_1 = p_r^2 + p_i^2,\ l_2 = p_r\, q_i - p_i\, q_r.$$

The first derivative for the real part of (2.39) is

$$(Re\, u)_x = \sqrt{\frac{6Al_1(1+4A^2)}{l_2}}\, k^2\, \cosh^{-1}(k\zeta)\, \tanh(k\zeta) \sin\left(\theta - \arctan(\frac{1}{2A})\right). \tag{2.40}$$

Thus, from (2.40) it follows that additional zeroes of the first derivative may appear if

$$k > \sqrt{\frac{l_2}{6A\, l_1}} \exp\left(\frac{\arctan(1/(2A))}{2\, A}\right). \tag{2.41}$$

The evolution of the real part of the solution (2.39) is illustrated in Fig. 2.3. Again we see that two initial maxima in Fig. 2.3(a) disappear, Fig. 2.3(e), then an initial minimum at $\zeta = 0$ is changed into a maximum, while two minima arise, Fig. 2.3(f-h). Therefore, our solution is breather- like. If (2.41) is not satisfied, there is a pulse solution whose spatial behavior is determined by the function $\cosh^{-1}(k\zeta)$ only with one extremum at $\zeta = 0$.

2.2 Asymptotic solutions

Particular exact solutions are insufficient for understanding physical processes. One can see that many equations consist in generalisations of the integrable equations like the KdV equation. Sometimes additional terms may be considered as small perturbations. Often straight asymptotic expansions are incorrect Cole (1968); Jeffrey and Kawahara (1982); Nayfeh (1973), and the matching asymptotic procedure Ablowitz and Segur (1981); Kodama and Ablowitz (1981) may be applied to find a solution in this case. The basic idea of the perturbation approach is to look for a solution of a perturbed nonlinear equation in terms of certain natural fast and slow variables. Often there is a need in only one fast variable, such as phase variable θ in the unperturbed problem. Depending upon the problem either slow time, $T = \varepsilon\, t$, or slow coordinate, $X = \varepsilon\, x$, $\varepsilon << 1$ are

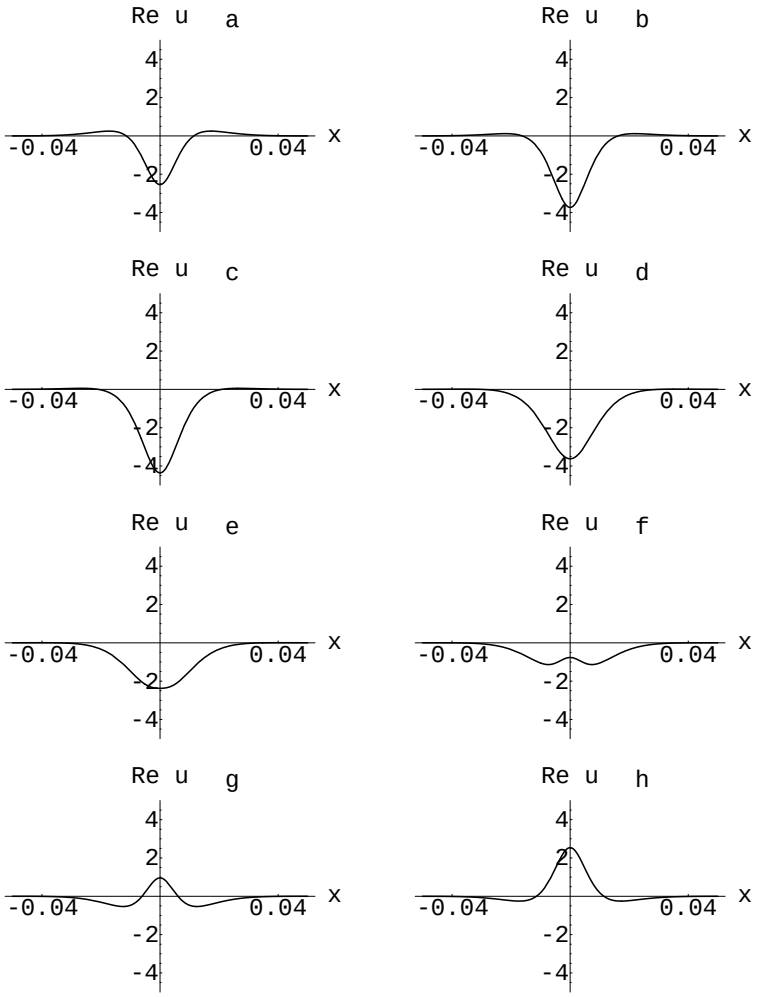

Fig. 2.3 Evolution of the pulse solution (2.39) *Re u vs x* for times $t = m\pi/\beta$, $0 < m < 8$. a)$m = 0$, b)$m = 1$, c)$m = 2$, d)$m = 4$, e)$m = 5$, f)$m = 6$, g)$m = 7$, h)$m = 8$.

introduced. Fast variable is generalized in a perturbed problem assuming either $\theta_x = 1$, $\theta_t = -V(T)$ or $\theta_x = P(X)$, $\theta_t = -1$. The functions $V(T)$ or $P(X)$ are defined to remove secular terms. Some of the appropriate secularity conditions are formed from Green's identity as follows. Assume a solution $u = u(\theta, T)$ is of the form

$$u(\theta, T) = u_0(\theta, T) + \varepsilon\, u_1(\theta, T) + ... \tag{2.42}$$

The leading order problem is nonlinear equation for u_0 whose solution is known. Then in the next order an inhomogeneous linear equation for u_1 holds

$$L(u_1) = F(u_0).$$

Here $L(u_1)$ is a linearized leading-order equation operator. Denoting by $v_i (i = 1, ..., M)$ the M solutions of the homogeneous adjoint problem,

$$L^A(v_i) = 0,\ i = 1, ..., M,$$

where L^A is the adjoint operator to L, we obtain that

$$L(u_1)v_i - L^A(v_i)u_1 = Fv_i$$

is always a divergence. Using the boundary conditions it may be integrated to give the secularity conditions. In particular, when $v_i \to 0$ as $|\theta| \to \infty$ while u_1 is bounded the secularity condition is:

$$\int_{-\infty}^{\infty} v_i F\, d\theta = 0. \tag{2.43}$$

Then either $V(T)$ or $P(X)$ are obtained from Eq.(2.43). Method may be used for finding perturbed cnoidal wave solutions. In this case integration in (2.43) is carrying over the period Rednikov *et. al* (1995); Svendsen and Buhr-Hansen (1978). It is to be noted that a simple quasistationary expansion is not uniformly valid on $|x| \to \infty$. Complete solutions is obtained using matching quasistationary solution to a nonstationary one for large $|\theta|$, e.g. $|\theta| \sim 1/\varepsilon$ Ablowitz and Segur (1981); Kodama and Ablowitz (1981).

Let us apply this method for a perturbed solitary wave solution of the DMKdV equation (1.13). Following Kliakhandler *et. al* (2000); Rednikov *et. al* (1995) assume that $\widetilde{\alpha}_i = \varepsilon\, \alpha_{\ i}$, $\varepsilon << 1$, and suppose that u depends upon a fast variable θ and a slow time T, such as

$$\theta_x = 1,\ \theta_t = -V(T),\ T = \varepsilon\, t.$$

Then equation (1.13) becomes

$$\alpha_3\, u_{\theta\theta\theta} - V\, u_\theta + 2\alpha_1\, u\, u_\theta + \varepsilon\, [u_T + \alpha_2\, u_{\theta\theta} + \alpha_4\, u_{\theta\theta\theta\theta} + \alpha_5\, (u\, u_\theta)_\theta] = 0. \tag{2.44}$$

The solution of Eq.(2.44) is sought in the form (2.42). In the leading order we get

$$\alpha_3\, u_{0,\theta\theta\theta} - V\, u_{0,\theta} + 2\alpha_1\, u_0\, u_{0,\theta} = 0. \tag{2.45}$$

We are interested in studying localized solutions vanishing together with its derivatives at $|\theta| \to \infty$. Then the leading order solution is

$$u_0 = \frac{6\,\alpha_3}{\alpha_1}\, b(T)^2 \cosh^{-2}\left(b(T)\,\theta\right) \tag{2.46}$$

with $V = 4\alpha_3\, b^2$. At order ε, we have

$$\alpha_3\, u_{1,\theta\theta\theta} - V\, u_{1,\theta} + 2\alpha_1\, (u_{\,0} u_1)_\theta = F, \tag{2.47}$$

$$F = -\left[u_{0,T} + \alpha_2\, u_{0,\theta\theta} + \alpha_4\, u_{0,\theta\theta\theta\theta} + \alpha_5\, (u_0\, u_{0,\theta})_\theta\right].$$

The operator acting on the function u_1 in the lhs of Eq.(2.47) is adjoint to that of the Eq.(2.45). Then the secularity condition (2.43) with $v_i = u_0$ yields the equation for b:

$$b_T = \frac{8}{15}\, b^3 \left(A + B\, b^2\right), \tag{2.48}$$

with

$$A = \alpha_2,\ B = \frac{4}{7}\left(\frac{6\alpha_3\alpha_5}{\alpha_1} - 5\alpha_4\right). \tag{2.49}$$

The behavior of b (or the sign of b_T) depends on the signs of A and B and on the value of $b_0 \equiv b(T = 0)$. Indeed, when both A and B are positive b diverges while for both negative values it will vanish. For $A < 0$, $B > 0$ the parameter b vanishes if $b_0 < \sqrt{-A/B}$ while it diverges if $b_0 > \sqrt{-A/B}$. The most interesting case occurs when $A > 0$, $B < 0$. Here b tends to $\sqrt{-A/B}$ independent of b_0. A quantitative description of the variation of b can be given. Equation (2.48) may be directly integrated giving the implicit dependence of b on T:

$$T = \frac{4\,B}{15A^2} \ln\left|\frac{b_0^2(A + B\, b^2)}{b^2(A + B\, b_0^2)}\right| - \frac{4(b_0^2 - b^2)}{15A\, b^2\, b_0^2}. \tag{2.50}$$

We see that b tends to infinity in finite time, $T = T^*$ for $A > 0$, $B > 0$,

$$T^* = \frac{4\,B}{15A^2} \ln\frac{b_0^2 B}{(A + B\, b_0^2)} + \frac{4}{15A\, b_0^2}, \tag{2.51}$$

A similar scenario occurs when $A < 0$, $B > 0$, $b_0 < \sqrt{-A/B}$. Hence, with our asymptotic approximation we can predict when blow-up could occur. On the other hand, for both $A < 0$, $B < 0$ and $A < 0$, $B > 0$, the quantity $b_0 > \sqrt{-A/B}$, b vanishes when T tends to infinity. Finally, when $A > 0$, $B < 0$, the quantity b approaches $\sqrt{-A/B}$ when T tends to infinity, and expression (2.50) provides an *analytical* description of the time-dependent process of the parameter-value selection of the solitary wave (2.46), see Fig. 1.17. In the last case, if we additionally assume $\alpha_3 = 2\alpha_1\alpha_4/\alpha_5$, the asymptotic "dissipative" solitary wave (2.46) will tend to the exact travelling solitary wave solution (1.12).

Function $u_1(\theta, T)$ is a solution of a linear inhomogeneous O.D.E., hence, it will contain free parameters depending on T like $b(T)$ in the leading order problem. Its definition allows to satisfy solvability condition in the next order problem and to avoid secular terms in the asymptotic expansion. Higher order approximations may be studied similarly. The first-order solution u_1 has been obtained in Rednikov *et. al* (1995) of the form:

$$u_1 = A_1 u_{0,\theta} + A_2\,\theta\cosh^{-2}(b(T)\,\theta) + A_3 u_{0,\theta}\log(\cosh(b(T)\,\theta)) +$$

$$A_4(1 - \tanh(b(T)\,\theta)),$$

where A_i may be found in Rednikov *et. al* (1995). One can see it predicts a plateau behind the solitary wave and does not vanish at minus infinity. Uniformly valid solution is found using the matching asymptotic procedure may be found in Rednikov *et. al* (1995). Perturbations of cnoidal wave solutions were studied, e.g., in Rednikov *et. al* (1995); Svendsen and Buhr-Hansen (1978). In this case the modulus of the Jacobian elliptic functions should be a function of a slow variable, corresponding expressions for the derivatives of the elliptic functions with respect to modulus may be found in Byrd and Friedman (1954); Newille (1951).

2.3 Numerical methods

One can see that both exact nor asymptotic solutions have severe limitations. In particular they satisfy specific initial conditions and do not allow to account for an arbitrary initial disturbance evolution. Therefore numerical simulations should be used. Two kinds of nonlinear equations,

considered here, may be written either

$$u_t = L(u) \tag{2.52}$$

or

$$u_{tt} = L(u) \tag{2.53}$$

where $L(u)$ is a certain nonlinear differential operator. Equations of the kind (2.52) will be called nonlinear evolution equations while nonlinear hyperbolic equations correspond to the class (2.53). Further only numerical methods are described which are used by the author and his coworkers in solving the problems considered in the book. Two main schemes are used, pseudo-spectral approach and finite-difference approach. More detailed information about numerical modelling of nonlinear wave equations may be found, in particular, in Berezin (1987); Dodd *et. al* (1982); Fletcher (1984); Mayer (1995); Sachdev (1987); Zwillenger (1989), see also references therein.

2.3.1 *Nonlinear evolution equations*

Among the equations of the kind (2.52) main attention has been paid to numerical solutions of the KdV equation, see Berezin (1987); Dodd *et. al* (1982) where various difference schemes are discussed. As noted in Berezin (1987) implicit three-levels schemes are rather simple and suitable for a realization. However, some of the straight finite-difference methods require rather small time step for stability, while long-time evolution should be studied. It becomes the smaller the higher is the order of a highest derivative term in NEE. In particular, it takes place for a simulation of the generalized fifth-order KdV equation (1.3), another example has been studied in Christov *et. al* (1997). The problem of an increase of the time step may be solved either by a modification of a difference scheme or by using a more effective solving procedure, in particular, the fourth-order Runge-Kutta finite-difference method. Besides simulation of Eq.(1.3) in Porubov *et. al* (2002), this method was effectively applied to study the evolution and interaction of Marangoni-Bénard solitary waves governed by Eq.(1.13) in Marchant (1996). The same equation has been numerically solved in Christov and Velarde (1995) using a four-stage scheme providing third-order approximation in time. The implicit predictor-corrector method has been applied to nonlinear diffusion equations in Sachdev (1987).

Pseudo-spectral methods have been adopted recently, there already exist monographs Fletcher (1984); Sachdev (1987) where they are explained in details, see also Zwillenger (1989) and references therein. In a pseudo-spectral scheme the space derivatives are approximated very accurately by means of the Fourier transforms, in particular, by the fast Fourier transform (FFT) algorithm. The fourth-order Runge-Kutta scheme may be used for the time derivative Kliakhandler (1999). It provides very mild stability restrictions on the time step. The pseudo-spectral numerical scheme has proved very efficient in solving dispersive and dissipative equations. The evolution of the initial monotonic solitary wave into radiating or oscillatory solitary waves was simulated in Benilov *et. al* (1993) for the fifth-order KdV equation. In a series of papers Salupere *et. al* (1997); Salupere *et. al* (2001) the solitary wave formation from a periodic input was studied for an equation similar to Eq.(1.3), while the paper Salupere *et. al* (1994) is devoted to the KdV soliton detection from a harmonic input. The use of the pseudo-spectral approach to account for an evolution of an initial localized pulse in framework of Eq.(1.3) is demonstrated in Sec. 1.2.1. Numerical solutions of the nonlinear diffusion equations are considered in Fletcher (1984); Sachdev (1987).

Finally, this method allows to study an evidence of the selected solitary waves Kliakhandler *et. al* (2000) predicted on the basis of the asymptotic analysis of Eq.(1.13) in previous section. To reveal the expected behaviour of the solutions, the following numerical technique has been employed. Since at the very late stage of the evolution the unstable waves are expected to be controlled by the finite-amplitude waves found in Kawahara (1983), we define the typical wavenumber $k_c = \sqrt{\alpha_2/2\alpha_4}$ corresponding to the most unstable linear mode in Eq.(1.13). The corresponding wavelength is $\lambda_c = 2\pi/k_c$. The length of spatial domain was chosen to be $256\lambda_c$, i.e. rather long. At the same time, the number of discretization points was chosen to be 4096, i.e. λ_c is covered by 16 points. The latter ensures fair resolution of the whole solutions computed. Periodic boundary conditions have been used for simulations. The pseudo-spectral technique was employed for the spatial discretization and the Runge-Kutta fourth order scheme for the time advance. The time step was chosen to be 0.01. The tests with smaller time steps and better resolution gave indistinguishable results. The control of the simulations in the Fourier space shows the good resolution of the computed solutions. First, it has been checked that the tendency to blow-up, Fig. 2.4(a), the damping, Fig. 2.4(b), and the selection have been observed at the α_i values prescribed by the theory in previous

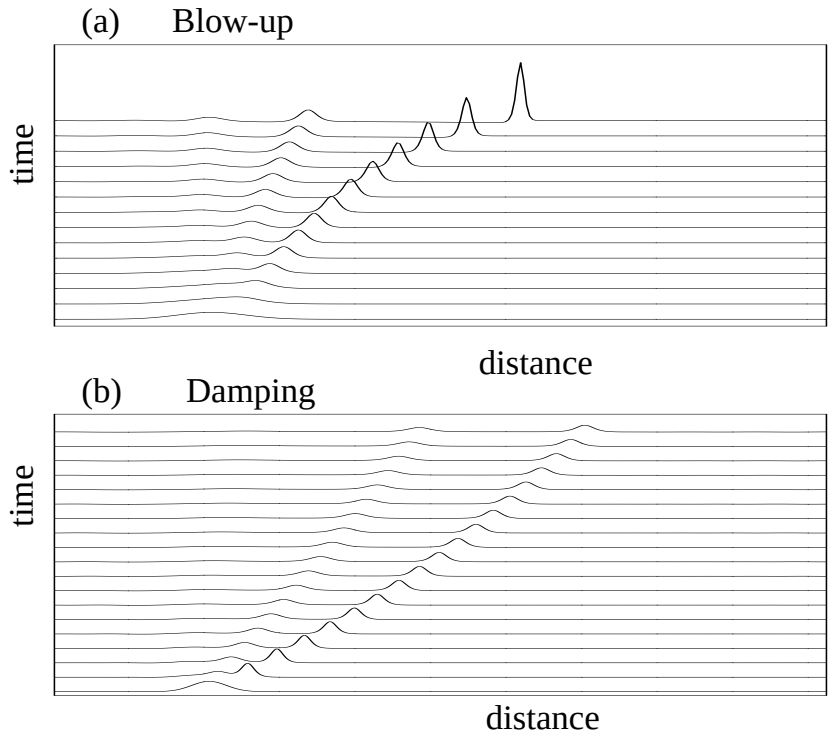

Fig. 2.4 Blow-up (a) and damping (b) of the initial conditions.

section. In the case of "blow-up", we found that the pulse tends to grow rapidly at the time t^* rather close to the predicted $t^* = T^*/\varepsilon$ from (2.51). This observation allows to find analytically "time-of-life" of the blowing solutions of Eq. (1.13).

Following Kliakhandler *et. al* (2000) let us discuss in detail the selection of "dissipative" solitary waves occurring at $A > 0$, $B < 0$. Choosing the parameter values $\varepsilon = 0.1$, $\alpha_1 = 1$, $\alpha_2 = 1$, $\alpha_3 = 1$, $\alpha_4 = 6/5$, $\alpha_5 = -2$, the resulting amplitude of the selected solitary wave is obtained using (2.46), (2.49) and $b = \sqrt{-A/B}$. The amplitude, $6\alpha_3 b^2/\alpha_1 = 0.583$ and the velocity $V = 4\alpha_3 b^2 = 0.389$. We consider both the selection occurring from "below" when the magnitude of an initial Gaussian pulse is smaller than that of the eventually selected solitary waves and the selection from "above" when the selected solitary wave amplitude is smaller than that of the initial pulse magnitude. This would permit to separate the selection mechanism from

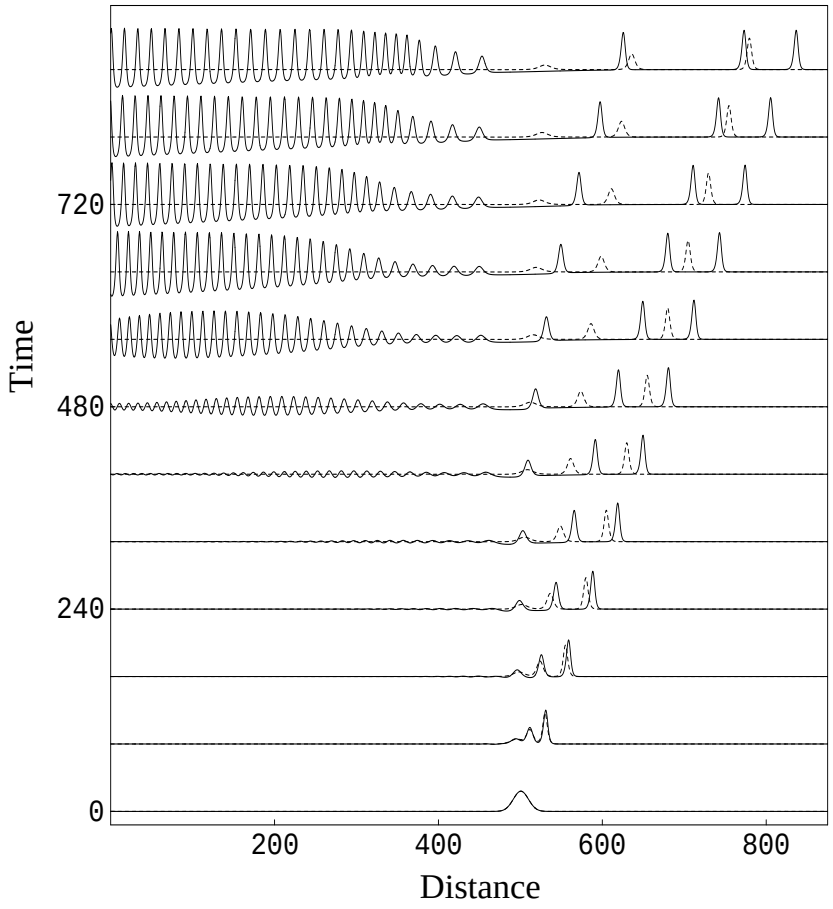

Fig. 2.5 "Dissipative" solitary wave selection from an initial Gaussian profile with amplitude 0.3 and width 36 units.

those originating from the *growing* unstable disturbances Kawahara (1983); Oron and Rosenau (1997). One can see in Fig. 2.5 that up to the time $t \sim 120$ an initial Gaussian pulse with the magnitude $0.3 < 0.583$ and width 36 breaks into a train of three localized pulses aligned in row of decreasing magnitude. Due to smallness of ε, the influence of the dissipative non-KdV terms is small at this stage. This may be seen by compar-

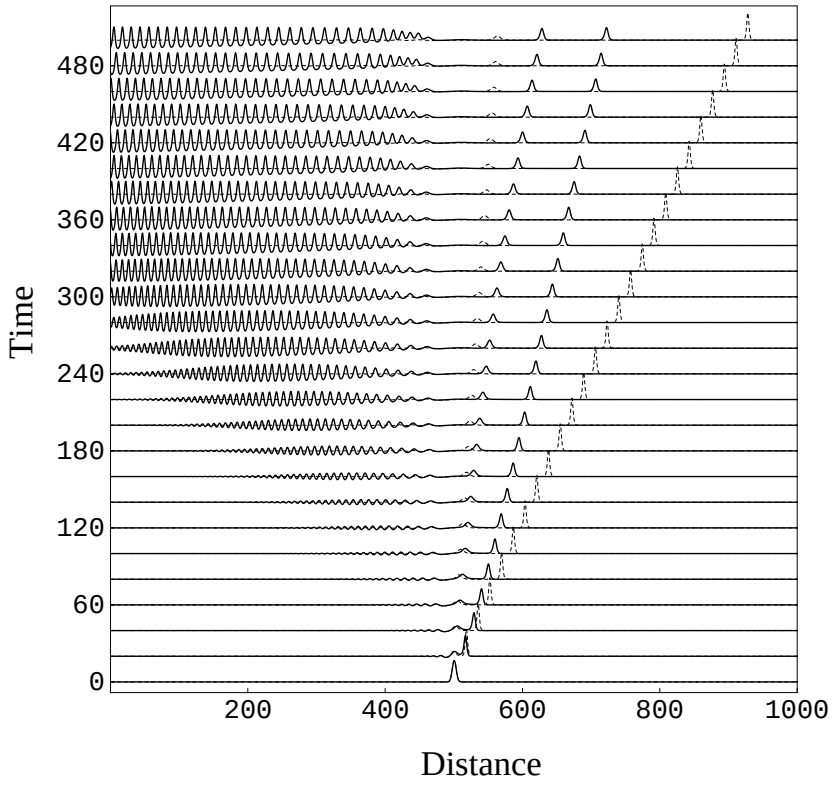

Fig. 2.6 "Dissipative" solitary wave selection from an initial Gaussian profile with amplitude 1 and width 12 units.

ison of solutions of Eq.(1.13), shown as solid lines, with pure KdV case, $\alpha_2 = \alpha_4 = \alpha_5 = 0$, shown by dashed lines. At later stages the initial pulse transforms into a train of the solitary waves. At nonzero ε each solitary wave amplitude and velocity tend to the values 0.585 and 0.38 in agreement with the theory of single solitary wave selection, while each of three KdV solitons continues propagation with its own amplitude and velocity. "Dissipative" solitary waves form a bound state Christov and Velarde (1995); Nekorkin and Velarde (1994) whose unequal spacing between equally high crests reflects the original separation of the solitary waves in the KdV stage when higher ideal solitons travel faster. The tail behind the train of solitary waves appear as a result of short wave instability similar to Kawahara (1983). However, the solitary waves have higher velocity than the velocity of growing wave packets. As a result, the solitary waves bound state es-

capes the destruction induced by the radiation that lags behind. A similar finding for the GKS equation was reported in Chang *et. al* (1995). We see on the last stages that the magnitude of the tail saturates. All these structures are quite well resolved and similar to those found in Kawahara (1983); Oron and Rosenau (1997). They are robust and remain the same under the mesh refinement and smaller time steps.

The selection process realized from "above" is shown in Fig. 2.6 when initial Gaussian pulse has the magnitude $1 > 0.583$ and the width 12. Two equal solitary waves with amplitude 0.585 and velocity 0.38 appear as a result of *decrease* of the magnitude of the initial pulse. Again the comparison with pure KdV case is shown by dashed lines. All features of the selection process are similar to the selection from "below".

Simulations of Eq.(1.13) with other values of parameters ε, α_i such that $A > 0$, $B < 0$, which are not reported here, show the same features of the selection process as described above.

2.3.2 *Nonlinear hyperbolic equations*

Among the equations of kind (2.53) we are especially interested in various Boussinesq-like long waves equations, that may be written in the form of so-called double-dispersive equation Erofeev and Klyueva (2002); Samsonov (2001)

$$u_{tt} - \alpha_1 u_{xx} - \alpha_2 (u^2)_{xx} - \alpha_3 u_{xxtt} + \alpha_4 u_{xxxx} = 0. \qquad (2.54)$$

At $\alpha_3 = 0$ it corresponds to the classic Boussinesq equation. Besides quadratic nonlinear term, $\alpha_2 (u^2)_{xx}$, cubic or higher-order nonlinearities may be considered Christou and Christov (2002); Soerensen *et. al* (1984); Soerensen *et. al* (1987); also higher-order derivative terms may be incorporated in Eq.(2.54) Christou and Christov (2000); Christov *et. al* (1996). A Fourier-Galerkin method were applied to computing localized solutions in Christou and Christov (2000); Christou and Christov (2002). An implicit difference scheme was developed in Christov and Maugin (1995); Christov and Velarde (1994); Christov and Velarde (1995) to account for numerical solutions of the Boussinesq equation and its generalizations where Newton's quasi-linearization of the nonlinear terms is employed. The solution in Soerensen *et. al* (1984); Soerensen *et. al* (1987) is obtained using the Gauss elimination.

There is an another method developed independently the USSR in 1953 Godunov and Ryaben'kii (1987); Samarskii and Nikolaev (1989) and in the

USA by L.H. Thomas (1949). That is why it is known in the West as the Thomas method Morton and Mayers (1994); Richtmyer and Morton (1967). As noted in Godunov and Ryaben'kii (1973), this method is justified for the solutions of linear problems. However, the author applied it more than ten years ago for a numerical solution of Eq.(2.54). One can see further in the book that it gives numerical results in a good agreement with analytical predictions. Previously the Thomas method was used for both nonlinear evolution equationsBerezin (1987) and hyperbolic equationAlexeyev (1999). Recently it was successfully applied in Bukhanovsky and Samsonov (1998); Porubov *et. al* (1998) for computing rather complicated hyperbolic nonlinear elastic systems.

Since the Thomas algorithm is not widely used for solutions of the nonlinear waves problems, it is useful to describe it in a more elaborate manner. Following Godunov and Ryaben'kii (1987); Godunov and Ryaben'kii (1973) consider a boundary problem:

$$a_n u_{n-1} + b_n u_n + c_n u_{n+1} = f_n,\ 0 < n < N, \tag{2.55}$$

$$u_0 = \varphi,\ u_N = \psi. \tag{2.56}$$

Let us assume

$$u_0 = L_{1/2} u_1 + K_{1/2},$$

where $L_{1/2} = 0$, $K_{1/2} = \varphi$. It allows to exclude u_0 from the equation (2.55) at $n = 1$, giving

$$u_0 = L_{3/2} u_2 + K_{3/2},$$

with $L_{3/2} = -c_1/b_1$, $K_{1/2} = (f_1 - a_1\varphi)/b_1$. Following this procedure one can obtain

$$u_n = L_{n+1/2} u_{n+1} + K_{n+1/2}, \tag{2.57}$$

with

$$L_{n+1/2} = -\frac{c_n}{b_n + a_n L_{n-1/2}},\ K_{n+1/2} = \frac{f_n - a_n L_{n-1/2}}{b_n + a_n L_{n-1/2}}.$$

Hence going from 1 to N one can calculate the coefficients $L_{n+1/2}$, $K_{n+1/2}$. Using (2.57) and the boundary conditions (2.56) at $n = N$, one can obtain u_{N-1}. Then coming back from $n = N-1$ to $n = 1$ one can find every u_n from (2.57) using already known $L_{n+1/2}$, $K_{n+1/2}$. It was noted

in Godunov and Ryaben'kii (1987); Godunov and Ryaben'kii (1973) that small amount of arithmetic operations together with a weak sensitivity to the calculation errors are the main advantages of the method.

Assume $u_n = u(x_n, t_j)$ is a mesh function of a solution of Eq.(2.54) while $v_n = u(x_n, t_{j-1})$, $w_n = u(x_n, t_{j-2})$ correspond to the mesh functions on previous time steps. Then we have for discretization of Eq.(2.54)

$$a_n = c_n = \alpha_3,\ b_n = -\triangle x^2 - 2\alpha_3,$$

$$f_n = \triangle x^2(w_n - 2v_n) - \alpha_1 \triangle t^2(v_{n-1} - 2v_n + v_{n+1}) + \alpha_3(2v_{n-1} - 4v_n + 2v_{n+1} -$$

$$w_{n-1} + 2w_n - w_{n+1}) - \alpha_4 \triangle t^2/\triangle x^2(v_{n-2} - 4v_{n-1} + 6v_n - 4v_{n+1} +$$

$$v_{n+2}) - \alpha_2 \triangle t^2(v_{n-1}^2 - 2v_n^2 + v_{n+1}^2),$$

where $\triangle t$, $\triangle x$ are time and space steps respectively. Uniqueness condition, $|b_n| > |a_n| + |c_n|$ Godunov and Ryaben'kii (1973), is always satisfied at positive α_3. The difference scheme is similar to those used in Soerensen *et. al* (1984); Soerensen *et. al* (1987) in the case $\alpha_4 = 0$ and with higher order nonlinearities being taken into account.

2.4 Use of Mathematica

Recently various symbolic mathematical programs were developed to provide huge analytical operations. One of the most powerful is the Mathematica developed by Wolfram (1999) that is used by the author on all stages of his studies. This section is not focused on the detailed description of the magnificent abilities of the program. Only some important features are considered in relation to the problems studied here.

Among the advantages of the Mathematica one can mention variety of the build-in mathematical functions. In particular, it works efficiently with the Weierstrass elliptic function $\wp$ that may be used for obtaining exact solutions. Indeed, the procedure described in Sec. 2.1 is based on the transformation of the problem of a solution of a PDE to the problem of the solution of algebraic equations for the ansatz parameters. These equations may be too complicated for manual operations, and use of the Mathematica allows to obtain solutions avoiding errors. Design of the Mathematica package provides an automatic finding of a solution. An example may be found in Parkes and Duffy (1996) where a package is presented to obtain

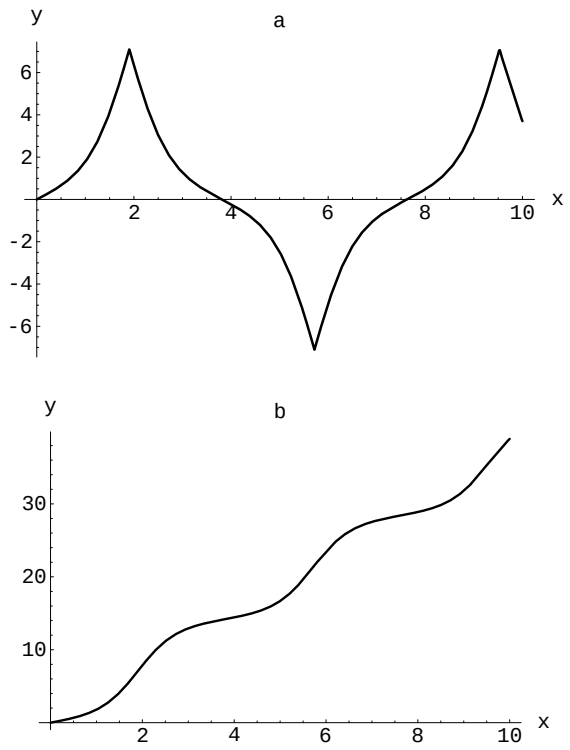

Fig. 2.7 a) Incorrect and b) correct representations of the function y.

solutions in terms of the hyperbolic tanh-function. However, it is unlikely that an automated method may be applied for finding periodic solutions. First, it is necessary to introduce the rules for the elliptic functions derivatives. Second, sometimes combinations like $g_2C - g_3 - 4C^3$ or $12C^2 - g_2$ should be kept in the solution for its convenient analysis, see Sec. 2.1.3. The Mathematica cannot do it automatically. Finally, it works simultaneously with all possible solutions of the algebraic equations that yields huge expressions at the intermediate stages of a solution and may result in falling down the evaluation. Hence, it is better to manage the substitution procedure step by step manually introducing the commands that provide the most efficient line of attack on the problem.

The algebraic manipulations should be used also for a check of the asymptotic solutions and for derivation of the governing nonlinear equa-

tions. Numerical abilities may be efficiently used for the analysis of analytical relationships, while Fortran, C++ or other languages are preferable for numerical simulations of nonlinear PDEs. The Mathematica possesses high-level graphic facilities, it admits representation of graphics in many formats including PostScript and Encapsulate PostScript. Almost all figures in the book are prepared using the Mathematica. Like analytical procedures graphics may be automatized. In particular, numerical data obtained using Fortran or C++ programs, may be represented by an automated procedure, see, e.g., Kliakhandler (1999).

Sometimes, the Mathematica gives incorrect results. In particular, the construction of the profiles shown in Figs. 2.1 and 2.2 requires calculation of the function $y = \Pi[\varphi,\, n,\, \kappa],\ \varphi = \arcsin(sn(k\ x))$ expressed through the elliptic integral of the third kind. Direct Mathematica command $\mathrm{Plot}[y, \{x, 0, 10\}]$ yields the profile shown in Fig. 2.7(a). One can see it contains the points where there is no first derivative of y. In order to obtain correct smooth profile it is necessary to define y as $y = \Pi[\psi,\, n,\, \kappa]$, where ψ is obtained using the Mathematica commands

$$\psi[x\_/;\ 0 \le x \le\ x_0] = \varphi;\ \psi[x\_/;\ x_0 \le x \le 3\ x_0] = \pi - \varphi;$$
$$\psi[x\_/;\ 3\ x_0 \le x \le 5\ x_0] = 2\pi + \varphi;$$
$$\psi[x\_/;\ 5\ x_0 \le x \le 7\ x_0] = 3\pi - \varphi;\ \text{etc.}$$

where $x_0 = K(\kappa)/k$, $K(\kappa)$ is the complete elliptic integral of the first kind, κ is the elliptic functions modulus. Then we obtain required smooth profile for y shown in Fig. 2.7(b) around which the profiles are developed in Figs. 2.1, 2.2.

Chapter 3

Strain solitary waves in an elastic rod

The theory of strain waves in solids began to develop over two hundred years ago, see about it Love (1927); McNiven and McCoy (1974). During the long period only linear theory of elasticity was considered since because of the engineering needs and poor experimental facilities. Now the study of the material properties Lurie (1990); Murnaghan (1951), acoustic signals Biryukov *et. al* (1991); Oliner (1978); Parker and Maugin (1987) etc. require mathematical models based on the nonlinear elasticity. Recent developments in general elastic theory may be found in Bland (1960); Lurie (1990); Maugin (1993); Maugin (1995); Murnaghan (1951), while nonlinear waves in solids were considered in Engelbrecht (1983); Engelbrecht (1997); Erofeev (2002); Erofeev and Klyueva (2002); Jeffrey and Engelbrecht(1994); Mayer (1995); Parker (1994); Parker and Maugin (1987); Samsonov (2001).

In order to go further it is necessary to define a notion of the word solid. In macroelasticity solid may be defined as a substance having a definite volume and shape and resisting forces that tend to alter its volume or shape. From the point of view of the theory of discrete media, solid may be considered as a crystalline material in which the constituent atoms are arranged in a 3D lattice with certain symmetries. As noted previously Jeffrey and Engelbrecht(1994); Samsonov (2001), these definitions complement each other allowing to take into account a model of elastic potential of atomic interactions, and to cover amorphous, porous or granular media.

When elastic features are one and the same in any direction we have isotropic solids. Sometimes anisotropy is important, e.g., in design of nonlinear acoustic devices Oliner (1978); Parker and Maugin (1987). Strain waves in solids may be classified as follows. Comparing the direction of the wave propagation with the particle motion one can distinguish longitudinal and shear waves. The former wave propagates along the direction of the

particle motion, the latter -perpendicular to it. Waves propagating inside solid are called bulk waves. In presence of a lateral surface, surface strain waves are possible. In this book main attention is paid to the longitudinal bulk waves in isotropic media and wave guides.

3.1 The sources of nonlinearities

Among the possible sources of nonlinearity we briefly consider so-called geometrical and physical nonlinearities since they affect the strain wave propagation to a greater extent. Other kinds of nonlinearities are considered in Engelbrecht (1997); Jeffrey and Engelbrecht(1994). The geometrical nonlinearity is described by the exact expression of the strain tensor always used in the theory of large deformations. Initially the position of a particle is accounted for a vector-radius $\overrightarrow{r}$, or an initial or reference configuration is defined. Loading forces provide the displacement of particle yielding the current or actual configuration characterized by an another vector-radius $\overrightarrow{R}$. Then the movement is described by the displacement vector, $\vec{V} = \overrightarrow{R}$ - $\overrightarrow{r}$. However, not only the positions of the particles vary during the deformation but also the distances between them. In order to describe the alteration of the distance a deformation or strain tensor is introduced. It is obtained from the difference between the squares of the arc length in the deformed (actual) and undeformed (reference) configuration. In the reference configuration the Cauchy-Green *finite* deformation tensor $\mathbf{C}$ is defined Lurie (1990), whose general form is

$$\mathbf{C} = \left[\overrightarrow{\nabla}\,\vec{V} + (\overrightarrow{\nabla}\,\vec{V})^T + \overrightarrow{\nabla}\,\vec{V}\cdot(\overrightarrow{\nabla}\,\vec{V})^T\right]/2$$

(written in terms of a vector gradient $\overrightarrow{\nabla}\,\vec{V}$ and its transpose $(\overrightarrow{\nabla}\,\vec{V})^T$). In rectangular Cartesian coordinates x_i the components of $\mathbf{C}$ may be written in a more familiar form

$$C_{ik} = \frac{1}{2}\left(\frac{\partial u_i}{\partial x_k} + \frac{\partial u_k}{\partial x_i} + \frac{\partial u_l}{\partial x_i}\frac{\partial u_l}{\partial x_k}\right),$$

where u_k are the components of the displacement vector $\vec{V}$.

As a result of a deformation process there appear stresses. Certainly they should be connected with the strains, and this is a source of the physical nonlinearity. It was found more than hundred years ago that Hook's linear law of elasticity is insufficient, see about it in Jeffrey and Engelbrecht(1994); Samsonov (2001). Since Piola-Kirchoff stress tensor is defined

in the reference configuration, through the volume density of the internal energy Π in adiabatic processes (or through the Helmgholtz free energy in thermoelastic processes),

$$P_{ik} = \frac{\partial \Pi}{\partial C_{ik}},$$

one can say the physical nonlinearity depends upon the structure of the internal (or free) strain energy density Π. The energy of deformation must be insensitive to the rotation of the reference frame. It was Murnaghan (1951) who supposed to develop the energy as a power series in the three invariants of the strain tensor,

$$\Pi \ = \ \frac{\lambda + 2\mu}{2} I_1^2 - 2\mu I_2 + \frac{l + 2m}{3} I_1^3 - 2m I_1 I_2 + n I_3, \qquad (3.1)$$

where $I_k, k = 1, 2, 3$ are the invariants of tensor $\mathbf{C}$:

$$I_1(\mathbf{C}) \ = \ tr\mathbf{C}, \ I_2(\mathbf{C}) \ = \ [(tr\mathbf{C})^2 - tr\mathbf{C}^2]/2, \ I_3(\mathbf{C}) = \det \mathbf{C}. \qquad (3.2)$$

The first two terms in (3.1)account for linear elasticity, hence the second order elastic moduli, or the Lamé coefficients (λ, μ), characterize linear elastic properties of the isotropic material. Other terms in (3.1) describe material or physical nonlinearity Lurie (1990); Murnaghan (1951). Accordingly, the third order elastic moduli, or the Murnaghan moduli (l, m, n) account for nonlinear elastic properties of the isotropic material. The energy may be written using another set of invariants,

$$J_1(\mathbf{C}) \ = \ tr\mathbf{C}, \ J_2(\mathbf{C}) \ = \ tr\mathbf{C}^2, J_3(\mathbf{C}) \ = \ tr\mathbf{C}^3,$$

in the form Lurie (1990)

$$\Pi \ = \ \frac{\lambda}{2} J_1^2 + \mu J_2 + \frac{\nu_1}{6} J_1^3 + \nu_2 J_1 J_2 + \nu_3 J_3. \qquad (3.3)$$

Since

$$J_1(\mathbf{C}) \ = I_1(\mathbf{C}) \ , \ J_2(\mathbf{C}) = I_1^2(\mathbf{C}) \ - 2I_2(\mathbf{C}),$$

$$J_3(\mathbf{C}) \ = I_1^3(\mathbf{C}) - 3I_1(\mathbf{C})I_2(\mathbf{C}) + 3I_3(\mathbf{C}),$$

Eqs.(3.1) and (3.3) coincide if $\nu_1 = 2l - 2m + n$, $\nu_2 = m - n/2$, $\nu_3 = n/4$. In some cases there is a need in more terms in Eq.(3.1):

$$\Pi = \frac{\lambda + 2\mu}{2} I_1^2 - 2\mu I_2 + \frac{l + 2m}{3} I_1^3 - 2m I_1 I_2 + n I_3 +$$

Table 3.1 Lame's and Murnaghan's modulii, $*10^{-9}N/m^2$

material	λ	μ	l	m	n
Polystyrene	1.71	0.95	-18.9	-13.3	-10
Steel Hecla 37	111	82.1	-459	-461	-358
Aluminium 2S	57	27.6	-299	-311	-228
Pyrex glass	13.5	27.5	14	92	420
SiO_2 melted	15.9	31.3	129	71	-44

$$a_1 I_1^4 + a_2 I_1^2 I_2 + a_3 I_1 I_3 + a_4 I_2^2, \tag{3.4}$$

The fourth order moduli (a_1, a_2, a_3, a_4) can be either positive or negative. However, mainly the third-order moduli data may be found in the literature Frantsevich *et. al* (1982); Lurie (1990), some of them are collected in Table 3.1.

The series expansions (3.1), (3.4) are convenient to account for the deformation of compressible materials (metals, polymers, etc.), whose yield point is small. For incompressible materials, like rubber, there exist another models, e.g., the Mooney model Lurie (1990). Its generalization, the Mooney-Rivlin model, may be used even for compressible materials, its application to nonlinear strain waves in a rod may be found, e.g., in Dai (1998).

3.2 Modelling of nonlinear strain waves in a free lateral surface elastic rod

3.2.1 *Statement of the problem*

Let us consider an isotropic, axially infinitely extended, free lateral surface cylindrical elastic rod, see Fig. 3.1. Axi-symmetry leads to using cylindrical Langrangian coordinates (x, r, φ), where x is the axis of the rod, $\varphi \in [0, 2\pi]$, $0 \leq r \leq R$. When torsions are neglected, the displacement vector is $\vec{V} = (u, w, 0)$. We shall consider the propagation of longitudinal strain waves of small but finite amplitude in the rod. Once the reference configuration is defined we use Hamilton's variation principle to obtain the governing equations together with the boundary conditions, setting to zero the variation of the action functional,

$$\delta S = \delta \int_{t_0}^{t_1} dt 2\pi \int_{-\infty}^{\infty} dx \int_0^R r \, \mathcal{L} dr = 0, \tag{3.5}$$

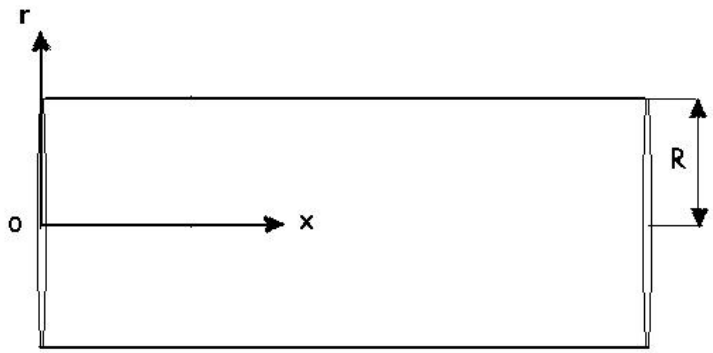

Fig. 3.1 Free lateral surface cylindrical rod

where, $\mathcal{L}$ is the Lagrangian density per unit volume, $\mathcal{L}$=$K - \Pi$, with Π defined by Eq.(3.1). For the kinetic energy density K we have

$$K = \frac{\rho_0}{2}\left[\left(\frac{\partial u}{\partial t}\right)^2 + \left(\frac{\partial w}{\partial t}\right)^2\right] \tag{3.6}$$

where ρ_0 is the rod material density at $t = t_0$. The integration in brackets in (3.5) is carried out at the initial time $t = t_0$. Initially, the rod is supposed to be in its natural, equilibrium state. In absence of torsions non-zero

components of the Cauchy-Green deformation tensor $\mathbf{C}$, are

$$C_{xx} = u_x + \frac{1}{2}(u_x^2 + w_x^2), C_{rr} = w_r + \frac{1}{2}(u_r^2 + w_r^2), C_{\varphi\varphi} = \frac{1}{r}w + \frac{1}{2r^2}w^2,$$
$$C_{rx} = \frac{1}{2}(u_r + w_x + u_x w_r + w_x w_r).$$

Hence the invariants in (3.2) may be written as

$$I_1(\mathbf{C}) = C_{xx} + C_{rr} + C_{\varphi\varphi},$$

$$I_2(\mathbf{C}) = C_{xx}C_{rr} + C_{xx}C_{\varphi\varphi} + C_{rr}C_{\varphi\varphi} - C_{rx}^2,$$

$$I_3(\mathbf{C}) = C_{\varphi\varphi}(C_{xx}C_{rr} - C_{rx}^2).$$

The following boundary conditions (b.c.) are imposed for a free lateral surface rod:

$$w \to 0, \qquad \text{at } r \to 0, \tag{3.7}$$

$$P_{rr} = 0\ , \qquad \text{at } r = R, \tag{3.8}$$

$$P_{rx} = 0, \qquad \text{at } r = R, \tag{3.9}$$

where the components P_{rr}, P_{rx} of the Piola - Kirchhoff stress tensor $\mathbf{P}$ are defined as

$$\begin{aligned} P_{rr} = {} & (\lambda + 2\mu)\, w_r + \lambda\, \frac{w}{r} + \lambda\, u_x + \frac{\lambda + 2\mu + m}{2}\, u_r^2 + \\ & \frac{3\lambda + 6\mu + 2l + 4m}{2}\, w_r^2 + (\lambda + 2l)\, w_r \frac{w}{r} + \frac{\lambda + 2l}{2}\frac{w^2}{r^2} + \\ & (\lambda + 2l)\, u_x w_r + (2l - 2m + n)\, u_x \frac{w}{r} + \frac{\lambda + 2l}{2}\, u_x^2 + \\ & \frac{\lambda + 2\mu + m}{2}\, w_x^2 + (\mu + m)\, u_r w_x, \end{aligned} \tag{3.10}$$

$$\begin{aligned} P_{rx} = {} & \mu\, (u_r + w_x) + (\lambda + 2\mu + m)\, u_r w_r + \frac{2\lambda + 2m - n}{2}\, u_r \frac{w}{r} + \\ & (\lambda + 2\mu + m)\, u_x u_r + \frac{2m - n}{2}\, w_x \frac{w}{r} + (\mu + m)\, w_x w_r + \\ & (\mu + m)\, u_x w_x\ . \end{aligned} \tag{3.11}$$

3.2.2 *Derivation of the governing equation*

Exception of torsions provides transformation of the initial 3D problem into a 2D one. Subsequent simplification is caused by the consideration of only long elastic waves with the ratio $R/L \ll 1$ between the rod radius R and typical wavelength L. The typical elastic strain magnitude B does not exceed the yield point of the material. Since Murnaghan's material have small yield points, one can assume $B \ll 1$. The Hamilton principle (3.5) yields a set of coupled equations for u and w together with the b.c. (3.8), (3.9). To obtain a solution in universal way one usually proceeds to the dimensionless form of the equations and looks for the unknown displacement vector components in the form of power series in the small parameters of the problem (for example R/L), hence, leading to an asymptotic solution of the problem. However, this procedure has some disadvantages. In particular, comparison of the predictions from the dimensionless solution to the experiments suffers from the fact that both B and L, are not well defined. In particular, solitary wave has an infinite wave length. Further, the coefficients of the nonlinear terms usually contain combinations of elastic moduli which may be also small in addition to the smallness of B something not predicted beforehand. Finally, this procedure gives equations of only first order in time, t, while general equations for displacements u and w are of the second order in time. Therefore the solution of the model equation will not satisfy two independent initial conditions on longitudinal strains or displacements Samsonov (2001).

An alternative is to simplify the problem making some assumptions about the behavior of longitudinal and/or shear displacements and/or strains in the elastic wave-guide. Referring to the elastic rod these relationships give explicit dependence of u and w upon the radius, while their variations along the rod axis are described by some unknown function and its derivatives along the axis of the rod. Then the application of Hamilton's principle (3.5) yields the governing equation in dimensional form for this function. This equation is of the second order of time, hence its solution can satisfy two independent initial conditions. Any combinations of elastic moduli appear in the coefficients of the equation, hence, subsequent scaling may take into account their orders when introducing small parameters.

For an elastic rod, the simplest assumption is the plane cross section hypothesis McNiven and McCoy (1974): the longitudinal deformation process is similar to the beards movement on the thread. Then every cross section of the rod remains flat, hence, $u = U(x,t)$ does not change along

the radius r. However, this assumption is not enough due to the Poisson effect, i.e., longitudinal and shear deformations are related. That is why Love (1927) proposed to use a relationship between w and u: $w = -r\,\nu\,U_x$, with ν the Poisson coefficient. Unfortunately, the plane cross-section hypothesis and Love's hypothesis do not satisfy the boundary conditions that demand vanishing of both the normal and tangential stresses, P_{rr} and P_{rx}, at the lateral surface of the rod with prescribed precision.

Another theory has been proposed in Porubov and Samsonov (1993) to find the relationships between displacement vector components satisfying b.c. on the lateral surface of the rod (3.8), (3.9) as well as the condition for w (3.7). Later it was developed in Porubov and Velarde (2000).

Since pure elastic wave are studied, $B \ll 1$, the "linear" and "nonlinear" parts of the relationships may be obtained separately. A power series approximations is used, as generally done for long wave processes. Accordingly, the longitudinal and shear displacement in *dimensional* form are:

$$u = u_L + u_{NL},\ u_L = u_0(x,t) + r\,u_1(x,t) + r^2 u_2(x,t) + ...,$$
$$u_{NL} = u_{NL0}(x,t) + r\,u_{NL1}(x,t) + ..., \tag{3.12}$$

$$w = w_L + w_{NL},\ w_L = w_0(x,t) + r\,w_1(x,t) + r^2 w_2(x,t) + ...,$$
$$w_{NL} = w_{NL0}(x,t) + r\,w_{NL1}(x,t) + ... \tag{3.13}$$

Substituting the linear parts u_L and w_L (3.12), (3.13) into the b.c. (3.7) and in the linear parts of b.c. (3.8), (3.9), and equating to zero terms at equal powers of r one obtains u_k and w_k. Using these results the nonlinear parts u_{NL}, w_{NL} are similarly obtained from the full b.c. We get $u_0(x,t) = U(x,t)$ while other u_k and w_k are expressed through U and its derivatives. Then (3.12), (3.13) are substituted into (3.1) and (3.6). Running the Hamilton principle (3.5) we obtain the single governing equation for the unknown function $U(x,t)$. In contrast to the theory based on the plane cross section hypothesis and the Love hypothesis, the present theory allows to account for nonzero b.c. for the stresses on the lateral surface of the rod.

3.3 Double-dispersive equation and its solitary wave solution

In order to derive the governing equation for longitudinal strain waves in a free lateral surface rod we assume that $B \sim R^2/L^2$. This assumption

provides a balance between nonlinearity and dispersion required for existence of the bell-shaped solitary waves of permanent shape. Substituting power series (3.12), (3.13) into the boundary conditions and equating to zero combinations at each power of the radius, we get

$$u = U + a_2\, r^2\, U_{xx}, \tag{3.14}$$

$$w = b_1\, r\, U_x + b_3 r^3\, U_{xxx} + B_1\, r\, U_x^2\ . \tag{3.15}$$

where

$$a_2 = \frac{\nu}{2},\ b_1 = -\nu,\ b_3 = \frac{\nu^2}{2(3-2\nu)},$$

$$B_1 = \frac{\nu(1+\nu)}{2} + \frac{(1-2\nu)(1+\nu)}{E}[l(1-2\nu)^2 + 2m(1+\nu) - n\nu].$$

Then kinetic and potential energy truncated approximations are

$$K = \frac{\rho_0}{2}(U_t^2 + \nu r^2[U_t U_{xxt} + \nu U_{xt}^2]), \tag{3.16}$$

$$\Pi = \frac{1}{2}\left(EU_x^2 + \frac{\beta}{3}U_x^3 + \nu E r^2 U_x U_{xxx}\right) \tag{3.17}$$

Here ν and E are the Poisson ratio and the Young modulus correspondingly,

$$\nu = \frac{\lambda}{2(\lambda+\mu)}, E = \frac{\mu(3\lambda+2\mu)}{\lambda+\mu},$$

while β is a nonlinear coefficient, $\beta = 3E + l(1-2\nu)^3 + 4m(1-2\nu)(1+\nu) + 6n\nu^2$. We have to truncate the approximations (3.14), (3.15), (3.16), (3.17) in order to be in an agreement with the five-constant Murnaghan approximation (3.1), where cubic nonlinear terms are neglected.

Comparing these relations with those obtained using cross-section and Love's hypothesis, $a_2 = 0$, $b_3 = 0$, $B_1 = 0$, one can see that only the term $a_2\, r^2\, U_{xx}$ makes its contribution into Eqs.(3.16), (3.17), while terms $b_3 r^3\, U_{xxx}$ and $B_1\, r\, U_x^2$ are needed to satisfy the boundary conditions on the lateral surface with prescribed accuracy.

Substituting (3.16), (3.17) into (3.5) one can obtain the so-called double-dispersive equation, DDE, for a strain function $v = U_x$,

$$v_{tt} - \alpha_1\, v_{xx} - \alpha_2\, (\, v^2)_{xx} - \alpha_3\, v_{xxtt} + \alpha_4\, v_{xxxx} = 0. \tag{3.18}$$

where

$$\alpha_1 = \frac{E}{\rho_0},\ \alpha_2 = \frac{\beta}{2\rho_0},\ \alpha_3 = \frac{\nu(\nu-1)R^2}{2},\ \alpha_4 = -\frac{\nu E R^2}{2\rho_0}.$$

For the first time DDE was derived independently by some authors, in framework of the plane cross section and Love's hypothesis, see about it Erofeev and Klyueva (2002); Samsonov (2001). The important difference is only in the values of the dispersive terms coefficients α_3 and α_4, in Samsonov (1988) it was $\alpha_3 = -\nu^2 R^2/2$, $\alpha_4 = \mu\nu^2 R^2/(2\rho_0)$.

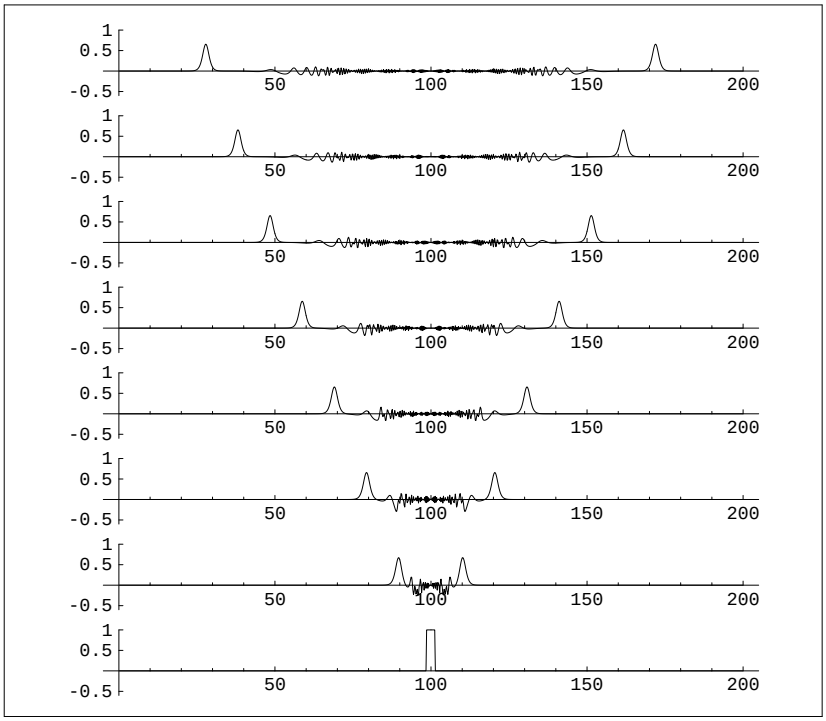

Fig. 3.2 Formation of solitary waves from an initial rectangular tensile pulse.

Eq.(3.18) possesses exact travelling solitary wave solution that may be obtained by direct integration,

$$v = A\cosh^{-2}(k\,(x - Vt)), \tag{3.19}$$

with

$$A = \frac{3(\rho_0 V^2 - E)}{\beta},\ k^2 = \frac{E - \rho_0 V^2}{2\nu R^2 (E + \rho_0(\nu - 1)V^2)}. \tag{3.20}$$

Accordingly, V^2 lies either inside the interval

$$\frac{E}{\rho_0(1-\nu)} < V^2 < c_*^2 = \frac{E}{\rho_0},\ \text{if}\ -1 < \nu < 0. \tag{3.21}$$

or in

$$c_*^2 < V^2 < \frac{E}{\rho_0(1-\nu)},\ \text{if}\ \nu > 0, \tag{3.22}$$

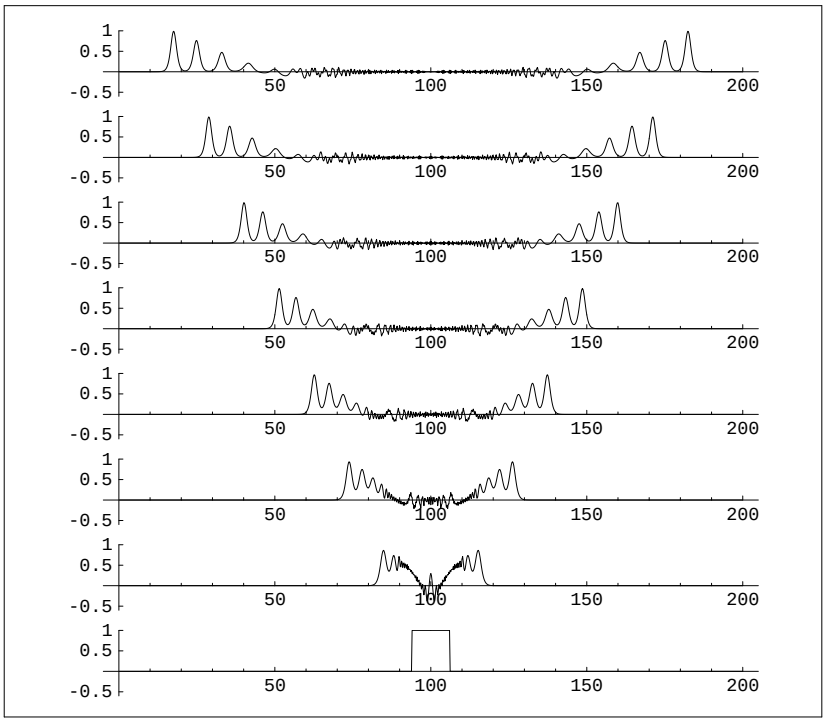

Fig. 3.3 Formation of a train of solitary waves from an initial rectangular tensile pulse.

When positive Poisson ratio is positive, more precisely, $1/2 \geq \nu > 0$, the sign of the amplitude is defined by the sign of β. The nonlinearity coefficient is the only coefficient carrying an information about the Murnaghan moduli. Hence, they define whether tensile or compression solitary wave

may propagate for a given elastic material of the rod. We see that it is the mixed dispersive term $\alpha_3\, v_{xxtt}$, who establishes the permitted *finite interval* for the wave velocity.

Exact solution requires specific initial conditions. It is of interest to know how rather arbitrary localized initial pulse evolves. To this purpose numerical simulation of the equation has been performed using numerical method explained in Sec. 2.3.2.

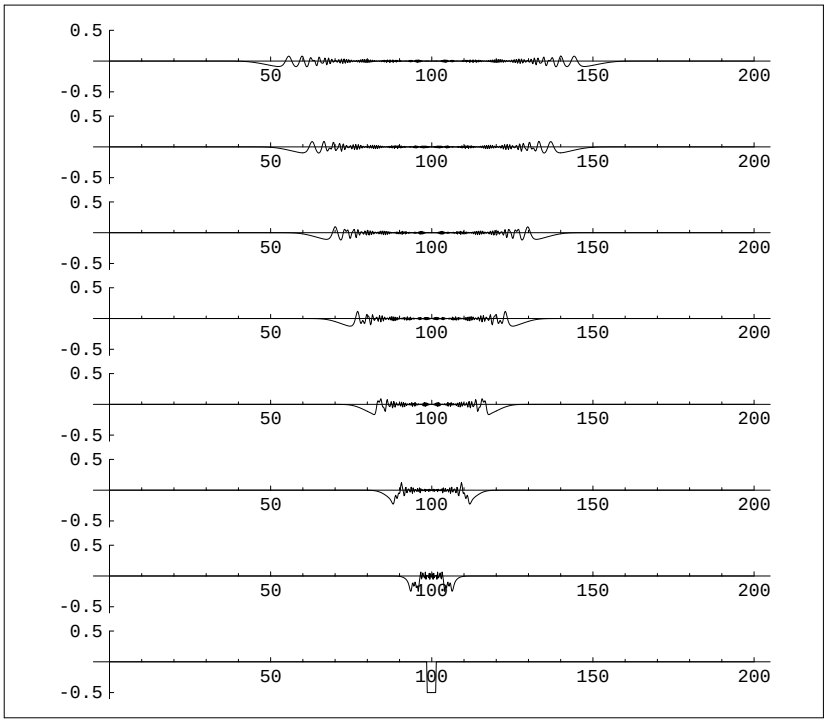

Fig. 3.4 Delocalization of an initial compression pulse.

It was found that rather arbitrary initial pulse splits into the train of solitary waves or evolves into small amplitude oscillating wave-packet according to the predictions about wave parameters done on the basis of exact single travelling solitary wave solution. Indeed, assume the material elastic features of the rod yield $\beta > 0$. Shown in Fig. 3.2 is the evolution of an initial tensile rectangular pulse into single solitary wave, while massive initial pulse splits into the sequence of solitary waves, see Fig. 3.3. However,

each solitary wave is accounted for the exact single travelling wave solution (3.19). Figure 3.4 demonstrates no solitary wave generation from the initial compression pulse. However, when the material of the rod possesses $\beta < 0$, only compressive solitary wave arises from an initial compression localized input. To sum up, single travelling wave exact solution provides correct predictions about solitary waves formation in an unsteady process of an arbitrary localized input evolution.

Finally, let us estimate the deviation from the plane cross section caused by the second terms in the expression (3.14). Indeed, the curvature h of the profile of longitudinal strain u along the radius of the rod is $h = |u_{rr}| / (1 + u_r^2)^{3/2} = |\nu U_{xx}| / (1 + \nu^2 r^2 U_{xx}^2)^{3/2}$. It was found in Porubov and Samsonov (1993)that the variation of longitudinal strain u along the radius is negligibly small when U_x is the solitary wave (3.19) that is important for the experimental observation of the waves.

3.4 Observation of longitudinal strain solitary waves

We briefly consider the recent successful experiments on solitary wave observation in a transparent rod, details may be found in Dreiden *et. al* (1995); Samsonov (2001). The optical methods were used because they are preferable to study transparent optical phase inhomogeneities. They allow not only to visualize inhomogeneity but also to determine its parameters, and on the other side, being contactless, they do not introduce any disturbances in an object under study. All optical methods record the alterations of refractive index in an object, when studying optically transparent phase inhomogeneities. Shadowgraphy is more convenient to record a considerable refractive index gradient, for example, caused by a strong shock wave propagation. It was shown theoretically in our case that a strain solitary wave is a propagating long density wave of small amplitude. Interferometry is the most appropriate for such waves study because it allows to observe and measure with sufficient accuracy even small refractive indices alterations.

Holographic interferometry method, used in the experiments Dreiden *et. al* (1995), has several advantages in comparison with the conventional optical interferometry. In particular, limitations to the optics quality are considerably lower because wave fronts to be compared pass through the same optical path. For this reason both waves are distorted *to the same extent* and possible defects in optical elements and experimental cell do not affect the resulting interference pattern. However, the choice of an optical

recording method allows to study, in general, only elastic materials, that are transparent for the given light wave length.

To check that the excited strain wave possesses indeed the solitary wave feature to conserve its shape, it is necessary to follow in observations a propagation along an extended elastic wave guide. However, in a wave guide made of material highly absorbing linear elastic waves, it will be sufficient to detect the constant shape wave propagation at much shorter distance.

Based on the results of the analysis presented above the transparent polystyrene SD-3 has been chosen as an appropriate material for a wave guide manufacturing. The elastic properties of it are given by a set of parameters $\nu = 0.35$; $\beta = \ -6 \cdot 10^{10}\ N/m^2$; $c_* = 1.8 \cdot 10^3\ m/sec$, see Frantsevich *et. al* (1982).

The experimental set-up used to generate and observe the strain solitons, consists of a basin where the rod is submerged into the water, a device to produce the initial shock wave, a holographic interferometer for the recording of a wave pattern, a synchronizer and a laser radiation energy meter. The waves inside the rod are generated from a primary shock wave produced in the water near the edge of the rod by laser vaporization of a metal target. The first exposure of the hologram is carried out to obtain the hologram of undisturbed wave guide. The second exposure is produced by a laser pulse synchronized with the prescribed stage of the wave propagation. Observations are carried out in the transversal direction, and two cut-off were made parallel to the rod axis in order to make transparent the central part of the rod. The carrier fringes on interferograms, obtained due to the reconstruction of doubly exposed holograms, occur due to the wedge turn between the exposures. The longitudinal strain wave patterns are recorded at various distances from the input edge of the rod, that are attained by the cell displacement along the axis of wave propagation.

The solitary wave parameters are calculated based on the data of the holography interferograms obtained. Typical interferogram is shown in Fig .3.5. Only central part of the PS rod is transparent thanks to the vertical cuts. Curved interference fringe is extracted from the area inside the rod and placed below the interferogram. Note that the interferometric pattern does not exhibit a standard bell-shaped image of a shallow water solitary wave since the strain solitary wave is, in fact, a *longitudinal* density wave in solids.

The solitary wave amplitude can be calculated using the interferometry fringe shift ΔK measured in the interference pattern, see Fig. 3.5. Let $2h$

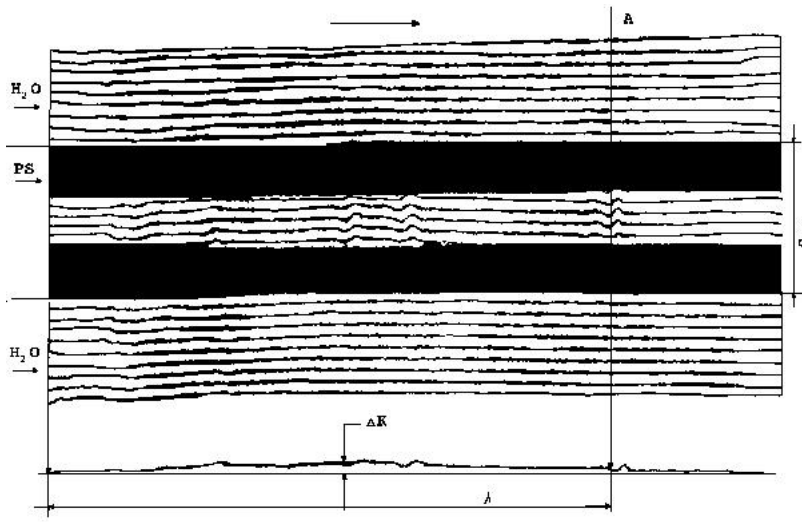

Fig. 3.5 Experimental observation of longitudinal strain solitary wave in an elastic rod(after Dreiden *et. al* (1995)).

be a distance passed by the recording light across the rod, i.e., precisely, the distance between two longitudinal cut-off. Before the deformation the phase variation $\Delta\phi_1$ of the light wave having the length λ, is caused by the laser light propagation along the distance $q - 2h$ through the water and the distance $2h$ through the rod (where q is the distance between the cell walls) Samsonov *et. al* (1998):

$$n_0(q - 2h) + 2hn_1 \;=\; \frac{\lambda}{2\pi}\Delta\phi_1. \tag{3.23}$$

Here n_0, n_1 are the refraction indices of water and the elastic material before deformation. After the deformation the refraction index value of the rod changes to n_2. Moreover, the distance, which light passes through the rod and water, varies due to the deformation of the rod. As a result we obtain the formula for the magnitude of the light wave phase variation $\Delta\phi_2$:

$$n_0(q - 2h - 2\Delta h) + n_2(2h + 2\Delta h) \;=\; \frac{\lambda}{2\pi}\Delta\phi_2. \tag{3.24}$$

Evidently, the interferometry fringe shift ΔK is defined as

$$\Delta K = \frac{\Delta\phi_2 - \Delta\phi_1}{2\pi}. \tag{3.25}$$

The new value of the refraction index of the deformed rod n_2 is caused by the local density variation:

$$\frac{\Delta\rho}{\rho} = \frac{n_2 - n_1}{n_1 - 1}. \tag{3.26}$$

On the other side, one can obtain the density variation from the solution of a static linear problem on uniaxial compression (or tension), see Lurie (1990), and as a result the following relationship is valid:

$$\frac{\Delta\rho}{\rho} = U_x(2\nu - 1). \tag{3.27}$$

Then we get finally from (3.25):

$$U_x = -\frac{\lambda\Delta K}{2h[(n_1 - 1)(1 - 2\nu) + \nu(n_1 - n_0)]}. \tag{3.28}$$

The amplitude is determined by the maximal fringe shift value. Derivation of the relationship (3.28) shows that the length L of the solitary pulse may be directly determined from the interferogram as the length of the fringe shift perturbation between two undisturbed areas.

In our experiments Dreiden *et. al* (1995) we used a long polystyrene rod, 149 mm long. The nonlinearity parameter $\beta < 0$ for polystyrene, and we can anticipate the appearance of only compression solitary wave. It is fairly long and keeps its shape on propagation. As follows from (3.28) the wave shown under interferogram in Fig. 3.5 is indeed a longitudinal compression wave. There is no any tensile wave around the observed wave, moreover, in the water surrounding the rod the interference patterns remains horizontal, i.e., undisturbed, that proves the wave that is measured propagates inside the rod. Therefore, the theory developed for an infinite cylindrical rod allows to predict an existence of solitary waves in a finite-length rod with vertical cuts.

Unfortunately only the wave amplitude may be measured more or less precisely, hence full quantitative comparison with the theory is impossible. The unsteady process of the solitary wave generation cannot be accounted for the theory. The propagation of a shock wave before the solitary wave

contradicts numerical results shown in Fig. 3.2. For a long time solitary waves were observed only in a wave guide made of polystyrene. Very recently they were generated also in a plexiglas rod Samsonov *et. al* (2003).

3.5 Reflection of solitary wave from the edge of the rod

Following Dreiden *et. al* (2001) let us consider a semi-infinite homogeneous rod, $-\infty < x < X$. The procedure developed in section 3.2 may be applied but now the elementary work done by the external forces should be included into the Hamilton principle, and the integration with respect to x is carried out over $-\infty < x < X$,

$$\delta \int_{t_0}^{t_1} dt \left[2\pi \int_{-\infty}^{X} dx \int_0^R r \; \mathcal{L} dr \right] + \int_{t_0}^{t_1} \delta A \, dt = 0. \tag{3.29}$$

The Lagrangian density per unit volume, $\mathcal{L}$=$K - \Pi$, is defined as before. According to Lurie (1990) we cannot call Eq.(3.29) *variation* principle since external forces are not necessary potential ones. Use of the Hamilton principle yields the DDE (3.18) as a governing equation for longitudinal waves together with the boundary conditions requiring zero values for v and its derivatives as $x \to -\infty$, while on the rod end, $x = X$, they depend upon the type of clamping. If the rod end is assumed free, the elementary work of external forces at the end of the rod, $x = X$, is zero, $\delta A = 0$, and Eq. (3.29) yields

$$v = 0, \; v_{xx} = 0. \tag{3.30}$$

When the end is clamped, the elementary work is not determined, but obvious kinematic reasons require zero displacement and its velocity,

$$U = 0, \; U_t = 0, \tag{3.31}$$

that may be rewritten in terms of strains,

$$v_x = 0, \; v_{xt} = 0. \tag{3.32}$$

Since DDE does not possess an exact solution describing interacting waves moving in opposite directions, it is necessary to apply an asymptotic technique, reducing DDE to a nondimensional form. Introducing the scales, L for x, L/c_0 for t, and B/L for v, where $c_0 = \sqrt{E/\rho_0}$ is the so-called rod velocity. A small parameter ε is chosen as $\varepsilon = B = R^2/L^2 << 1$, to balance nonlinearity and dispersion.

Assume the asymptotic solution v depends, in addition to x, t, on a slow time $\tau = \varepsilon t$. The solution is sought in power series in ε:

$$v = v_0 + \varepsilon v_1 + \dots . \tag{3.33}$$

Substituting (3.33) into dimensionless DDE, and equating the terms with the same power of ε we obtain the D'Alembert solution for v_0:

$$v_0 = v_{01}(\theta, \tau) + v_{02}(\psi, \tau), \tag{3.34}$$

where $\theta = x + t$, $\psi = x - t$. At order ε there is a linear equation for v_1,

$$2v_{1,\theta\psi} = 2v_{01,\theta\tau} - 2v_{02,\psi\tau} + \frac{\beta}{2E}\left((v_{01}^2)_{\theta\theta} + 2v_{01,\theta}v_{02,\psi} + (v_{02}^2)_{\psi\psi}\right) + \frac{\nu^2}{2}(v_{01,\theta\theta\theta\theta} + v_{02,\psi\psi\psi\psi}) \tag{3.35}$$

The absence of secular terms leads to two uncoupled KdV equations for the functions v_{01} and v_{02},

$$2v_{01,\tau} - \frac{\beta}{2E}(v_{01}^2)_\theta - \frac{\nu^2}{2}v_{01,\theta\theta\theta} = 0, \tag{3.36}$$

$$2v_{02,\tau} + \frac{\beta}{2E}(v_{02}^2)_\psi + \frac{\nu^2}{2}v_{02,\psi\psi\psi} = 0, \tag{3.37}$$

and the bounded solution of Eq. (3.35) is

$$v_1 = \frac{\beta}{E}v_{01}v_{02} + v_{11}(\theta, \tau) + v_{12}(\psi, \tau). \tag{3.38}$$

Substituting the soliton solutions of the KdV equations (see Chapter 1) into the leading order solution (3.34), we obtain

$$v_0 = \frac{6E\nu^2}{\beta}\ k^2\ [\cosh^{-2}\left(k[x + (1 + \varepsilon\nu^2k^2)t - x_{01}\right) + \cosh^{-2}\left(k[x - (1 + \varepsilon\nu^2k^2)t - x_{02}]\right)]. \tag{3.39}$$

where x_{01} are the constant phase shifts. It follows from (3.39) that the type of the strain wave depends upon the sign of β like in previous section. Both conditions (3.32) on the clamped end are satisfied if $x_{02} = 2X - x_{01}$. In this case reflection of the solitary wave occurs with no change of its shape. On the contrary, one cannot satisfy boundary conditions (3.30) at a free end of

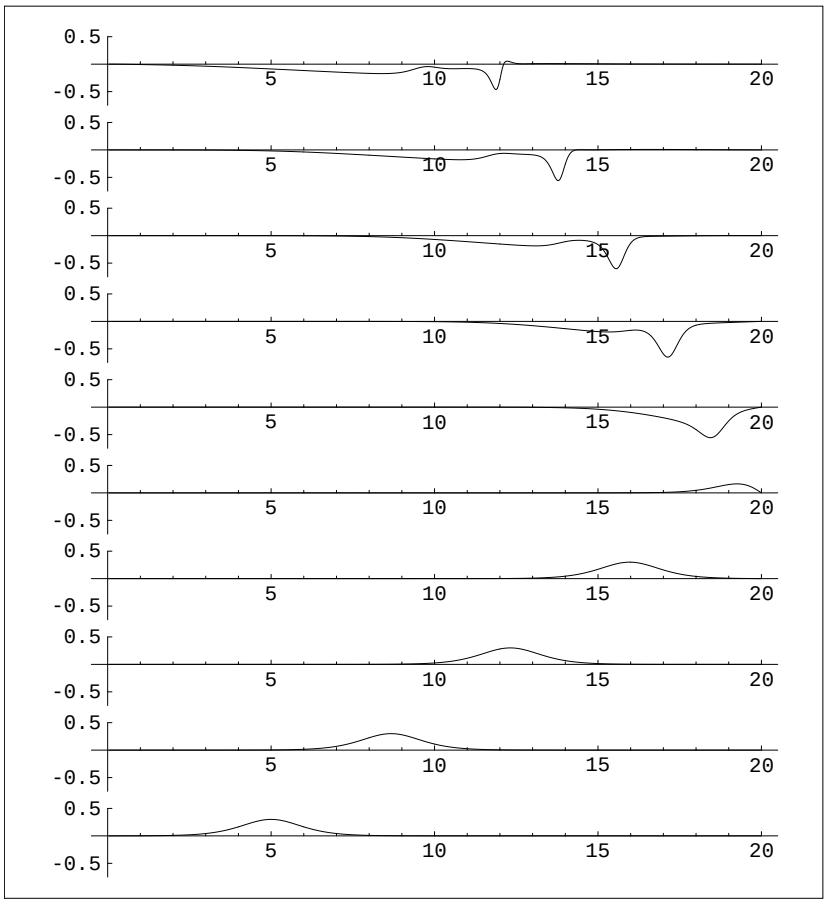

Fig. 3.6 Reflection of the solitary wave from a free end of the rod.

the rod. It means that the reflected solitary wave does not propagate but disappears due to dispersion.

It may be clearly seen from numerical simulation of the reflection Dreiden *et. al* (2001). Again the implicit finite-difference scheme explained in Sec. 2.3.2, is used. Implementation of the boundary conditions at the end of the rod is effected by means of symmetric continuation of the calculation area beyond the real rod end, so that the area of calculation would occupy the interval $0 < x < 2X$. In case of free end of the rod the sign of β in the interval $X < x < 2X$ is chosen opposite to that used in the interval $0 < x < X$. Initial pulses are assumed to be the equal magnitude KdV

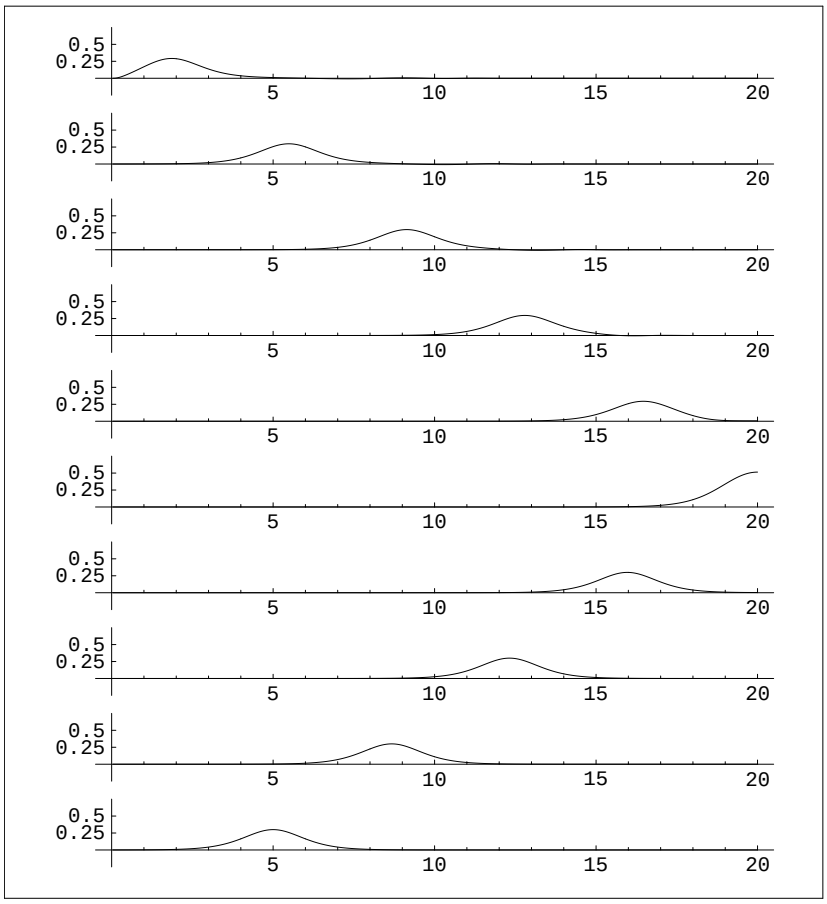

Fig. 3.7 Reflection of the solitary wave from a fixed end of the rod.

solitons located centrally symmetric relative to the genuine end $x = X$. The type of an initial solitary wave depends upon the sign of β. In particular, if $\beta > 0$ the initial solitary wave in the interval $0 < x < X$ is a tensile wave, while in the interval $0 < x < 2X$ we impose the same tensile solitary wave for the clamped end or the compression solitary wave for the free end. Initial velocities of the solitary waves are chosen equal and taken to be directed towards each other.

The reflection from the free end is shown in Fig. 3.6. The right-hand side of the figure corresponds to the free end. It is seen that the amplitude of the solitary wave propagating from left to right decreases as it reaches

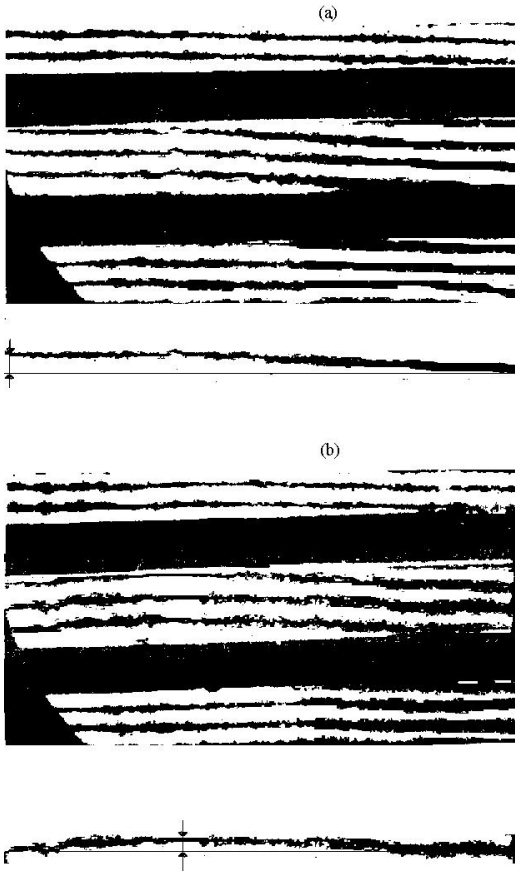

Fig. 3.8 Observation of a reflection of the solitary wave from a free end of the rod.

the end of the rod. The reflected wave is of opposite, first, its amplitude grows, then the wave is dispersed, and no localized strain wave is observed near the input end of the rod.

In case of the clamped end numerical results are shown in Fig. 3.7. In agreement with the theory the amplitude of the solitary wave is seen to be nearly twice as large when it reaches the end of the rod. The reflected wave has the same amplitude and velocity as the incident one. Keeping its

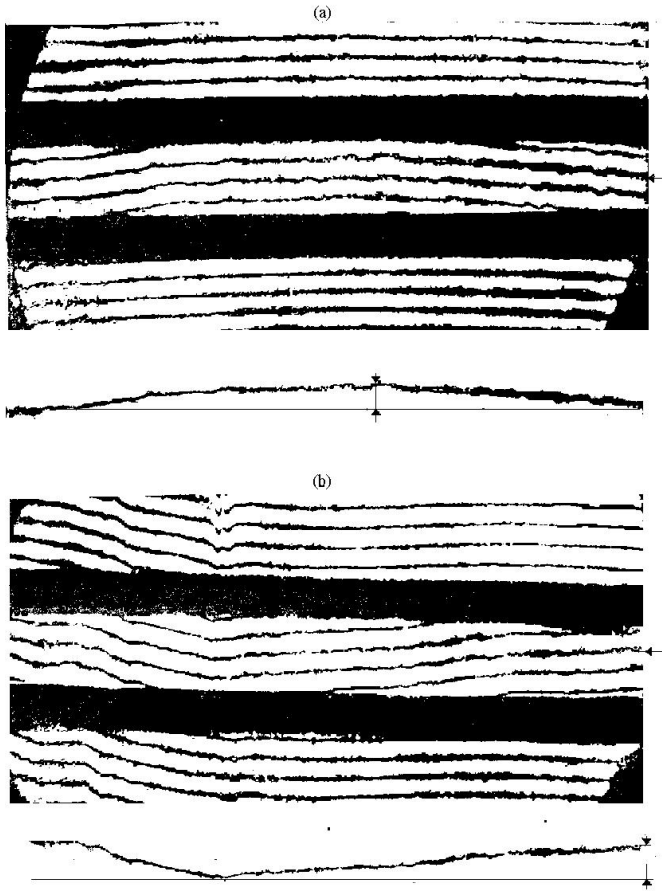

Fig. 3.9 Reflection of the solitary wave from a clamped end of the rod.

shape, the reflected wave propagates towards the input end of the rod.

Experimental observation of the solitary strain wave reflection were carried out in Dreiden *et. al* (2001) using the same technique as for the study of the solitary wave propagation. Shown in Fig. 3.8 is the reflection from the free end. Footnotes in Fig. 3.8(a) and Fig. 3.8(b) demonstrate the decrease of the amplitude of the initially generated compression localized wave shown in Fig. 3.8(a), cf. with the first and the fifth stages in Fig. 3.7. It was found in experiments the absence of any reflected localized waves

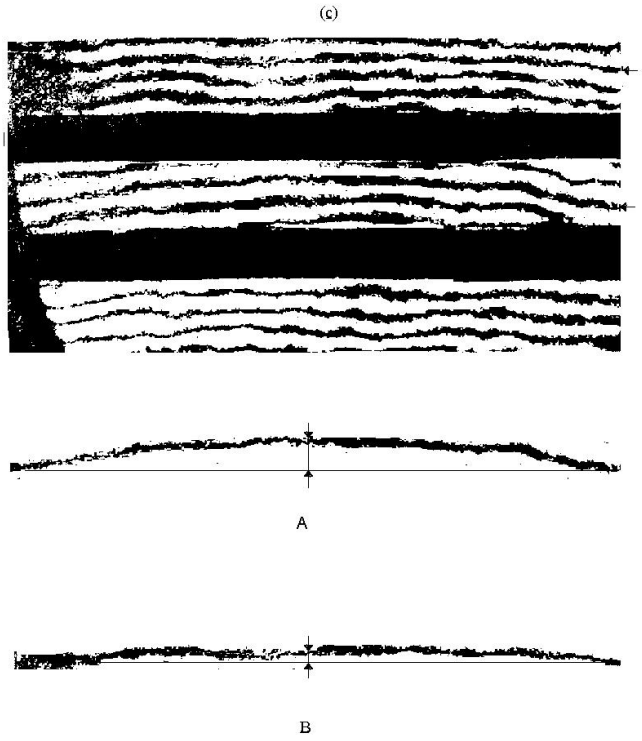

Fig. 3.10 Reflected wave comes back to the input end of the rod.

moving towards the input end of the rod, cf. with the last stage of Fig. 3.6. Hence all observations verify theoretical predictions.

Figures 3.9, 3.10 demonstrate the reflection of the strain solitary wave from the rod end attached to the right to a massive brass plate. The material of the plate is chosen so as to avoid penetration of the wave energy outside the rod. It was found experimentally in Dreiden *et. al* (2001) that the acoustic resistance of the plate should be much greater than that of the material of the rod (polystyrene). It is seen that the amplitude of the

incident solitary wave, Fig. 3.9(a), is almost doubled by the fixed end of the rod, Fig. 3.9(b)in an agreement with the first and the fifth stages in Fig. 3.7. Figure 3.10 shows the reflected solitary wave moving to the left at a distance of 140 mm from the fixed end. It has the same amplitude and velocity as the incident one, cf. the last stages in Fig. 3.7. In order to see it is necessary to subtract the fringe shift outside the rod (marked by B in Fig. 3.10) from the fringe shift measured inside the rod (marked by A in Fig. 3.10). The wave observed in experiments demonstrates the main feature of the solitary waves to keep their shapes after collisions, hence it confirms also the fact that the observed localized wave is indeed the strain solitary wave predicted by the theory.

Chapter 4

Amplification of strain waves in absence of external energy influx

As we seen in the previous chapter, strain solitary wave propagates without change of the shape in an uniform rod with a free lateral surface. However, the wave may still exist even in presence of an external medium or when a material of the rod is microstructured. At the same time, the shape of the wave varies when the balance between nonlinearity and dispersion is destroyed. The simplest reason is the varying cross section of the rod.

4.1 Longitudinal strain solitary wave amplification in a narrowing elastic rod

The section is devoted to the theoretical and experimental description of the propagation and amplification of the strain solitary wave (soliton) in a cylindrical nonlinearly elastic rod with varying cross section. We call it an inhomogeneous rod in the following for convenience, while the rod with permanent cross section will be called the homogeneous one. We follow Samsonov *et. al* (1998) where the results presented below were published for the first time.

4.1.1 *Governing equation for longitudinal strain waves propagation*

Let us consider the wave propagation problem for an isotropic infinite nonlinearly elastic compressible rod with varying cross section, see Fig. 4.1. Introducing the cylindrical Lagrangian coordinate system (x, r, φ), where x is the axis along the rod, $\varphi \in [0, 2\pi]$, $0 \leq r \leq R(x) \leq R_0$, R_0- const, one can write the displacement vector $\vec{V} = (u, w, 0)$, if torsions are neglected. Basic equations, describing the nonlinear wave propagation in the initial

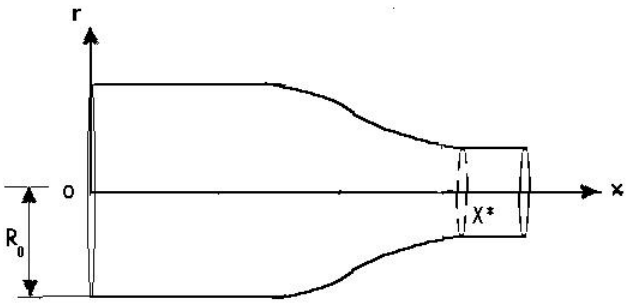

Fig. 4.1 Free lateral surface cylindrical rod with varying cross section.

configuration, are obtained from the Hamilton variation principle (3.5).

We are studying long nonlinear longitudinal strain waves (density waves), that allows to do some simplifications, namely, the relationships between longitudinal and transversal displacements u and w. To find them one needs to satisfy the boundary conditions on the free lateral rod surface $r = R(x)$, namely, the absence of both the normal and tangential stresses at every moment. We introduce the small parameter ε, taking into account that the waves under study should be *elastic* waves with sufficiently small magnitude B, $B << 1$, as well as sufficiently long waves with the length L, so as the ratio $R_0/L << 1$, where R_0 is the maximal value of $r(x)$ along the rod . The most important case occurs when both nonlinear and dispersive features are *in balance* and *small enough:*

$$\varepsilon = B = \left(\frac{R_0}{L} \right)^2 << 1. \tag{4.1}$$

The boundary conditions have the form (3.7)-(3.9). The unknown func-

tions u, w are expanded in a power series (3.12), (3.13). Substituting them into the boundary conditions and following the procedure explained in Sec. 3.2, one can obtain

$$u_L \;=\; U(x,t) + r^2\frac{\nu}{2}U_{xx}, \quad w_L = -r\;\nu U_x \;- r^3\frac{\nu^2}{2(3-2\nu)}U_{xxx}. \tag{4.2}$$

$$w_{NL} = r\left[\frac{\nu(1+\nu)}{2} + \frac{(1-2\nu)(1+\nu)}{E}\left(l(1-2\nu)^2 + 2m(1+\nu) - n\nu\right)\right]U_x^2, \tag{4.3}$$

Higher order terms may be obtained by the same way, however, they will be omitted here because of no influence on the final model equation for the longitudinal strain waves equation to be derived using the Hamilton principle (3.5). Substituting expansions (3.12), (3.13) with (4.2), (4.3) into the formulas for K and Π, one can find respectively:

$$K \;=\; \frac{\rho_0}{2}\left(U_t^2 + \nu r^2\left[U_t U_{xxt} + \nu U_{xt}^2\right]\right), \tag{4.4}$$

$$\Pi \;=\; \frac{1}{2}\left(EU_x^2 + \frac{\beta}{3}U_x^3 + \nu E r^2 U_x U_{xxx}\right). \tag{4.5}$$

where $\beta \;=\; 3E + 2l(1-2\nu)^3 + 4m(1+\nu)^2(1-2\nu) + 6n\nu^2$ becomes the only coefficient depending on the nonlinear elasticity of the rod, it coincides with that obtained in Sec. 3.2.3. Substituting (4.4), (4.5) into (3.5) and calculating $\delta S = 0$, one can obtain the following nonlinear equation:

$$\begin{aligned} U_{tt} - \frac{c_*^2}{R^2}\frac{\partial}{\partial x}\left[R^2 U_x\right] &= \frac{1}{R^2}\frac{\partial}{\partial x}\left[\frac{\beta}{2\rho_0}R^2U_x^2 - \frac{\nu}{4}\frac{\partial}{\partial x}(R^4U_{tt}) + \frac{\nu^2}{2}R^4U_{xtt}\right] \\ &+ \frac{1}{R^2}\frac{\partial}{\partial x}\left[\frac{\nu c_*^2}{4}\left(R^4U_{xxx} + \frac{\partial^2}{\partial x^2}\left(R^4U_x\right)\right)\right] - \frac{\nu R^2}{4}U_{xxtt}, \end{aligned} \tag{4.6}$$

where c_* is the so-called "rod" wave velocity, $c_*^2 \;=\; E/\rho_0$.

Let us consider now the rod which cross section varies slowly along the $x-$ axis, which is described by a function $R = R(\gamma x)$, $\gamma \;<<\; 1$. Introducing the notation: $v \;=\; U_x$, $\tau \;=\; tc_*$ and differentiating the equation (4.6) on x, we obtain an equation

$$v_{\tau\tau} - \frac{\partial}{\partial x}\frac{1}{R^2}\frac{\partial}{\partial x}\left(R^2 v + \frac{\beta R^2}{2E}(v^2) + aR^4 v_{\tau\tau} - bR^4 v_{xx} - 4bR^3R_x v_x\right) \;=\; 0, \tag{4.7}$$

with the dispersion terms coefficients a and b, $a = -[\nu(1-\nu)]/2$, $b = -\nu/2$. Two first terms here describe a common linear wave, the third governs the nonlinearity, and the two following terms are responsible for dispersive features of the rod, while the last term, being of the same order, looks like a dissipative one, it occurs due to the cross section variation.

4.1.2 *Evolution of asymmetric strain solitary wave*

To describe the evolution of a travelling strain wave v we introduce the phase variable θ and the slow variable $X \equiv \gamma x$, as follows:

$$\theta_\tau \;=\; -1, \quad \theta_x \;=\; A(X). \tag{4.8}$$

Using the asymptotic method explained in Sec. 2.2, the solution of Eq. (4.7) is obtained in new variables in the power series in γ:

$$v = v_0 + \gamma v_1 + \dots. \tag{4.9}$$

Substitution (4.9) into the equation (4.7) gives in leading order of γ the ODE reduction of the nonlinear double dispersive equation (3.18) for v_0:

$$(1-A^2)v_{0,\theta\theta} - A^2\frac{\beta}{2E}(v_0^2)_{\theta\theta} - R^2A^4(a-b)v_{0,\theta\theta\theta\theta} = 0,$$

whose solitary wave solution is Samsonov (2001):

$$v_0 \;=\; \frac{3E}{\beta}\;\alpha\;\cosh^{-2}\left(k(X)[\theta-\theta_0(X)]\right), \tag{4.10}$$

depending upon the varying parameter $\alpha = \alpha(X)$, $\alpha > 0$, while A, k are expressed through it:

$$A^2 \;=\; \frac{1}{1+\alpha},\; k^2 \;= \frac{\alpha(1+\alpha)}{4R^2[a(1+\alpha)-b]}. \tag{4.11}$$

Since the parameters of the solitary wave depends upon the slow coordinate, the wave is asymmetric like shown in Fig. 1.18.

Both A and k will be real in Eq.(4.11) for most standard elastic materials (having the Poisson coefficient $\nu > 0$) if the value of the function α is inside an interval :

$$0 \;<\; \alpha \;<\; \frac{\nu}{1-\nu}, \tag{4.12}$$

Then the type of the strain wave (4.10) (compression or tensile one) is defined only by the sign of the nonlinear coefficient β, which depends on the elasticity of the rod material, respectively.

Let us study a distortion of the solitary strain wave due to the "geometrical" inhomogeneity considered. Indeed an inmogeneous linear equation holds for v_1 at order $O(\gamma)$

$$(1-A^2)v_{1,\theta\theta} - A^2\frac{\beta}{E}(v_1 v_0)_{\theta\theta} - R^2A^4(a-b)v_{1,\theta\theta\theta\theta} = F, \tag{4.13}$$

where

$$\begin{aligned} F = \frac{R_X}{R}A(2v_{0,\theta} + \frac{\beta}{E}(v_0^2)_\theta + \nu R^2[3(\nu-1)+5A^2]v_{0,\theta\theta\theta}) + \\ A_X(v_{0,\theta} + \frac{\beta}{2E}(v_0^2)_\theta + \nu R^2[\frac{\nu-1}{2} + 3A^2]v_{0,\theta\theta\theta}) + \\ A(2v_{0,\theta X} + \frac{\beta}{E}(v_0^2)_{\theta X} + \nu R^2[\frac{\nu-1}{2} + 2A^2]v_{0,\theta\theta\theta X}). \end{aligned}$$

Then the equation for the amplitude α arises from the secular term absence condition (2.43):

$$\left(\ln\frac{R^2\alpha^2}{2kA^3}\right)_X + \frac{4bk^2R^2A^4}{5}\left(\ln 2R^4\alpha^2Ak\right)_X = 0, \tag{4.14}$$

that after use of Eq.(4.11) is reduced to a nonlinear first order ODE for an amplitude variation

$$\frac{R_X}{R} = \alpha_X\left(\frac{1}{6(1-D+\alpha)} - \frac{1}{2\alpha} - \frac{1}{3(1-D_1+\alpha)} - \frac{1}{3(1-D_2+\alpha)}\right), \tag{4.15}$$

where:

$$D = \frac{b}{a} = \frac{1}{(1-\nu)},\ D_{1,2} = \frac{2\pm\sqrt{9-5\nu}}{5(1-\nu)}.$$

Taking the restrictions for α, Eq.(4.12), into account, we conclude that the expansion in the brackets on the right- hand side of Eq.(4.15) is always positive. Therefore the unbounded growth of the amplitude of the solitary wave occurs with the radius decrease, while the increase of the radius is accompanied by the decay of the amplitude. When the radius no longer alters at $X > X^*$, see Fig. 4.1, the amplitude and the velocity of the solitary wave remain constant. The solitary wave evolution in this case is similar to that shown in Fig. 1.19. However, there is no tendency to a finite value

α^* in the solutions of Eq.(4.15), and the values of the wave parameters at $X > X^*$ are not fixed by the equation coefficients, they are defined by the initial condition. Hence this is not a *selection* of the solitary wave when *any* initial conditions provide one and the same solitary waves, see Sec. 1.3.

Direct integration of Eq.(4.15) yields

$$\frac{R^6\alpha^3\left[\nu+\alpha(2\nu-6/5)-\alpha^2(1-\nu)\right]^2}{(1-\nu)[\nu-\alpha(1-\nu)]} = \text{const.} \tag{4.16}$$

Routine analysis of the functions v_0, Eq.(4.10), and $v_{0,x}$ shows that the distortion of the wave shape takes place apart from the amplitude variation. When the bell-shaped solitary wave propagates along the narrowing rod, its front side becomes steeper while the back one becomes smoother. Vice versa, the front side of the solitary wave, moving along the expanding rod, becomes smoother, while the back one - steeper. The equation for the determination of an extremum of a derivative $v_{0,x}$

$$\gamma\frac{R_X}{R}+[k(1-\gamma\theta_{0,X})+\gamma k_X[\theta-\theta_0(X)]]\tanh\left(k[\theta-\theta_0(X)]\right) \;=\; 0. \tag{4.17}$$

shows that for the wave propagation along the narrowing rod ($R_X < 0$) the extremum is achieved for $\theta-\theta_0(X) > 0$, while in an expanding rod ($R_X > 0$) - for an inverse sign. Then the asymmetric solitary wave accelerates in the narrowing rod and decelerates in the expanding one in comparison with the same solitary wave moving along a uniform (homogeneous) rod.

The exact formulas (4.11), (4.16) may be easily simplified to describe the wave parameters variations. The range of the strain wave amplitude is restricted by a physical condition of the strain elasticity:

$$\mid\sqrt{1+2C_{xx}}-1\mid \;<\; e_0, \tag{4.18}$$

where e_0 is the yield point of a material, and for most of elastic materials its value lies in the interval $10^{-4}-10^{-3}$ Frantsevich *et. al* (1982). Therefore α will have to be small enough, and the following approximations follow from Eqs. (4.11), (4.16):

$$A \;=\; 1,\; k^2 \;=\; \frac{\alpha}{4R^2(a-b)},\; \frac{\alpha}{\alpha_0} \;=\left(\frac{R_0}{R}\right)^2. \tag{4.19}$$

The most important feature of the solution of Eq.(4.13) is in the appearance of a plateau, propagating behind the solitary wave (4.10) with much less velocity Samsonov (2001). The amplitude of the plateau is negative for the narrowing rod and positive when the wave propagates along the expanding rod.

4.1.3 *Experimental observation of the solitary wave amplification*

We used the same experimental technique as used for the study of the strain solitary wave propagation in a homogeneous rod, see Sec. 3.3. The choice of the rod cross sections variation is caused by two reasons. First, we were going to observe a geometrical inhomogeneity influence just on the strain solitary wave, secondly, the experimental setup limitations should be taken into account. Measurements of the solitary wave amplitude in a homogeneous rod resulted in an estimation of the parameter $\varepsilon = O(10^{-3})$. When the inhomogeneity parameter γ is chosen to be $\gamma << \varepsilon$, then the possible variation of the initial rod radius ($R_0 = 5$ mm) at the distance 100 mm along the axis will be of order 0.1 mm or 2 % from the initial value. The estimation of the amplitude change in this case by means of an approximation (4.19) shows that such a magnitude corresponds to the oscillations of the observed solitary wave front Dreiden *et. al* (1995). So it seems hardly possible to detect such a deviation using our experimental setup. Therefore the inhomogeneity parameter should be chosen as $\gamma >> \varepsilon$.

It has to be noted, however, that an unsteady process takes place in experiments in contrast to the quasistationary process governed by the asymptotic solution obtained above. When $\gamma >> \varepsilon$ the inhomogeneity will change the initial pulse earlier than both nonlinearity and dispersion, and the strain solitary wave will hardly appear from an initial shock. Thus the rod cross section should remain constant at the distance required for the solitary wave generation and separation, and begin vary only after it. Experiments on the solitary wave generation in a homogeneous rod, see Sec. 3.4, showed that a solitary wave appears even at the distance of 60 mm (ca. 10 R_0) approximately from the input edge of the rod. Based on this analysis, a rod of 140 mm long was made of polystyrene with uniform and narrowing parts, as is shown in Fig. 4.2, and two cut offs were made on the lateral surface for the observation purposes. The rod radius decreases linearly from the value $R_0 = 5$ mm to the value $R = 2.75$ mm along the distance 70 mm. In this case the inhomogeneity parameter $\gamma = 0.032$ is

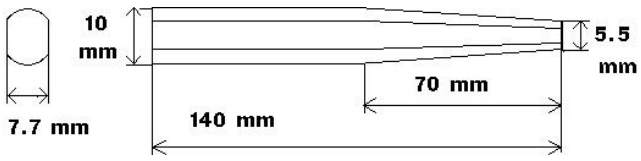

Fig. 4.2 Polysteryne rod with variable cross section and cut-offs.

much greater than the typical solitary wave amplitude $\approx 10^{-4}$Dreiden *et. al* (1995) for the homogeneous rod.

The shape of the strain wave was reconstructed by means of Eq.(3.28) using the following values of parameters: $n_0 = 1.33$, $n_1 = 1.6$, $\Lambda = 7 \cdot 10^{-7}$ m, $\nu = 0.35$. It must be taken into account that light passes the different distances $2h$ in different cross sections. At the interval where the cross section remains uniform , we have $2h = 2h_0 = 7.75 \cdot 10^{-3}$ m, while the measured cross section for the tapered rod part as well as the inteferograms may be found in Samsonov *et. al* (1998). The enlargement

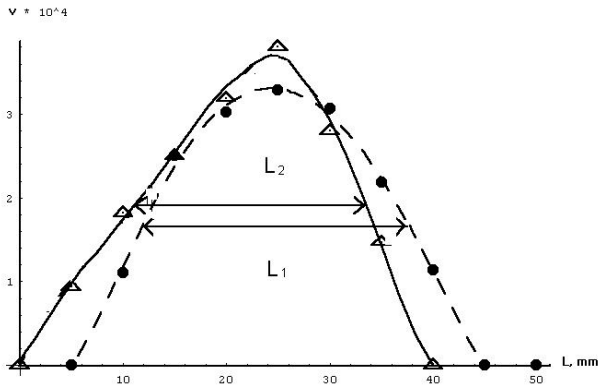

Fig. 4.3 Amplification of longitudinal strain solitary wave. Two graphs "strain v vs. solitary pulse width L" are drawn after interpolation. Solid circles • and the dashed interpolative line both correspond to experimental data measured on a 40-60 mm interval of the rod length; open triangles △ and the solid interpolative line correspond to them on a 75 - 125 mm interval.

of the amplitude scale allows to visualize the main features of the solitary wave in the tapered rod, see Fig. 4.3. Some features predicted by our theory appear in experiments, namely, the increase of the amplitude, the steepness

of the wave front and smoothness of its back, i.e., asymmetric deformation of the bell-shaped solitary wave. Moreover, the characteristic width of the pulse, $L_1 = 25,2$ mm, in the homogeneous part of the rod at the one-half amplitude level is visibly greater than the similar value, $L_2 = 22,3$ mm, in the narrowing part, hence the width of the localized strain solitary pulse decreases along the tapered rod.

The measurement of the wave amplitude is supposed to be quite plausible for the comparison with the theory. One can see that the maximal amplitude of the strain solitary wave is achieved at the distances 60 and 95 mm from the rod input edge, respectively. Then from the estimation (3.28) we obtain the solitary wave magnitudes equal to $3.29 \cdot 10^{-4}$ in the interval 40-90 mm, and to $3.83 \cdot 10^{-4}$ for the interval 75-125 mm. Therefore the solitary wave magnitude increases 1.16 times. The estimation using the simplified formulas (4.19), and a length dependence of the kind $R = R_0 - \gamma(x - 70)$ gives the amplification as 1.31 times, which is in a good agreement with the experimental data.

However, some new theoretical results cannot be checked in experiments, namely:

-The experimental setup does not allow to measure directly the solitary wave acceleration caused by the narrowing cross section along the rod.

-Like in case of the homogeneous rod, the precise measurement of the wave width is impossible.

-There is no observation of a plateau.

4.2 Strain solitary waves in an elastic rod embedded in another elastic external medium with sliding

Stresses on the lateral surface of an elastic wave guide, e.g., an elastic rod, may appear due to its interaction with the surrounding external medium, as in some technological devices. Various types of contact models can be used at the interface between the rod and the external medium. The full (strong) contact model is used when there is continuity of both normal and shear stresses, and displacements. Alternatively, in a weak contact, friction may appear at the interface, hence a discontinuity in the shear stresses. Slippage provides another form of contact at the interface, in which only the continuity of the normal stresses and displacements is assumed. Surface stresses may also arise due to the imperfect manufacturing of the lateral surface of the wave guide and are formally like the "surface tension" on the

free surface of a liquid Biryukov *et. al* (1991), Nikolova (1977).

The analytical solution of the contact problem is rather difficult even in the framework of the linear elasticity theory, see Kerr (1964) and references therein. However, considerable progress has been achieved to account for short nonlinear surface acoustic waves propagating along the interface between elastic media Parker (1994); Parker and Maugin (1987).

Recently, in the studies of strain waves in a rod interacting with an elastic external medium, attention was mostly focused on the propagation of*surface* strain waves along the lateral rod surface *perpendicular* to its axis (see, e.g., Gulyaev and Polsikova (1978); Shevyakhov (1977)). Here, however, we shall consider *bulk* density strain waves, propagating *along* the rod axis. Although rather useful in the study of free lateral surface rods, the so- called plane cross section hypothesis and Love's relationship fail to properly account for contact problems, because they rule out normal stresses at the rod lateral surface, hence there is discontinuity of normal stresses at the interface of the rod and the external medium. Most of the results in this section were first published in Porubov *et. al* (1998).

4.2.1 *Formulation of the problem*

Let us consider an isotropic, axially infinitely extended, elastic rod surrounded by another albeit different elastic medium, in which it may slide without friction, see Fig. 4.4. We shall consider the propagation of longitudinal strain waves of small but finite amplitude in the rod. Axi-symmetry leads to using cylindrical Lagrangian coordinates (x, r, φ), where x is the axis of the rod, $\varphi\ \epsilon[0, 2\pi]$, $\quad 0 \leq r\ \leq\ R$. When torsions are neglected, the displacement vector is $\vec{V}\ =\ (u, w, 0)$. We choose Murnaghan's approximation (3.1) for deformation energy for the rod. The displacement vector for the *linearly* elastic external medium may be written as $\vec{V_1}\ =\ (u_1, w_1, 0)$. Its density is noted by ρ_1, and its elastic properties are characterized by the Lamé coefficients $(\lambda_1,\ \mu_1)$. Any disturbances due to the wave propagation inside the rod are transmitted to the external medium through displacements and stresses normal to the rod surface only when contact with *slippage* is considered. Disturbances are assumed to decay to zero in the external medium far from the rod. The normal strains as well as the displacements inside the rod are smaller than those along the rod axis. Thus we assume that displacements and strains are infinitesimal in the external medium, hence as already said it is a linear elastic one. Then for the

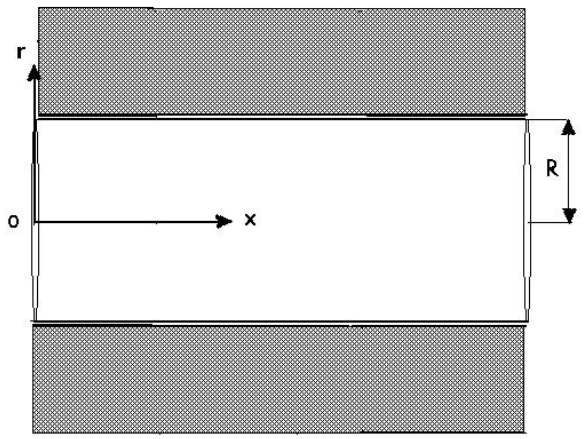

Fig. 4.4 Cylindrical rod surrounded by an external elastic medium.

external medium we have:

$$\rho_1 u_{1,tt} - (\lambda_1 + 2\mu_1)\, u_{1,zz} - (\lambda_1 + \mu_1)\left(w_{1,rz} + \frac{w_{1,x}}{r}\right) - \lambda_1\left(u_{1,rr} + \frac{u_{1,r}}{r} + w_{1,rx} + \frac{w_{1,x}}{r}\right) = 0 \quad (4.20)$$

$$\rho_1 w_{1,tt} - (\lambda_1 + 2\mu_1)\left(w_{1,rr} + \frac{w_{1,r}}{r} - \frac{w_1}{r^2}\right) - \mu_1\, w_{1,xx} - (\lambda_1 + \mu_1)\, u_{1,rx} = 0 \quad (4.21)$$

The following boundary conditions (b.c.) are imposed:

$$w \to 0, \qquad \text{at } r \to 0, \quad (4.22)$$

$$w = w_1, \qquad \text{at } r = R, \quad (4.23)$$

$$P_{rr} = \sigma_{rr}, \qquad \text{at } r = R, \quad (4.24)$$

$$P_{rx} = 0,\ \sigma_{rx} = 0, \qquad \text{at } r = R, \tag{4.25}$$

$$u_1 \to 0,\ w_1 \to 0 \qquad \text{at } r \to \infty. \tag{4.26}$$

where P_{rr}, P_{rx} denote the components of the Piola - Kirchhoff stress tensor $\mathbf{P}$, see Eqs. (3.10), (3.11). The quantities σ_{rr} and σ_{rz} are the corresponding components of the linear stress tensor in the surrounding, external medium:

$$\sigma_{rr} = (\lambda_1 + 2\mu_1)\, w_{1,r} + \lambda_1 \frac{w_1}{r} + \lambda_1\, u_{1,x} \tag{4.27}$$

$$\sigma_{rx} = \mu_1\, (u_{1,r} + w_{1,x}) \tag{4.28}$$

The conditions (4.23)-(4.25) define the *sliding* contact, while the longitudinal displacements u and u_1 are left free at the interface $r = R$.

The Piola- Kirchhoff tensor coincides with the linear stress tensor for infinitesimally small strains. Note that the coefficients in P_{rr} and P_{rx} depend upon both the second order Lamé coefficients λ and μ and the Murnaghan moduli, l, m, n. Hence the tensor $\mathbf{P}$ takes into account both the geometrical and material nonlinearities.

The linear equations (4.20) and (4.21) are solved together with the boundary conditions (4.23), (4.25), (4.26), assuming that the displacement w at the interface is a given function of x and t, hence $w(x, t, R) \equiv W(x, t)$. Then the linear shear stress σ_{rr} at the interface $r = R$ is obtained as a function of W and its derivatives, thus providing the dependence only on the rod characteristics in the right hand side of the b.c. (4.24). The same is valid for the elementary work done by external forces at $r = R$:

$$\delta A = 2\pi \int_{-\infty}^{\infty} \sigma_{rr}\, \delta w\, dx\,. \tag{4.29}$$

Satisfaction of the b.c. on the rod lateral surface yields the relationships between displacements and strains inside the rod, see Sec. 3.2, allowing to derive only one nonlinear equation for long longitudinal waves using Hamilton's principle (3.29) with the Lagrangian density per unit volume, $\mathcal{L}{=}K - \Pi$, with Π, K and δA defined by Eqs. (3.1), (3.6) and (4.29) correspondingly.

4.2.2 *External stresses on the rod lateral surface*

First, the linear problem (4.20), (4.21) will be solved with the boundary conditions (4.23), (4.25), (4.26). As we focus attention on *travelling* waves along the axis of the rod we assume that all variables depend only upon the phase variable $\theta = x - ct$, where c is the phase velocity of the wave. Assuming that the unknown functions $u_1,\ w_1$ are

$$u_1 \ = \ \Phi_\theta + \Psi_r + \frac{\Psi}{r}, \qquad\qquad w_1 \ = \ \Phi_r - \Psi_\theta, \tag{4.30}$$

then Φ and Ψ satisfy the equation:

$$\Phi_{rr} + \frac{1}{r}\Phi_r + (1 - \frac{c^2}{c_l^2})\Phi_{\theta\theta} \ = \ 0, \tag{4.31}$$

$$\Psi_{rr} + \frac{1}{r}\Psi_r - \frac{1}{r^2}\Psi + (1 - \frac{c^2}{c_\tau^2})\ \Psi_{\theta\theta} = \ 0, \tag{4.32}$$

where c_l and c_τ are the velocities of the bulk longitudinal and shear linear waves in the external medium, respectively. They depend on the density and the Lamé coefficients, $c_l^2 = (\lambda_1 + 2\mu_1)/\rho_1$, and $c_\tau^2 = \mu_1/\rho_1$.

To solve equations (4.31), (4.32)we introduce the Fourier transforms of Φ and Ψ:

$$\widetilde{\Phi} = \int_{-\infty}^{\infty} \Phi \exp(-k\,\theta)\, d\theta, \quad \widetilde{\Psi} = \int_{-\infty}^{\infty} \Psi \exp(-k\,\theta)\, d\theta$$

that reduces Eqs. (4.31), (4.32) to the Bessel equations :

$$\widetilde{\Phi}_{rr} + \frac{1}{r}\ \widetilde{\Phi}_r - k^2\alpha\ \widetilde{\Phi} = 0, \tag{4.33}$$

$$\widetilde{\Psi}_{rr} + \frac{1}{r}\ \widetilde{\Psi}_r - \frac{1}{r^2}\ \widetilde{\Psi} - k^2\beta\ \widetilde{\Psi} = 0, \tag{4.34}$$

with $\alpha = 1 - c^2/c_l^2$, and $\beta = 1 - c^2/c_\tau^2$. The ratios between c, c_l and c_τ define the signs of α and β, hence three possible sets of solutions to the equations (4.33), (4.34) appear, vanishing at infinity due to b.c. (4.26). Using the boundary conditions (4.23), (4.25),we obtain the following relationships for the Fourier images of normal stresses at the lateral surface $r = R$:

I) when $0 < c < c_\tau$:

$$\widetilde{\sigma}_{rr}= \frac{\mu_1 \widetilde{W}}{1-\beta}\left(\frac{2(\beta-1)}{R}+\frac{k(1+\beta)^2 K_0(\sqrt{\alpha}kR)}{\sqrt{\alpha}\, K_1(\sqrt{\alpha}kR)}-\frac{4k\sqrt{\beta}K_0(\sqrt{\beta}kR)}{K_1(\sqrt{\beta}kR)}\right) \tag{4.35}$$

II) when $c_\tau < c < c_l$

$$\widetilde{\sigma}_{rr}= \frac{\mu_1 \widetilde{W}}{1-\beta}\left(\frac{2(\beta-1)}{R}+\frac{k(1+\beta)^2 K_0(\sqrt{\alpha}kR)}{\sqrt{\alpha}\, K_1(\sqrt{\alpha}kR)}-\frac{4k\sqrt{\beta}J_0(\sqrt{-\beta}kR)}{J_1(\sqrt{-\beta}kR)}\right) \tag{4.36}$$

III) when $c > c_l$

$$\widetilde{\sigma}_{rr}= \frac{\mu_1 \widetilde{W}}{1-\beta}\left(\frac{2(\beta-1)}{R}+\frac{k(1+\beta)^2 J_0(\sqrt{-\alpha}kR)}{\sqrt{-\alpha}\, J_1(\sqrt{-\alpha}kR)}-\frac{4k\sqrt{\beta}J_0(\sqrt{-\beta}kR)}{J_1(\sqrt{-\beta}kR)}\right) \tag{4.37}$$

where J_i and K_i $(i = 0, 1)$ denote the corresponding Bessel functions.

We shall see in the next section that in the long wave limit the normal stress σ_{rr} has one and the same functional form at the lateral surface of the rod in all three cases (4.35)- (4.37). The main difference in the stress (and strain) fields in the external medium is how they vanish at infinity. This depends on the monotonic decay of K_i and the oscillatory decay of J_i when $R \to \infty$. Note that the dependence of the strain wave behavior on the velocities of bulk linear waves, c_l, c_τ, is known, in particular, for acoustic transverse Love waves propagating in an elastic layer superimposed on an elastic half-space Jeffrey and Engelbrecht(1994); Parker and Maugin (1987).

4.2.3 *Derivation of strain-displacement relationships inside the rod*

To solve the nonlinear problem inside the elastic rod, we have to simplify the relationships between longitudinal and shear displacements u and w following the procedure explained in Sec. 3.2. These relationships are obtained, using conditions on the free lateral surface $r = R$, namely, the simultaneous absence of the tangential stresses and the continuity of the normal ones. We search for *elastic* strain waves with sufficiently small magnitude $B << 1$, and a *long* wavelength relative to the rod radius R, $R/L << 1$. L scales the wavelength along the rod. An interesting case appears when there is balance between (weak) nonlinearity and (weak) dispersion as for

a rod with free lateral surface. Then

$$\varepsilon \;=\; B \;=\; \left(\frac{R}{L}\right)^2 \;<<\; 1. \tag{4.38}$$

is the smallness parameter of the problem. The linear part of longitudinal strain along the rod axis, C_{xx}, is u_x. Then choosing L as a scale along x, one gets $B\,L$ as a scale for the displacement u. Similarly, the linear part of transverse strain, C_{rr}, is w_r. We use the scale $B\,R$ for the displacement w, by choosing R as a length scale along the rod radius. Then with $|kR| << 1$ in (4.35) - (4.37), we have a power series expansion in kR. It allows to obtain analytically an inverse Fourier transform for $\sigma_{rr} = k_1 r^2\, w + k_2 r^{-1}\, w_{xx}$ and to write the conditions (4.24), (4.25) in dimensionless form at the lateral surface $r = 1$ as:

$$\begin{aligned}
&(\lambda+2\mu)\, w_r + (\lambda - k_1)\, w + \lambda\, u_x + \frac{\lambda+2\mu+m}{2}\, u_r^2 + \\
&\varepsilon(\frac{3\lambda+6\mu+2l+4m}{2} w_r^2 + (\lambda+2l)\, w\, w_r + \frac{\lambda+2l}{2}\, w^2 + (\lambda+2l)\, u_x w_r + \\
&(2l-2m+n)\, u_x\, w \;\; + (\mu+m)\, u_r w_x + \frac{\lambda+2l}{2}\, u_x^2 - k_2 \;\; w_{xx}) + \\
&\varepsilon^2 \frac{\lambda+2\mu+m}{2}\, w_x^2 = O(\varepsilon^3),
\end{aligned} \tag{4.39}$$

$$\begin{aligned}
&\mu\, u_r + \varepsilon(\mu\, w_x + (\lambda+2\mu+m)\, u_r w_r + 0.5(2\lambda+2m-n)\, u_r\, w + \\
&(\lambda+2\mu+m)\, u_x\, u_r) + \varepsilon^2(0.5(2m-n)\, w\, w_x + \\
&(\mu+m)\,(w_x w_r + u_x w_x)) = \; O(\varepsilon^3)
\end{aligned} \tag{4.40}$$

At the rod lateral surface $W \equiv w$, $W_{xx} \equiv w_{xx}$. Moreover, for $0 \;<\; c \;<\; c_\tau$:

$$k_1 \;=\; -\,2\mu_1,\; k_2 \;=\; \frac{\mu_1 c^2(\gamma - \log\, 2)}{c_\tau^2}, \tag{4.41}$$

while for $c_\tau \;<\; c \;<\; c_l$:

$$k_1 \;=\; \frac{2\mu_1(4c_\tau^2 - c^2)}{c^2},\; k_2 \;=\; \frac{\mu_1 c_\tau^2}{c^2}\left(1 - \frac{c^2}{c_\tau^2} + (2 - \frac{c^2}{c_\tau^2})^2(\gamma - \log\, 2)\right), \tag{4.42}$$

and for $c \;> c_l$:

$$k_1 \;=\; \frac{2\mu_1[c^2(c_\tau^2 - c_l^2) + 3c_l^2 c_\tau^2 - 4c_\tau^4]}{c_\tau^2(c_l^2 - c^2)},\; k_2 \;=\; \frac{\mu_1 c^2}{4c_\tau^2}. \tag{4.43}$$

with $\gamma = 0.5772157$ Euler's constant.

The unknown functions $u,\ w$ will be found in power series of ε:

$$u \ = \ u_0 + \varepsilon u_1 + \varepsilon^2 u_2 + \ldots, \quad w \ = \ w_0 + \varepsilon w_1 + \varepsilon^2 w_2 + \ldots. \tag{4.44}$$

Substituting (4.44) in (4.39), (4.40), and equating to zero all terms of the same order of ε, we find that the plane cross-section hypothesis and Love's relation are valid in the leading order only:

$$u_0 \ = \ U(x,t), \quad w_0 \ = \ r\, C\, U_x \ , \tag{4.45}$$

with

$$C = \frac{\lambda}{k_1 - 2(\lambda+\mu)}. \tag{4.46}$$

To order $O(\varepsilon)$ we get:

$$u_1 \ = \ - \ r^2 \frac{C}{2} U_{xx}, \quad w_1 = r^3\, D\, U_{xxx} + r\, Q\, U_x^2, \tag{4.47}$$

with coefficients

$$D = \frac{\lambda(\lambda + 2k_2)}{2(k_1 - 2(\lambda+\mu))(2(2\lambda+3\mu) - k_1)} \tag{4.48}$$

$$Q = \frac{\lambda + 2l + 2C(\lambda + 4l - 2m + n) + 2C^2(3\lambda + 3\mu + 4l + 2m)}{2(k_1 - 2(\lambda+\mu))} \tag{4.49}$$

The higher order terms in the series (4.44) may be obtained in a similar way, but are omitted here being unnecessary to obtain an evolution equation for the strain waves.

4.2.4 *Nonlinear evolution equation for longitudinal strain waves along the rod and its solution*

Now we can derive the equation for the strain waves along the rod. First of all, substituting (4.44) into the potential deformation energy density Π (3.1), one can get in dimensionless form that

$$\Pi = a_1\, U_x^2 + \varepsilon \left[a_2 r^2 U_x U_{xxx} + a_3 U_x^3 \right] + O(\varepsilon^2), \tag{4.50}$$

with

$$a_1 = \frac{\lambda + 2\mu}{2} + 2\lambda C + 2(\lambda+\mu)C^2,$$

$$a_2 = -\frac{\lambda + 2\mu}{2} C - \lambda C^2 + 4\lambda D + 8(\lambda + \mu) C D,$$

$$a_3 = \frac{\lambda + 2\mu}{2} + \lambda C + \lambda C^2 + 2(\lambda + \mu)C^3 + 2Q [\lambda + 2(\lambda + \mu)C] + l \left[\frac{1}{3} + 2C + 4C^2 + \frac{8}{3}C^3\right] + m \left[\frac{2}{3} - 2C^2 + \frac{4}{3}C^3\right] + n C^2.$$

For the kinetic energy we have:

$$K = \frac{\rho_0}{2} \left[U_t^2 - \varepsilon r^2 C(U_t U_{xxt} - C U_{xt}^2)\right] + O(\varepsilon^2) \tag{4.51}$$

Substituting (4.50), (4.51) and (4.29) into (3.29) and using Hamilton's variational principle, we obtain the following equation for a longitudinal strain wave, $v = U_x$:

$$v_{tt} - b_1 \, v_{xx} - \varepsilon \left(b_2 \, v_{xxtt} + b_3 \, v_{xxxx} + b_4 \, (v^2)_{xx}\right) = 0, \tag{4.52}$$

with

$$b_1 = \frac{2(a_1 - k_1 C^2)}{\rho_0}, \; b_2 = \frac{C(1 + C)}{2},$$
$$b_3 = \frac{a_2 - 2C(k_2 \, C + 2 \, k_1 \, D)}{\rho_0}, \; b_4 = \frac{3(a_3 - k_1 \, C \, Q)}{\rho_0}. \tag{4.53}$$

Equation (4.52) is nothing but the double dispersive equation (3.18), it admits, in particular, *exact* travelling solitary wave solution. Note that the coefficients depend now upon the wave velocity, c, due to (4.41)- (4.43). The terms of order $O(\varepsilon^2)$ have been neglected, when deriving equation (4.52). Therefore we assume $c^2 = c_0^2 + \varepsilon \, c_1 + ...$ and consider the coefficients $b_2 - b_4$ depending on c_0 only, while the coefficient b_1 may depend also on c_1 as $b_1 = b_{10}(c_0) + \varepsilon \, b_{11}(c_0, c_1)$. Then the solitary wave solution has the form:

$$v = A \, m^2 \cosh^{-2} (m \, \theta), \tag{4.54}$$

with

$$A = \frac{6(b_{10} b_2 + b_3)}{b_4}. \tag{4.55}$$

To leading order the phase velocity is obtained from the equation

$$c_0^2 = b_{10}(c_0), \tag{4.56}$$

Table 4.1 Phase velocities of waves in a polystyrene rod embedded indifferent media. All velocities are measured in $10^{-3}\frac{m}{\sec}$

material	c_τ	c_l	c_{01}	c_{02}	c_{03}	model
Quartz	3.78	6.02	2.06	2.1 or 7.15	2.13 or 5.77	I
Iron	3.23	5.85	2.08	2.1 or 6.32	2.11 or 5.15	I
Copper	2.26	4.7	2.07	2.11 or 4.33	2.12 or 3.68	I, II
Brass	2.12	4.43	2.06	2.11 or 4.02	2.12 or 3.45	I, II
Aluminium	3.08	6.26	2.05	2.11 or 5.75	2.13 or 4.97	I, II
Lead	1.09	2.41	2.01	–	1.83 or 2.06	-

and for the function $c_1$we get the equation

$$c_1 = b_{11} + 4k^2(b_{10}b_2 + b_3), \tag{4.57}$$

where the wave number k remains a free parameter.

4.2.5 *Influence of the external medium on the propagation of the strain solitary wave along the rod*

Let us estimate the influence of the external medium on the solitary wave propagation along the rod. First of all, we have to solve Eq.(4.56) for all three possible cases (4.41) -(4.43). As ε must not exceed the yield point of the elastic material (its usual value is less than 10^{-3}) we have to compare with c_l and c_τ the values obtained for c_0, rather than for c.

For the case (4.41), the velocity c_0 is obtained from (4.57) as

$$c_0^2 = \frac{(3\lambda + 2\mu)\mu + \mu_1(\lambda + 2\mu)}{\rho_0(\lambda + \mu + \mu_{1)}}. \tag{4.58}$$

It appears always higher than the wave velocity in a free rod.

For the model (4.42), Eq. (4.56) yields

$$c_0^4 - A_1\, c_0^2 + A_2 = 0 \tag{4.59}$$

where

$$A_1 = \frac{(3\lambda + 2\mu)\mu + \mu_1(\lambda + 2\mu) + 4\mu_1\rho_0 c_\tau^2}{\rho_0(\lambda + \mu + \mu_{1)}},\ A_2 = \frac{4\mu_1 c_\tau^2(\lambda + 2\mu)}{\rho_0(\lambda + \mu + \mu_{1)}}.$$

Finally, for the model (4.43), Eq. (4.56) provides

$$c_0^4 - B_1\, c_0^2 + B_2 = 0 \tag{4.60}$$

Table 4.2 Phase velocities of waves in a lead rod embedded in differentexternal media. All velocities are measured in $10^{-3}\frac{m}{\sec}$

material	c_τ	c_l	c_{01}	c_{02}	c_{03}	model
Quartz	3.78	6.02	2.06	2.55 or 4.39	7.51	I,II,III
Iron	3.23	5.85	2.2	2.47 or 4.91	2.73 or4.81	I, II
Copper	2.26	4.7	2.11	–	–	I
Brass	2.12	4.43	2.08	–	–	I
Aluminium	3.08	6.26	2.03	–	–	I
Polystyrene	1.01	2.1	1.83	0.38 or 1.81	1.84 or 2.06	II, III

with

$$B_1 = \frac{(3\lambda+2\mu)\mu c_\tau^2 + (c_\tau^2 - c_l^2)\mu_1(\lambda+2\mu) + 4\mu_1\rho_0 c_\tau^4 + c_\tau^2 c_l^2\rho_0(\lambda+\mu-3\mu_1)}{\rho_0(c_l^2\mu_1 - c_\tau^2(\lambda+\mu+\mu_1))}$$

$$B_2 = \frac{c_\tau^2 c_l^2[3\mu_1(\lambda+2\mu) - \mu(3\lambda+2\mu)] - 4\mu_1 c_\tau^4(\lambda+2\mu)}{\rho_0(c_l^2\mu_1 - c_\tau^2(\lambda+\mu+\mu_1))}.$$

Table 4.1 contains some quantitative estimates for a polystyrene rod and Table 4.2 for a lead rod, respectively, both embedded in different external media. The quantities c_{01}, c_{02} and c_{03} denote velocities calculated from Eqs.(4.58), (4.59) and (4.60), respectively. Comparing velocities c_{0i} relative to c_τ and c_l we can justify the applicability of cases (4.41)- (4.43). This is noted by symbols I-III, respectively, in the last column of Tables 4.1 and 4.2. Indeed, the model (4.41) is better for the contact with a polystyrene rod, while no solitary wave may propagate when the external medium is lead. However, a solitary wave may propagate along a lead rod embedded in a polystyrene external medium, as it follows from Table 4.2. Note that there exist pairs of materials, for which two or even all three models of sliding contact allow a solitary wave propagation. Thus the balance between nonlinearity and dispersion may be achieved at different phase velocities of the strain nonlinear waves. This result is of importance when generating strain solitary waves in a rod embedded in an external elastic medium.

Therefore, strain solitary waves can propagate only with velocities from the intervals around c_{0i}. Note that the solitary wave is a bulk (density) wave inside the rod and, simultaneously, it is a surface wave for the external medium. Then, an important difference appears relative to long nonlinear Rayleigh surface waves in Cartesian coordinates: in our case more than one velocity interval exists where solitary waves may propagate. The

main difference between modes lies in the different rate of wave decay in the external medium, that follows from the different behavior of Bessel's functions at large values of their arguments.

Now let us consider the influence of the type of external medium on the existence of either compression or tensile longitudinal strain localized waves. Using the data from Table 4.1 to compute the value of A (4.55) for a polystyrene rod, it yields that its sign may change according to the values of the parameters of the material used for the external medium. Therefore the solitary wave (strain!) amplitude (4.54) may change its sign. The amplitude is negative for a free lateral surface rod and it remains negative if the external medium is, say, quartz, brass, copper or iron. However, the sign changes if $c_0 = c_{02}$ and the external medium is aluminium. Therefore, one can anticipate, in particular, that for a rod embedded in aluminium an initial pulse with velocity close to c_{02} may transform only into a tensile solitary wave while an initial pulse with velocity close to c_{01} evolves to become a compression solitary wave.

Finally, let us consider the influence on the sign of c_1(4.57). For case I, $b_{11} = 0$, hence the sign is defined by the sign of the quantity $(b_{10}b_2 + b_3)/b_4$. For polystyrene it is, generally, negative for all the external media in Table 4.1, while for a free lateral surface it is positive. Thus, the velocity, c, of a *nonlinear* wave in a rod embedded in an external medium is lower than the *linear* wave velocity, c_0, while for a free surface rod nonlinear waves propagate faster than linear waves. On the other hand, the nonlinear wave velocity, c, in a polystyrene rod embedded in external medium is higher than the linear wave velocity for a rod with free lateral surface, $c^* = \sqrt{E/\rho_0}$.

4.2.6 *Numerical simulation of unsteady strain wave propagation*

Numerical simulation of unsteady nonlinear wave processes in elastic rods with *free lateral surface* shows that for $A < 0$ only initial compression pulses provide a solitary wave (4.54) or a wave train, while tensile initial pulses do not become localized and are destroyed by dispersion. On the contrary, for $A > 0$ only tensile strain solitary waves may appear, see Figs. 3.2, 3.3 , and initial compression pulses are destroyed like in Fig. 3.4. Let us consider now the case when the rod lateral surface is partly free along the axis and the other part is subjected to a sliding contact with an external elastic medium, as it is shown in Fig. 4.5. Then the nonlinear strain wave propagation is described in each part by its own equation (4.52). Matching

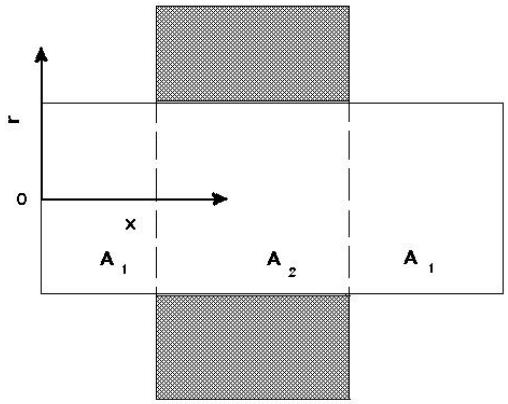

Fig. 4.5 Cylindrical rod partly embedded into an external elastic medium with sliding.

is provided by the continuity of strains and its derivatives. Assume that for the free surface part ($k_1 = 0$, $k_2 = 0$) $A = A_1$, $m = m_1$, while for the embedded one, $A = A_2$, $m = m_2$. Let the initial solitary wave (4.54) moves from left to right in Fig. 4.5 far from the embedded part, which is supposed to be undeformed at the initial time. It was found in Samsonov (1988) that the mass M conservation in the form

$$\frac{d}{dt}M = 0,\ M = \int\limits_{-\infty}^{\infty} v\, dx \tag{4.61}$$

is satisfied by equation (4.52). Then using Eqs.(4.54) and (4.55) we get for the mass M_1

$$M_1 = 2\, A_1\, m_1, \tag{4.62}$$

The wave evolution along the embedded part, depends on the ratio between A_1 and A_2. Similar to the unsteady processes inside a rod with the free lateral surface, see Sec. 3.2, an initial strain solitary wave will be destroyed in the embedded part, if $sgnA_2$ differs from $sgnA_1$. Otherwise another solitary wave or a wave train will appear. When the initial pulse is

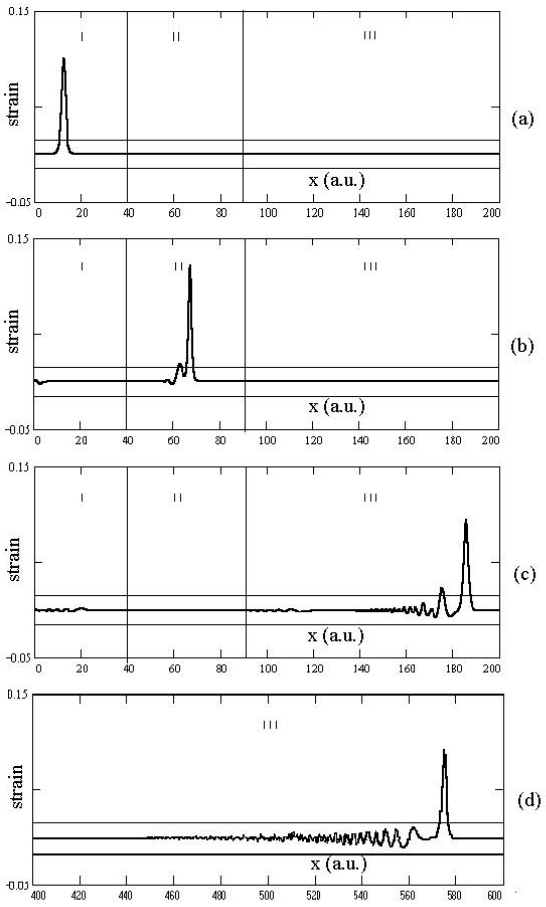

Fig. 4.6 Amplification and reconstruction of a strain solitary wave.

not massive enough one can see in Fig. 3.2, that only one new solitary wave appears but there is an oscillatory decaying tail. However, the contribution of the tail to the mass M is negligibly small relative to the solitary wave contribution, hence

$$M_2 = 2\,A_2\,m_2. \tag{4.63}$$

Comparing M_1 and M_2, according to Eq.(4.61) it follows

$$A_1\, m_1 = A_2\, m_2. \tag{4.64}$$

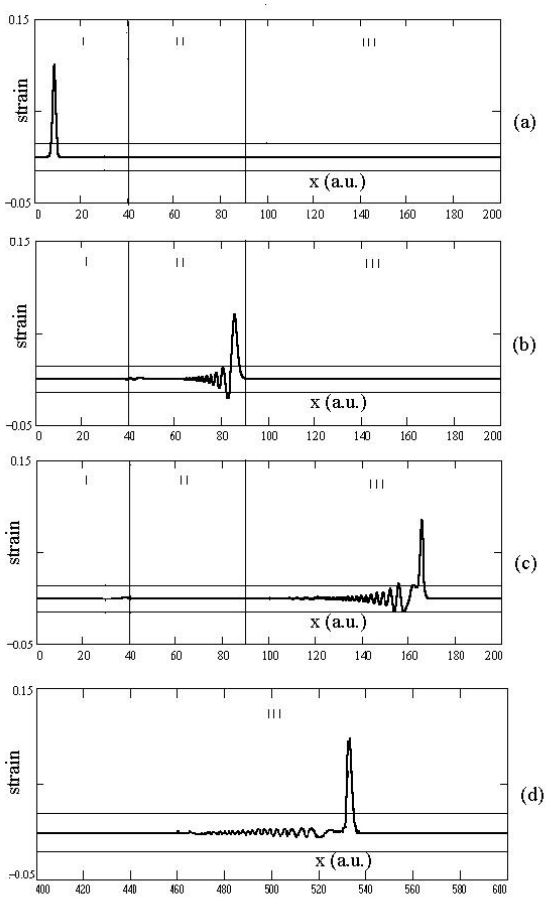

Fig. 4.7 Attenuation and reconstruction of a strain solitary wave.

Therefore, if $A_2 < A_1$ the amplitude of the solitary wave increases while its width, proportional to m^{-1}, decreases, hence there is focusing of the solitary wave. On the contrary, when $A_2 > A_1$ attenuation of the solitary wave

is provided by the simultaneous decrease of the amplitude and the increase of the wave width. Numerical simulations confirm our theoretical estimates.

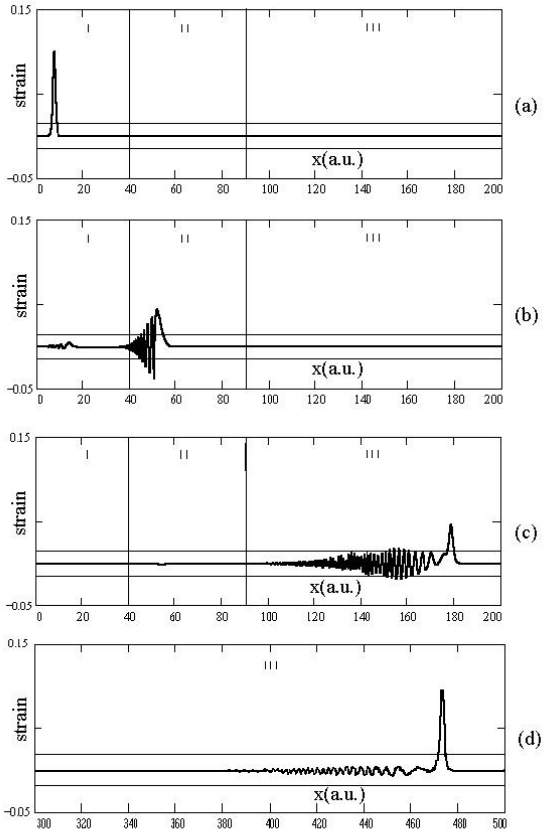

Fig. 4.8 Delocalization and reconstruction of a strain solitary wave.

In Fig. 4.6 the evolution of a strain tensile solitary wave is shown in a rod, having a central part embedded in an external medium. The value of A in the central part II, A_2, is positive but smaller than the value of A_1 in the surrounding free lateral surface parts I and III, $A_1 > A_2 > 0$. In the

embedded part II (Fig. 4.6(b)) the solitary wave amplitude exceeds the amplitude of the initial solitary wave in Fig. 4.6(a), while its width becomes narrower than that of the initial wave. Therefore an increase in amplitude of the elastic strain solitary wave is possible even in an *uniformly* elastic rod. This may overtake the yield point inside the elastically deformed rod, hence the possible appearance of cracks or plasticity zones. In our case the deformations of the wave front and rear are equal. Hence, the solitary wave remains symmetric on amplification at variance with the strain solitary wave amplification in a rod with diminishing cross section. Moreover, a *plateau* develops in the tail of the solitary wave in geometrically inhomogeneous rod. These differences could be caused by the absence of mass (and energy) conservation for strain solitary waves in a narrowing (expanding) rod.

In the case treated here, the solitary wave does not loose mass, M, hence its original shape is recovered when traversing part III in Fig. 4.6(c,d). One can see that an oscillatory tail of the solitary wave in Fig. 4.6(d) is less pronounced than the tail in Fig. 4.6(c), in agreement with (4.64). Again there is no solitary wave selection since the parameters of the recovered wave depends upon that of the original one.

When $A_2 > A_1 > 0$, an initial tensile strain solitary wave, Fig. 4.7(a), is drastically attenuated as soon as it enters the embedded area, Fig. 4.7(b), and its amplitude decreases while its width becomes larger. Again both the reconstruction of the initial wave profile and the damping of its tail are observed in the third part of a rod with free lateral surface, part III in Fig. 4.7(c,d).

Consider now the case of different signs of A_i and assume that $A_1 > 0$ on both free surface parts. One can see in Fig.4.8 how an initial tensile solitary wave, Fig. 4.8(a), is destroyed in the embedded part II, Fig. 4.8(b), in agreement with our previous results on the unsteady processes occurring for a free surface rod. However, a strain wave is localized again in the third part of a rod with free lateral surface, Fig. 4.8(c), part III , and finally recovers its initial shape in Fig. 4.8(d). Again damping of the tail behind the solitary wave is observed. Accordingly, both compression and tensile initial pulses may produce localized strain solitary waves in a rod partly embedded in an external elastic medium with sliding.

Moreover, the amplitude of the solitary wave generated in such a manner, may be greater than the magnitude of the initial pulse. This case is shown in Figs. 4.9, 4.10 where $A_1 < 0$, $A_2 > 0$ and $|A_1| < A_2$. One can see in Fig. 4.9 how an initially localized rectangular tensile pulse, Fig. 4.9(a), is

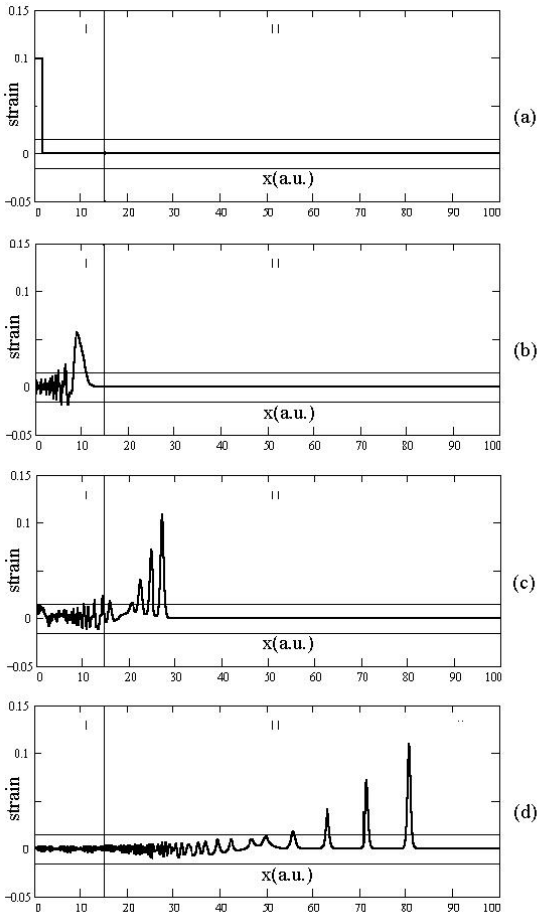

Fig. 4.9 Generation of a tensile strain solitary wave train in a rod. The elastic properties of the rod are chosen such that tensile wave propagation cannot occur in the absence of contact with an external medium.

destroyed in the free surface part I, Fig.4.9(b). However, a wave train of solitary waves appears, when a destroyed strain wave comes to the embedded part, Figs. 4.9(c,d). The amplitude of the first solitary wave in Fig. 4.9(d) exceeds the magnitude of the initial rectangular pulse in Fig. 4.9(a). In the absence of surrounding external medium this rod wave-guide does not

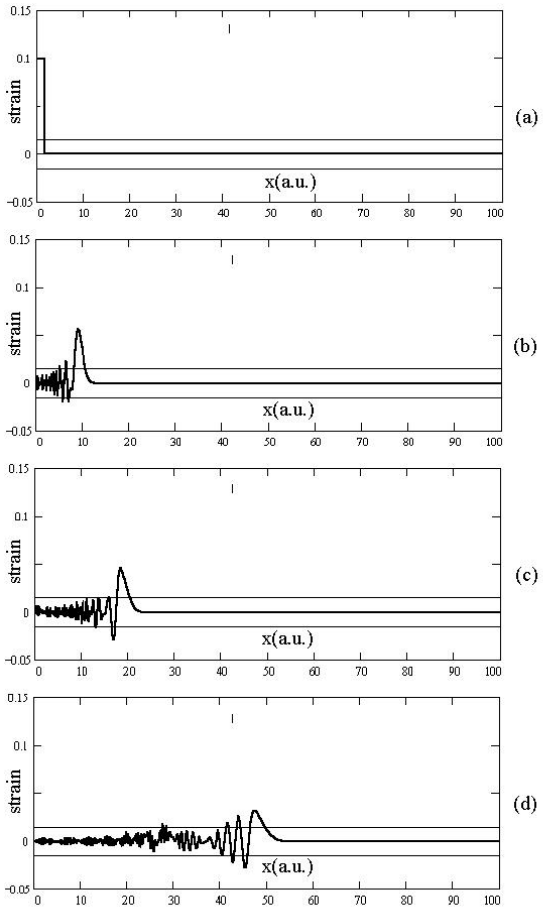

Fig. 4.10 Delocalization of a strain solitary wave in the absence of external medium.

support tensile solitary wave propagation, and a strain wave is delocalized as shown in Fig. 4.10.

4.3 Strain solitary waves in an elastic rod with microstructure

Classic elastic theory cannot account for phenomena caused by the microstructure of a material. A particular case is a dispersion of strain waves in an elastic medium. The influence of microstructure may provide dissipative effects Cermelli and Pastrone (1997); Engelbrecht and Braun (1998); Maugin and Muschik (1994), it will be studied in Chapter 6, now consideration is restricted by the non-dissipative case.

The present section refers to the study of nonlinear solitary waves inside cylindrical rod with microstructure following Porubov (2000). The problem is solved using the "pseudo-continuum" Cosserat model and the Le Roux continuum model. A procedure is developed for derivation of the model equation for long longitudinal strain waves inside the rod. The influence of the microstructure on the solitary wave propagation and amplification is studied.

4.3.1 *Modelling of non-dissipative elastic medium with microstructure*

The theory of microstructure has been developed recently, see Engelbrecht and Braun (1998); Eringen (1968); Mindlin (1964); Nowacki (1975); Nowacki (1986a) and references therein. Most of results belong to the linear theory of elasticity, however, there are findings in the field of the nonlinear theory Engelbrecht and Braun (1998); Eringen (1968). Strain waves were studied mainly in the linear approximation Eringen (1968); Mindlin (1964); Nowacki (1975); Nowacki (1986a). Only a few works are devoted to the nonlinear waves in microstructured non-dissipative media Engelbrecht and Braun (1998); Erbay *et. al* (1991); Erofeev and Potapov (1993); Erofeev (2002); Savin *et. al* (1973a); Savin *et. al* (1973b). Waves in elastic *wave guides* with microstructure were out of considerable investigation. Also the values of the parameters characterizing microstructure, are unknown as a rule, only a few experiments may be mentioned, Savin *et. al* (1973b); Potapov and Rodyushkin (2001).

Recall some basic ideas following Eringen (1968). Suppose the macroelement of an elastic body contains discrete micromaterial elements. At any time the position of a material point of the αth microelement may be

expressed as

$$\mathbf{x}^{(\alpha)} = \mathbf{x} + \xi^{(\alpha)},$$

where $\mathbf{x}$ is the position vector of the center of mass of the macroelement, $\xi^{(\alpha)}$ is the position of a point in the microelement relative to the center of mass. The motion of the center of mass depends upon the initial position $\mathbf{X}$ and time t, $\mathbf{x} = \mathbf{x}(\mathbf{X}, t)$, while for $\xi^{(\alpha)}$ the axiom of affine motion is assumed,

$$\xi^{(\alpha)} = \chi_K(\mathbf{X}, t)\ \mathbf{\Xi}_K^{(\alpha)},$$

where $\mathbf{\Xi}^{(\alpha)}$ characterizes initial position of a point relative to the center of mass. Then the square of the arc length is $(ds^{(\alpha)})^2 = d\mathbf{x}^{(\alpha)} d\mathbf{x}^{(\alpha)}$, and the difference between the squares of arc length in the deformed and undeformed body is

$$\begin{aligned}(ds^{(\alpha)})^2 - (dS^{(\alpha)})^2 = (&x_{k,K}\, x_{k,L} - \delta_{KL} + 2x_{k,K}\, \chi_{kM,L}\, \Xi_M + \\ &\chi_{kM,K}\, \chi_{kN,L}\, \Xi_M\, \Xi_N) dX_K\, dX_L + \\ &2\left(x_{k,K}\, \chi_{kL} - \delta_{KL} + \chi_{kL}\, \chi_{kM}\, \Xi_M\right) dX_K\, d\Xi_L + \\ &\chi_{kK}\, \chi_{kL} d\Xi_K\, d\Xi_L. \end{aligned} \tag{4.65}$$

where δ_{KL} is the Kronecker delta. Let us introduce vector of macrodisplacements, $\mathbf{U}(\mathbf{X}, t)$ and tensor of microdisplacements, $\mathbf{\Phi}(\mathbf{X}, t)$,

$$\begin{aligned} x_{k,K} &= (\delta_{LK} + U_{L,K})\delta_{kL}, \\ \chi_{kK} &= (\delta_{LK} + \Phi_{LK})\delta_{kL} \end{aligned}$$

Then three tensors characterizing the behavior of microstructured medium follow from (4.65),

$$\begin{aligned} C_{KL} &= \frac{1}{2}\left(U_{K,L} + U_{L,K} + U_{M,K} U_{M,L}\right), \\ E_{KL} &= \Phi_{KL} + U_{L,K} + U_{M,K}\, \Phi_{ML}, \\ \Gamma_{KLM} &= \Phi_{KL,M} + U_{N,K}\, \Phi_{NL,M}, \end{aligned}$$

where C_{KL} is the Cauchy-Green macrostrain tensor , E_{KL} is the tensor of a reference distortion, Γ_{KLM} is the tensor of microdistortion. Tensor of the second rank E_{KL} accounts for the microelements motion relative to the center of mass of the macroelement, while tensor of the third rank Γ_{KLM} characterizes relative motion of the microelements of one another.

The density of the potential energy Π should be the function of these tensors, $\Pi = \Pi(C_{KL}, E_{KL}, \Gamma_{KLM})$, more precisely upon the invariants of them. The bulk density of the kinetic energy has the form Mindlin (1964)

$$K = \frac{1}{2}\rho_0 \left(U_{M,t}^2 + J_{KN}\, \Phi_{KM,t}\, \Phi_{NM,t}\right), \tag{4.66}$$

where ρ_0 is macrodensity of the elastic material, J_{KN} is the inertia tensor. Elastic media with central symmetry posses simpler representation, $J_{KN} = J^* \delta_{KN}$.

One of the main problem is to define integrity basis of three tensors $C_{KL}, E_{KL}, \Gamma_{KLM}$ Spencer (1971); Eringen and Suhubi (1964). Moreover, the basic invariants of the third and higher rank tensors have not been studied. That is why the models were developed based on the additional assumption on a relationship between $\mathbf{U}$ and $\mathbf{\Phi}$. One of them is the pseudo-continuum Cosserat model . According to it

$$\Phi_{KL} = -\varepsilon_{KLM}\Phi_M,\ \Phi_M = \frac{1}{2}\varepsilon_{MLK}U_{K,L}, \tag{4.67}$$

where ε_{KLM} is the alternating tensor. The first relationship represents the classic Cosserat model when only rotations of solid microelements are possible. The last expression in (4.67) accounts for the pseudo-continuum Cosserat model when micro-rotation vector $\mathbf{\Phi}$ coincides with the macro-rotation vector. In this case the density of the potential energy my be either $\Pi = \Pi(C_{KL}, \Gamma_{KLM})$ or $\Pi = \Pi(C_{KL}, \Phi_{K,L})$ Nowacki (1975); Nowacki (1986a); Savin *et. al* (1973b). Tensor E_{KL} has the form

$$E_{KL} = \frac{1}{2}\left(U_{K,L} + U_{L,K} + U_{M,K}U_{M,L} - U_{M,K}U_{L,M}\right),$$

and only linear part of E_{KL} coincides with those of C_{KL}. Assume the microstructure is sufficiently weak to be considered in the linear approximation Nowacki (1975); Nowacki (1986a); Savin *et. al* (1973b), and the Murnaghan model is valid for the macro-motion. Then the density of the potential energy may be written as

$$\Pi = \frac{\lambda + 2\mu}{2}I_1^2 - 2\mu I_2 + \frac{l + 2m}{3}I_1^3 - 2mI_1I_2 + nI_3 + 2\mu M^2(\Phi_{K,L}\Phi_{K,L} + \eta\Phi_{K,L}\Phi_{L,K} + \beta\Phi_{K,K}\Phi_{L,L}), \tag{4.68}$$

where λ and μ are the Lamé coefficients, (l, m, n) are the third order elastic moduli, or the Murnaghan moduli, M, η and β are the microstructure constants, I_p, $p = 1, 2, 3$ are the invariants of the tensor $\mathbf{C}$, see Eq.(3.2).

Another simplified microstructure model was used by some authors, see Erofeev and Potapov (1993); Mindlin (1964); Savin *et. al* (1973a). Sometimes it is referred to as the Le Roux continuum Erofeev (2002). According to it

$$\Phi_{KL} = -U_{L,K},\ \Gamma_{KLM} = -U_{L,KM}.$$

When microstructure is weak and may be considered in the linear approximation the linear part of E_{KL} is zero tensor. It means that there is no difference between deformation of elastic microelement and elastic macrostructure. In this case $\Pi = \Pi(C_{KL}, \Gamma_{KLM})$. Assume again the Murnaghan model for the macro part of the energy density and use the linear Mindlin's model Mindlin (1964) for its micro part one can obtain

$$\begin{aligned}\Pi \ = \ & \frac{\lambda + 2\mu}{2} I_1^2 - 2\mu I_2 + \frac{l + 2m}{3} I_1^3 - 2mI_1 I_2 + nI_3 + a_1 \Gamma_{KKM}\Gamma_{MLL} + \\ & a_2 \Gamma_{KLL}\Gamma_{KMM} + a_3 \Gamma_{KKM}\Gamma_{LLM} + a_4 \Gamma_{KLM}^2 + a_5 \Gamma_{KLM}\Gamma_{MLK}.\end{aligned} \tag{4.69}$$

where a_i, $i = 1 - 5$, are the constant microstructure parameters.

4.3.2 *Nonlinear waves in a rod with pseudo-continuum Cosserat microstructure*

Let us consider the propagation of a longitudinal strain wave in an isotropic cylindrical *compressible* nonlinearly elastic rod, see Fig. 3.1. We take cylindrical Lagrangian coordinates (x, r, φ) where x is directed along the axis of the rod, $-\infty < x < \infty$; r is the coordinate along the rod radius, $0 \leq r \ \leq \ R$; φ is a polar angle, $\varphi \ \epsilon [0, 2\pi]$. Neglecting torsions the displacement vector is $\mathbf{U} = \ (u, w, 0)$. Then nonzero components of the macrostrain tensor $\mathbf{C}$ are

$$\begin{aligned}& C_{xx} = u_x + \frac{1}{2}(u_x^2 + w_x^2), C_{rr} = w_r + \frac{1}{2}(u_r^2 + w_r^2), C_{\varphi\varphi} = \frac{w}{r} + \frac{w^2}{2r^2}, \\ & C_{rx} = C_{xr} = \frac{1}{2}\left(u_r + w_x + u_x u_r + w_x w_r\right).\end{aligned} \tag{4.70}$$

while nonzero components of the rotation tensor $\Phi_{K,L}$ are

$$\Phi_{\varphi,x} = w_{xx} - u_{rx}, \Phi_{\varphi,r} = w_{xr} - u_{rr}. \tag{4.71}$$

The governing equations together with the boundary conditions are obtained using the Hamilton variation principle (3.5), where the Lagrangian

density per unit volume, $\mathcal{L}$=$K-\Pi$, with K and Π defined by Eqs.(4.66) (4.68) correspondingly.

The following boundary conditions (b.c.) are imposed:

$$w \to 0, \qquad \text{at } r \to 0, \tag{4.72}$$

$$P_{rr} = 0\,, \qquad \text{at } r = R, \tag{4.73}$$

$$P_{rx} = 0, \qquad \text{at } r = R, \tag{4.74}$$

where the components P_{rr}, P_{rx} of the modified Piola - Kirchhoff stress tensor $\mathbf{P}$ are defined from (3.5) with (4.66), (4.68), (4.70) and (4.71) being taken into account:

$$\begin{aligned} P_{rr} = (\lambda+2\mu)\, w_r + \lambda\,\frac{w}{r} + \ \lambda\, u_x + \frac{\lambda+2\mu+m}{2}\, u_r^2 + (\lambda+2l)\, w_r\frac{w}{r} + \\ \frac{\lambda+2l}{2}\frac{w^2}{r^2} + (\lambda+2l)\, u_x w_r + (2l-2m+n)\, u_x\frac{w}{r} + \\ \frac{\lambda+2l}{2}\, u_x^2 + \frac{\lambda+2\mu+m}{2}\, w_x^2 \ + (\mu+m)\, u_r w_x + \\ \frac{3\lambda+6\mu+2l+4m}{2}\, w_r^2 + 4\mu M^2(u_{rrx} - w_{xxr}), \end{aligned} \tag{4.75}$$

$$\begin{aligned} P_{rx} = \mu\,(u_r + w_x) + (\lambda+2\mu+m)\, u_r w_r + (2\lambda+2m-n)\, u_r\frac{w}{2r} + \\ (\lambda+2\mu+m)\, u_x u_r + \frac{2m-n}{2}\, w_x\frac{w}{r} + (\mu+m)\, w_x w_r + \\ (\mu+m)\, u_x w_x \ + 4\mu M^2[w_{xxx} - u_{xxr} + \frac{1}{r}\,(r(w_{xr} - u_{rr}))_r - \\ \frac{1}{2}J^*(u_{rtt} - w_{xtt})]. \end{aligned} \tag{4.76}$$

Exception of torsions provides transformation of the initial 3D problem into a 2D one. Subsequent simplification is caused by the consideration of only long elastic waves with the ratio between the rod radius R and typical wavelength L is $R/L \ll 1$. The typical elastic strain magnitude B is also small, $B \ll 1$. Then the procedure from Sec. 3.2.2 is applied to find the relationships between displacement vector components satisfying b.c. on the lateral surface of the rod (4.73), (4.74) as well as the condition for w (4.72). An additional parameter $\gamma = M^2/R^2$ is introduced to characterize the microstructure contribution. Accordingly, the longitudinal and shear displacement in *dimensional* form are sought in the form (3.12), (3.13).

Substituting the linear parts u_L and w_L (3.12), (3.13) into the b.c. (4.72) and in the linear parts of b.c. (4.73), (4.74), and equating to zero terms at equal powers of r one obtains u_k and w_k. Using these results the nonlinear parts u_{NL}, w_{NL} are similarly obtained from the full b.c. We get

$$u = U(x,t) + \frac{\nu r^2}{2}\frac{1+4\gamma}{1-4\gamma}U_{xx}, \tag{4.77}$$

$$\begin{aligned} w \ &= -\nu r U_x \ - \frac{\nu}{2(3-2\nu)(1-4\gamma)}\left[\nu + 4\gamma(2+\nu)\right] r^3 U_{xxx} - \\ &(1+\nu)\left[\frac{\nu}{2} + \frac{(1-2\nu)}{E}\left(l(1-2\nu)^2 + 2m(1+\nu) - n\nu\right)\right] r U_x^2, \end{aligned} \tag{4.78}$$

where ν is the Poisson ratio, E is the Young modulus. Other terms from the series (3.12), (3.13) for $i > 3$ may be found in the same way, however, they are omitted here because of no influence on the final model equation for the strain waves. Substituting Eqs.(4.77), (4.78) into Eq.(3.5), and using Hamilton's principle we obtain that longitudinal strains, $v = U_x$, obey a double dispersive nonlinear equation:

$$v_{tt} - \alpha_1\, v_{xx} - \alpha_2 (\, v^2)_{xx} + \alpha_3\, v_{xxtt} - \alpha_4\, v_{xxxx} = 0, \tag{4.79}$$

where $\alpha_1 = c_*^2 = E/\rho_0$, $\alpha_2 = \beta/(2\rho_0)$, $\beta = 3E + 2l(1-2\nu)^3 + 4m(1+\nu)^2(1-2\nu) + 6n\nu^2$, $\alpha_3 = \nu(1-\nu)R^2/2$,

$$\alpha_4 = \frac{\nu E R^2}{2\rho_0}\frac{1+4\gamma}{1-4\gamma}.$$

Hence the microstructure affects only dispersion in Eq.(4.77). The solitary wave solution of Eq.(4.77) is

$$v = \frac{3E}{\beta}\left(\frac{V^2}{c_*^2} - 1\right)\cosh^{-2}(k\,(x - Vt)), \tag{4.80}$$

where V is a free parameter while the wave number k is defined by

$$k^2 = \frac{\rho_0(V^2 - c_*^2)}{2\nu E R^2\left(\frac{1+4\gamma}{1-4\gamma} - \frac{(1-\nu)V^2}{c_*^2}\right)}. \tag{4.81}$$

Therefore the contribution of the microstructure results in the widening of the permitted solitary wave velocities,

$$1 < \frac{V^2}{c_*^2} < \frac{1}{1-\nu}\frac{1+4\gamma}{1-4\gamma}.$$

Also the characteristic width of the solitary wave proportional to $1/k$ becomes larger relative to the wave width in pure elastic case, $\gamma = 0$. We consider γ to be rather small due to the experimental data from Savin *et. al* (1973b). Then the type of the solitary wave (compression/tensile) is defined by the sign of the nonlinearity parameter β like in the case without microstructure, see Sec. 3.3.

4.3.3 *Nonlinear waves in a rod with Le Roux continuum microstructure*

The procedure of obtaining the governing equations is similar to those used in previous subsection. The nonzero components of the tensor Γ_{KLM} are

$$\Gamma_{xxx} = -u_{xx}, \Gamma_{xxr} = \Gamma_{rxx} = -u_{xr}, \Gamma_{xrx} = -w_{xr},$$
$$\Gamma_{xrr} = \Gamma_{rrx} = -w_{xr}, \Gamma_{rxr} = -u_{rr}, \Gamma_{rrr} = -w_{rr}.$$

The b.c. (4.73), (4.74) are satisfied for the strain tensor components

$$\begin{aligned} P_{rr} = (\lambda + 2\mu)\, w_r + \lambda(\frac{w}{r} + \ u_x) + \frac{\lambda + 2\mu + m}{2}\, u_r^2 + (\lambda + 2l)\, w_r \frac{w}{r} + \\ + \frac{\lambda + 2l}{2} \frac{w^2}{r^2} + (\lambda + 2l)\, u_x w_r + (2l - 2m + n)\, u_x \frac{w}{r} + \\ \frac{\lambda + 2l}{2}\, u_x^2 + \frac{\lambda + 2\mu + m}{2}\, w_x^2 \ + (\mu + m)\, u_r w_x + \\ \frac{3\lambda + 6\mu + 2l + 4m}{2}\, w_r^2 + 2J^*(2u_{xtt} + w_{rtt}) - 2a_1 u_{xxx} - \\ 2(a_1 + 2a_2) w_{xxr} - 2(a_1 + a_2) \frac{1}{r} \left(r(w_{rr})\right)_r - a_1 \frac{1}{r} \left(r(u_{xr})\right)_r , \end{aligned} \quad (4.82)$$

$$\begin{aligned} P_{rx} = \mu\, (u_r + w_x) + (\lambda + 2\mu + m)\, u_r w_r + (2\lambda + 2m - n)\, u_r \frac{w}{2r} + \\ (\lambda + 2\mu + m)\, u_x u_r + \frac{2m - n}{2}\, w_x \frac{w}{r} + (\mu + m)\, w_x w_r + \\ (\mu + m)\, u_x w_x \ + 2J^* u_{rtt} - a_1 w_{xrr} - 2(a_1 + 2a_2) u_{xxr} - \\ 2a_2 \frac{1}{r} \left(r(u_{rr})\right)_r . \end{aligned} \quad (4.83)$$

Then the approximations for the components of the displacement vector have the form

$$u = U(x,t) + \frac{\nu r^2}{2} \frac{1}{1 - N} U_{xx}, \quad (4.84)$$

$$w = -\nu r U_x - \frac{4J^*(2-\nu)(1+\nu)(1-2\nu)}{E(3-2\nu)R^2} r^3 U_{xtt} - \frac{\nu^2-(1-2\nu)(1-N)(G(1-\nu)-2\nu N)}{2(3-2\nu)(1-N)} r^3 U_{xxx} - (1+\nu)\left[\frac{\nu}{2} + \frac{(1-2\nu)}{E}\left(l(1-2\nu)^2 + 2m(1+\nu) - n\nu\right)\right] r U_x^2, \quad (4.85)$$

where $G = 2a_1/\mu R^2$, $N = 2a_2/\mu R^2$. Like in previous section the governing equation for longitudinal strain $v = U_x$ is the double dispersive equation (4.79) whose coefficients are defined now as

$$\alpha_1 = c_*^2, \alpha_2 = \frac{\beta}{2\rho_0}, \alpha_3 = \frac{\nu R^2}{2(1-N)} - \frac{\nu^2 R^2}{2} + 2J^*\nu(2-\nu), \alpha_4 = \frac{\nu c_*^2 R^2}{2(1-N)},$$

while the solitary wave solution has the form

$$v = \frac{3E}{\beta}\left(\frac{V^2}{c_*^2} - 1\right) \cosh^{-2}(k\,(x - Vt)), \quad (4.86)$$

where V is a free parameter, and the wave number k is defined by

$$k^2 = \frac{(1-N)\rho_0(V^2 - c_*^2)}{2\nu E R^2\left[c_*^2 - V^2\,(1-\nu(1-N) + 4J^*(1-N)(2-\nu)/R^2)\right]}. \quad (4.87)$$

Physically reasonable case corresponds to rather small N, $N < 1$. Then the influence of the microstructure yields an alteration of the permitted solitary wave velocities interval,

$$1 < \frac{V^2}{c_*^2} < \frac{1}{1-\nu(1-N) + 4J^*(1-N)(2-\nu)/R^2}.$$

The widening or narrowing of the interval depends upon the relationship between N and the parameter of microinertia J^*. Again the type of the solitary wave is governed by the sign of the nonlinearity parameter β. At the same time the characteristic width of the solitary wave proportional to $1/k$ turns out smaller than the wave width in a pure macroelastic case, $N = 0$, $J^* = 0$.

4.3.4 *Concluding remarks*

It is to be noted that the assumption of the linear contribution of the microstructure is correct since its nonlinear contribution, being weaker, may provide alterations only in the neglected higher-order nonlinear and dispersion terms in the governing equation both the Cosserat and the Le

Roux models. Hence we don't need in the additional nonlinear terms in the density of the potential energy Π thus avoiding the additional unknown parameters (like Murnaghan's third order moduli) describing the nonlinear contribution of the microstructure Eringen and Suhubi (1964); Erofeev (2002).

The alterations of the amplitude and the wave width, caused by the microstructure, have been found in both case under study. The important result is in the opposite changing of the wave width which gives a possibility to distinguish the Cosserat and the Le Roux models in possible experiments.

The dispersion caused by the microstructure may be observed experimentally, and numerical data on microstructure parameters my be obtained Savin *et. al* (1973b). In experiments on the solitary waves propagation, see Sec. 3.4, the amplitude and the width of the wave may be measured. Therefore expressions (4.80), (4.81) provide possible estimation of the parameter M in the pseudo-continuum Cosserat model. In case of the LeRoux continuum there is an extra parameter J^*, see Eqs.(4.86), (4.87), and parameters N and J^* cannot be estimated separately.

The microstructure and the surrounding medium provide similar deviations in the governing double dispersive equation. Hence the analysis in Sec. 4.2.6 may be used if we consider a rod only part of which contains the microstructure. Then the amplification/attenuation (but not a selection) of the strain solitary wave occurs similar to that shown in Figs. 4.6-4.10.

Chapter 5

Influence of dissipative (active) external medium

Now we study the role played by dissipation/energy influx often present in a realistic case. Dissipative/active effects may be caused by internal features of the elastic material, hence, an irreversible part should be included into the stress tensor in addition to the reversible one depending only upon the density of the Helmholtz energy. Accordingly, the governing equations for nonlinear strains will contain dissipative/active terms. Dissipation/energy influx may also occur in an elastic wave guide through phenomena occurring at or through its lateral surface, and this case is considered further in this Chapter. Presence of external medium makes a problem more complicated. However, the Hamiltonian formalism described in Chapter 3 may be applied since a wave guide remains pure elastic, all dissipative/active factors come through the elementary work done by the external forces, and therefore Eq.(3.29) may be used.

5.1 Contact problems: various approaches

External medium affects the lateral surface of a wave guide through the normal and tangential stresses. In some cases only normal stresses may act like in the slippage contact. Various contact problems are widely considered, see, e.g., Galin (1980); Goryacheva (1998); Goryacheva (2001); Hähner and Spencer (1998); Johnson (1985); Kalker *et. al* (1997); Kerr (1964); Nikitin (1998). Both elastic and viscoelastic interactions are studied their in the linear approximation. Main attention is paid to the static loading and to the interaction forces caused by the relative movement of the contacting bodies. Of special interest if the contact with friction Goryacheva (1998); Goryacheva (2001); Hähner and Spencer (1998); Kalker *et. al* (1997); Nikitin (1998); Stefański *et. al* (2000) . Various generalizations of the

Coulomb-Amonton law (dependence on the sliding velocity and the apparent area of contact) are studied Elmer (1997); Goryacheva (2001); Hähner and Spencer (1998); Nikitin (1998); Pöschel and Herrmann (1993); Stefański *et. al* (2000). However, it was noted in Hähner and Spencer (1998); Nikitin (1998); Stefański *et. al* (2000) that the classical Coulomb-Amonton approach is sufficient when the relative velocity of the sliding bodies is small.

Sometimes the problem of the interaction with an external medium may be solved directly. It means that we formulate the equation for a wave guide and the medium and impose the corresponding continuity conditions on the lateral surface of the wave guide. An example may be found in Sec. 4.2 where dissipationless sliding contact with an elastic external medium is considered. The difficulties of elastic contact stress theory may arise because the displacement at any point in the contact surface depends upon the distribution of pressure throughout the whole contact Johnson (1985). In this case the solution of an integral equation for the pressure is required. Another problem arises when an external medium is not elastic, and its behavior cannot be described by the equations of elasticity. The difficulties mentioned above may be avoided if the response of a wave guide is more interesting then the displacements and stresses distribution in the external medium. In this case the problem reduces to a development of a relatively simple foundation models to account for an influence of the external medium in terms of the wave guide displacements and/or strains at the lateral surface. Variety of the foundation models are collected in Kerr (1964). The models are designed replacing an external medium with interacting spring and dissipative elements. In particular, when only springs are considered and their shear interactions are assumed the so-called Winkler-Pasternak model holds Kerr (1964); Pasternak (1954); Winkler (1867). According to it the pressure p is expressed through the shear displacement w

$$p = kw - G\nabla^2 w,$$

where ∇^2 is the Laplace operator in x and y, k and G are the constant foundation moduli. One can see its similarity with the response of the external medium in case of the sliding contact, see Sec. 4.2.3. Hence foundation models are physically reasonable since they correspond to the results obtained from the contact problem solutions.

It was Kerr (1964) who developed a viscoelastic foundation model.

Based on the results of footing load tests performed on a snow base he proposed a viscoelastic model for the interaction between an elastic body and the external snow (or permafrost) medium. He assumed Newton's law for the viscous behavior thus including a dissipative elements besides springs. This model will be studied in the following two sections where its mathematical expression is presented. Now we only mention it provides the influence on a wave guide only through the normal stresses. Classic case of a dissipative action through the tangential stresses corresponds to the dry friction contact Hähner and Spencer (1998); Nikitin (1998). Here the foundation model is proposed in Sec. 5.4 when the external medium affects a lateral surface of an elastic rod both by the normal and the tangential stresses but dissipative (active) influence is provided by the tangential stresses.

5.2 Evolution of bell-shaped solitary waves in presence of active/dissipative external medium

5.2.1 *Formulation of the problem*

Let us consider the propagation of a longitudinal strain wave in an isotropic cylindrical elastic rod embedded in an external medium subjected to Kerr's viscoelastic contact model. Most of results were first obtained by Porubov and Velarde (2000) [1]. We take cylindrical Lagrangian coordinates (x, r, φ) where x is directed along the axis of the rod, $-\infty < x < \infty$, r is the radial coordinate, $0 \leq r \leq R$, φ is a polar angle, $\varphi \, \epsilon[0, 2\pi]$. Assuming that torsions can be neglected, then the displacement vector is $\vec{V} = (u, w, 0)$. According to Kerr (1964) the external medium yields a normal stress P^*_{rr} on the lateral surface of the rod $r = R$:

$$P^*_{rr} = -\frac{k}{r} w - \eta \, w_t + \chi \, r^2 \, w_{xxt}, \tag{5.1}$$

where t is a time, k is the stiffness coefficient of the medium, η is the viscocompressibility coefficient of the external medium, χ is the viscosity coefficient of the external medium. All three coefficients, k, η and χ, are positive and constant in framework of the Kerr model, however, we consider a more general case with the coefficients of either sign.

The evolution of nonlinear waves is obtained in the reference configuration using Hamilton's principle Eq.(3.29)), where the Lagrangian density

[1] Reprinted with permission from Elsevier Science

per unit volume, $\mathcal{L}$, is defined as before in the book. Again we choose Murnaghan's approximation (3.1) for the deformation energy. Due to (5.1) the elementary work, δA, is:

$$\delta A = 2\pi \int_{-\infty}^{\infty} P^*_{rr}\, \delta w\, dx\,. \tag{5.2}$$

The boundary conditions (b.c.) are:

$$w \to\ 0, \qquad\qquad \text{at } r\ \to\ 0, \tag{5.3}$$

$$P_{rr}\ = P^*_{rr}\ , \qquad\qquad \text{at } r\ =\ R, \tag{5.4}$$

$$P_{rx}\ =\ 0, \qquad\qquad \text{at } r\ =\ R, \tag{5.5}$$

where the components $P_{rr},\ P_{rx}$ of the Piola - Kirchhoff stress tensor $\mathbf{P}$ are defined by Eqs. (3.10), (3.11).

5.2.2 *Dissipation modified double dispersive equation*

For the longitudinal and shear displacements inside the rod we assume that:

(i) pure elastic waves have strain magnitude $B << 1$;

(ii) a characteristic strain wave length L is greater then the rod radius R, $R/L << 1$.

Let us obtain the approximations satisfying b.c. (5.3)- (5.5). According to the procedure developed in Chapter 3 the unknown functions $u,\ w$ are expanded in a power series (3.12), (3.13). Substituting them into the boundary conditions and following the approach from Sec. 3.2 we get

$$u = U + a_2\, r^2\, U_{xx} + a_3\, r^3\, U_{xxt}, \tag{5.6}$$

$$\begin{aligned} w = b_1\, r\, U_x + b_2\, r^2\, U_{xt} + \ r^3\, (b_{31}\, U_{xxx} + b_{32}\ U_{xtt}) + \\ r^4\, (b_{41}\ U_{xxxt} + b_{42}\ U_{xttt}) + B_1\, r\, U_x^2 + B_2\, r^2\, U_x\, U_{xt}. \end{aligned} \tag{5.7}$$

where the explicit forms for the coefficients are given by

$$a_2 = \frac{\lambda}{2(2(\lambda+\mu)+k)},\ a_3 = -\frac{\lambda\,\eta}{3(2(\lambda+\mu)+k)(3\lambda+4\mu+k)},$$

$$b_1 = -2\,a_2,\ b_2 = -3\,a_3,\ b_{31} = -\frac{\lambda\, a_2}{2(2\lambda+3\mu)+k},$$

$$b_{32} = \frac{3\eta\, a_3}{2(2\lambda+3\mu)+k},\ b_{41} = -\frac{2\chi\, a_2 + \eta\, b_{31} + \lambda\, a_3}{5\lambda+8\mu+k},\ b_{42} = -\frac{\eta\, b_{32}}{5\lambda+8\mu+k},$$

$$B_1 = -\frac{2\, b_1(\lambda+4l-2m+n) + 8a_2^2[3(\lambda+\mu)+2(2l+m)] + \lambda + 2l}{2(2(\lambda+\mu)+k)},$$

$$B_2 = -\frac{2\eta\, B_1 + 12a_2\ a_3[3(\lambda+\mu)+2(2l+m)] - 3\, a_3(\lambda+4l-2m+n)}{3\lambda+4\mu+k}.$$

Note that a_2, b_2, b_{42} are always positive, while a_3, b_1, b_{31}, b_{32} are always negative, while the remaining coefficients may have either sign. Due to (3.1) we have to truncate the series (5.6), (5.7), hence, omitting nonlinear terms of order three and higher. Neglecting cubic nonlinear terms we have to neglect simultaneously the "corresponding" higher order linear derivative terms. It was shown in that solitary waves appear as a result of the balance between nonlinearity and dispersion when B is of order $(R/L)^2$. The "largest" of the cubic terms is $rU_x^3 \sim RB^3 \sim R(R/L)^6$. Then, the "corresponding" comparable linear term is r^5U_{xxxxx}, while quadratic terms are $r^3U_xU_{xxx}$ and $r^3(U_{xx})^2$. Similar terms with spatio-temporal mixed derivatives are of the same order. Higher order terms may be added if terms like I_1^4 are taken into account, see (3.4).

Using Hamilton's principle we obtain that longitudinal strains, $v = U_x$, obey a dissipation modified double dispersive nonlinear equation (DMDDE):

$$v_{tt} - \alpha_1\, v_{xx} - \alpha_2\, v_{xxt} - \alpha_3(\, v^2)_{xx} - \alpha_4\, v_{xxxx} + \alpha_5\, v_{xxtt} -$$

$$\alpha_6\, (v^2)_{xxt} - \alpha_7\, v_{xxxxt} + \alpha_8\, v_{xttt} = 0. \tag{5.8}$$

The explicit forms of the coefficients α_i, $i = 1, ..., 8$, are

$$\alpha_1 = \frac{8a_2^2\,(2(\lambda+\mu)+k) - 8\lambda\, a_2 + \lambda + 2\mu}{\rho_0},\ \alpha_2 = \frac{8R\,\eta\, a_2^2}{\rho_0},$$

$$\alpha_3 = \frac{3}{\rho_0}[\lambda\left(\frac{1}{2} + 2B_1 - 2a_2(1+4B_1) + 4a_2^2(1-4a_2)\right) +$$

$$\mu\left(1 - 8a_2B_1 - 16a_2^3\right) - 4ka_2B_1 +$$

$$l\left(\frac{1}{3} - 4a_2(1 - 4a_2 + \frac{16}{3}a_2^2)\right) + \frac{2}{3}m(1 - 4a_2^2(3+4a_2)) + 4na_2^2],$$

$$\alpha_4 = \frac{R^2}{\rho_0}\left[(\lambda + 2\mu - 4\lambda\, a_2)\, a_2 + 4(\lambda - 2(2\lambda + 2\mu + k)\, a_2)\, b_{31}\right],$$

$$\alpha_5 = \frac{R^2}{2\rho_0}[2\rho_0\, a_2(1 - 2a_2) - 8\lambda\, b_{32} + 9(9\lambda + 10\mu + 4k)a_3^2 +$$

$$16(2\lambda + 2\mu + k)a_2\, b_{32}],\ \alpha_6 = -\frac{8R\, a_2\, \eta B_1}{\rho_0},\ \alpha_7 = -\frac{8R^3\, a_2}{\rho_0}\left[\eta\, b_{31} + \chi\, a_2\right],$$

$$\alpha_8 = \frac{4R^3\, \eta}{\rho_0}\left[4a_2\, b_{32} + 9a_3^2\right].$$

The coefficients in Eq.(5.8) may take either sign depending upon the material properties of the rod and the values of k, η and χ. Higher order terms, $(v^3)_{xx}$, v_{6x} etc., have been neglected when deriving Eq.(5.8) in accordance with the early given arguments.

5.2.3 *Exact solitary wave solutions of DMDDE*

In the moving frame, $\theta = x - V\,t$, we assume that $v = v(\theta)$ and obtain from (5.8) the following ODE:

$$(V^2 - \alpha_1)v + \alpha_2\, V\, v' - \alpha_3\, v^2 - (\alpha_4 - \alpha_5\, V^2)v'' + \alpha_6\, V\, (v^2)' + V(\alpha_7 - \alpha_8 V^2)v''' +$$

$$P + P_1\theta = 0, \tag{5.9}$$

where a dash, $'$, denotes $\partial/\partial\theta$; P and P_1 are constants of integration. We are interested in bell- shaped or kink- shaped solitary waves when $v \to const$ at $\mid \theta \mid \to \infty$, hence, $P_1 = 0$. It is seen that Eq.(5.9) coincides with the ODE reduction of the DMKdV Eq.(1.13) obtained in the study of long waves in surface tension gradient-driven flows Nekorkin and Velarde (1994); Nepomnyashchy and Velarde (1994). Its most general exact solution expressed in terms of the Weierstrass elliptic function has been obtained in Sec. 2.1.3. Here we restrict consideration to its bell-shaped solitary wave limit,

$$v = A\, k^2\, \cosh^{-2}(k\,\theta) - B, \tag{5.10}$$

with

$$A = \frac{6(\alpha_6\alpha_7 - \alpha_1\,\alpha_6\,\alpha_8 + \alpha_2\,\alpha_3\,\alpha_8)}{\alpha_6^2},\ B = \frac{A}{3}k^2 + \frac{\alpha_2}{2\alpha_6},$$

$$V^2 = \alpha_1 - \frac{\alpha_2\,\alpha_3}{\alpha_6}. \tag{5.11}$$

provided

$$\alpha_6(\alpha_4\alpha_6 - \alpha_3\alpha_7) = (\alpha_1\alpha_6 - \alpha_2\alpha_3)(\alpha_5\alpha_6 - \alpha_3\alpha_8). \tag{5.12}$$

Thus, the elastic features of the rod and the values of the parameters k, η and χ of the external medium determine the existence of exact bell-shaped strain wave solution (5.10) as well as the sign of its amplitude, A, hence, the propagation of either compression or tensile strain solitary waves. The relationship (5.12) provides simultaneously a balance between nonlinearity (v^2) and dispersion ($v^{''}$) and another balance between nonlinear active/dissipative ($(v^2)^{'}$) and linear active/dissipative ($v^{'''}$) terms .

With Eqs.(5.11), (5.12) taken into account, Eq.(5.9) may be written as

$$(V\frac{\partial}{\partial\theta} - \frac{\alpha_3}{\alpha_6})\left(\alpha_2 v + \alpha_6\, v^2 + \frac{\alpha_6(\alpha_4 - \alpha_5 V^2)}{\alpha_3}\, v^{''} - \frac{\alpha_6\, P}{\alpha_3}\right) = 0. \tag{5.13}$$

The ODE reduction of the Boussinesq (or KdV) equation appears in brackets. However, here the wavenumber k is not a free parameter of the solution (5.10), as it is prescribed by the behaviour as $\mid\theta\mid\rightarrow\infty$. In particular, when a solution decaying at infinity is considered, then

$$k^2 = -\frac{\alpha_2}{4(\alpha_7 - \alpha_8\, V^2)}, \tag{5.14}$$

thus implying yet another restriction on the coefficients,

$$\alpha_8\left(\alpha_1 - \frac{\alpha_2\,\alpha_3}{\alpha_6}\right) - \alpha_7 > 0. \tag{5.15}$$

Eq. (5.8) also admits kink-type solutions of the form

$$v = A\,k^2\cosh^{-2}(k\theta) + D\,k\,\tanh(k\theta) + C, \tag{5.16}$$

with

$$A = \frac{6(\alpha_7 - \alpha_8\, V^2)}{\alpha_6},\; D = \frac{6(\alpha_3(\alpha_7 - \alpha_8\, V^2) - \alpha_6(\alpha_4 - \alpha_5\, V^2))}{5\alpha_6},$$
$$C = \frac{V^2 - \alpha_1}{2\alpha_3}. \tag{5.17}$$

There are two possibilities for k and V. On the one hand

$$k = \frac{1}{10}\left|\frac{\alpha_4 - \alpha_5\, V^2}{V(\alpha_7 - \alpha_8\, V^2)} - \frac{\alpha_3}{\alpha_6}\right|, \tag{5.18}$$

where V is a solution of the cubic equation,

$$\alpha_3^3\alpha_8\,V^3-\alpha_6(\alpha_6^2-\alpha_3^3\,\alpha_5)V^2-(\alpha_3^3\,\alpha_7+\alpha_2\,\alpha_3\,\alpha_6^2)V+\alpha_6(\alpha_1\alpha_6^2+\alpha_3^2\,\alpha_4)=0. \tag{5.19}$$

On the other hand,

$$k^2=\frac{1}{4}\left(\frac{6\alpha_3^2}{\alpha_6^2}-\frac{(V^2-\alpha_1)\alpha_6+\alpha_2\alpha_3 V}{\alpha_3 V(\alpha_7-\alpha_8\,V^2)}\right), \tag{5.20}$$

where V is a solution of another cubic equation,

$$6\alpha_3\alpha_8\,V^3+\alpha_6\alpha_7V^2-6\alpha_3\alpha_7\,V+\alpha_4\,\alpha_6=0. \tag{5.21}$$

Therefore, we have in both cases the kink-shaped solution (5.16) with prescribed parameters. An initial prestressed state of the rod may transform into a different one as the wave passes. The loading or unloading of the rod depends upon the sign of D, hence on the elastic features of the rod and on the parameter values of the external medium.

5.2.4 *Bell-shaped solitary wave amplification and selection*

Let us consider the case when the influence of the external medium is weak, and all coefficients of the active/dissipative terms in DMDDE (5.8) are small relative to the other coefficients, i.e., $\alpha_2=\varepsilon\,\beta_2$, $\alpha_6=\varepsilon\,\beta_6$, $\alpha_7=\varepsilon\,\beta_7$, $\alpha_8=\varepsilon\,\beta_8$, $\varepsilon<<1$. Then Eq.(5.8) may be written as

$$v_{tt}-\alpha_1\,v_{xx}-\alpha_3(\,v^2)_{xx}-\alpha_4\,v_{xxxx}+\alpha_5\,v_{xxtt}=$$

$$\varepsilon\left(\beta_2\,v_{xxt}+\beta_6\,(v^2)_{xxt}+\beta_7\,v_{xxxxt}-\beta_8\,v_{xxttt}\right). \tag{5.22}$$

We see that the left hand side of Eq.(5.22) is the double dispersive equation. Thus at $\varepsilon=0$, Eq.(5.22) admits an exact bell-shaped solitary wave solution. For nonzero ε we assume that a solution of Eq.(5.22) is a function of the phase variable θ and the slow time T, $v=v(\theta,\,T)$, with

$$\theta_x=1,\ \theta_t=-V(T),\ T=\varepsilon\,t.$$

Then from (5.22) we get that

$$(V^2-\alpha_1)v_\theta-\alpha_3(\,v^2)_\theta-(\alpha_4-\alpha_5V^2)\,v_{\theta\theta\theta}=$$

$$\varepsilon(2V[v_T+\alpha_5\,v_{\theta\theta T}]+V_T[v+\alpha_5\,v_{\theta\theta}]-V\frac{\partial^2}{\partial\theta^2}[\beta_2\,v+\beta_6\,v^2+$$
$$(\beta_7\,-\beta_8V^2)\,v_{\theta\theta}])+O(\varepsilon^2). \tag{5.23}$$

The solution of Eq.(5.23) is sought using the method explained in Sec. 2.2.2 in the form

$$v = v_0 + \varepsilon v_1 + ... \tag{5.24}$$

Substituting (5.24) into (5.23) in the leading order we have

$$(V^2 - \alpha_1)v_{0,\theta} - \alpha_3(\, v_0^2)_\theta - (\alpha_4 - \alpha_5 V^2)\, v_{0,\theta\theta\theta} = 0 \tag{5.25}$$

The exact solitary wave solution of Eq.(5.25) has the form

$$v_0 = A(T)\cosh^{-2}(k(T)\,\theta), \tag{5.26}$$

with

$$A = \frac{3(V^2 - \alpha_1)}{2\,\alpha_3},\ k^2 = \frac{V^2 - \alpha_1}{4(\alpha_4 - \alpha_5 V^2)}. \tag{5.27}$$

Accordingly, $s = V^2$ may lie either inside the interval

$$\alpha_1 < s < \frac{\alpha_4}{\alpha_5},\ \text{if}\ \alpha_4 - \alpha_1\alpha_5 > 0, \tag{5.28}$$

or in

$$\frac{\alpha_4}{\alpha_5} < s < \alpha_1,\ \text{if}\ \alpha_4 - \alpha_1\alpha_5 < 0. \tag{5.29}$$

Only the interval (5.28) is acceptable for a free rod with positive Poisson ratio. The interval (5.29) exists if the viscocompressibility coefficient is greater than a given value, $\eta > \eta^*$, with

$$\eta^* = \frac{\sqrt{\rho_0}(k + 3\lambda + 4\mu)}{\sqrt{4k + 9\lambda + 10\mu}}.$$

The correction v_1 (5.24) obeys the inhomogeneous linear equation

$$(V^2 - \alpha_1)v_{1,\theta} - 2\alpha_3\,(v_0\, v_1)_\theta - (\alpha_4 - \alpha_5 V^2)\, v_{1,\theta\theta\theta} = F, \tag{5.30}$$

where F is

$$F = 2V[v_{0,T} + \alpha_5\, v_{0,\theta\theta T}] + V_T[v_0 + \alpha_5\, v_{0,\theta\theta}] -$$

$$V\frac{\partial^2}{\partial\theta^2}\left[\beta_2\, v_0 + \beta_6\, v_0^2 + (\beta_7\, - \beta_8 V^2)\, v_{0,\theta\theta}\right].$$

The operator M acting on the function v_1 in Eq.(5.30) is adjoint to the operator

$$M^A = (\alpha_1 - V^2)\partial_\theta + 2\alpha_3\, v_0\partial_\theta + (\alpha_4 - \alpha_5 V^2)\,\partial_\theta^3.$$

Table 5.1 Selection of solitary wave velocity for the case $\alpha_4 - \alpha_1\alpha_5 > 0$.

q_1	s_{1q}	s_{2q}	s_0	s^*
> 0	$(\alpha_1; s_Q)$	$(\alpha_4/\alpha_5; \infty)$	$(\alpha_1; s_Q)$	s_{1q}
> 0	$(\alpha_1; s_{2q})$	$(s_{1q}; s_Q)$	$(\alpha_1; s_{2q})$	s_{1q}
> 0	$(\alpha_1; s_Q)$	$(s_Q; \alpha_4/\alpha_5)$	$(\alpha_1; s_Q)$	s_{1q}
> 0	$(\alpha_1; s_Q)$	$(s_Q; \alpha_4/\alpha_5)$	$(s_Q; \alpha_4/\alpha_5)$	s_{2q}
> 0	$(s_Q; s_{2q})$	$(s_{1q}; \alpha_4/\alpha_5)$	$(s_{1q}; \alpha_4/\alpha_5)$	s_{2q}
> 0	$(0; \alpha_1)$	$(s_Q; \alpha_4/\alpha_5)$	$(s_Q; \alpha_4/\alpha_5)$	s_{2q}
< 0	$(0; \alpha_1)$	$(\alpha_1; s_Q)$	$(\alpha_1; s_Q)$	s_{2q}
< 0	$(\alpha_1; s_{2q})$	$(s_{1q}; s_Q)$	$(s_{1q}; s_Q)$	s_{2q}
< 0	$(s_Q; s_{2q})$	$(s_{1q}; \alpha_4/\alpha_5)$	$(s_Q; s_{2q})$	s_{1q}
< 0	$(s_Q; \alpha_4/\alpha_5)$	$(\alpha_4/\alpha_5; \infty)$	$(s_Q; \alpha_4/\alpha_5)$	s_{1q}

Then using Eq.(5.25) one can obtain the solvability condition (2.43) for Eq.(5.30),

$$\int_{-\infty}^{\infty} v_0 \, F \, d\theta = 0, \tag{5.31}$$

which yields the equation for the function s,

$$s_T \, Q_3(s) = s \, (s - \alpha_1)^2 (q_1 \, s^2 + q_2 \, s + q_3), \tag{5.32}$$

with

$$Q_3(s) = \alpha_1\alpha_4(5\alpha_4 - \alpha_1\alpha_5) + 2\alpha_4(11\alpha_1\alpha_5 - 10\alpha_4) \, s -$$

$$3\alpha_5(17\alpha_4 - 5\alpha_1\alpha_5) \, s^2 - 30\alpha_5^2 \, s^3, \tag{5.33}$$

$$q_1 = 12\alpha_5\beta_6 - 5\alpha_3\beta_8, \; q_2 = 12\beta_6(\alpha_4 - \alpha_1\alpha_5) + \alpha_3(7\beta_2\alpha_5 - 5\beta_7 + 5\alpha_1\beta_8), \tag{5.34}$$

$$q_3 = \alpha_3(7\beta_2\alpha_4 + 5\alpha_1\beta_7) - 12\alpha_1\alpha_4\beta_6.$$

Important features of the behavior of s may be established analyzing (5.32) without integration. Note that $Q_3(\alpha_1) = -15\alpha_1(\alpha_4 - \alpha_1\alpha_5)^2$ while $Q_3(\alpha_4/\alpha_5) = \alpha_4/\alpha_5 \, (\alpha_4 - \alpha_1\alpha_5)^2$, and Q_3 always changes its sign inside the interval $(\alpha_1, \alpha_4/\alpha_5)$ permitted for s. The most interesting evolution of s is realized when s tends to the finite constant value s^* as $T \to \infty$. The values of s^* are the solutions of equation

$$q_1 \, s^2 + q_2 \, s + q_3 = 0. \tag{5.35}$$

First, consider the case $\alpha_4 - \alpha_1\alpha_5 > 0$. Then $\alpha_1 < s < \alpha_4/\alpha_5$, and Q_3 cannot have more than one root inside the interval (5.28). Assume that the root of Q_3 is s_Q while real roots of Eq.(5.35) are $s_{1q} < s_{2q}$. We denote by s_0 the initial value of s. All possibilities of the solitary wave velocity selection are collected in Table 5.1. The most interesting case corresponds to q_1 positive when $s_{1q} \in (\alpha_1; s_Q)$, $s_{2q} \in (s_Q; \alpha_4/\alpha_5)$. Table 5.1 shows (see third and fourth rows) that two different solitary waves may be selected depending on the initial value s_0. Moreover, any initially initial solitary wave with velocity s_0 from the permitted interval (5.28) transforms into a dissipative solitary wave (5.26). Here we are dealing with the selection of a symmetric solitary wave. It occurs according to Fig. 1.17, the only difference is the presence of two thresholds, s_{1q} and s_{2q}.

When Eq.(5.35) has no multiple root, $s_{1q} = s_{2q} = s_q$, s tends to $s^* = s_q$ at $q_1 > 0$ if

$$\alpha_1 < s_q < s_Q,\ \alpha_1 < s_0 < s_q, \text{or } \ s_Q < s_q < \alpha_4/\alpha_5,\ s_q < s_0 < \alpha_4/\alpha_5.$$

For negative values of q_1 we also have two possibilities

$$\alpha_1 < s_q < s_Q,\ \alpha_1 < s_0 < s_Q, \text{or } \ s_Q < s_q < \alpha_4/\alpha_5,\ s_Q < s_0 < s_q.$$

The same analysis may be performed for the case $\alpha_4 - \alpha_1\alpha_5 < 0$. Under conditions (5.12) the asymptotic solution (5.26) coincides with the exact solution (5.10).

We consider here in details only the cases when the velocity tends to one or another root of Eq.(5.35). Other possibilities corresponding to the blow-up or the damping of the solitary wave (5.26) may be similarly studied.

There remains the problem of whether solitary wave selection is achieved in finite or infinite time. Eq. (5.32) may be integrated in the general case giving the implicit dependence of s on T. In order to avoid cumbersome algebra we consider one particular case only, $\alpha_1 = 1$, $\beta_2 = 1$, $\alpha_3 = 1$, $\alpha_4 = 2$, $\alpha_5 = 1$, $\beta_6 = 2$, $\beta_7 = 1$, $\beta_8 = 1$, $\varepsilon = 0.1$. Then the permitted interval for s is $(1, 2)$, and $Q_3(s)$ has only one root, $s_Q = 1.588$, inside this interval. For the roots of Eq.(5.35) we have $s_{1q} = 1.324$, $s_{2q} = 1.745$. Therefore, this is the case of complete selection when all initially dissipationless solitons with initial velocity from the interval $1 < s_0 < 1.588$ transform into a dissipative solitary wave with velocity $s^* = 1.588$. When $1.588 < s_0 < 2$ they go to a dissipative solitary wave with $s^* = 1.745$. Integration of Eq. (5.32) yields

$$\exp T = \left|\frac{s_0 - s_{1q}}{s - s_{1q}}\right|^{p_1} \left|\frac{s_0 - s_{2q}}{s - s_{2q}}\right|^{p_2} \left(\frac{s-1}{s_0 - 1}\right)^{p_3} \left(\frac{s_0}{s}\right)^{p_4} \exp\left[\frac{p_5(s - s_0)}{(s-1)(s_0 - 1)}\right],$$

with $p_1 = 7.904$, $p_2 = 0.420$, $p_3 = 8.980$, $p_4 = 0.657$, $p_5 = 4.286$. One can see that $s \to s_{1q}$ or $s \to s_{2q}$ at $T \to \infty$. Hence the wave amplitudes tend to $A_1 = 3(s_{1q} - \alpha_1)/2\,\alpha_3$ or to $A_2 = 3(s_{2q} - \alpha_1)/2\,\alpha_3$.

Of special interest is the evolution of an arbitrary initial pulse. It cannot be described by the asymptotic solution. We already noted the similarity between the governing equation (5.8) and the DMKdV equation (1.13). For the last equation it was found that the single wave asymptotic solution accounts for a behaviour of the solitary waves generated from an arbitrary input, see Sec. 2.3.1. Hence we can anticipate the evolution of the initial localized strains according to that shown in Figs. 2.4-2.6.

5.2.5 *Concluding remarks*

We have obtained a nonlinear equation, DMDDE (5.8), governing the evolution of bulk longitudinal long nonlinear strain waves in an elastic rod immersed inside an active/ dissipative medium. There is an interesting similarity with the results found for free surface shear long waves in a thermoconvective liquid layer described by a dissipation modified Korteweg-de Vries equation (DMKdV), see Christov and Velarde (1995); Garazo and Velarde (1991); Nekorkin and Velarde (1994); Velarde *et. al* (1995); Nepomnyashchy and Velarde (1994). Indeed, in the "travelling wave" limit the ODE reduction of our DMDDE (5.9) is functionally identical to the corresponding ODE reduction of the DMKdV equation Christov and Velarde (1995); Nekorkin and Velarde (1994). Consequently, all exact travelling wave solutions for the latter equation are valid in our case. The dynamical system representation of Eq.(5.9),

$$\begin{aligned} \dot{v} &= y, \\ \dot{y} &= z, \\ \dot{z} &= -\beta\, z - \alpha\, v\, y - \nu\, y - G(v) + P, \end{aligned}$$

with

$$\alpha = \frac{2\alpha_6}{\alpha_7 - \alpha_8 V^2},\ \beta = -\frac{\alpha_4 - \alpha_5 V^2}{V(\alpha_7 - \alpha_8 V^2)},\ \nu = \frac{\alpha_2}{\alpha_7 - \alpha_8 V^2},$$

$$G(v) = \frac{\alpha_1 - V^2}{V(\alpha_7 - \alpha_8 V^2)}\, v + \frac{\alpha_3}{V(\alpha_7 - \alpha_8 V^2)}\, v^2.$$

coincides with the system studied by Nekorkin and Velarde (1994); Velarde *et. al* (1995) when $P = 0$. Therefore, we can transfer to the lon-

gitudinal strain waves all the results about the existence of pulses, "bound solitons" and "chaotic states" found for the DMKdV equation in Christov and Velarde (1995); Nekorkin and Velarde (1994); Velarde *et. al* (1995).

In order to get conservation laws for DMDDE (5.8) we have to rewrite it as

$$v_t = -g_x,$$
$$g_t = \alpha_1\, v_x + \alpha_2\, v_{xt} + \alpha_3(\, v^2)_x + \alpha_4\, v_{xxx} - \alpha_5\, v_{xtt} +$$

$$\alpha_6\, (v^2)_{xt} + \alpha_7\, v_{xxxt} - \alpha_8\, v_{xttt}.$$

Then the time evolution of the wave energy for the solutions vanishing at $\pm\infty$ is governed by the equation

$$\frac{\partial}{\partial t} \int\limits_{-\infty}^{\infty} v\, g\, dx = \alpha_2 \int\limits_{-\infty}^{\infty} v_x\, g_{\,x} dx + \alpha_6 \int\limits_{-\infty}^{\infty} v_x^2\, g_x\, dx -$$

$$\alpha_7 \int\limits_{-\infty}^{\infty} v_{xx}\, g_{xx}\, dx + \alpha_8 \int\limits_{-\infty}^{\infty} v_{xt}\, g_{xt}\, dx. \tag{5.36}$$

Thus, instead of energy conservation we have an input-output energy balance that at the steady state gives a vanishing l.h.s. Indeed, the first term in the right-hand side of (5.36) accounts for the energy input while energy output is provided by the third term. The second term in (5.36) may play a stabilizing or a destabilizing role depending on the sign of α_6. The last term in (5.36) is absent in the corresponding balance law for the DMKdV equation Garazo and Velarde (1991); Nepomnyashchy and Velarde (1994). Here it diminishes the role of the third term in (5.36). These linear mixed derivative terms in (5.8) appear due to the influence of the Poisson effect on the kinetic energy density, K, and on the work, A, done by external forces. These terms decide the existence of either exact compression or tensile solitary wave solutions. Moreover, due to Eq.(5.15) there is no exact solution decaying at $|\theta| \to \infty$ if $\alpha_8 = 0$. The corresponding variation of velocity of the kink-shaped solution depends upon α_8 due to Eqs.(5.19), (5.21). Both the compression and tensile asymptotic solutions occur due to the mixed terms with the velocities from the intervals (5.28), (5.29). Finally, two sets of the selected solitary wave parameters result from the nonzero coefficient q_1 (5.34) in the equation (5.35).

Our predictions about strain solitary wave selection may help to the possible experimental generation of active/dissipative solitary waves in a rod partly embedding in an external medium with the Kerr contact. Indeed, strain solitary waves may be effectively generated inside a rod with a free boundary based on the analysis of the exact travelling solitary wave solution of the governing double dispersive equation (Eq.(5.8) with k, η and χ equal to zero). Also we have shown that the external medium, e.g., the permafrost may be responsible for large wave amplification. Thus our results permit to delineate the yield point of the material. The domain of validity of Kerr's model could be estimated comparing theory with experiments.

5.3 Strain kinks in an elastic rod embedded in an active/dissipative medium

There are two main types of nonlinear solitary waves which could propagate keeping its shape, bell-shaped and kink-shaped solitary waves. The bell-shaped solitary wave usually appears as a result of a balance between nonlinearity and dispersion. Nonlinearity in a pure elastic rod is caused by the finite stress values and the elastic material properties while dispersion results from the finite transverse size of the rod. They are in balance when, for instance, the strain wave magnitude, B, and the wave length, L, are such that $B = O(R^2/L^2) << 1$, where R is the rod radius. Here we address the question of whether besides bell-shaped solitary waves also kink-shaped waves may propagate in an elastic rod. The kink-shaped localized traveling structure may be sustained by different balances. There is a balance between cubic nonlinearity and dispersion, e.g., resulted in the kink solution of the modified Korteweg-de Vries (MKdV) equation case Ablowitz and Segur (1981). Another possibility occurs when nonlinearity is balanced by dissipation (or accumulation), e.g., the kink solution of the Burgers equation Sachdev (1987); Whitham (1974). The inclusion of cubic nonlinearity requires to extend the widely used so-called "five constants" Murnaghan energy model, Eq.(3.1), to a more general "nine constants" Murnaghan model, Eq.(3.4). In view of a possible experimental test of our predictions we consider dissipative (active) phenomena occurring at the lateral boundary of an otherwise purely elastic and hence non-dissipative rod in the bulk Kerr (1964). It allows us to cover both possibilities for longitudinal strain kink propagation. There is also interest in the analytical study of the simultaneous influence of dis-

persion, nonlinearity and dissipation (or accumulation) on the evolution, particularly, amplification, of kinks. As we seen before, mathematically the description of these processes requires inclusion of derivatives of high order in the model equation. Below we shall use the results obtained in Porubov and Velarde (2002) [2].

5.3.1 *Formulation of the problem*

Again we consider the propagation of a longitudinal strain wave in an isotropic cylindrical *compressible* elastic rod embedded in an external medium subjected to Kerr's viscoelastic contact on the lateral surface of the rod $r = R$:

$$P^*_{rr} = -\frac{k}{r}w - \eta\, w_t, \tag{5.37}$$

As will be seen later, the third term in Eq.(5.1) now does nor affect the wave behavior. Again both k and η are assumed to be of either sign.

We choose nine constants Murnaghan's approximation for the density of the potential energy, Eq.(3.4). Thus besides the third order elastic moduli, or the Murnaghan moduli (l, m, n) we are now dealing with the fourth order moduli (a_1, a_2, a_3, a_4) account also for nonlinear elastic properties of the isotropic material. Like Murnaghan's third order moduli moduli, they can be either positive or negative.

Otherwise the statement of the problem is similar to that of the previous section with the exception of the components P_{rr}, P_{rx} of the Piola - Kirchhoff stress tensor $\mathbf{P}$ that are now written in framework of the nine-constants theory, Eq.(3.4),

$$\begin{aligned} P_{rr} = {} & (\lambda + 2\mu)\, w_r + \lambda\, (u_x + \frac{w}{r}) + \frac{\lambda + 2\mu + m}{2}\, (u_r^2 + \ w_x^2\ ) + \\ & \frac{3\lambda + 6\mu + 2l + 4m}{2}\, w_r^2 + (2l - 2m + n)\, u_x \frac{w}{r} + \\ & \frac{\lambda + 2l}{2}\, (u_x^2 + \frac{w^2}{r^2} + 2w_r \frac{w}{r} + 2u_x w_r) + (\mu + m)\, u_r w_x + \\ & (l + 4a_1 + a_2) \left(\frac{w^3}{r^3} + \frac{3ww_r^2}{r} + u_x^3 + 3u_x w_r^2 \right) + (3m - a_2) u_r w_r w_x + \\ & \frac{2l - 2m + n + 24a_1 + 10a_2 + 2a_3 + 4a_4}{2} \left(\frac{u_x w^2}{r^2} + \frac{u_x^2 w}{r} + \frac{2u_x w w_r}{r} \right) + \end{aligned}$$

[2]Reprinted with permission from Elsevier Science

$$(2l-\mu+12a_1+4a_2+2a_4)\left(u_x^2w_r+\frac{w^2w_r}{r^2}\right)+$$
$$(2m-n-2a_2-a_3-2a_4)\frac{u_rww_r}{2r}+2(l+2m+2a_1)w_r^3+$$
$$(2m+\mu-a_2-a_4)u_ru_xw_x+\frac{4l-2a_2-a_3-2a_4}{4}\left(\frac{u_r^2w}{r}+\frac{ww_x^2}{r}\right)+$$
$$\frac{2l+5m-a_2}{2}\left(u_r^2w_r+w_rw_x^2\right)+\frac{2l+2m-a_2-a_4}{2}\left(u_r^2u_x+u_xw_x^2\right), \tag{5.38}$$

$$P_{rx}=\mu\,(u_r+w_x)+(\lambda+2\mu+m)\,(u_rw_r+u_xu_r)+(2\lambda+2m-n)\,u_r\frac{w}{2r}+$$
$$\frac{2m-n}{2}\,w_x\frac{w}{r}+(\mu+m)\,(w_xw_r+u_xw_x)+\frac{2m+a_4}{4}\left(3u_r^2w_x+w_x^3\right)+$$
$$\frac{4l+2m-n-4\mu-2a_2-2a_3}{4}u_rw^2+\frac{2m-n-2a_2-2a_3}{4}\frac{w^2w_x}{r^2}+$$
$$\frac{2m-n-2a_2-a_3-2a_4}{2}\left(\frac{u_xw_xw}{r}+\frac{w_rw_xw}{r}\right)+\frac{4m+a_4}{4}u_r^3+$$
$$(2m+\mu-a_2-a_4)u_xw_rw_x+\frac{4m-4\mu+3a_4}{4}u_rw_x^2+$$
$$\frac{4l-2a_2-a_3-2a_4}{2}\left(\frac{u_xu_rw}{r}+\frac{u_rw_rw}{r}\right)+(2l+2m-a_2-a_4)u_xu_rw_r+$$
$$\frac{2l+5m-a_2}{2}(u_ru_x^2+u_rw_r^2)+\frac{3m-a_2}{2}\left(w_xw_r^2+u_x^2w_x\right). \tag{5.39}$$

5.3.2 *Combined dissipative double-dispersive equation*

Besides assumptions (i), (ii) from Sec. 5.2.2, we now assume that (iii) $B\sim R/L$ to provide a balance between nonlinearity and dissipation (or accumulation).

Like before we first obtain the relationships between the longitudinal and shear displacements,

$$u=U+q_2\,r^2\,U_{xx}, \tag{5.40}$$

$$w=b_1\,r\,U_x+b_2\,r^2\,U_{xt}+\,r^3\,(b_{31}\,U_{xxx}+b_{32}\,U_{xtt})+$$
$$+B_1\,r\,U_x^2+B_2r\,U_x^3+B_3\,r^2\,U_x\,U_{xt}. \tag{5.41}$$

where the explicit forms for the coefficients are given by

$$q_2=\frac{\lambda}{2(2(\lambda+\mu)+k)},\ b_1=-2\,q_2,\ b_2=\frac{2\,q_2\,\eta}{3\lambda+4\mu+k},$$

$$b_{31} = -\frac{\lambda\, q_2}{2(2\lambda+3\mu)+k},\ b_{32} = -\frac{\eta\, b_2}{2(2\lambda+3\mu)+k},$$

$$B_1 = -\frac{2\, b_1(\lambda+4l-2m+n)+2b_1^2[3(\lambda+\mu)+2(2l+m)]+\lambda+2l}{2(2(\lambda+\mu)+k)},$$

$$\begin{aligned} B_2 = -\frac{1}{(2(\lambda+\mu)+k)}\{&B_1[\lambda+4l-2m+n+2b_1(3\lambda+3\mu+4l+2m)]+\\ &1+4a_1+a_2+\frac{1}{2}b_1[6l-2\mu-2m+n+48a_1+18a_2+2a_3+8a_4]+\\ &\frac{3}{2}b_1^2[2+2l-2m+n+32a_1+12a_2+2a_3+4a_4]+\\ &b_1^3[4-\mu+4l+4n+32a_1+8a_2+2a_4]\}, \end{aligned}$$

$$B_3 = -\frac{2\eta\, B_1 - b_2\{2q_2\,[3(\lambda+\mu)+2(l+m)]-(\lambda+4l-2m+n)\}}{3\lambda+4\mu+k}.$$

Note that q_2, b_2 are always positive, while b_1, b_{31}, b_{32} are always negative when the coefficients in (5.37) are positive (Kerr's model), and the other coefficients B_i, $i = 1 \div 3$, have different signs. Due to the chosen nine-constant model we have to truncate the series (5.40), (5.41), hence, omitting higher order nonlinear terms and the "corresponding" higher order linear derivative terms due to the assumption (iii). The "largest" of the quartic terms is $rU_x^4 \sim RB^4 \sim R(R/L)^4$. Then, the "corresponding" comparable linear term is r^4U_{xxxx}, while the cubic term is $r^3U_x^2U_{xxx}$. Similar terms with spatio-temporal mixed derivatives are of the same order.

Substituting (5.40), (5.41) into (3.29), and using Hamilton's principle (3.29) we obtain that longitudinal strains, $v = U_x$, obey a combined dissipative double-dispersive (CDDD) nonlinear equation:

$$v_{tt} - \alpha_1\, v_{xx} - \alpha_2\, v_{xxt} - \alpha_3(\,v^2)_{xx} - \alpha_4\, v_{xxxx} + \alpha_5\, v_{xxtt} -$$

$$\alpha_6\,(v^2)_{xxt} - \alpha_7\,(\,v^3)_{xx} = 0. \tag{5.42}$$

The explicit forms of the coefficients α_i, $i = 1 \div 7$, are

$$\alpha_1 = \frac{8q_2^2\,(2(\lambda+\mu)+k)-8\lambda\, q_2+\lambda+2\mu}{\rho_0},,\ \alpha_2 = \frac{8R\,\eta\, q_2^2}{\rho_0},$$

$$\alpha_3 = \frac{3}{\rho_0}[\lambda\left(\frac{1}{2}+2B_1-2q_2(1+4B_1)+4q_2^2(1-4q_2)\right)+$$

$$\mu\left(1-8q_2B_1-16q_2^3\right)-4kq_2B_1+$$

$$l\left(\frac{1}{3}-4q_2(1-4q_2+\frac{16}{3}q_2^2)\right)+\frac{2}{3}m(1-4q_2^2(3+4q_2))+4nq_2^2],$$

$$\alpha_4=\frac{R^2}{\rho_0}\left[(\lambda+2\mu-4\lambda\,q_2)\,q_2+4b_{31}(\lambda-2(2\lambda+2\mu+k)\,q_2)\right],$$

$$\alpha_5 = \frac{R^2}{\rho_0}[\rho_0\,q_2(1-2q_2)+2k(b_2^2+4q_2b_{32})+(9\lambda+10\mu)b_2^2/2-4\{\lambda-$$

$$4q_2(\lambda+\mu)\}b_{32}],$$

$$\alpha_6=-\frac{8R\,q_2\eta B_1}{\rho_0}$$

$$\begin{aligned}\alpha_7=\frac{4\,kB_2}{\rho_0}\left[B_1-4q_2\right]+\frac{4}{\rho_0}\{&l[1/2+4q_2(16q_2^3-8q_2^2+3q_2-1)+\\&2B_1(1-4q_2)^2]+m[1-4q_2^2+8q_2(B_1+2q_2^2)(1+2q_2)]+\\&2nq_2[q_2-4q_2^2-2B_1]+\lambda[1/8+2q_2^2(1+4q_2^2)+B_1(1+2B_1+8q_2^2)+\\&2B_2(1-4q_2)]+\mu[1/4+8q_2^4+2B_1(B_1-4q_2-4q_2^2)-8q_2B_2]+\\&a_1[1-16q_2+96q_2^2-256q_2^3+256q_2^4]+4a_2q_2[16q_2^3-24q_2^2+9q_2-1]+\\&4a_3q_2^2[1-4q_2]+16a_4q_2^2[1-q_2]^2\}.\end{aligned}$$

All coefficients in Eq.(5.42) are always positive in framework of the Kerr model, with the exception of α_3 and α_6 and α_7 that can be of different signs depending upon the material properties of the rod.

Note that we have obtained Eq.(5.42) in dimensional form without use of the multiple scales method and hence terms of different orders may occur, simultaneously. Indeed, due to the above given assumptions, (i) and (ii), in general, the last four terms in (5.42) are smaller than the others and hence are considered small perturbations to the other four terms. We shall refer to this case as the weakly dispersive limit. Note that the coefficients α_3, α_6 and α_7 depend on the third and fourth elastic moduli. In contrast to the second order moduli (Lamé coefficients) they may be of different signs Lurie (1990). Accordingly, their combination in α_3 may be quantitatively small while not so in α_7, and then the terms $\alpha_3(\,v^2)_{xx}$ and $\alpha_7\,(\,v^3)_{xx}$ may, quantitatively, be of the same order. Then the dissipative term, $\alpha_2\,v_{xxt}$, $\alpha_2 = O(1)$, will overcome the nonlinearity and drastically alter the wave

shape before the nonlinearity comes to play. However, if the influence of the external medium is weak enough, k and η are small, $\alpha_2 << 1$, the significant balance will be between the quadratic-cubic nonlinearities and dispersion, slightly perturbed by the influence of dissipative terms. We shall call it the weakly dissipative limit. Therefore, the advantage of equation (5.42) is that it embraces different important cases, for which we shall below give exact, asymptotic and numerical solutions.

5.3.3 *Exact solutions*

Assuming that the solution of Eq.(5.42) depends only upon the phase variable $\theta = x - c\,t$, then in the moving frame Eq.(5.42) becomes the O.D.E.

$$v^{''} + \beta_1 v^{'} + \beta_2 v + \beta_3 v^2 + \beta_4 (v^2)^{'} + \beta_5 v^3 = N, \tag{5.43}$$

where a dash denotes differentiation with respect to θ; N is a constant, and

$$\beta_1 = \frac{\alpha_2 c}{\alpha_5 c^2 - \alpha_4},\ \beta_2 = \frac{c^2 - \alpha_1}{\alpha_5 c^2 - \alpha_4},\ \beta_3 = \frac{\alpha_3}{\alpha_4 - \alpha_5 c^2},$$

$$\beta_4 = \frac{\alpha_6 c}{\alpha_5 c^2 - \alpha_4},\ \beta_5 = \frac{\alpha_7}{\alpha_4 - \alpha_5 c^2}.$$

Eq.(5.43) is a particular case of the equation (2.16) studied in Sec. 2.1.3. Among exact solutions obtained there we consider two bounded solutions:

(i) kink-shaped solitary wave solution

$$v \;=\; A\,m\,\tanh(m\,\theta) + B. \tag{5.44}$$

with

$$A = \frac{\beta_4 \pm \sqrt{\beta_4^2 - 2\beta_5}}{\beta_5},\ B = -\frac{\beta_1 - A\,\beta_3}{2\beta_4 - 3A\,\beta_5},$$

$$m^2 = \frac{(3A^2\beta_5 - 4A\beta_4)(3\beta_2\beta_5 - \beta_3^2) + 4\beta_4(\beta_2\beta_4 - \beta_1\beta_3) + 3\beta_1^2\beta_5}{2(1 - A\beta_4)(2\beta_4 - 3A\beta_5)^2}. \tag{5.45}$$

(ii) bounded periodic solution

$$v = \frac{m}{\sqrt{-\beta_5}}\ \frac{cn(m\,\theta,\,\kappa)\,sn(m\,\theta,\,\kappa)\,dn(m\,\theta,\,\kappa)}{C_1 + cn^2(m\,\theta,\,\kappa)} - \frac{\beta_3}{3\beta_5}. \tag{5.46}$$

with

$$C_1 = \frac{1 - 2\kappa^2 + \sqrt{\kappa^4 - \kappa^2 + 1}}{3\kappa^2},\ m^2 = \frac{\beta_2 + 3\beta_1^2}{4\sqrt{\kappa^4 - \kappa^2 + 1}},$$

and the following restrictions on the coefficients:

$$\beta_4 = -\frac{1}{2}\sqrt{-\beta_5},\ \beta_3 = 3\beta_1\sqrt{-\beta_5}. \tag{5.47}$$

The periodic wave solution (5.46) has a functional form different from both the KdV cnoidal wave and the MKdV bounded periodic solutionAblowitz and Segur (1981). Note also that the solution (5.46) exists only for non vanishing β_4, hence only in the presence of the nonlinear dissipative term $\beta_4(v^2)^{'}$ in Eq.(5.43). Equation (5.42), or its equivalent dynamical system, exhibits a more complicated balance between nonlinearity, dispersion and (linear and nonlinear) dissipation required for the periodic nonlinear wave than the standard balance between nonlinearity and dispersion that supplies both the KdV and the MKdV periodic solutions. When $\kappa = 1$ we have $C_1 = 0$, and the solution (5.43) tends to the kink-shaped solution (5.44) like the MKdV periodic solution, while the KdV cnoidal wave solution becomes the bell-shaped or solitary wave solution in the analogous limit, see Fig. 1.6.

The dissipationless limit of Eq.(5.43), $\beta_1 = \beta_4 = 0$, is

$$v^{''} + \beta_2 v + \beta_3 v^2 + \beta_5 v^3 = N. \tag{5.48}$$

It corresponds to the O.D.E. reduction of the combined KdV-MKdV (CKdV) equation. The CKdV equation possesses the one-parameter kink solution (5.44) with (5.45) if $\beta_1 = \beta_4 = 0$. However, a periodic solution of Eq.(5.48), having a kink limit at $\kappa = 1$, has a form different from (5.46):

$$v = \frac{\sqrt{2}m\kappa}{\sqrt{-\beta_5}}\ sn(m\,\theta,\,\kappa) - \frac{\beta_3}{3\beta_5},$$

with $m^2 = (3\beta_2\beta_5 - \beta_3^2)/(3\beta_5(1 + \kappa^2))$. Moreover, Eq.(5.48) has a variety of bell-shaped solitary wave solutions.

If $\alpha_4 \div \alpha_7$ are equal to zero we get from Eq.(5.42) the O.D.E. reduction of the Burgers equation,

$$\alpha_2 c\, v^{'} + (c^2 - \alpha_1)v - \alpha_3 v^2 = N. \tag{5.49}$$

Its kink solution has the functional form like (5.44) but with

$$A = -\frac{\alpha_2 c}{\alpha_3} \equiv \frac{\beta_1}{\beta_3},\ B = \frac{c^2 - \alpha_1}{2\alpha_3} \equiv -\frac{\beta_2}{2\beta_3},\ m - free. \tag{5.50}$$

There are two free parameters, the phase velocity c and the wave number m. If the boundary conditions are

$$v \to h_1 \text{ at } \theta \to \infty,\ v \to h_2 \text{ at } \theta \to -\infty,$$

then for the kink-shaped solution of Eq. (5.43)

$$\frac{\beta_4 \pm \sqrt{\beta_4^2 - 2\beta_5}}{\beta_5} m = \frac{h_1 - h_2}{2},\ \frac{\beta_1 - A\,\beta_3}{2\beta_4 - 3A\,\beta_5} = -\frac{h_1 + h_2}{2}$$

while the Burgers model (5.49) gives

$$m = \frac{(h_1 - h_2)\beta_3}{2\beta_1},\ \frac{\beta_2}{2\beta_3} = -\frac{h_1 + h_2}{2}.$$

The coefficients β_i depend upon the phase velocity c, and the elastic features of the material of the rod and the parameters of the external medium. Hence, for the Burgers model any pair of h_j define phase velocity and the wave number, while in general for the one-parameter solution (5.44), (5.45) as well as for the MKdV kink solution the boundary conditions imply additional restrictions on the parameters of the problem.

5.3.4 *Weakly dissipative (active) case*

When the viscocompressibility coefficient η is small, i.e. when the external medium is of little influence we can take $\alpha_2 = \delta\widetilde{\alpha}_2$, $\alpha_6 = \delta\widetilde{\alpha}_6$, $\delta << 1$. Then Eq.(5.42) is the perturbed combined double-dispersive equation,

$$v_{tt} - \alpha_1\, v_{xx} - \alpha_3(\, v^2)_{xx} - \alpha_7\,(\, v^3)_{xx} - \alpha_4\, v_{xxxx} + \alpha_5\, v_{xxtt} =$$

$$\delta(\widetilde{\alpha}_2\, v_{xxt} + \widetilde{\alpha}_6\,(v^2)_{xxt}) \tag{5.51}$$

For nonzero δ we assume that a solution of Eq.(5.51) is a function of the phase variable $\theta = x - ct$, $v = v(\theta)$. Then from Eq.(5.51) we get that

$$(c^2 - \alpha_1)v_\theta - \alpha_3(\, v^2)_\theta - \alpha_7\,(\, v^3)_\theta - (\alpha_4 - \alpha_5 c^2)\, v_{\theta\theta\theta} =$$

$$-\delta\, c\frac{\partial^2}{\partial\theta^2}\left[\widetilde{\alpha}_2\, v + \widetilde{\alpha}_6\, v^2\right] + O(\delta^2). \tag{5.52}$$

The solution of Eq.(5.52) is sought in the form

$$v = v_0 + \delta v_1 + ... \tag{5.53}$$

Substituting (5.53) into (5.52) in the leading order we have the O.D.E. underlying the CKdV equation,

$$(c^2 - \alpha_1)c_{0,\theta} - \alpha_3(\, v_0^2)_\theta - \alpha_7\,(\, v_0^3)_\theta - (\alpha_4 - \alpha_5 c^2)\, v_{0,\theta\theta\theta} = 0. \tag{5.54}$$

We look for a solution satisfying the boundary conditions

$$v_0 \to h_\pm,\ v_i \to 0,\ i > 0,\ \text{at}\ \theta \to \pm\infty,$$

and with all derivatives of v_i with respect to θ vanishing at infinity. For a kink $h_+ \neq h_-$.

The exact kink solution of Eq.(5.54) has the form

$$v_0 = A\, m \tanh(m\,\theta) - \alpha_3/(3\alpha_7), \tag{5.55}$$

with

$$A = \sqrt{\frac{2(\alpha_5 c^2 - \alpha_4)}{\alpha_7}}\, m,\ m^2 = \frac{3\alpha_1\alpha_7 - \alpha_3^2 - 3\alpha_7 c^2}{6(\alpha_4 - \alpha_5 c^2)}. \tag{5.56}$$

The correction v_1 (5.53) obeys the inhomogeneous linear equation

$$(c^2 - \alpha_1)v_{1,\theta} - 2\alpha_3\,(v_0\, v_1)_\theta - 3\alpha_7\,(v_0^2\, v_1)_\theta - (\alpha_4 - \alpha_5 c^2)\, v_{1,\theta\theta\theta} =$$

$$-c\frac{\partial^2}{\partial\theta^2}\left[\widetilde{\alpha}_2\, v_0 + \widetilde{\alpha}_6\ v_0^2\right], \tag{5.57}$$

whose solution satisfies the b.c. only when

$$3\widetilde{\alpha}_2\alpha_7 - 2\alpha_3\widetilde{\alpha}_6 = 0 \tag{5.58}$$

and has the form

$$v_1 = \frac{\widetilde{\alpha}_6\, m\, A}{2(\alpha_5 c^2 - \alpha_4)}\theta\, v_{0,\theta}.$$

Numerical integration of Eq.(5.51) allows exploration of the kink evolution outside the range imposed by condition (5.58). Case $\widetilde{\alpha}_2 < 0$, corresponding to dominating damping in the linearized Eq.(5.51) is depicted in Fig. 5.1 while Fig. 5.2 shows the evolution when $\widetilde{\alpha}_2 > 0$, hence corresponding to accumulation. In both figures the steepness of the wave front (i.e. $m = const$) and the phase velocity of the initial MKdV kink (5.55), left

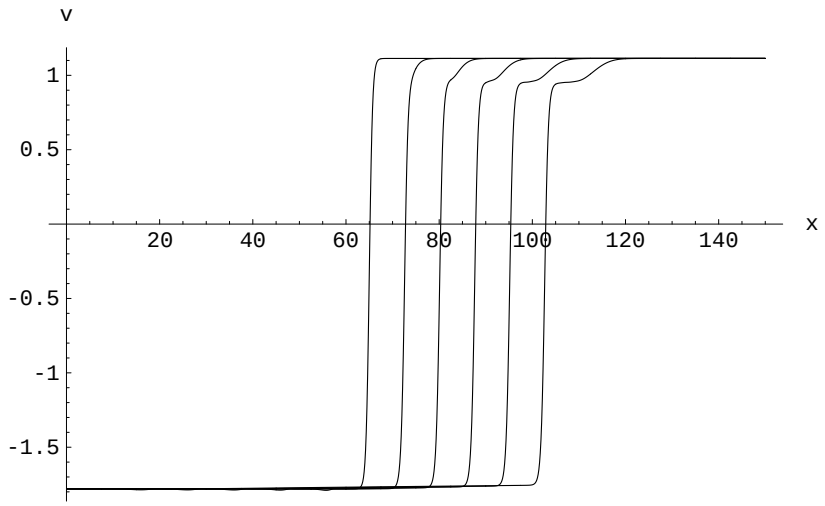

Fig. 5.1 Numerical simulation of the MKdV kink evolution with weak dissipation.

profile, remain one and the same. The influence of dissipation (accumulation) shows in the growth experienced by the *shelves* before and behind wave fronts, with more dramatic effect in the wave front. The length of the shelf increases like the length of the shelf behind the perturbed KdV soliton Ablowitz and Segur (1981) but the height also increases. As a result no quasistationary profile is possible during the evolution of the perturbed MKdV kink at variance with the result found for the bell-shaped strain solitary wave in Porubov and Velarde (2000).

5.3.5 *Weakly dispersive case*

Let us now take into account all assumptions from Sec. 5.3.2 to obtain the dimensionless form of Eq.(5.42). Assume the scale for v is B, for x is L, and for t is L/c_0 where c_0 is a characteristic velocity of the wave. The small parameter of the problem is $\varepsilon = B = R/L$. Suppose that our dimensionless solution $\overline{v}$ depends upon the phase variable $\theta = \overline{x} - c\overline{t}$ and that $c = 1 + \varepsilon c_1 + \varepsilon^2 c_2 + ...$ Then from Eq.(5.42) we get

$$(c_0^2 - \alpha_1)\overline{v}_{\theta\theta} + \varepsilon\left(2c_0^2 c_1 \overline{v}_{\theta\theta} - \alpha_3(\overline{v}^2)_{\theta\theta} + \overline{\alpha}_2 c_0 \overline{v}_{\theta\theta\theta}\right) +$$

$$\varepsilon^2(c_0^2 c_1[2c_2 + c_1]\overline{v}_{\theta\theta} + \overline{\alpha}_2 c_0 c_1 \overline{v}_{\theta\theta\theta} +$$

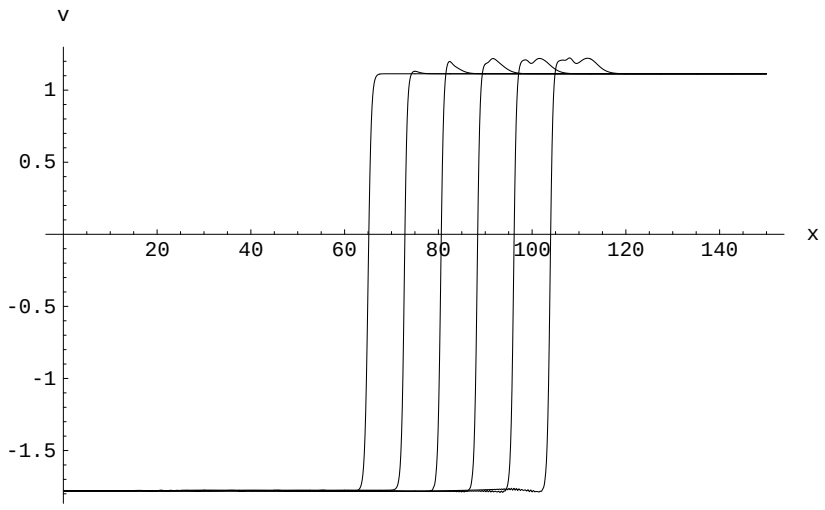

Fig. 5.2 Numerical simulation of the MKdV kink evolution with weak accumulation

$$[\overline{\alpha}_5 c_0^2 - \overline{\alpha}_4]\overline{v}_{\theta\theta\theta\theta} - \alpha_7\,\overline{v}_{\theta\theta}^3 + \overline{\alpha}_6 c_0 \overline{v}_{\theta\theta\theta}^2) = O(\varepsilon^3). \tag{5.59}$$

with $\overline{\alpha}_2 = \alpha_2/R$, $\overline{\alpha}_4 = \alpha_4/R^2$, $\overline{\alpha}_5 = \alpha_5/R^2$, and $\overline{\alpha}_6 = \alpha_6/R$. The solution is sought in the form

$$\overline{v} = \overline{v}_0 + \varepsilon\,\overline{v}_1 + ... \tag{5.60}$$

The boundary conditions are the same as for the kink solution in the weakly dissipative case. In the leading order we have $c_0 = \sqrt{\alpha_1}$, while the next order yields the equation

$$\frac{\partial^2}{\partial\theta^2}\left(2\alpha_1 c_1\,\overline{v}_0 - \alpha_3\,\overline{v}_0^2 + \overline{\alpha}_2\sqrt{\alpha_1}\,\overline{v}_{0,\theta}\right) = 0. \tag{5.61}$$

In brackets we have the O.D.E. reduction of Burgers equation whose kink-shaped solution is

$$\overline{v}_0 = -\frac{\overline{\alpha}_2\sqrt{\alpha_1}}{\alpha_3}\,m\,\tanh(m\theta) + \frac{\alpha_1 c_1}{\alpha_3}, \tag{5.62}$$

In the following higher order we get an inhomogeneous linear ordinary differential equation for $\overline{v}_1(\theta)$,

$$\frac{\partial^2}{\partial\theta^2}\left(2\alpha_1 c_1\,\overline{v}_1 - 2\alpha_3\overline{v}_0\,\overline{v}_1 + \overline{\alpha}_2\sqrt{\alpha_1}\,\overline{v}_{1,\theta}\right) =$$

$$[\overline{\alpha}_4 - \overline{\alpha}_5\alpha_1\,]\overline{v}_{0,\theta\theta\theta\theta} + \alpha_7\,\overline{v}^3_{0,\theta\theta} - \overline{\alpha}_6\sqrt{\alpha_1}\overline{v}^2_{0,\theta\theta\theta} - \alpha_1 c_1[2c_2 + c_1]\overline{v}_{0,\theta\theta} -$$

$$\overline{\alpha}_2\sqrt{\alpha_1}c_1\overline{v}_{0,\theta\theta\theta},$$

whose solution, decaying at infinity, is

$$\overline{v}_1 = \overline{v}_{0,\theta}\left[b_1\theta + b_2 Log(\cosh(m\theta)) + b_3\right], \tag{5.63}$$

provided that

$$c_2 = \frac{1}{2\alpha_3^2 c_1}\left(\alpha_7\left[3\alpha_1 c_1^2 - \overline{\alpha}_2^2 m\right] - c_1^2\right),$$

where $b_3 = const$, while b_i, $i = 1, 2$, depend upon the coefficients of Eq.(5.59),

$$b_1 = \frac{c_1}{\overline{\alpha}_2\alpha_3^2}\left(\alpha_1[\overline{\alpha}_2\alpha_7 - 2\alpha_3\overline{\alpha}_6] - \overline{\alpha}_2\alpha_3^2\right),$$
$$b_2 = \frac{1}{\sqrt{\alpha_1}\overline{\alpha}_2\alpha_3^2}\left(2[\alpha_1\overline{\alpha}_5 - \overline{\alpha}_4]\alpha_3^2 + \alpha_1\overline{\alpha}_2[2\alpha_3\overline{\alpha}_6 - \overline{\alpha}_2\alpha_7]\right).$$

We see that b_1, b_2 remain nonzero even when $\alpha_6 = \alpha_7 = 0$. The influence of dispersion is provided by b_2 only. If $b_2 = b_3 = 0$ then $\overline{v}$ may be written as

$$\overline{v} = -\frac{\overline{\alpha}_2\sqrt{\alpha_1}}{\alpha_3}\, m\, \tanh(m[1 + \varepsilon b_1]\theta) + \frac{\alpha_1 c_1}{\alpha_3} + O(\varepsilon^2). \tag{5.64}$$

Then the first term in (5.63) affects the smoothness of the wave front in the solution (5.60). Shown in Fig. 5.3(a) is the case $b_1 > 0$, while Fig. 5.3(b) accounts for negative values of b_1. The dashed line in Fig. 5.3 accounts for the unperturbed Burgers kink (5.44), (5.50), while solution (5.64) is shown with a solid line. Correspondingly, in Fig. 5.4 it is shown the influence of the second term ($b_1 = b_3 = 0$) on the shape of the solution $\overline{v}$ (5.60) vs Burgers kink (dashed line) for $b_2 < 0$ in Fig. 5.4(a) and for $b_2 > 0$ in Fig. 5.4(b). Note the asymmetric disturbance of the profile near the upper and lower states of the solution that are exchanged with the opposite sign of b_2. The case $b_1 = b_2 = 0$ corresponds to a constant phase shift of the unperturbed Burgers kink solution.

The features of a quasistationary asymptotic solution can be observed when studying the time-dependent process of the kink formation. Numerical integration of Eq.(5.42) with an initial condition in the form of a Burgers kink-shaped wave (5.44), (5.50) shows that the wave attracts the profile described by the asymptotic solution even at moderate ε. The time evolution

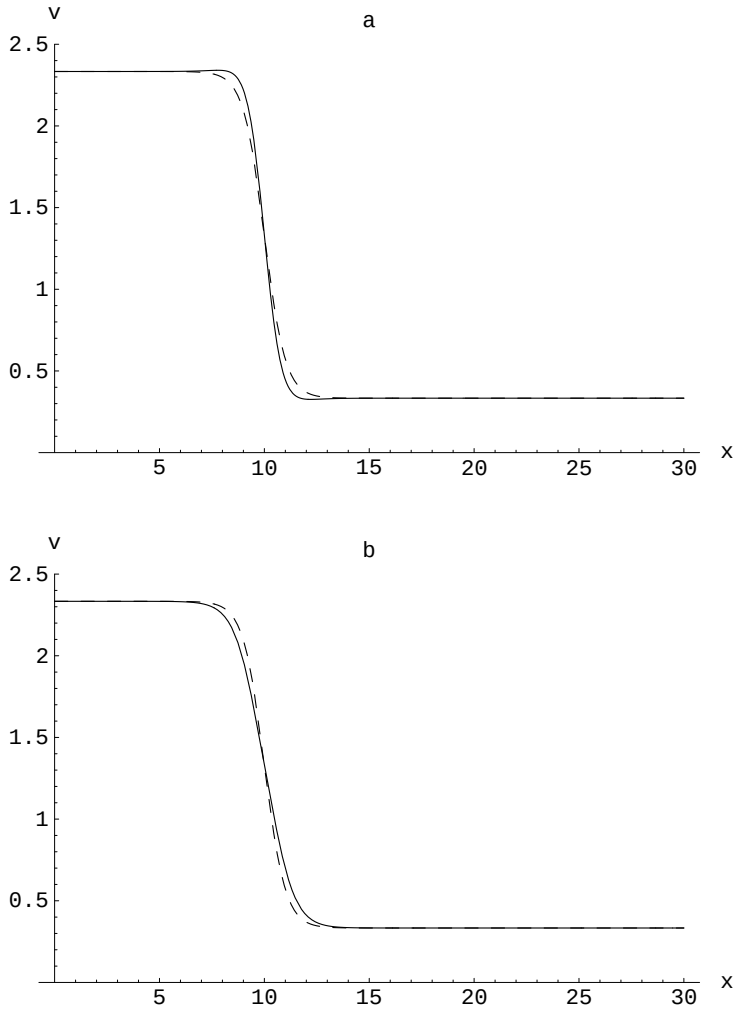

Fig. 5.3 Smoothness of the Burgers kink profile due to the first term in the first order asymptotic solution: (a) $b_1 > 0$, (b) $b_1 < 0$.

of the wave at $\varepsilon = O(1)$ is shown in Figs. 5.5, 5.6 where the propagation of the undisturbed Burgers kink is shown with a dashed line; the left profile corresponds to the initial Burgers kink. The values of the coefficients in Eq.(5.42) have been chosen such that b_2, is negative for Fig. 5.5 and positive

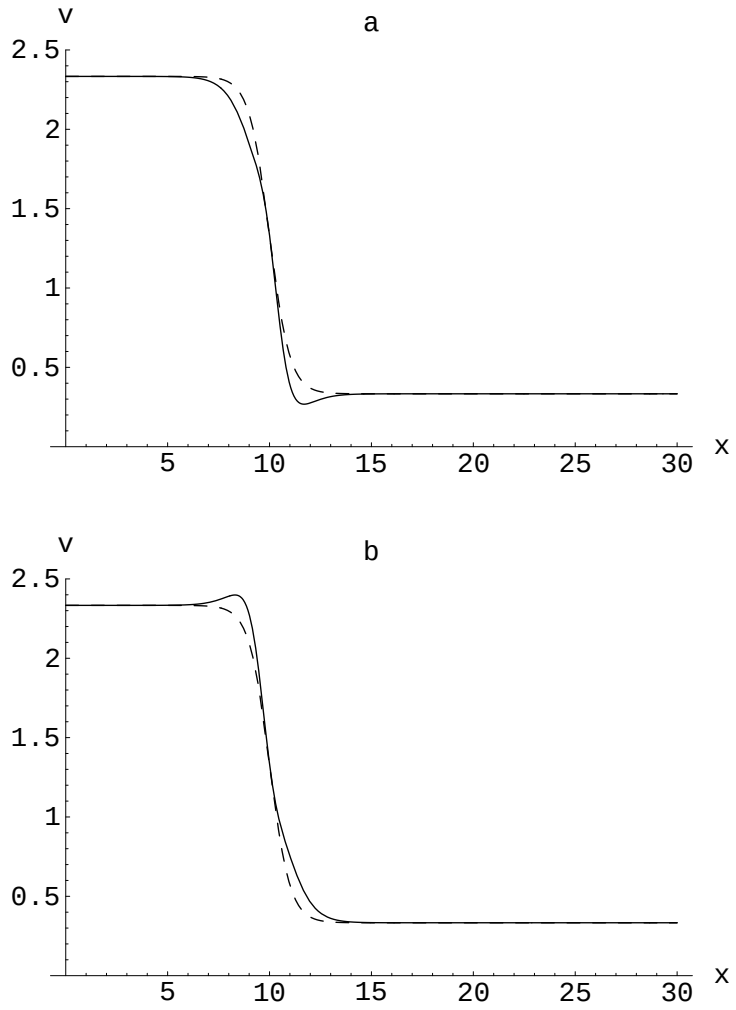

Fig. 5.4 Disturbances on the Burgers kink profile due to the second term in the first order asymptotic solution: (a) $b_2 < 0$, (b) $b_2 > 0$.

for Fig. 5.6. The three most right solid line profiles show that the quasistationary perturbed kink-shaped waves are rather close to the corresponding asymptotic profiles shown in Figs. 5.5, 5.6. The phase velocity remains one and the same during the whole time and practically equal to the velocity of

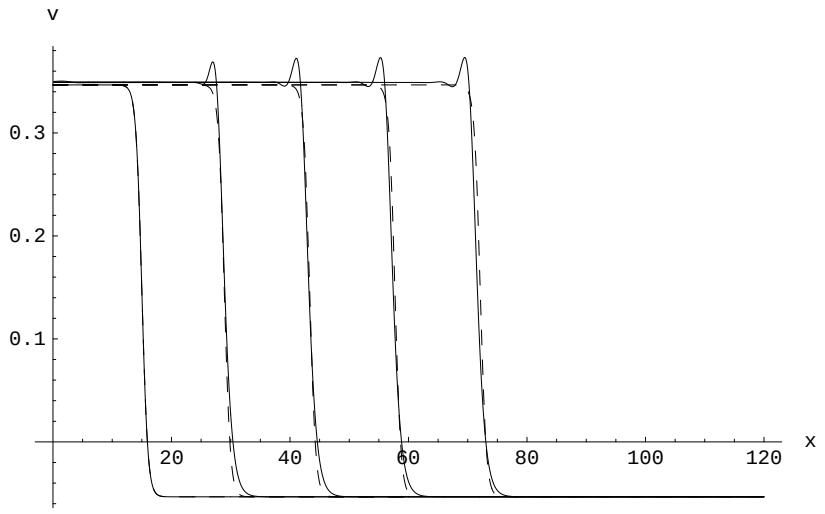

Fig. 5.5 Numerical simulation of the Burgers kink evolution into the quasistationary profile in the weakly dispersive case at $b_2 < 0$.

the initial Burgers kink. Any other initial kink different from the Burgers one, diverges even when dispersion is small.

5.3.6 *Summary of results and outlook*

We have shown that kinks can propagate in a compressible elastic rod, of radius R, when the wave characteristics, amplitude and wavelength, are such that $B \sim R/L << 1$, a cubic nonlinearity of the elastic material is taken into account and dissipation exists e.g. due to the rod being embedded in an external viscoelastic medium. We have found in the weakly dispersive limit how the kink-shaped wave is selected. In contrast to the bell-shaped solitary wave selection in previous section now only the wave number tends to a prescribed finite value, as Eq.(5.64) indicates. Other possibilities exist for an exact travelling wave solution (5.44) of Eq.(5.42) as well for the perturbed MKdV kink when the additional condition (5.58) is satisfied.

High order terms do not significantly alter the wave structure in the weakly dispersive case. In such circumstance Eq.(5.42) can be approximated with $\alpha_6 = \alpha_7 = 0$ and hence without using the fourth-order elastic moduli, a_i. This is very important from the point of view of application because for most materials the values of a_i are unknown. However, if dis-

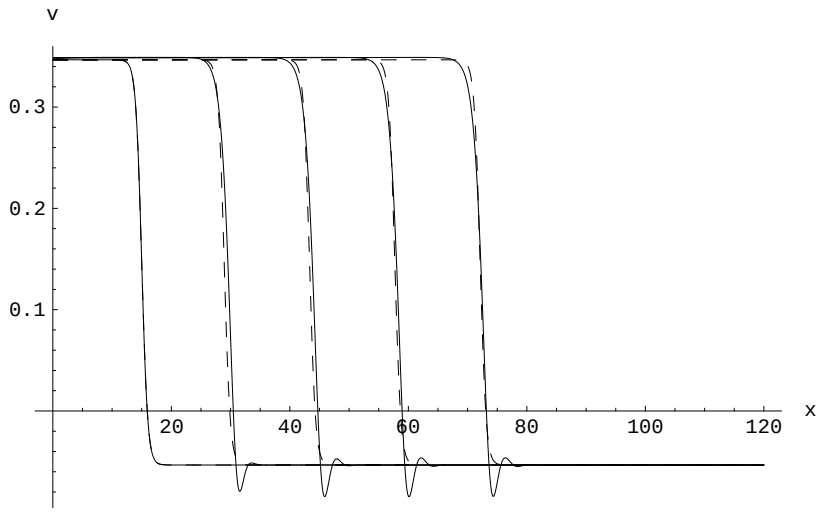

Fig. 5.6 Numerical simulation of the Burgers kink evolution into the quasistationary profile in the weakly dispersive case at $b_2 > 0$.

persion becomes significant those terms must be taken into consideration for a correct description of the strain kinks. In particular they provide the nontrivial condition $3\alpha_2\alpha_7 - 2\alpha_3\alpha_6 = 0$, that allows the propagation of a quasistationary perturbed kink in the weakly dissipative case.

The influence of dissipation on the balance between nonlinearity and dispersion appears affecting wave evolution much more drastically than what dispersion does to the Burgers nonlinearity-dissipation balance. However, we have no kink selection in the weakly dissipative (active) case when all wave parameters tend to *finite* values. This seems due to the absence of "dissipative (active)" cubic nonlinear terms in the r.h.s. of Eq.(5.51). However, adding a term like $(v^3)_{xxt}$ is not permitted by the assumptions in Sec. 5.3.2. Indeed, $(v^3)_{xxt}$ and $(v^4)_{xx}$ will be of the same order, and thus the corresponding "dissipative" quartic nonlinearity demands a simultaneous quintic nonlinear term, and so on.

Exact solutions obtained account for the case when the dispersion, dissipation and nonlinearity are of the same order. The existence of these solutions require additional restrictions studied in Sec. 5.3.3. Moreover numerical simulations in the weakly dispersive case point to a formal validity of the results from Sec. 5.3.5 when dispersion is not small.

As a useful aspect of our analytical study is that obtaining exact and

asymptotic solutions allow reliable testing points for time-dependent numerical integration. Analytic solutions could be also the starting points for the numerical search of homoclinic and heteroclinic trajectories yielding solutions of possibly more complicated form than those described in this report. On the other hand, we have shown that an external medium, e.g., permafrost, may be responsible for the amplification of both the strain kink and bell-shaped solitary waves, see Sec. 5.2. This may be used to locate zones of potential plasticity. In view of the lack of experimental data on the fourth order moduli our results may help in finding these moduli using the linear algebraic relationships between them and the kink wave amplitude and velocity obtained using B_2.

Finally, note that our solutions may also be used to account for the evolution of surface waves in a heated liquid layer subjected to variations of surface tension. Indeed, when $A/H = H/L << 1$, the evolution of surface waves with surface deformation η of amplitude A and wavelength L in a layer of depth H is governed by the equation Porubov (1995):

$$\eta_t + \gamma_1(\eta^2)_x + \gamma_2\eta_{xx} + \varepsilon\left(\gamma_3\eta_{xxx} + \gamma_4(\eta^2)_{xx} + \gamma_5(\eta^3)_x\right) = 0, \qquad (5.65)$$

Eq.(5.65) describes waves past an instability threshold. Its O.D.E. reduction coincides with Eq.(5.43). Note that Eq.(5.65) accounts only for the weakly dispersive case. Contrary to the elastic bulk dissipation–free rod inside the liquid layer here the dissipation is caused by fluid viscosity and heat diffusion.

5.4 Influence of external tangential stresses on strain solitary waves evolution in a nonlinear elastic rod

5.4.1 *Formulation of the problem*

Let us use the same notations as in previous sections. The elementary work, δA, done by normal and tangential external forces at the lateral surface of the rod, $r = R$, now is:

$$\delta A = 2\pi \int_{-\infty}^{\infty} (P^*_{rr}\, \delta w + P^*_{rx}\, \delta u) dx\,. \qquad (5.66)$$

We assume the external medium yields a normal stress P^*_{rr} ,

$$P^*_{rr} = -\frac{k_1}{r} w + k_2 r\, w_{xx}, \qquad (5.67)$$

where k_i are the stiffness coefficients of the external medium, both k_1 and k_2 are positive and constant. It corresponds to the Pasternak (1954) model based on the representation of the contact by means of the interacting spring elements, see also Kerr (1964) and references therein. Tangential stresses on the lateral surface are assumed in the form:

$$P^*_{rx} = k_d P^*_{rr}, \tag{5.68}$$

that relates to the Coulomb-Amonton law Hähner and Spencer (1998); Nikitin (1998) when $k_d > 0$ is a friction coefficient. We consider a more general model, k_d is of either sign, in order to account for the influence of an active external medium providing an energy influx .

Hence the boundary conditions (b.c.) are:

$$w \to 0, \qquad \text{at } r \to 0, \tag{5.69}$$

$$P_{rr} = P^*_{rr}\ , \qquad \text{at } r = R, \tag{5.70}$$

$$P_{rx} = P^*_{rx}\ , \qquad \text{at } r = R, \tag{5.71}$$

where the components P_{rr}, P_{rx} of the Piola - Kirchhoff stress tensor $\mathbf{P}$ are defined by Eqs. (3.10), (3.11).

5.4.2 *Derivation of the governing equation*

Simplifications follows from the natural assumptions are similar to those used in previous sections:

(i) pure elastic strain waves have magnitude $B << 1$;

(ii) long elastic strain waves have a characteristic length L such that relative to the rod radius R, $R/L << 1$.

(iii)$B \sim R^2/L^2$.

Let us obtain the relationships between longitudinal and shear displacements satisfying b.c. (5.69)- (5.71). According to the procedure developed in Sec. 3.2 the unknown functions u, w are expanded in a power series (3.12), (3.13) that yields in our case:

$$u = U + k_d\, a_1 r\, U_x + a_2\, r^2\, U_{xx} + k_d\, A_1\, r\, U_x^2, \tag{5.72}$$

$$w = b_1\, r\, U_x + k_d\, b_2\, r^2\, U_{xx} + b_3 r^3\, U_{xxx} + B_1\, r\, U_x^2\ . \tag{5.73}$$

where

$$a_1 = -\frac{k_1}{\mu} b_1,\ a_2 = -\frac{[\mu^2(3\lambda + 4\mu + k_1) + 2\,k_d^2\,k_1^2\lambda\,]b_1}{2\mu^2(3\lambda + 4\mu + k_1)},$$

$$b_1 = -\frac{\lambda}{2(\lambda+\mu)+k_1},\ b_2 = \frac{k_1\lambda\,b_1}{\mu(3\lambda+4\mu+k_1)},\ b_3 = \frac{(k_2\,b_1 - \lambda a_2)}{2(2\lambda+3\mu)+k_1},$$

$$A_1 = -\frac{k_1}{\mu} B_1,$$

$$B_1 = -\frac{\lambda + 2l + 2(\lambda + 4l - 2m + n)b_1 + 2[3(\lambda+\mu) + 4l + 2m]b_1^2}{2(2(\lambda+\mu)+k_1)}.$$

Note that a_1, a_2, are always positive, b_1- b_3 are always negative, while nonlinear term coefficients A_1, B_1 have different but opposite signs. Due to the chosen five-constant theory (3.1) we have to truncate the series (5.6), (5.7) like before in order to omit negligibly small higher-order nonlinear terms and the "corresponding" higher order linear derivative terms due to the assumption (iii).

Substituting Eqs.(5.72), (5.73) into Eq.(3.29) we obtain that longitudinal strains, $v = U_x$, obey a nonlinear dispersive-dissipative equation

$$v_{tt} - \alpha_1\,v_{xx} - \alpha_2\,(\,v^2)_{xx} - \alpha_3\,v_{xxtt} + \alpha_4\,v_{xxxx} = k_d(\beta_1 v_x + \beta_2\,(v^2)_x + \beta_3 v_{xxx}), \tag{5.74}$$

where

$$\alpha_1 = \frac{\lambda + 2\mu + 4[\lambda + b_1(\lambda+\mu)]b_1 + 2k_1\,(b_2 - b_1^2)}{\rho_0} + \frac{3\,k_1^2 k_d^2 b_1^2}{\mu\rho_0},$$

$$\beta_1 = -\frac{2k_1 b_1}{\rho_0 R}, \beta_2 = -\frac{2k_1 B_1}{\rho_0 R}$$

$$\alpha_2 = \frac{3}{\rho_0}[\frac{1}{2}(1+2b_1)(1+2b_1^2) + \mu\left(1+2b_1^3\right) + \frac{1}{3}l\left(1+2b_1^3\right) +$$

$$\frac{2}{3}m(1+2b_1)(1-b_1)^2 + nb_1^2 + \{\lambda + 2b_1(\lambda+\mu) + 2k_1b_1\}B_1 +$$

$$\frac{k_1^2 k_d^2 b_1^2}{\mu^2}\left((\lambda + \frac{1}{2}m)(1+2b_1) + \mu(1+b_1) - \frac{1}{4}nb_1 - \frac{\mu}{b_1}B_1\right)],$$

$$\alpha_3 = \frac{R^2}{2}(b_1^2 - 2a_2) + \frac{R^2\, k_1^2 k_d^2 b_1^2}{2\mu^2}, \beta_3 = \frac{2R[k_2\mu b_1 - k_1\mu(a_2 b_1 + b_3) - k_1^2 k_d^2 b_1 b_2]}{\mu\rho_0}$$

$$\alpha_4 = \frac{R^2}{2\rho_0}\,[a_2\{4\mu a_2 - 2(\lambda+2\mu) - 4b_1(\lambda-\mu)\} + \mu\, b_1^2 - 8b_3\{\lambda + 2b_1(\lambda+\mu)\}] +$$

$$\frac{2R^2 b_1}{\rho_0}[k_2\mu b_1 - k_1 b_3(\mu - k_1)] + \frac{R^2 k_d^2}{2\mu^2\rho_0}[b_2^2(9\lambda + 10\mu)\mu^2 +$$

$$k_1\{b_2[4\mu^2(a_2+1) + 2\mu(\mu - 3\lambda)] - 4k_2\mu b_1^2\} + k_1^2 b_1\{4\mu b_3 + (\lambda + 2\mu)b_1\}].$$

When $k_d = 0$ Eq.(5.74) becomes the double dispersive equation (DDE) accounting for nonlinear strain waves in a free lateral surface rod.

5.4.3 *Symmetric strain solitary waves*

Even at $k_d = 0$ Eq.(5.74) is nonitegrable by the Inverse Scattering Transform method Ablowitz and Segur (1981). Hence, only particular, usually travelling wave, exact solutions may be obtained. There exist different approaches based on the assumptions of the appropriate ansatz for a solutions. More general solutions are found in terms of the elliptic functions see Sec. 2.1. However, up to now only localized strain waves were observed in experiments, see Sec. 3.4, and main attention is paid here on the exact solutions vanishing at infinity. Assume the solution of Eq.(5.74) depends only upon the phase variable $\theta = x - c\,t$, then in the moving frame Eq.(5.74) becomes the O.D.E.

$$v''' + k_d\gamma_1 v'' + \gamma_2 v' + \gamma_3 v v' + k_d\gamma_4 v^2 + k_d\gamma_5 v = 0, \qquad (5.75)$$

where a dash denotes differentiation with respect to θ, and

$$\gamma_1 = \frac{\beta_3}{\alpha_3 c^2 - \alpha_4},\ \gamma_2 = \frac{\alpha_1 - c^2}{\alpha_3 c^2 - \alpha_4},\ \gamma_3 = \frac{2\alpha_2}{\alpha_3 c^2 - \alpha_4},$$

$$\gamma_4 = \frac{\beta_2}{\alpha_3 c^2 - \alpha_4},\ \gamma_5 = \frac{\beta_1}{\alpha_3 c^2 - \alpha_4}.$$

Following the procedure from Sec. 2.1. we compare the leading-order derivative term, v''', and the nonlinear term, vv'. One can see they are in balance when a solution has the second order pole. Hence, general periodic solution may be expressed using either the Weierstrass elliptic function , $v = a_1\wp(\theta, g_1, g_2) + b_1$, or the Jacobian elliptic function, $v = a_2 cn^2(p\theta, \kappa) + b_2$.

Localized solitary wave solution are of interest here. Since they correspond to the limit $\kappa \to 1$, one can assume the solution of the form:

$$v = G\cosh^{-2}(p\theta). \tag{5.76}$$

Substituting (5.76) into Eq.(5.75) and equating to zero coefficients at corresponding powers of $\tanh(p\theta)$ one obtains

$$p^2 = \frac{c^2-\alpha_1}{4(\alpha_3 c^2-\alpha_4)},\ G = \frac{3(c^2-\alpha_1)}{2\alpha_2}, \tag{5.77}$$

$$2\gamma_4 = \gamma_1\gamma_3,\ \gamma_5 = \gamma_1\gamma_2. \tag{5.78}$$

The first of the conditions (5.78) defines the phase velocity,

$$c^2 = \frac{\alpha_4\beta_2+\alpha_2\beta_3}{\alpha_3\beta_2},$$

while the second one imposes a restriction on the equation coefficients,

$$\alpha_2\alpha_3\beta_1 + (\alpha_4-\alpha_1\alpha_3)\beta_2 + \alpha_2\beta_3 = 0.$$

When conditions (5.78) hold Eq. (5.75) may be rewritten as

$$[\frac{\partial}{\partial\theta} + k_d\gamma_1](v^{''} + \gamma_2 v + \frac{1}{2}\gamma_3 v^2) = 0,$$

whose solution vanishing at infinity is obtained from the equation

$$v^{''} + \gamma_2 v + \frac{1}{2}\gamma_3 v^2 = 0. \tag{5.79}$$

Eq. (5.79) is nothing but ODE reduction of the DDE integrated twice. Its solitary wave solution is (5.76), (5.77), while the phase velocity c remains a free parameter. Hence the general solution (5.76), (5.77), (5.78) is supported simultaneously by a balance between nonlinearity, $\gamma_3 vv^{'}$, and dispersion, $v^{'''}$(like DDE's solution), and by a balance between active/dissipative terms, $k_d\gamma_1 v^{''}$, $k_d\gamma_4 v^2$, $k_d\gamma_5 v$. The last balance is realized under conditions (5.78).

The coefficients α_i, β_j depend on the elastic features of the material of the rod and the parameters of the external medium. They define the sign of the wave amplitude G, hence either compression, $G<0$, or tensile, $G>0$, wave may propagate in the rod.

Solitary wave solution exists under specific initial condition in the form of (5.76) at $t=0$. It is known that in non-dissipative case even rather arbitrary initial pulse splits into the train of solitary waves each being

accounted for the travelling solitary wave exact solution of the DDE, see Sec. 3.3. When dissipation/accumulation predominates it destroys initial pulse before balance between nonlinearity and dispersion become to play, and no localized waves appear.

Consider now a weakly dissipative case, $k_d << 1$, when nonlinearity and dispersion dominate over dissipation/accumulation. Assume a solution of Eq.(5.74) depends upon the phase variable θ and the slow time T, $v = v(\theta, T)$, with

$$\theta_x = 1,\ \theta_t = -c(T),\ T = k_d\, t.$$

Then asymptotic solution of Eq.(5.74) is sought in the form

$$v = v_0(\theta) + k_d v_1(\theta) + ...$$

In the leading order we get

$$(c^2 - \alpha_1)v_{0,\theta} - (\alpha_3 c^2 - \alpha_4)v_{0,\theta\theta\theta} - 2\alpha_2 v_0 v_{0,\theta} = 0, \tag{5.80}$$

whose one-parameter solution has the form of (5.76), but c now depends upon T. At order $O(k_d)$ there is an inhomogeneous linear equation for v_1,

$$(c^2 - \alpha_1)v_{1,\theta} - (\alpha_3 c^2 - \alpha_4)v_{1,\theta\theta\theta} - 2\alpha_2 (v_0 v_1)_\theta = F, \tag{5.81}$$

where

$$F = 2cv_{0,T} + c_T v_0 - 2\alpha_3 c v_{0,\theta\theta T} - \alpha_3 c_T v_{0,\theta\theta\theta} + \beta_1 v_0 + \beta_2 v_0^2 + \beta_3 v_0^{''}.$$

The operator acting on the function v_1 in Eq.(5.81) is adjoint to that in Eq.(5.80). We look for a solution satisfying the boundary conditions

$$v_i \to 0,\ i \succeq 0,\ \text{at } |\theta| \to \infty, \tag{5.82}$$

Then the Fredholm alternative,

$$\int_{-\infty}^{\infty} v_0 F\, d\theta = 0, \tag{5.83}$$

provides the absence of secular terms. It yields the equation defining the phase velocity c,

$$\begin{aligned}\alpha_2 c_T Q_6(c) = (\alpha_1 - c^2)(\alpha_3 c^2 - \alpha_4)(6\alpha_3\beta_2 c^4 + [5\alpha_2\alpha_3\beta_1 - \\ 6\beta_2(\alpha_4 + \alpha_1\alpha_3) - \alpha_2\beta_3]c^2 - 5\alpha_2\alpha_4\beta_1 + \\ 6\alpha_1\alpha_4\beta_2 + \alpha_1\alpha_2\beta_3).\end{aligned} \tag{5.84}$$

where

$$Q_6(c) = 30\alpha_3^2 c^6 - 3\alpha_3(11\alpha_4 + 10\alpha_1\alpha_3)c^4 + 2\alpha_4(11\alpha_1\alpha_3 + 10\alpha_4)c^2 - \alpha_1^2\alpha_3\alpha_4 - 5\alpha_1\alpha_4^2.$$

Eq. (5.84) may be integrated giving the dependence c on T in an implicit form. However, important features of the evolution of c may be established studying the sign of c_T without integration. The stationary solutions of (5.84) $c_1 = \sqrt{\alpha_1}$ and $c_2 = \sqrt{\alpha_4/\alpha_3}$ correspond to $p = 0$ or $p \to \infty$ in (5.77). Other stationary solutions are defined from the equation

$$6\alpha_3\beta_2 c^4 + [5\alpha_2\alpha_3\beta_1 - 6\beta_2(\alpha_4 + \alpha_1\alpha_3) - \alpha_2\beta_3]c^2 - 5\alpha_2\alpha_4\beta_1 + 6\alpha_1\alpha_4\beta_2 + \alpha_1\alpha_2\beta_3 = 0. \tag{5.85}$$

Due to (5.77) $(\alpha_1 - c^2)(\alpha_3 c^2 - \alpha_4) < 0$, and the sign of c_T depends upon the signs of the polynomial $Q_6(c)$ and the quartic polynomial in the r.h.s. of Eq. (5.84). When c_T keeps its sign as time passes possible scenarios for evolution of c are either vanishing or diverging to infinity. More interesting case is realized when, in particular, real roots of Eq.(5.85), $c_1^* < c_2^*$, are located in the interval, $q_1 < c_1^* < c_2^* < q_2$, where q_1, q_2 are real neighboring roots of $Q_6(c)$. If $\alpha_3\beta_2 > 0$ and $Q_6(c) > 0$ at $q_1 < c < q_2$, we have $c_T > 0$ when $c_1^* < c < c_2^*$ and $c_T < 0$ when $q_1 < c < c_1^*$ or $c_2^* < c < q_2$. It means that if an initial velocity, $c(T = 0) \equiv c_0$ lies in the intervals $c_1^* < c_0 < c_2^*$ or $c_2^* < c < q_2$, the velocity $c(T)$ tends to the *finite* value $c_s = c_2^*$ at $T \to \infty$. If $Q_6(c) < 0$, c tends to $c_s = c_1^*$. To put this another way, the value of velocity is *selected* according to the governing equation coefficients. The wave amplitude $G(c)$ is selected like velocity c according to (5.77). It was called in Sec. 1.3 the selection from below when $c_0 < c_s$, Fig. 1.17 (a), while the case $c_0 > c_s$ is referred to by the selection from above, Fig. 1.17(b). We see the waves remain symmetric with respect to their maximums, their amplitudes increase (decrease) while their widths decrease (increase).

Based on Eq. (5.84) the solution of Eq.(5.81) is

$$v_1 = \frac{C(\alpha_1 - c^2)}{2\alpha_2}[1 - \tanh(p\theta)] + [C + \frac{(\alpha_1\alpha_3 - \alpha_4)c^2 c_T}{(\alpha_1 - c^2)^2(\alpha_3 c^2 - \alpha_4)}\theta]v_0 + [C_1 + \frac{C}{2}\theta - \frac{(\alpha_1\alpha_3 - \alpha_4)c^2 c_T}{(\alpha_1 - c^2)^2(\alpha_3 c^2 - \alpha_4)}\theta^2]v_{0,\theta},$$

where C_1 is a constant,

$$C = 12p[\alpha_3^2\beta_2 c^8 + \alpha_3(5\alpha_2\alpha_3 c_T - 2\alpha_1\alpha_3\beta_2 - 2\alpha_4\beta_2 - \alpha_2\beta_3)c^6 + (\beta_2\{\alpha_1^2\alpha_3^2 + 4\alpha_1\alpha_3\alpha_4 + \alpha_4^2\} + \alpha_2\beta_3\{2\alpha_1\alpha_3 + \alpha_4\} - 11\alpha_2\alpha_3\alpha_4 c_T)c^4 + (\alpha_2\alpha_4 c_T\{2\alpha_1\alpha_3 + 5\alpha_4\} - \alpha_1\{2\alpha_4\beta_2[\alpha_1\alpha_3 + \alpha_4] + \alpha_2\beta_3[\alpha_1\alpha_3 + 2\alpha_4]\})c^4 - \alpha_1^2\alpha_4(\alpha_4\beta_2 + \alpha_2\beta_3)]/\{5\alpha_2(\alpha_1 - c^2)^3(\alpha_3 c^2 - \alpha_4)\}$$

One can check that evolution of the solution $v = v_0(\theta, T) + k_d v_1(\theta, T)$ does not significantly differ from that of the solution $v = v_0(\theta, T)$. However, it does not vanish at $\theta \to -\infty$, and a plateau appears behind the solitary wave. The standard matching asymptotic procedure should be used to complete the uniformly valid asymptotic solution satisfying boundary conditions (5.82), see Ablowitz and Segur (1981) for details. Absence of plateau requires additional restrictions on the equation coefficients. Note that neither exact solitary wave solution (5.76) nor asymptotic *selected* solitary wave solution exists at $\beta_2 = 0$, $\beta_3 = 0$, and two values of the selected wave parameters exist thanks to the mixed dispersion term in Eq.(5.74), when $\alpha_3 \neq 0$.

5.4.4 *Evolution of asymmetric solitary waves*

Another asymptotic solution may be found when $k_d << 1$ is considered but now it is assumed that a solution of Eq.(5.74) is a function of the phase variable θ and the slow coordinate X, $v = v(\theta, X)$, with

$$\theta_x = P(X),\ \theta_t = -1,\ X = k_d\, x.$$

Then from (5.74) we get that

$$(1 - \alpha_1 P^2)v_\theta - 2\alpha_2 v\, v_\theta - (\alpha_3 - \alpha_4 P^2)\, v_{\theta\theta\theta} = k_d(2P[\alpha_1 v_X + \alpha_2\, v_X^2 +$$

$$(\alpha_3 - 2\alpha_4 P^2)v_{\theta\theta X}] +$$

$$P_X[\alpha_1 v + \alpha_2\, v_\theta^2 + (\alpha_3 - 6\alpha_4 P^2)v_{\theta\theta}] + P[\beta_1 v + \beta_2 v^2 + p^2\beta_3 v_{\theta\theta}]) + O(k_d^2). \quad (5.86)$$

The solution of Eq.(5.86) is sought in the form

$$v = v_0(\theta,\, X) + k_d v_1(\theta,\, X) + ..., \quad (5.87)$$

and satisfies boundary conditions (5.82). Substituting (5.87) into (5.86) we have a nonlinear O.D.E. for v_0 in the leading order,

$$(1-\alpha_1 P^2)v_{0,\theta} - 2\alpha_2 v_0\, v_{0,\theta} - (\alpha_3 - \alpha_4 P^2)\, v_{0,\theta\theta\theta} = 0. \tag{5.88}$$

Its solution,

$$v_0 = \frac{3(1-\alpha_1 P^2)}{2\alpha_2 P^2}\cosh^{-2}(p\theta),\; p^2 = \frac{1-\alpha_1 P^2}{4P^2(\alpha_3 - \alpha_4 P^2)} \tag{5.89}$$

now accounts for a solitary wave with parameters varying with respect to X. Depending upon the function $P(X)$ the solitary wave (5.89) may be symmetric or asymmetric with respect to its core (or maximum) at different points in time, see Fig. 1.18. The evolution of the solitary wave may be described solving the next order problem where an inhomogeneous linear equation holds,

$$(1-\alpha_1 P^2)v_{1,\theta} - 2\alpha_2 (v_0\, v_1)_\theta - (\alpha_3 - \alpha_4 P^2)\, v_{1,\theta\theta\theta} = F, \tag{5.90}$$

with

$$\begin{aligned} F = {} & 2P[\alpha_1 v_{0,X} + \alpha_2\, v_{0,X}^2 + (\alpha_3 - 2\alpha_4 P^2)v_{0,\theta\theta X}] + \\ & P_X[\alpha_1 v_0 + \alpha_2\, v_{0,\theta}^2 + (\alpha_3 - 6\alpha_4 P^2)v_{0,\theta\theta}] + \\ & P[\beta_1 v_0 + \beta_2 v_0^2 + P^2\beta_3 v_{0,\theta\theta}]. \end{aligned}$$

Like in previous section the solvability condition (5.83) yields the equation for the function $s = P^2$,

$$\alpha_2 H_3(s) s_X \;=\; s\,(\alpha_1 s - 1)(\alpha_3 - \alpha_4\, s)(6\alpha_3\beta_2 + [5\alpha_2\alpha_3\beta_1 -$$

$$6\beta_2(\alpha_4 + \alpha_1\alpha_3) - \alpha_2\beta_3]s - [5\alpha_2\alpha_4\beta_1 - 6\alpha_1\alpha_4\beta_2 - \alpha_1\alpha_2\beta_3]s^2), \tag{5.91}$$

where

$$H_3(s) = \alpha_1\alpha_4(\alpha_1\alpha_3 + 5\alpha_4)s^3 - 2\alpha_4(11\alpha_1\alpha_3 + 10\alpha_4)s^2 +$$

$$3\alpha_3(5\alpha_1\alpha_3 + 17\alpha_4)s - 30\alpha_3^2.$$

Analysis of the solutions of Eq.(5.91) may be done similar to that in the previous section. Again besides decay or an infinite growth of s one can describe its selection (from below and from above) to the values s_s obtained from the equation

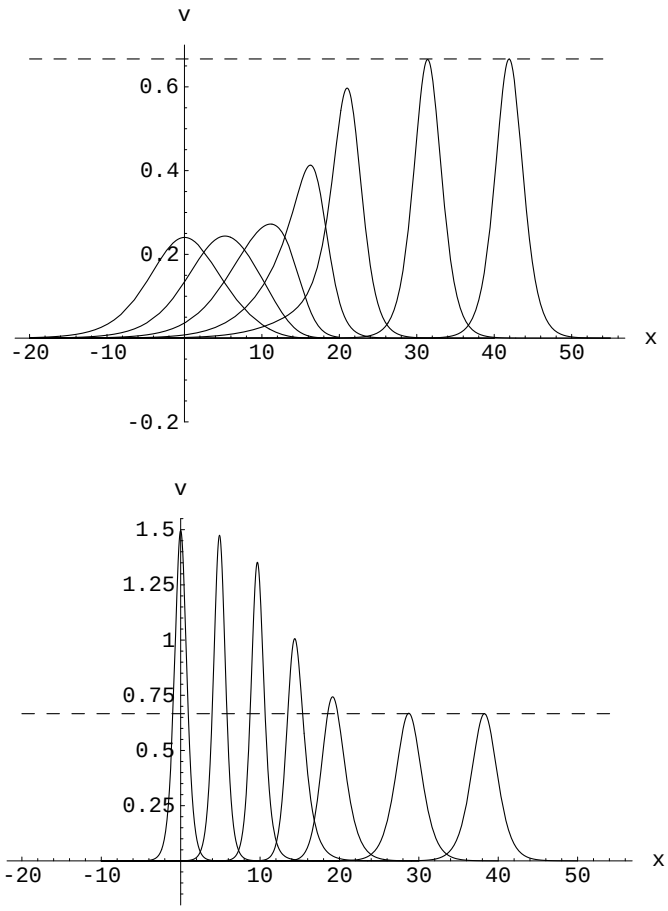

Fig. 5.7 Selection of the solitary waves governed by the solution (5.89), (5.91): (a) from below (b) from above.

$$[5\alpha_2\alpha_4\beta_1 - 6\alpha_1\alpha_4\beta_2 - \alpha_1\alpha_2\beta_3]s^2 - [5\alpha_2\alpha_3\beta_1 - 6\beta_2(\alpha_4 + \alpha_1\alpha_3) - \alpha_2\beta_3]s -$$

$$6\alpha_3\beta_2 = 0. \tag{5.92}$$

We see that after substitution $s = 1/c^2$ we get $H_3(s) = Q_6(c)/c^6$ while Eqs. (5.92) coincides with Eq. (5.85). It means that parameters of the selected solitary waves (5.76) and (5.89) are the same as well as the conditions required for the selection.

In Fig. 5.7 it is shown the temporal evolution of the solitary wave (5.89) whose amplitude and velocity vary according to Eq.(5.91). The parameters are chosen so as an initial profile is symmetric. We see that the initial wave increases, Fig. 5.7(a), or decreases, Fig. 5.7(b), into the asymmetric solitary wave. However, it transforms back into the symmetric wave during the selection both from below and from above as shown in the last two stages in Fig. 5.7(a) and Fig. 5.7(b).

We have studied how the external tangential dissipative (active) forces may support an evolution of the long strain solitary waves in an elastic rod. The conditions are found analytically when the selection of the solitary wave occurs both from below and from above. It is shown that both asymptotic solutions predict evolution into the symmetric selected solitary waves.

Previously, it was found analytically and in experiments the formation of asymmetric strain solitary wave in a narrowing rod, see Sec. 4.1 where the governing equation corresponds to Eq.(5.74) with $\beta_1 = \beta_1(x)$, $\beta_2 = 0$, $\beta_3 = 0$. In experiments only narrowing part of the rod was observed where a conversion to an asymmetric wave occurs, and there is no solitary wave selection.

Chapter 6

Bulk active or dissipative sources of the amplification and selection

Now the attention is paid on the situations when active/dissipative forces act inside a solid body. It is known that variation formulations used before in the book cannot be applied in the presence of volume dissipative effects unless some modifications are proposed. Thus Lord Rayleigh (1945) involved so-called dissipation function describing forces which depend upon temporal derivatives of the variables. Dissipation function is included into variation formulation through its elementary work. Another idea has been used in Maugin (2000) to develop a variation formulation in thermoelasticity. New variable has been introduced, called thermacy, into the relation for the free energy density.

Another approach is of phenomenological kind. The coupled governing equations are derived in the form of a hyperbolic equation of motion (or the equation with main hyperbolic part) and the equation for a variable responsible for dissipation (e.g., microdisplacement, temperature etc.). The last equation is usually parabolic and is obtained phenomenologically. This modelling is connected with the concept of internal variables Engelbrecht and Braun (1998); Maugin (1990); Maugin (1999); Maugin and Muschik (1994). Application of the internal variables to the wave problems may be found in Engelbrecht (1997); Engelbrecht *et. al* (1999); Engelbrecht and Maugin (1996); Maugin (1999). According to this theory, elastic stress or strain may be considered as observable variables in the usual sense of the word. Its behavior is described by the hyperbolic equation. In order to compensate our lack of description of the internal structure of material or the heat processes, another variables are introduced called internal variables. They are usually governed by the equations of parabolic type (i.e., diffusive). Various phenomenologocal model for viscoelastic biologocal media are discussed in Alekseev and Rybak (2002).

Below some active/dissipative problems are considered, namely, waves in microstructured solids, seismic waves, waves in a medium with moving defects, and thermoelastic waves. All processes are governed by coupled dissipative nonlinear partial differential equations. We do not consider here viscoelastic materials describing by the integro- differential equations, see about it, e.g., Christensen (1971); Engelbrecht (1979).

6.1 Nonlinear bell-shaped and kink-shaped strain waves in microstructured solids

The classical theory of elasticity cannot account for effects caused by the microstructure of a material. The theory of microstructures has been developed recently, see Capriz (1989); Engelbrecht and Braun (1998); Eringen (1968); Maugin and Muschik (1994); Mindlin (1964) and references therein quoted. Most results belong to the linear theory of elasticity, however, there are findings in the field of the nonlinear theory Engelbrecht and Braun (1998); Eringen (1968); Eringen and Suhubi (1964); Erofeev and Potapov (1993); Maugin and Muschik (1994). An important problem is the lack of data on the microstructure parameters, but a few works can be mentioned Savin *et. al* (1973b) where attempts to measure them were done. Also experiments were performed in Potapov and Rodyushkin (2001). Strain waves may be useful in developing a possible method to estimate the microparameters since shape, amplitude and velocity of the strain wave can carry informations about the microstructure.

Strain waves in microstructured medium were studied mainly in the linear approximation Eringen (1968); Mindlin (1964). Only a few works are devoted to the nonlinear waves in microstructured non-dissipative media Engelbrecht and Braun (1998); Erofeev and Potapov (1993); Sillat (1999) while the influence of the dissipative microstructure on the evolution of non-linear waves has been discussed in Cermelli and Pastrone (1997); Engelbrecht (1997); Engelbrecht and Braun (1998); Engelbrecht and Khamidullin (1988) The influence of dissipation/accumulation may be described by various methods, see Engelbrecht (1983) and references therein. Recently in a series of papers Cermelli and Pastrone (1997); Engelbrecht *et. al* (1999) the influence of dissipation on a shock propagation was studied in the one dimensional case while inertia of the microstructure was neglected into account together with the gradient of the microfield . Later numerical simulations were performed to account for the evolution of

periodic waves Sillat (1999).

Below we follow Porubov and Pastrone (2001). The model discussed in Cermelli and Pastrone (1997); Engelbrecht *et. al* (1999) is modified including both the inertia of the microstructure and the gradient of the microfield . As a result the nonlinear PDE with dispersion and dissipative (active) terms is derived. It is shown that it is able to describe both the bell-shaped and kink-shaped longitudinal strain solitary waves. The simultaneous influence of the accumulation/dissipation on the evolution is studied, and the selection of quasistationary dissipative solitary waves is found. A possibility of the estimation of the microstructure parameters is proposed on the basis of the results obtained here.

6.1.1 *Modelling of a microstructured medium with dissipation/accumulation*

Let us recall some basic ideas following Eringen (1968); Mindlin (1964). The motion of a material particle is characterized by the displacement vector with components $U_J(x_J, t)$. We suppose that the material particle contains discrete micromaterial elements whose displacements are accounted by the microdisplacement vector with components $U_J^{'}(x_J^{'}, t)$. Following Eringen (1968); Mindlin (1964), we assume the microdisplacement depends linearly on the microcoordinates $x_J^{'}$: $U_J^{'}(x_J^{'}, t) = x_K^{'}\psi_{KJ}(x, t)$. Hence the microdisplacement gradient is given by $\partial_I^{'}U_J^{'} = \psi_{IJ}$, thus avoiding dependence upon microcoordinates. In a reference configuration, the fundamental strains are given by: the Cauchy-Green macrostrain tensor , C_{IJ}, the distortion tensor, $E_{IJ} = \partial_I U_J - \psi_{IJ}$, and the microdisplacement gradient, $\Gamma_{IJK} = \partial_I \psi_{JK}$. This kinematical model is valid for particular families of microstructures only; if one needs a model to describe wider class of phenomena (solids with affine microstructures, liquid crystals, fluid with micro-bubbles, etc.), we refer to the references given in Cermelli and Pastrone (1997); Engelbrecht *et. al* (1999).

Let us assume the following:
(i) the movement is one dimensional, all variables depend upon the coordinate x and the time t;
(ii) the macromotion if small but finite. Then the geometrical nonlinearity is described by the only macrostrain $C_{XX} = U_x + 1/2U_x^2$, while the Murnaghan model is valid to account for the physical nonlinearity;
(iii) the microstructure is sufficiently weak to be considered in the linear approximation, $E_{XX} = U_x - \psi$, $\psi = \psi_{XX}$, $\Gamma_{XXX} = \psi_x$. Now and in the

following small lower indices denote differentiation.
(iv) the external forces are negligible.

Then the one dimensional governing equations may be written as in Mindlin (1964),

$$\rho U_{tt} = \sigma_x + \tau_x, \tag{6.1}$$

$$I\ \psi_{tt} = \eta_x + \tau, \tag{6.2}$$

where ρ is the macro-density, I characterizes micro inertia. In dissipationless case components σ_{eq}, τ_{eq} and η_{eq} of the tensors σ_{IJ}, τ_{IJ} and η_{IJK} are defined through the derivatives of the free energy W,

$$\sigma_{IJ} = \frac{\partial W}{\partial C_{IJ}},\ \tau_{IJ} = \frac{\partial W}{\partial E_{IJ}},\ \eta_{IJK} = \frac{\partial W}{\partial \Gamma_{IJK}},$$

which in the one dimensional limit Mindlin (1964); Murnaghan (1951) is reduced to:

$$\sigma_{eq} = (\lambda + 2\mu)U_x + \beta U_x^2,\ \tau_{eq} = D(U_x - \psi),\ \eta_{eq} = G\psi_x. \tag{6.3}$$

Here λ, μ are the Lame coefficients, $\beta = 3/2(\lambda + 2\mu) + l + 2m$, D and G are constant parameters. Assume the following representations in the general case,

$$\sigma = \sigma_{eq} + AU_{xt} + a\psi_t,\ \tau = \tau_{eq} + BU_{xt} + b\psi_t,\ \eta = \eta_{eq} + FU_{xxt} + f\,\psi_{xt}. \tag{6.4}$$

Note that A and a, B and b, F and f have the same dimensions. Dissipation inequality imposes some restrictions on the involved parameters Cermelli and Pastrone (1997); Engelbrecht (1983); Engelbrecht *et. al* (1999); Maugin and Muschik (1994). The reason of our assumption may be seen considering the linearized case in absence of the microstructure. Then we have for σ:

$$\sigma = (\lambda + 2\mu)U_x + AU_{xt},$$

that relates to the Voigt model, see, e.g., Bland (1960), the simplest extension of the Hook law to the viscoelastic media Alekseev and Rybak (2002). Our model may be considered as a generalization of the Voigt model of microstructured solids. Let us remark that the Voigt model accounts for the influence of the dissipation only. We would like to consider a more general case to account also for the energy influx to the strain wave caused by the microstructure. Hence the coefficients in Eq.(6.4) may be of different signs. Certainly, constitutive equations (6.4) are of phenomenological kind, since strictly speaking, they are not rigorously deduced within the

general framework of Rational Continuum Mechanics, but we do not want to go further in details here. In the following a more general constitutive equations will be derived according the basic assumptions and methods of Continuum Mechanics. Equation (6.4) can be seen as a particular case, obtained via proper additional assumptions.

Substituting Eqs.(6.3), (6.4) into Eqs. (6.1), (6.2) and introducing the functions $v = U_x$ and ψ as unknown variables, we obtain the coupled equations

$$\rho v_{tt} = (\lambda+2\mu+D)v_{xx} - D\psi_{xx} + \beta(\,v^2)_{xx} + (A+B)v_{xxt} + (a+b)\psi_{xxt}, \quad (6.5)$$

$$I\,\psi_{tt} = D(v-\psi) + Bv_t + b\psi_t + G\,\psi_{xx} + F\,v_{xxt} + f\,\psi_{xxt}. \quad (6.6)$$

Further simplifications follow considering only long waves with characteristic length $L >> 1$. Moreover, the macro strain v is elastic and does not exceed the yield point. Since the Murnaghan model is chosen, we are dealing with those elastic materials whose yield points are small, hence, the characteristic strain magnitude V is also small, $V << 1$. Let us introduce L as a scale for x, V- as a scale for v and ψ, L/c_0, as a scale for t, $c_0^2 = (\lambda + 2\mu)/\rho$ as a characteristic velocity. The microinertia term I depends upon the square of a typical size p of a microstructure element. Then I may be rewritten as $I = \rho p^2 I^*$, I^* being dimensionless. Using dimensional analysis, one can assume $G = p^2 G^*$, G^* having the dimension of stress. The influence of dissipation/accumulation may be conveniently described supposing $A = dA^*$, $a = da^*$, $B = dB^*$, $b = db^*$, $F = dF^*$, $f = df^*$, where d has the dimension of a length. Then three positive dimensionless parameters appear in Eqs.(6.5), (6.6):

(a) $\varepsilon = V << 1$ accounting for elastic strains;

(b) $\delta = p^2/L^2 << 1$, characterizing the ratio between the microstructure size and the wave length;

(c) $\gamma = d/L$, characterizing the influence of the dissipation.

Then the dimensionless governing equations are (we keep the notations for variables):

$$v_{tt} - (1 + \frac{D}{\lambda+2\mu})v_{xx} + \frac{D}{\lambda+2\mu}\psi_{xx} = \varepsilon\frac{\beta}{\lambda+2\mu}(\,v^2)_{xx} +$$

$$\gamma\left[\frac{(A^*+B^*)c_0}{\lambda+2\mu}v_{xxt} + \frac{(a^*+b^*)c_0}{\lambda+2\mu}\psi_{xxt}\right], \quad (6.7)$$

$$D\psi = Dv + \gamma c_0 \left[B^* v_t + b^* \psi_t\right] + \delta \left[G^* \psi_{xx} - (\lambda + 2\mu) I^* \psi_{tt}\right] + \gamma\delta c_0 \left[F^* v_{xxt} + f^* \psi_{xxt}\right]. \tag{6.8}$$

In absence of the microstructure, B^*, D, F^*, G, a^*, b^*, and δ are equal to zero, the only equation for v is of the form

$$v_{tt} - v_{xx} - \varepsilon \frac{\beta}{\lambda + 2\mu} (v^2)_{xx} - \gamma \frac{(A^* + B^*) c_0}{\lambda + 2\mu} v_{xxt} = 0. \tag{6.9}$$

Assume dissipation is weak. If we expand the solution of Eq.(6.8) in the form :

$$\psi = \psi_0 + \gamma\, \psi_1 + \delta\, \psi_2 + \gamma\delta\, \psi_3 + \gamma^2 \psi_4 + ..., \tag{6.10}$$

with

$$\begin{aligned}
&\psi_0 = v,\ \psi_1 = \frac{(B^* + b^*) c_0}{D} v_t,\ \psi_2 = \frac{G^*}{D} v_{xx} - \frac{(\lambda + 2\mu) I^*}{D} v_{tt},\\
&\psi_3 = \frac{[(F^* + f^*) D + (B^* + 2b^*) G^*] c_0}{D^2} v_{xxt} - \frac{(\lambda + 2\mu)(B^* + 2b^*) c_0 I^*}{D^2} v_{ttt},\\
&\psi_4 = \frac{b^* (B^* + b^*) c_0^2}{D^2} v_{tt}.
\end{aligned} \tag{6.11}$$

we obtain, by substituting (6.10), (6.11) into Eq.(6.7), the governing nonlinear PDE for the macrostrain $v(x,t)$,

$$v_{tt} - v_{xx} - \varepsilon\alpha_1 (v^2)_{xx} - \gamma\alpha_2\, v_{xxt} + \delta(\alpha_3\, v_{xxxx} - \alpha_4\, v_{xxtt}) +$$

$$\gamma\delta(\alpha_5\, v_{xxxxt} + \alpha_6\, v_{xxttt}) + \gamma^2 \alpha_7 v_{xxtt} = 0, \tag{6.12}$$

where

$$\begin{aligned}
&\alpha_1 = \frac{\beta}{\lambda + 2\mu},\ \alpha_2 = \frac{(A^* + a^*) c_0}{\lambda + 2\mu},\ \alpha_3 = \frac{G^*}{\lambda + 2\mu}, \alpha_4 = I^*,\\
&\alpha_5 = \frac{[(F^* + f^*) D + (B^* + b^* - a^*) G^*] c_0}{(\lambda + 2\mu) D},\\
&\alpha_6 = \frac{I^* (a^* - B^* - b^*) c_0}{D},\ \alpha_7 = \frac{a^* (B^* + b^*)}{\rho D}.
\end{aligned}$$

Comparing Eq.(6.12) with Eq.(6.9) we see that the inclusion of the gradient of microdistortion provides the dispersion v_{xxxx}, while the inertia of the microstructure gives us mixed dissipation and dispersion terms. The

evolution of nonlinear strain wave depends upon the ratio between parameters ε, γ and δ. This is the reason we retain terms quadratic in these parameters in the expansion of the solution (6.10). Sometimes they can be considered " negligibly small", sometimes-not, according to the different effects we want to point out, as it will be explained in the following.

There are two main types of nonlinear travelling solitary waves which could propagate keeping its shape, bell-shaped and kink-shaped solitary waves. The bell-shaped solitary wave usually appears as a result of a balance between nonlinearity and dispersion. The kink-shaped localized travelling structure may be sustained by different balances, one possibility occurs when nonlinearity is balanced by dissipation (or accumulation), another case corresponds to the simultaneous balance between dispersion, nonlinearity and dissipation (or accumulation). Typical shapes of the waves are shown in Figs. 1.1–1.5.

6.1.2 *Bell-shaped solitary waves*

The balance between nonlinearity and dispersion takes place when $\delta = O(\varepsilon)$. If in addition $\gamma = 0$, we have the nondissipative case governed by the double dispersive equation,

$$v_{tt} - v_{xx} - \varepsilon(\alpha_1 (v^2)_{xx} - \alpha_3 v_{xxxx} + \alpha_4 v_{xxtt}) = 0. \tag{6.13}$$

Its exact bell-shaped travelling solitary wave solution arises as a result of balance between nonlinear and dispersive terms. It satisfies the boundary conditions

$$\frac{\partial^k}{\partial x^k} v \to 0 \ \text{ for } \ |x| \to \infty, \ k = 0, 1, 2, 3, \tag{6.14}$$

and takes the form (see section 3):

$$v = \frac{6k^2(\alpha_4 c^2 - \alpha_3)}{\alpha_1} \cosh^{-2}(k\theta), \tag{6.15}$$

where $\theta = x - ct$, c is a free parameter,

$$k^2 = \frac{c^2 - 1}{4\varepsilon(\alpha_4 c^2 - \alpha_3)}. \tag{6.16}$$

Hence, the solitary wave (6.15) exists when $c^2 > \max\{1, \alpha_3/\alpha_4\}$ or when $0 < c^2 < \min\{1, \alpha_3/\alpha_4\}$. In the first case longitudinal tensile waves propagate, while in the second case only compressive waves propagate.

In general, Eq.(6.12) possesses an exact travelling bell-shaped solution vanishing at infinity Kudryashov (1988); Parkes and Duffy (1996),

$$v = -\frac{60ck^3\gamma\delta}{\varepsilon\alpha_1}(\alpha_5 + \alpha_6 c^2)\cosh^{-2}(k\,(x-ct))[\tanh(k\,(x-ct)) \pm 1], \quad (6.17)$$

where

$$k = \pm\frac{2\gamma c\alpha_2}{\delta(\alpha_3 - \widetilde{\alpha}_4 c^2)},$$

$\widetilde{\alpha}_4 = \alpha_4 + \varepsilon^2/\delta\,\alpha_7$, the phase velocity c is defined from the overdetermined system of bi-quadratic equations,

$$(\delta\alpha_4 - \gamma^2\alpha_7)c^4 - [\delta(\alpha_3 + \widetilde{\alpha}_4) + 24\gamma^2\alpha_2^2]c^2 + \delta\alpha_3 = 0,$$

$$(\delta\widetilde{\alpha}_4{}^2 + 16\gamma^2\alpha_2\alpha_6)c^4 + (16\gamma^2\alpha_2\alpha_5 - 2\delta\alpha_3\widetilde{\alpha}_4)c^2 + \delta\alpha_3^2 = 0,$$

hence, the exact solution (6.17) exists only for particular values of the coefficients in such equations.

When $\delta = O(\varepsilon)$, $\gamma << 1$, Eq.(6.12) is considered as dissipation perturbed double dispersive equation (6.13). The asymptotic solution is sought as a function of the phase variable θ and the slow time T, $v = v(\theta, T)$, with

$$\theta_x = 1,\ \theta_t = -c(T),\ T = \gamma\, t.$$

Then from (6.12) we get that

$$(c^2-1)v_\theta - \varepsilon\alpha_1(\,v^2)_\theta + \varepsilon(\alpha_3 - \alpha_4 c^2)\,v_{\theta\theta\theta} =$$

$$\gamma\left(2c[v_T - \varepsilon\alpha_4\,v_{\theta\theta T}] + c_T[v - \varepsilon\alpha_4\,v_{\theta\theta}] - c\frac{\partial^2}{\partial\theta^2}\left[\alpha_2\,v - \varepsilon(\alpha_5 + \alpha_6 c^2)\,v_{\theta\theta}\right]\right) +$$

$$O(\gamma^2). \quad (6.18)$$

The solution of Eq.(6.18) is sought in the form

$$v = v_0(\theta, T) + \gamma v_1(\theta, T) + ... \quad (6.19)$$

where v_i, $i = 0, 1, ...$, satisfy boundary conditions (6.14) at $|\theta| \to \infty$. Substituting (6.19) into (6.18) we have in the leading order

$$(c^2 - \alpha_1)v_{0,\theta} - \varepsilon\alpha_1(\,v_0^2)_\theta + \varepsilon(\alpha_3 - \alpha_4 c^2)\,v_{0,\theta\theta\theta} = 0. \quad (6.20)$$

The exact solitary wave solution of Eq.(6.20) has the form (6.15) with $c = c(T)$. The first order term v_1 in the solution (6.19) obeys the inhomogeneous linear equation

$$(c^2 - \alpha_1)v_{1,\theta} - 2\varepsilon\alpha_1\,(v_0\,v_1)_\theta + \varepsilon(\alpha_3 - \alpha_4 c^2)\,v_{1,\theta\theta\theta} = F, \tag{6.21}$$

where F is

$$F = 2c[v_{0,T} - \varepsilon\alpha_4\ v_{0,\theta\theta T}] + c_T[v_0 - \varepsilon\alpha_4\ v_{0,\theta\theta}] -$$

$$c\frac{\partial^2}{\partial\theta^2}\left[\alpha_2\,v_0 - \varepsilon(\alpha_5\ + \alpha_6 c^2)\ v_{0,\theta\theta}\right].$$

The operator M acting on the function v_1 in Eq.(6.21) is adjoint to the operator

$$M^A = (c^2 - 1)\partial_\theta - 2\varepsilon\alpha_1\,v_0\partial_\theta + \varepsilon(\alpha_3 - \alpha_4 c^2)\ \partial_\theta^3.$$

Then using (6.20) and boundary conditions at infinity one can obtain the solvability condition for Eq.(6.21),

$$\int_{-\infty}^{\infty} v_0\ F\,d\theta = 0, \tag{6.22}$$

which yields the equation for the function $s = c^2$,

$$7\varepsilon\,s_T\ Q_3(s) = 2s\,(s - \alpha_1)^2(q_1\,s^2 + q_2\,s + q_3), \tag{6.23}$$

with

$$Q_3(s) = 30\alpha_4^2\,s^3 + 3\alpha_4(17\alpha_3 + 5\alpha_4)\,s^2 + 2\alpha_3(10\alpha_3 + 11\alpha_4)\,s - \alpha_3(\alpha_4 + 5\alpha_3),$$

$$q_1 = 5\alpha_6,\ q_2 = 5\alpha_5 - 7\alpha_2\alpha_4 - 5\alpha_6,\ q_3 = 7\alpha_2\alpha_3 - 5\alpha_5. \tag{6.24}$$

Important features of the behaviour of s may be established analyzing Eq.(6.23) without integration. There may be decay or infinite growth of the initial velocity and the amplitude of the solitary wave (6.15). However, the most interesting evolution of s is realized when s (and hence the amplitude of the solitary wave) tends to the finite constant value s^* as $T \to \infty$. Hence the solitary wave in microstructured solids may be also selected. Indeed, the values of s^* are the real positive solutions of equation

$$q_1\,s^2 + q_2\,s + q_3 = 0. \tag{6.25}$$

Assume real roots of Eq.(6.25) are $s_{1q} < s_{2q}$. We denote by s_0 the initial value of s while the real root of Q_3 is s_Q. The sign of s_T needed for $s \to s_{nq}$ depends upon the sign of $Q_3(s)$ around $s = s_{nq}$, the sign of q_1, and the permitted interval defined from (6.16). When s_Q is the only real root of Q_3, and $s_Q < s_{1q}$ the amplification of the solitary wave with $s^* = s_{1q}$ occurs at $q_1 > 0$ if $s_Q < s_0 < s_{1q}$ while at $q_1 < 0$ it amplifies by $s^* = s_{2q}$ if $s_{1q} < s_0 < s_{2q}$. The attenuation of the wave to $s^* = s_{1q}$ happens when $q_1 > 0$, $s_{1q} < s_0 < s_{2q}$, in case $q_1 < 0$ wave with initial velocity $s_0 > s_{2q}$ decreases to $s^* = s_{2q}$. When $s_{1q} < s_Q < s_{2q}$ there is no selection for $q_1 > 0$, while for negative q_1 the double selection is realized. Thus, waves with $s_0 < s_{1q}$ amplify up to $s^* = s_{1q}$, but waves with $s_Q < s_0 < s_{2q}$ increase up to $s^* = s_{2q}$. Similarly, the attenuation to $s^* = s_{1q}$ happens for the waves with $s_{1q} < s_0 < s_Q$, while the waves with $s_0 > s_{2q}$ attenuate by $s^* = s_{2q}$. If $s_Q > s_{2q}$ there is no double selection, the wave evolution is similar to the case $s_Q < s_{1q}$. The situation when Q_3 has three real roots within or outside the interval $[s_{1q}, s_{2q}]$ may be analyzed in the same manner. Thus the stationary values of the solitary wave parameters are prescribed by the equation coefficients.

Amplification, attenuation and selection of the bell-shaped solitary wave $v = v_0$ is shown in Fig. 1.17. One can see that the solitary wave keeps its localized bell-shaped form. In the case of amplification, the wave amplitude increases, while the width decreases; the attenuation is provided by simultaneous decrease of the amplitude and the increase of the width. The addition of correction γv_1 does not change significantly the profile of $v = v_0$. It is relevant to notice that the solution (6.19) is not uniformly valid: the matching asymptotic expansions method Ablowitz and Segur (1981) should be applied to complete the solution, even if it does not modify the behaviour of the wave near its core.

6.1.3 *Kink-shaped solitary waves*

The equation (6.12) possesses also exact travelling kink-shaped solution Kudryashov (1988); Parkes and Duffy (1996), in the form

$$v \;=\; \sum_{i=0}^{3} A_{\,i}\, \tanh^i(k\,\theta), \tag{6.26}$$

with three possible sets of parameters $A_{\,i}$, k . There are no free parameters in the solution, and additional restrictions on the equation coefficients are

needed.

When dispersion is weak, i.e., $\varepsilon^2 < \delta < \varepsilon$ and $\gamma = O(\varepsilon)$, the nonlinearity is balanced by the dissipation/accumulation only. Then Eq.(6.12) may be rewritten as

$$v_{tt} - v_{xx} - \varepsilon(\alpha_1 (v^2)_{xx} + \alpha_2 v_{xxt}) = -\delta(\alpha_3 v_{xxxx} - \widetilde{\alpha}_4 v_{xxtt}) -$$

$$\varepsilon\delta(\alpha_5 v_{xxxxt} + \alpha_6 v_{xxttt}), \tag{6.27}$$

whose solution is sought in the form

$$v = v_0 + \delta v_1 + ... \tag{6.28}$$

where $v_i = v_i(\theta = x - ct)$ satisfies the boundary conditions

$$v_0 \to h_\pm,\ v_i \to 0,\ i > 0, \quad \text{for} \quad \theta \to \pm\infty, \tag{6.29}$$

and all derivatives of v_i with respect to θ vanish at infinity. For a kink $h_+ \neq h_-$. In the leading order the kink solution has the form

$$v \ = \ A\, m\, \tanh(m\,\theta) + B, \tag{6.30}$$

with

$$A = -\frac{\alpha_2 c}{\alpha_1},\ B = \frac{c^2 - 1}{2\varepsilon\alpha_1}. \tag{6.31}$$

There are two free parameters, the phase velocity c and the wave number m which are defined from the boundary conditions,

$$m = \frac{(h_- - h_+)\alpha_1}{2c\alpha_2},\ c^2 = 1 + \varepsilon\alpha_1(h_+ + h_-).$$

Next order solution v_1 consists of two parts, $v_1 = v_{1d} + v_{1a}$, where dispersive perturbation of the kink vanishing at infinity is accounted for the solution,

$$v_{1d} = \frac{2(\widetilde{\alpha}_4 c^2 - \alpha_3)m^2}{\varepsilon\alpha_1} \cosh^{-2}(m\theta) \log \mathrm{sech}(m\theta), \tag{6.32}$$

while higher order dissipative/active terms contribution is

$$v_{1a} = \frac{2(\alpha_5 + \alpha_6 c^2)cm^3}{\alpha_1} \cosh^{-2}(m\theta)\,(3\tanh(m\theta) - 2m\theta)\,. \tag{6.33}$$

The alterations of the kink shape in absence of higher order dissipative/active terms, $\alpha_5 = \alpha_6 = 0$, depend upon the sign of $(\alpha_4 c^2 - \alpha_3)/\alpha_1$. Typical profiles of $v = v_0 + \delta v_{1d}$ with v_{1d} defined by (6.32) are shown in Fig. 6.1 for different values of α_3 with other parameters values fixed:

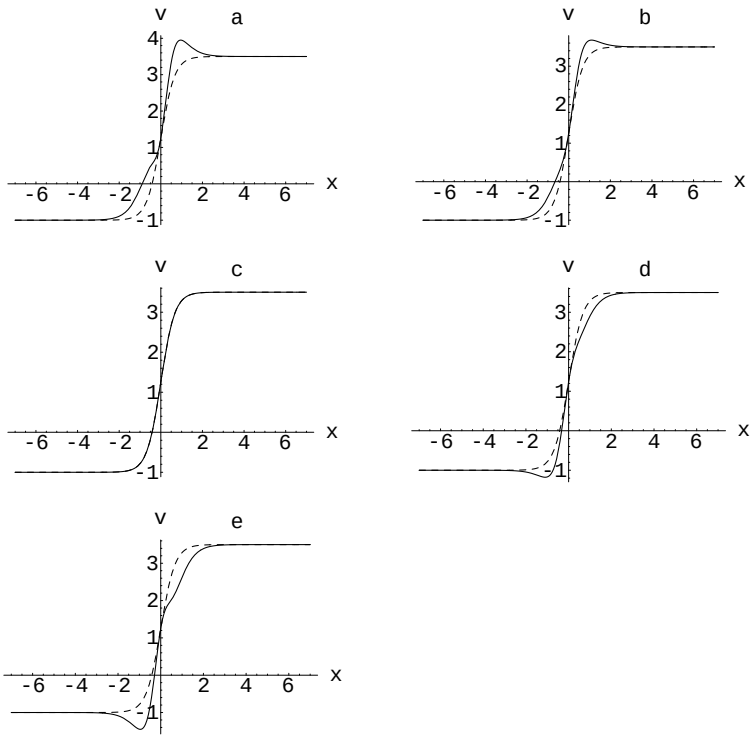

Fig. 6.1 Influence of weak dispersion on the shape of the kink-shaped wave. Shown by dashed line is the unperturbed kink.

$\alpha_1 = 1$, $\alpha_2 = -1$, $\widetilde{\alpha}_4 = 1$, $c = 1.5$, $m = 1.5$, $\varepsilon = 0.5$, $\delta = 0.1$. The "non-symmetric" disturbances of the kink shape are seen in Fig. 6.1(a), where $\alpha_3 = -2.5$; they become weaker when α_3 tends to zero. In Fig. 6.1(b) the value is $\alpha_3 = -0.5$, while undisturbed kink appears in Fig. 6.1(c) where $\alpha_3 = 2.25$. Then the disturbances develop on another "side" of the kink, as shown in Figs. 6.1(d,e) with $\alpha_3 = 5$, 7, correspondingly, and we have the mirror profile of those shown in Fig. 6.1(a, b). Fig. 6.1 shows the amplification of the kink-shaped wave since the difference between its maximum and its minimum is larger than in the undisturbed case. In contrast to the bell-shaped wave now the amplification is accompanied by the alteration of the wave profile. One can note the similarity with the profile in Fig. 1.5 of the exact kink-shaped solution of DMKdV equation. In Fig. 6.2 it is shown what happens with the kink (6.30) when there is no dispersion,

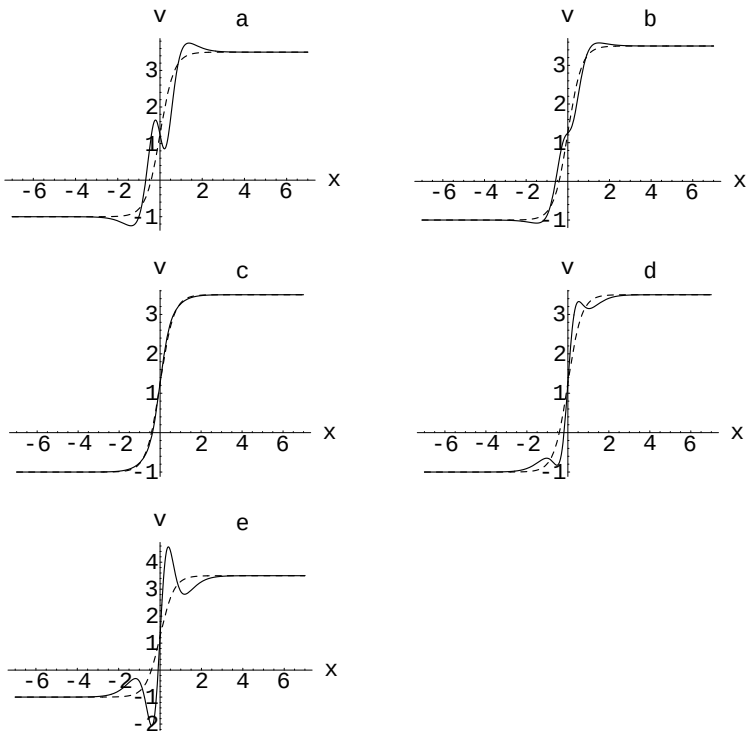

Fig. 6.2 nfluence of weak higher order dissipation on the shape of the kink-shaped wave . Shown by dashed line is the unperturbed kink.

$\alpha_3 = \alpha_4 = 0$. The profiles of $v = v_0 + \delta v_{1a}$ with v_{1a} defined by (6.33) correspond to $\alpha_1 = 1$, $\alpha_2 = -1$, $\alpha_5 = 1.5$, $c = 1.5$, $m = 1.5$, $\varepsilon = 0.5$, $\delta = 0.1$. In Fig. 6.2(a) $\alpha_6 = -2.5$, it varies from $\alpha_6 = -1.5$, Fig. 6.2(b) to $\alpha_6 = -0.5$, Fig. 6.2(c) where there are no disturbances. We have $\alpha_6 = 0.5$ in Fig. 6.2(d), while Fig. 6.2(e) corresponds to $\alpha_6 = 2.5$. Two main distinctions may be mentioned in comparison with profiles shown in Fig. 6.1. First, the disturbances of the kink shape are "symmetric" independently of the sign of α_6. Second, there are no mirror profiles arising at distinct signs of α_6.

The case $\delta = O(\varepsilon)$, $\gamma = O(\varepsilon)$ corresponds to the simultaneous balance between nonlinearity, dispersion and dissipation/accumulation, perturbed

by the higher order dissipative/active terms,

$$v_{tt} - v_{xx} - \varepsilon[\alpha_1(v^2)_{xx} + \alpha_2 v_{xxt} - \alpha_3 v_{xxxx} + \widetilde{\alpha}_4 v_{xxtt}] =$$

$$-\varepsilon^2(\alpha_5 v_{xxxxt} + \alpha_6 v_{xxttt}), \tag{6.34}$$

The solution of Eq.(6.34) is sought in the form

$$v = v_0 + \varepsilon v_1 + \varepsilon^2 v_2 ... \tag{6.35}$$

where boundary conditions (6.29) hold. Substituting (6.35) into (6.34) in the leading order we obtain the D'Alembert equation. Consider only one wave travelling to the left and assume v depends upon phase variable $\theta = x - ct$ with $c = 1 + \varepsilon c_1 + \varepsilon^2 c_2 ....$ Then at order ε the ODE equation for v_0 is,

$$2c_1 v_{0,\theta} - \alpha_1(v_0^2)_\theta + \alpha_2 v_{0,\theta\theta} + (\alpha_3 - \widetilde{\alpha}_4) v_{0,\theta\theta\theta} = 0. \tag{6.36}$$

Equation (6.36) possesses the exact kink-shaped solution Vlieg-Hultsman and Halford (1991),

$$v_0 = A \tanh(m\theta)\mathrm{sech}^2(m\theta) + B \tanh(m\theta) + C, \tag{6.37}$$

with

$$A = \frac{3\alpha_2^2}{50\alpha_1(\widetilde{\alpha}_4 - \alpha_3)},\ B = \frac{3\alpha_2^2}{25\alpha_1(\widetilde{\alpha}_4 - \alpha_3)},\ C = \frac{c_1}{\alpha_1},\ m = \frac{\alpha_2}{10(\alpha_3 - \widetilde{\alpha}_4)}.$$

It follows from (6.29) that

$$h_+ - h_- = 2B,\ c_1 = \frac{\alpha_1}{2}(h_+ + h_-),$$

and the solution exists under special boundary conditions. The influence of higher order terms may be studied in a similar way as done for the solution (6.28).

6.1.4 *Concluding remarks*

We have found that various features of the microstructure provide corresponding terms in the governing equation (6.12). Thus inertia yields mixed derivative terms v_{xxtt}, v_{xxttt} , while dispersion v_{xxxx} and higher order dissipative/active term v_{xxxxt} are due to the micro-deformation gradient. Dispersion is required for the existence of the bell-shaped solitary waves in an elastic microstructured medium. The dispersive term v_{xxtt} determines, in

particular, the existence of either exact compression or tensile solitary wave solutions (see Eqs.(6.15), (6.16)), while the higher order dissipative/active term $\alpha_6\, v_{xxttt}$ provides nonzero q_1 in Eq.(6.25), namely two stationary finite velocities of the solitary wave. Dispersion terms also account for the alterations in the kink-shaped wave profile, see Fig. 6.1, while higher order dissipative/active terms are responsible for a saturation which prevents unbounded growth of the bell-shaped solitary wave.

We see that pairs B^*, b^* and F^*, f^* appear in the expressions for the equation coefficients only in combinations $B^* + b^*$, $F^* + f^*$. Hence, one could reduce the number of the microstructure parameters in the model (6.4). At the same time there is a need of both A and a, since a^* appears in the expression for α_4 independently from A^*. The ratio between the small parameters, ε, δ and γ, allows to estimate the size p of the microstructure and the parameter d which influence the dissipation/accumulation effects. According to this ratio the governing equation (6.12) may describe either bell-shaped or kink- shaped solitary waves.

The solutions of Eq.(6.12) allow to describe in an *explicit form* the amplification of both types of the waves, as well as the selection of the solitary wave, when its parameters tend to the *finite* values prescribed by the coefficients of the governing equation. The relationships among these parameters define the thresholds that separate the parameters of the initial solitary waves which will be amplified or attenuated. The wave amplitude and velocity depend upon macro- and micro-properties of the microstructured medium through the analytical relationships, explicitly given above.

An application of the results obtained here consists in a possible estimation of the microstructure parameters on the basis of the strain wave behaviour. In principle, the measurements of the solitary wave amplitude and velocity allow to obtain the parameters of the microstructure using elastic macro-moduli known beforehand.

The asymptotic solution (6.19) describing bell-shaped solitary wave selection may help to explain transfer of the strain energy by the microstructure. Let us assume one single solitary wave with initial velocity $\sqrt{s_{01}}$, so that it will be attenuated propagating in the microstructured medium. Hence, it looses its energy which is absorbed by the microstructure. If another wave travels with an initial velocity $\sqrt{s_{02}}$, it will be amplified and it means that we need a source of energy to justify the amplification. A possible explanation could be that the energy stored by the microstructure is released because of the passing wave. Certainly the solution cannot describe an energy exchange between the waves but it gives us the range of

the microstructure parameters when the energy transmission is possible. The predictions of the asymptotic solution may be valid even in a more complicated unsteady process of the formation of solitary waves from an arbitrary input, see, e.g., Sec. 2.3.1. where the equation is considered rather similar to ours. Like here its single solitary wave asymptotic solution has been obtained in Sec. 2.2, and the conditions were found for the decay or a selection of a single solitary wave. Then the evolution of an initial arbitrary pulse has been studied numerically. It was found that the initial pulse splits into a *sequence* of solitary waves but each of them evolves according to the *single* solitary wave analytical solution.

6.2 Nonlinear seismic solitary waves selection

6.2.1 *Modelling of nonlinear seismic waves*

The influence of microstructure may explain phenomena caused by the energy input/output. Thus, recently the phenomenological theory has been developed in Engelbrecht (1997); Engelbrecht and Khamidullin (1988) to account for the seismic waves propagation in a horizontal layer. It was proposed to describe longitudinal strain waves evolution by the nonlinear equation,

$$u_t + u\,u_x + d\,u_{xxx} = \varepsilon f(u), \tag{6.38}$$

where f is the body force related to the so-called dilation mechanism,

$$f(u) = -\left(a_1 u - a_2 u^2 + a_3 u^3\right), \tag{6.39}$$

a_1, a_2, a_3 are positive constants and ε is a small parameter. Eq. (6.38) may describe an appearance of microseisms. The internal energy is stored in a geophysical medium, while propagating seismic waves may release the locked-in internal energy. Additional energy influx yields an amplification of the wave.

The basic idea of the seismic waves modelling is originated from the dilation theory in fracture mechanics Zhurkov (1983). It was assumed there that negative density fluctuations play an essential role in the strength of solids. These fluctuations are called dilatons. They may be considered as short-lived objects which are able to absorb energy from a surrounding medium. Accumulation of the energy may happen only up to a certain threshold value, then it is released, and the dilaton breaks generating

a crack. Qualitatively similar phenomena were recognized in Kozák and Šilený (1985) studying seismic energy release to explain the earthquake mechanism. The necessary condition for the fracturing of the medium under load is the existence of an inhomogeneity like a tectonic fault, an inclusion etc. Hence it was assumed in Kozák and Šilený (1985) to consider a medium as a two-dimensional homogeneous space containing a linear inhomogeneity compressed uniaxially, which is the structure that simulates commonly occurring geological faults subjected to tectonic stress with a predominant orientation. The area, affected by the loading, increases until the stress field achieves a threshold. Then a seismic-energy-releasing events occur. A similar dilatancy model has been proposed in Gusev (1988) to explain the nature of earthquake precursors. In particular, it was assumed that the mechanism of seismic radiation is connected with rapid dilatancy variations.

The theory developed in Gusev (1988); Kozák and Šilený (1985) is linear. Preliminary results, mainly qualitative, were obtained in Nikolaev (1989) to clarify the role of the simultaneous influence of nonlinearity and dissipation on the seismic waves evolution. However, the most important contribution to nonlinear description of the seismic waves has been done in Engelbrecht (1997); Engelbrecht and Khamidullin (1988). In order to govern a medium that may store and release the energy it was proposed in Engelbrecht (1997); Engelbrecht and Khamidullin (1988) to consider the Earth crust as a certain hierarchy of elastic blocks connected by thin interface layers. The layers are inhomogeneities where the energy is pumped, stored and released. Hence the interface layers behave like dilatons. Derivation of Eq.(6.38) in Engelbrecht (1997); Engelbrecht and Khamidullin (1988) is based on a model where the classic elasticity basic equations are complemented by the inclusion of the body force to account for the dilaton mechanism, and the phenomenological expression for the body force (6.39) closes the basic equations.

In absence of the body force, $f = 0$, Eq.(6.38) is the celebrated Korteweg-de Vries equation, whose exact travelling one-parameter solitary wave solution arises as a result of a balance between nonlinearity, $u\,u_x$, and dispersion, $d\ u_{xxx}$. Body force f plays a dissipative/active role destroying this balance. When all terms in the expression for f are dissipative, the solitary wave decays, while there is an infinite growth in a pure active case. The most interesting scenario happens in the mixed dissipative-active case. In particular, numerical results in Engelbrecht (1997); Engelbrecht and Khamidullin (1988) demonstrate transformation of an ini-

tial KdV soliton into a new stable localized bell-shaped wave with the amplitude and velocity prescribed by the equation coefficients.

The nature of the terms in f depend upon the values of the coefficients a_1, a_2, a_3, but numerical simulations cannot describe the intervals of their values required for the appearance of the stable localized waves. In order to obtain this information a procedure is developed below. Most of the results were first published in Porubov *et. al* (2003). First, the *unsteady* process of the transformation of the KdV soliton into the solitary wave with prescribed parameter values is described analytically. Then it is demonstrated numerically that solitary waves selection
(i) in presence of the solitary waves interactions;
(ii) when an initial profile is arbitrary;
(iii) when the parameter ε is not small
happens in *quantitative* agreement with asymptotic solution.

6.2.2 *Asymptotic solution of the governing equation*

Let us assume that $\varepsilon << 1$. Furthermore the function u depends upon a fast variable ξ and a slow time T , such as

$$\xi_x = 1,\ \xi_t = -V(T),\ T = \varepsilon\, t.$$

Then equation (6.38) becomes

$$d\, u_{\xi\xi\xi} - V\, u_\xi + u\, u_\xi + \varepsilon\, \left[u_T + a_1 u - a_2 u^2 + a_3 u^3\right] = 0. \tag{6.40}$$

The solution u of Eq.(6.40) is sought in the form:

$$u(\xi, T) = u_0(\xi, T) + \varepsilon\, u_1(\xi, T) + ... \tag{6.41}$$

In the leading order we have

$$d\, u_{0,\xi\xi\xi} - V\, u_{0,\xi} + u_0\, u_{0,\xi} = 0. \tag{6.42}$$

Equation (6.42) contains coefficients $V = V(T)$, hence, its exact solitary wave solution will have slowly varying parameters,

$$u_0 = 12\, d\, k(T)^2 \cosh^{-2}\left(k(T)\, \xi\right) \tag{6.43}$$

with $V = 4dk^2$.

In the next order an inhomogeneous linear differential equation for u_1 appears,

$$d\,u_{1,\xi\xi\xi} - V\,u_{1,\xi} + (u_0\,u_1)_\xi = F, \tag{6.44}$$

with

$$F = -\left[u_{0,T} + a_1 u_0 - a_2 u_0^2 + a_3 u_0^3\right].$$

Due to (6.43)

$$u_{0,T} = \frac{2k_T}{k}\,u_0 + \frac{k_T}{k}\,\xi\,u_{0,\xi}\,.$$

The solvability condition for Eq.(6.44) is

$$\int_{-\infty}^{\infty} u_0\,F\,d\xi = 0. \tag{6.45}$$

Then it follows from (6.45) that k obeys the equation

$$k_T = -\frac{2}{105}\,k\left(3456a_3d^2k^4 - 336a_2dk^2 + 35a_1\right), \tag{6.46}$$

that may be rewritten in terms of the solitary wave amplitude $Q = 12\,d\,k(T)^2$ as

$$Q_T = -\frac{4}{105}\,Q(24a_3Q^2 - 28a_2Q + 35a_1). \tag{6.47}$$

The roots of the equation,

$$24a_3Q^2 - 28a_2Q + 35a_1 = 0,$$

are

$$Q_1 = \frac{14a_2 - 2\sqrt{49a_2^2 - 210a_3a_1}}{24a_3},\ Q_2 = \frac{14a_2 + 2\sqrt{49a_2^2 - 210a_3a_1}}{24a_3}. \tag{6.48}$$

The behavior of the solitary wave amplitude, Q, depends on the value of $Q_0 \equiv Q(T=0)$. Indeed, Q will diverge at $Q_0 < Q_1$, when $Q_1 < Q_0 < Q_2$ parameter Q will grow up to Q_2, while if $Q_0 > Q_2$ it will decrease by Q_2. Hence parameters of the solitary wave tends to the finite values prescribed by the equation coefficients a_i and is selected.

A more quantitative description of the variation of Q can be given in order to see at what time the selected values are achieved. Equation (6.47)

may be directly integrated over the range $(0, T)$ giving the implicit dependence of Q on T:

$$T = \frac{35}{32a_3Q_1Q_2(Q_2 - Q_1)}$$

$$\left(Q_2 \log \frac{(Q - Q_1)}{(Q_0 - Q_1)} - Q_1 \log \frac{(Q - Q_2)}{(Q_0 - Q_2)} + (Q_2 - Q_1) \log \frac{Q}{Q_0}\right) \qquad (6.49)$$

One can see that T tends to infinity when $Q \to Q_2$, and expression (6.49) provides an *analytical* description of the time-dependent process of the parameter-value selection of the solitary wave (6.43).

With Eq.(6.47) being taken into account, the solution for u_1 is

$$u_1 = A_1[\tanh(k\xi) - 1] + [3A_1 + 2A_2\xi]\cosh^{-2}(k\xi) + [C - 3kA_1\xi - A_2\,\xi^2 - A_3 \log(\cosh(k\xi))]\tanh(k\xi)\cosh^{-2}(k\xi), \qquad (6.50)$$

where $C = const$,

$$A_1 = \frac{1152a_3d^2k^4 - 168a_2dk^2 + 35a_1}{35k},$$

$$A_2 = \frac{3456a_3d^2k^4 - 336a_2dk^2 + 35a_1}{35},\ A_3 = \frac{1728a_3d^2k^3}{35}.$$

We see that u_1 does not vanish at $\xi \to -\infty$, and a plateau appears behind a solitary wave. It may be of negative or positive amplitude depending upon the sign of A_1. A uniformly valid solution vanishing at $\xi \to -\infty$ may be obtained by the standard procedure described in Ablowitz and Segur (1981).

One can make now some important conclusions. If we formally assume $a_2 = 0$, $a_3 = 0$, both the behavior of the solitary wave parameters and the sign of the amplitude of plateau are defined by the sign of a_1. Indeed when $a_1 > 0$, the amplitude and velocity of the wave decreases in time according to Eq.(6.47), while $A_1 > 0$, and the plateau is negative. On the contrary, at negative a_1 we have an increase of the wave amplitude and positive plateau. In general case the plateau may be negative both in case of an increase and a decrease of the solitary wave. We also see that the increase of the amplitude is accompanied by the decrease of the wave width.

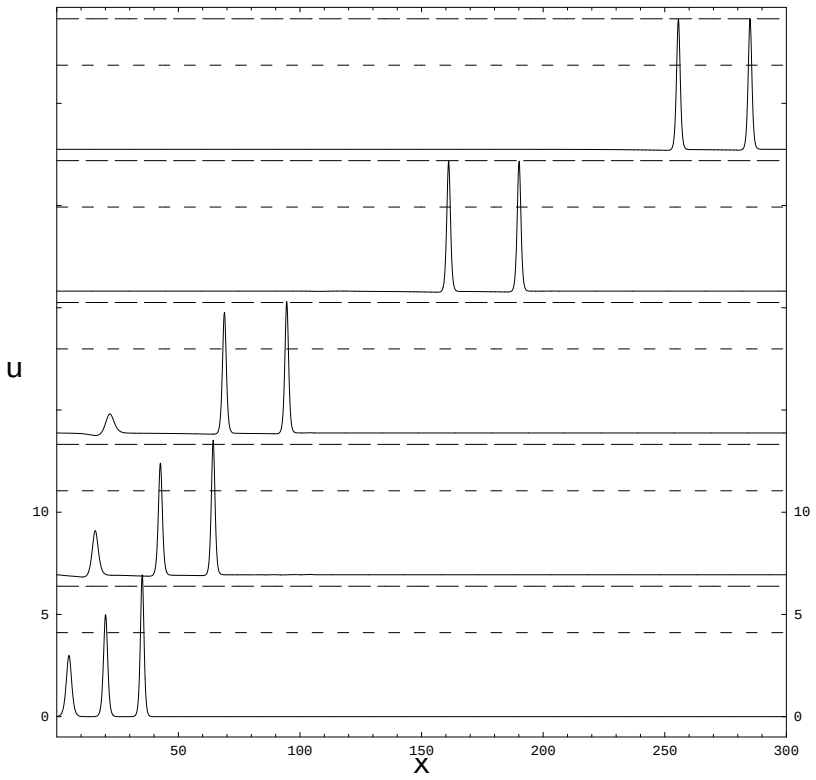

Fig. 6.3 Evolution of three solitary waves in absence of their interaction.

6.2.3 *Numerical simulations*

An asymptotic solution requires specific initial conditions while an evolution of an arbitrary initial disturbance as well as interactions between nonlinear localized waves are of practical interest. It may be described only numerically, however, it is important to know whether analytical predictions may be used for a design of numerics, since the behavior of the waves is sensitive to the values of the equation coefficients and the initial conditions.

We use for computations a pseudo-spectral method whose computation code was designed in Kliakhandler (1999). The program computes solutions of 1D scalar PDEs with periodic boundary conditions. It evaluates spatial derivatives in Fourier space by means of the Fast Fourier Transform, while

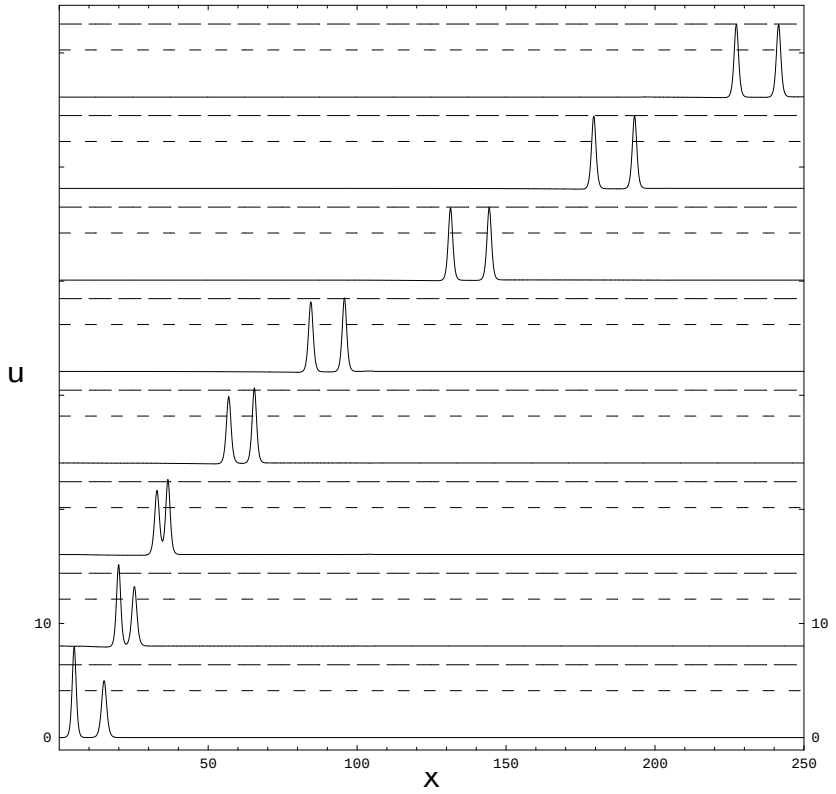

Fig. 6.4 Selection of two solitary in presence of their interaction.

the time discretization is performed using the fourth-order Runge–Kutta method. This scheme appears to have a good stability with respect to the time step and was already successfully used for the modelling of the solitary wave selection in a convective fluid, see Sec. 2.3.1. More detailed information about the code may be found in Kliakhandler (1999).

We choose the parameter values identical to that used in numerics in Engelbrecht (1997): $a_1 = 1$, $a_2 = 0.5$, $a_3 = 0.0556$, $d = 0.5$, $\varepsilon = 0.1$. Following the analysis from the previous section one obtains $Q_1 = 4.11$, $Q_2 = 6.38$, and the selection occurs for single solitary waves with initial amplitudes from the interval $4.11 < Q_0 < 6.38$. Numerical results for the single wave evolution confirm analytical solutions and agree with the

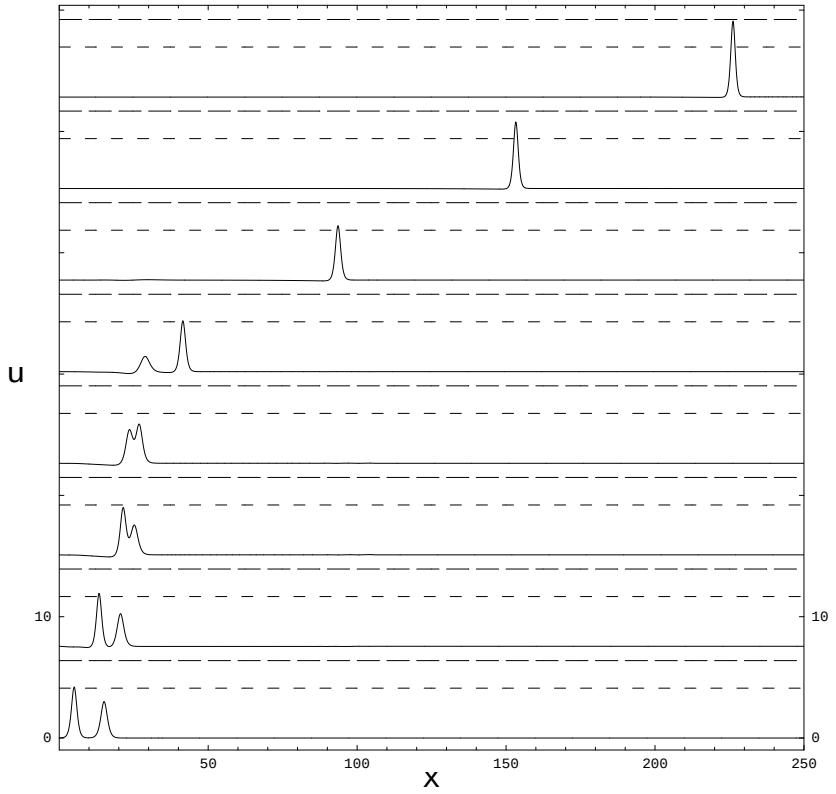

Fig. 6.5 Selection of one solitary wave and decay of another one in presence of their interaction.

numerical results in Engelbrecht (1997).

Then the initial conditions are changed to the profile containing three solitary waves each accounting for Eq.(6.43) at $T = 0$. First, the waves are located so as to avoid their interactions, see the first stage in Fig. 6.3. The initial amplitudes are chosen so as the values of the amplitudes of the first two solitary waves are brought into the selection interval, while the amplitude of the last one is below $Q_1 = 4.11$. For convenience here and in the following figures thresholds 4.11 and 6.38 are shown by dashed lines at each stage. One can see in Fig. 6.3 that the amplitudes of the first two solitary waves tend to the value $Q_2 = 6.38$, while the last solitary

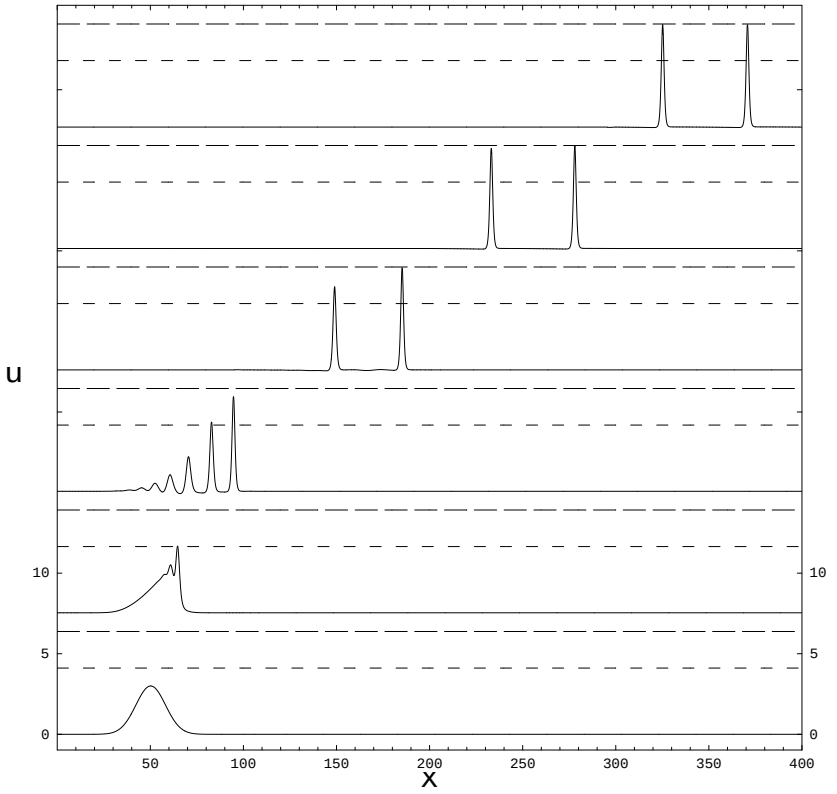

Fig. 6.6 Evolution of an initial Gaussian profile and formation of two selected solitary waves.

wave decays. Hence each solitary wave evolves according to the asymptotic solution.

Let us re-arrange the initial positions of the solitary waves in order to include their interactions. First we take two larger initial solitary waves. One can see in Fig. 6.4 that the interaction does not affect the selection, and again both solitary waves evolve in agreement with the theory. When the second initial solitary wave from Fig. 6.3 is moved behind the third one, its selection occurs despite the interaction, while the smaller wave decays. The process is shown in Fig. 6.5.

One can see in Fig. 6.6 that an initial Gaussian pulse produces a train of solitary waves of different magnitude in agreement with the KdV theory.

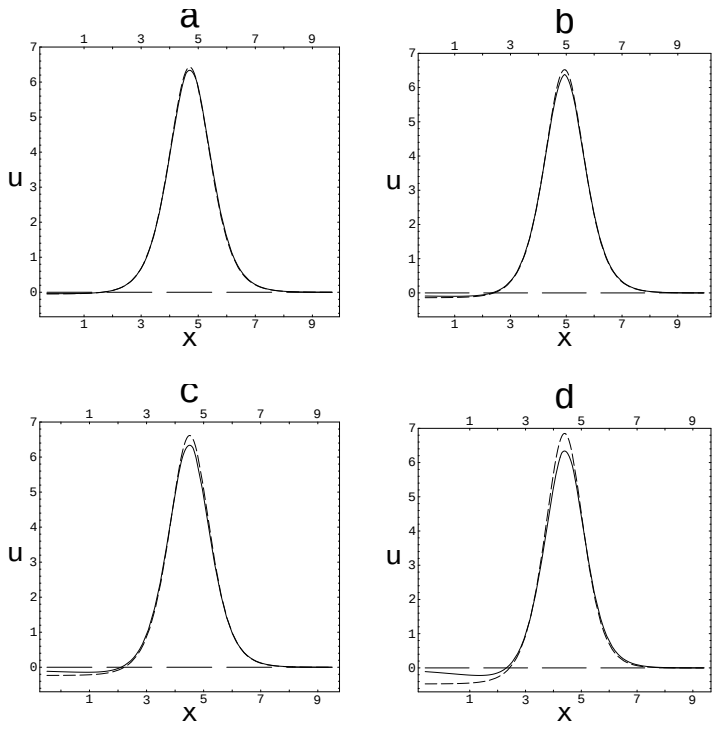

Fig. 6.7 Comparison of asymptotic (dashed line) and numerical (solid line) solutions at various ε: a)$\varepsilon = 0.1$, b)$\varepsilon = 0.3$, c)$\varepsilon = 0.5$, d)$\varepsilon = 1$.

Then, the selection of those solitary waves occurs whose amplitudes come to the selection interval prescribed by the theory. Note that two leading solitary waves are selected from below while other solitary waves generated from the input, vanish.

Finally, the influence of the small parameter value is studied. In Fig. 6.7 we see that the solitary waves continue to evolve according to the asymptotic solution with growth in ε. Two main deviations are observed. First is the difference in amplitudes, it is caused by the increase of the contribution of u_1 into the asymptotic solution. The difference in the shape of plateau is shown in Fig. 6.8 where we see the decrease of its length. At larger $\varepsilon = 10$ the plateau almost disappears, see Fig. 6.9, however, the initial solitary wave amplitude $Q_0 = 5$ still tends to the value $Q_2 = 6.38$. Selection from above still occurs for $Q_0 > Q_2$. At the same time we observe a decay of

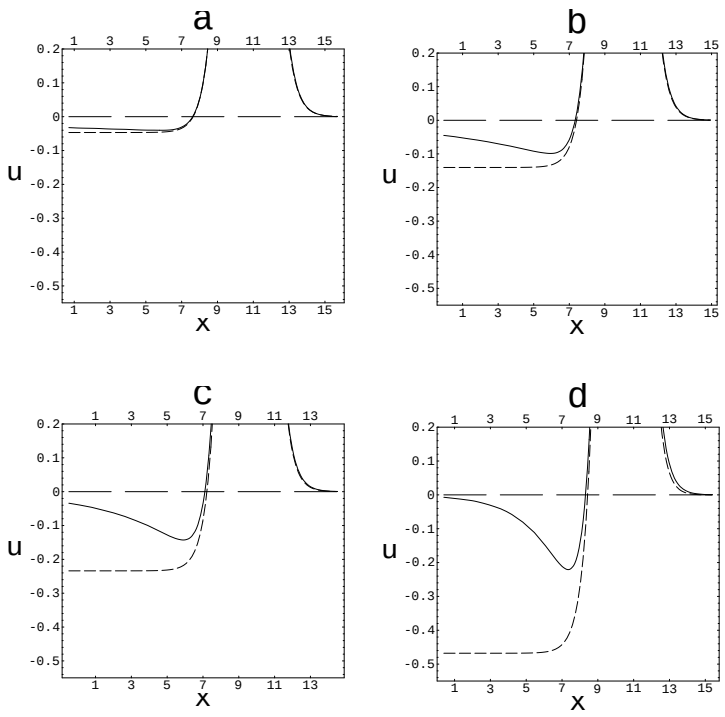

Fig. 6.8 Comparison of plateau in asymptotic (dashed line) and numerical (solid line) solutions at various ε: a)$\varepsilon = 0.1$, b)$\varepsilon = 0.3$, c)$\varepsilon = 0.5$, d)$\varepsilon = 1$.

the initial solitary wave with the amplitude less than $Q_0 = 3$ that already differs from the theoretical predictions, $Q_0 < Q_1 = 4.11$.

6.3 Moving defects induced by external energy flux

6.3.1 *Basic concepts and derivation of governing equations*

Recently it was found that point defects may be generated in a solid subjected to the laser radiation, see Mirzoev *et. al* (1996) and references therein. Point defect is described as a distortion in a crystal lattice in the area equal to the atomic volume. The simplest point defects in the crystal are the interstitial atom, or an atom occupying a position among the atomic equilibrium positions in an ideal lattice, and the vacancy, or a specific site in the

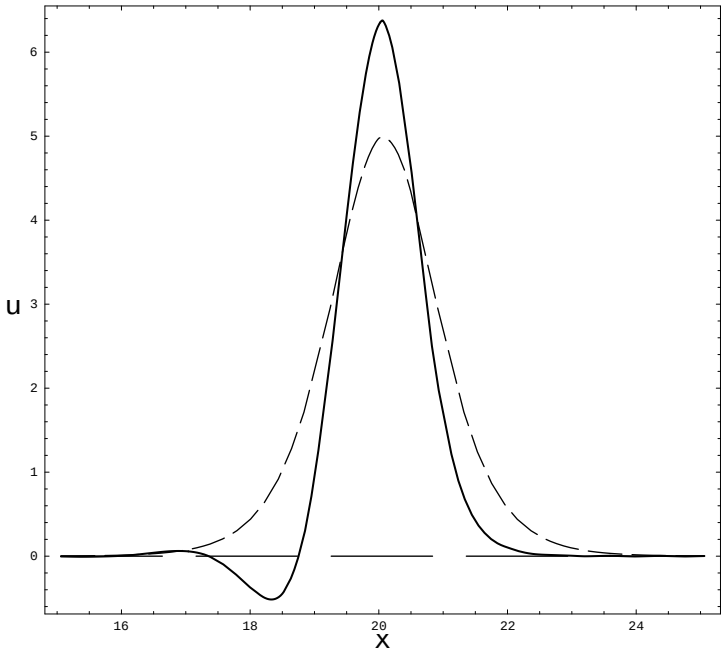

Fig. 6.9 Evolution of an initial KdV soliton (dashed line) at $\varepsilon = 10$.

lattice of the crystal where atoms are absent Kosevich (1981). Generation of defects due to the laser radiation may be explained using interaction of strain, temperature and defect-concentration fields Mirzoev *et. al* (1996).

Let us consider an isotropic solid where a concentrated energy influx (e.g., laser beam) produces moving point defects. Following Mirzoev *et. al* (1996) assume $n_j(x,t)$ be the concentration of defects of the kind j ($j = v$ for vacancies, $j = i$ for interstitial atoms) at a point $r(x,y,z)$ at time t. The main processes responsible for the temporal evolution of a defect are generation, recombination and diffusion. Then the kinetics of the point defects is governed by the equation

$$n_{j,t} = q_0 + q_\varepsilon U_x + D_j n_{j,xx} - \beta_j n_j, \tag{6.51}$$

where q_0 is a velocity of the defects generation in absence of the strain, next

term in the r.h.s. of Eq.(6.51) accounts for a contribution of a strain into the defects generation, D_j is the diffusion coefficient of the defect of the kind j, β_j is a recombination velocity at sinks Mirzoev and Shelepin (2001). Volume mutual recombination of the defects of different kind is neglected.

It is important that point defects cause deformation of a medium at macroscopic distances. In elasticity single defect is described by the volume density of the force, f ,

$$\mathbf{f}(\mathbf{r}) = -K\,\Omega_0\,\nabla\delta(\mathbf{r}),$$

where K is the bulk modulus, Ω_0 is a dilatation parameter representing the change in the volume of a crystal as a result of a formation of the one defect, while defect is located in the coordinate origin Kosevich (1981). For vacancies we have $\Omega_0 < 0$, while $\Omega_0 > 0$ corresponds to the interstitial atoms. Combinations of the point defects yield defect of the dipole kind that may be accounted for

$$\mathbf{f}(\mathbf{r}) = -K\,\Omega_{ik}\,\nabla_k\delta(\mathbf{r}),$$

where Ω_{ik} is a symmetric tensor. When dipole is axi-symmetric, we have

$$\Omega_{ik} \ = \Omega_0\delta_{ik} + \Omega_1(l_i l_k - 1/3\delta_{ik}),$$

where $\mathbf{l}$ is a unit vector of the dipole axis, Ω_1 defines deviator of the tensor Ω_{ik} Kosevich (1981). The average parameters of the crystal specimen may be introduced if a typical distance between defects is considerably less than the gradient of a strain field. Then we have in one-dimensional case

$$f = -K\,\Omega_j\,n_{j,x}, \tag{6.52}$$

where evolution of the concentration of defects is accounted for Eq. (6.51).

6.3.2 *Nonlinear waves in a medium*

One-dimensional governing equation in an elastic medium with moving defects may be obtained similar to Eq.(6.12) for a microstructured medium. We start with the coupled equations for n_j, Eq.(6.51), and for nonlinear longitudinal displacement $U(x,t)$,

$$\rho U_{tt} = \sigma_x, \tag{6.53}$$

where σ,

$$\sigma = (\lambda + 2\mu)U_x + (3/2(\lambda + 2\mu) + l + 2m)U_x^2 - K\,\Omega_j\,n_j.$$

is written with Eq. (6.52) being taken into account. Equations (6.53), (6.51) are simply uncoupled yielding the governing equation for the strain waves $v = U_x$,

$$v_{tt} - a_1 v_{xx} - a_2(\,v^2)_{xx} - a_3 v_{xxt} + a_4 v_{ttt} - a_5 v_{xxtt} + a_6 v_{xxxx} -$$

$$a_7(\,v^2)_{xxt} + a_8(\,v^2)_{xxxx} = 0, \tag{6.54}$$

where

$$a_1 = \frac{\lambda + 2\mu}{\rho} - \frac{K\,\Omega_j q_\varepsilon}{\rho\beta_j},\ a_2 = \frac{3(\lambda + 2\mu) + 2(l + m) + 3n}{4\rho},\ a_3 = \frac{(\lambda + 2\mu)}{\beta_j \rho},$$

$$a_4 = \frac{1}{\beta_j},\ a_5 = \frac{D_j}{\beta_j},\ a_6 = \frac{(\lambda + 2\mu)D_j}{\rho\beta_j},\ a_7 = \frac{a_2}{\beta_j},\ a_8 = \frac{a_2 D_j}{\beta_j}.$$

We see from Eq. (6.54) that presence of the moving defects provides a dispersion in an elastic medium, $a_5 v_{xxtt}$ and $a_6 v_{xxxx}$, as well as dissipative/active terms. The coefficients in Eq.(6.54) do not depend upon $K\,\Omega_j$ with the exception of a_1. Equation (6.54) is similar to Eq.(5.42) in Sec. 5.3 describing the influence of an external dissipative/active medium on the waves evolution in a rod. Various simplified cases may be considered:

(i) $\beta_j >> 1$;

(ii) $D_j << 1$;

(iii) $\beta_j >> 1, D_j << 1,\ D_j = O(1/\beta_j)$.

In case (i) recombinations at sinks are strong, quadratic nonlinearity in Eq.(6.54) predominates, and the formation of shocks is possible. Weakly dispersive case (ii) corresponds to the weak defects diffusion. An analysis is already done in Sec. 5.3 where stable kink waves with a "hat" are found, see Figs. 5.5, 5.6. Simultaneous weak diffusion and strong recombinations in case (iii) provide weakly dissipative/active case which has been also studied in Sec. 5.3. When dissipation is negligibly small, the influence of the higher-order nonlinear term $a_8(\,v^2)_{xxxx}$ may affect the wave behavior. Nondissipative limit of Eq.(6.54) is similar to a particular case of Eq.(1.3) that possesses oscillatory and multi-humps solitary wave solutions. However, it was shown in Sec. 1.2 that no stable bell-shaped solitary waves arise in absence of higher-order derivative terms (like $a_9\ v_{6x}$ or corresponding mixed derivative terms) in Eq.(6.54).

6.3.3 *Nonlinear waves in a plate*

Equation for longitudinal displacements in a plate already includes a dispersion even in absence of defects Mirzoev and Shelepin (2001):

$$U_{tt} - c_s^2 U_{xx} - \beta_N U_x U_{xx} - l^2(U_{ttxx} - c_\tau^2 U_{xxxx}) = -\frac{K\,\Omega_j}{\rho} n_{j,x} \qquad (6.55)$$

where

$$c_s^2 = \frac{E}{\rho(1-\nu^2)},\ \beta_N = \frac{3E}{\rho(1-\nu^2)} + \frac{2(1-2\nu)}{\rho(1-\nu)^3}[(1-2\nu)^2 l + 2(1-\nu+\nu^2)m],$$

$$l^2 = \frac{\nu^2 h^2}{12(1-\nu)^2},\ c_\tau^2 = \frac{\mu}{\rho(1-\nu^2)},$$

where h is the width of the plate. Again the evolution of the defects is accounted for Eq.(6.51). Note that nonlinearity parameter β_N does not depend upon the Murnaghan modulus n.

Uncoupling of Eqs. (6.51), (6.55) in case of the elastic plate is performed similar to the previous case giving the governing equation for the longitudinal strains of the form

$$v_{tt} - a_1 v_{xx} - a_2(v^2)_{xx} - a_3 v_{xxtt} + a_4 v_{xxxx} -$$

$$b_1 v_{xxt} + b_2 v_{ttt} - b_3(v^2)_{xxt} - b_4 v_{xxttt} + b_5 v_{xxxxt} +$$

$$c_1(v^2)_{xxxx} + c_2 v_{xxxxtt} - c_3 v_{xxxxxx} = 0, \qquad (6.56)$$

where

$$a_1 = c_s^2 - \frac{K\,\Omega_j q_\varepsilon}{\rho\beta_j},\ a_2 = \frac{\beta_N}{2},\ a_3 = \frac{D_j}{\beta_j} + l^2,\ a_4 = \frac{c_s^2 D_j}{\beta_j} + c_\tau^2 l^2,$$

$$b_1 = \frac{c_s^2}{\beta_j},\ b_2 = \frac{1}{\beta_j},\ b_3 = \frac{\beta_N}{2\beta_j},\ b_4 = \frac{l^2}{\beta_j},\ b_5 = \frac{c_\tau^2 l^2}{\beta_j},$$

$$c_1 = \frac{\beta_N D_j}{2\beta_j},\ c_2 = \frac{l^2 D_j}{\beta_j},\ c_3 = \frac{c_\tau^2 l^2 D_j}{\beta_j}.$$

Equation (6.56) is close to Eq. (5.8) when the c_i's terms in Eq.(6.56) are negligibly small. Now dispersion appears as a result of the plate finite width also, and no weakly dispersive case is considered. Case $\beta_j >> 1$ now corresponds to the perturbed double-dispersive equation. There are

two kinds of perturbations. Active/dissipative perturbations are accounted for the b_i's terms while c_i's terms in Eq.(6.56) play the role of higher-order nonlinearity and dispersion. Hence weakly active/dissipative case is realized if additionally $D_j << 1$. Then we can use the results obtained in Sec. 5.2 to account for the bell-shaped solitary wave selection. When $D_j >> 1$, c_i's terms dominate over b_i's terms, and we obtain from Eq. (6.56) the hyperbolic analog of Eq.(1.3) studied in Chapter 1. Thanks to nonzero dispersion, now stable oscillatory and multi-humps strain solitary wave solutions are realized, see Figs. 1.7–1.16.

Eqs. (6.51), (6.55) are uncoupled in a different manner if $\beta_j << 1$. In this case Mirzoev and Shelepin (2001) derived the governing equation for the strain $v = U_x$,

$$v_t + c_s v_x + \beta_d v_{xxx} + \gamma_N \ v_x^2 = gv - \zeta v_{xx} + \mu v_{xxxx}, \tag{6.57}$$

where

$$\beta_d = \frac{l^2(c_s^2 - c_\tau^2)}{2},\ \gamma_N = \frac{\beta_N}{\rho c_s},\ g = \frac{q_\varepsilon K\,\Omega_j}{\rho c_s^2},\ \zeta = \beta_j l^2,\ \mu = D_j l^2.$$

Equation (6.57) may be considered as a perturbed KdV equation. Then its asymptotic solution is obtained using the procedure explained in Chapter 2. The most interesting case is realized when small parameters q_ε, D_j and β_j are of the same order. Then one can write $g = \varepsilon g^*, \zeta = \varepsilon\zeta^*, \mu = \varepsilon\mu^*$, $\varepsilon << 1$. The fast variable θ and the slow time T are introduced as before, $\theta_x = 1$, $\theta_t = -V(T)$, $T = \varepsilon t$, and the solution of Eq.(6.57) may be obtained using the procedure from Chapter 2 to describe the selection of localized longitudinal strain wave as a result of the interactions with moving defects.

6.4 Thermoelastic waves

In thermoelasticity the deformation and temperature fields affect each other. As a result governing equations for the strains and the temperature should be coupled. Very often the influence of the temperature on the strains is negligibly small. However, thermoelasticity is important to study attenuation of the waves that is observed in experiments. Of special interest are the processes in polymers arising due to the laser irradiation Kartashov and Bartenev (1988). Linear thermoelastic waves were studied extensively, analytical results for a medium may be found in Kartashov and Bartenev (1988); Nowacki (1975); Nowacki (1986b), while numerical simu-

lations are performed in Berezovski *et. al* (2000); Berezovski and Maugin (2001). Nonlinear surface wave attenuation is considered in Mayer (1990); Mayer (1995), nonlinear bulk waves are studied in a medium in Engelbrecht and Maugin (1996) and in a rod in Potapov and Semerikova (1988).

Derivation of the equations may be done by various approaches. First, the balance laws are used. In contrast to liquid, the transfer of heat in solids is caused by the heat conduction only. Usually the equation of the heat conduction is obtained from the energy conservation law Engelbrecht (1983); Engelbrecht and Nigul (1981); Landau *et. al* (1987); Maugin (1995); Maugin (1999); Nowacki (1975); Nowacki (1986b):

$$T\,\frac{\partial S}{\partial t} = div(\kappa \nabla T), \tag{6.58}$$

where S is the entropy per unit volume, T is the absolute temperature, κ is the thermal conductivity. Usually the last coefficients is assumed to be constant while the entropy is expressed through the temperature and the displacements u_i. Then Eq. (6.58) is rewritten in the form, see, e.g., Landau *et. al* (1987),

$$C_v\,\frac{\partial T}{\partial t} + \frac{C_p - C_v}{\alpha_T}\frac{\partial}{\partial t} div(\mathbf{u}) = \kappa \nabla T, \tag{6.59}$$

where C_p, C_v are the specific heat per unit volume at fixed density and volume respectively, α_T is the heat extension coefficient. The Fourier law of thermal conduction, $Q = -\kappa\,\nabla T$, is used to obtain Eqs. (6.58), (6.59). However, it predicts an infinite velocity of a thermal wave. In order to describe the finite velocity, the modification of the law is needed. In particular, the generalized law has been proposed in Likov (1967)

$$Q = -\kappa\,\nabla T - \tau^* Q_t,$$

that takes into account an inertia of the heat flux, τ^* is a time of the heat flux relaxation.

Balance of linear momentum provides the second equation of thermoelasticity,

$$\rho_0 \mathbf{u}_{tt} = Div \mathbf{P}^*, \tag{6.60}$$

where $\mathbf{P}^*$ is the Piola-Kirchoff tensor expressed through the free energy density $W(\mathbf{u},T)$, $\mathbf{P}^* = \partial W/\partial \nabla \mathbf{u}$. Usually only the term linear in $\nabla \mathbf{u}$, $\alpha_T(T - T_0)\nabla \mathbf{u}$, is included into W. Hence Eq.(6.60) contains the linear

term depending on the temperature while nonlinearity is caused by the same reasons as in pure elastic case, see Chapter 3.

Equations of thermoelasticity may be derived using the variational methods Fares (2000); Maugin (2000); Nowacki (1975); Nowacki (1986b); Rayleigh (1945). However, usually only Eq.(6.60) is derived from the Hamilton principle while the heat equation is introduced additionally Fares (2000). It was Maugin (2000) who proposed the modification of the free energy density so as to get all field equations, balance laws and constitutive relations for the theory of materially inhomogeneous, finitely deformable, thermoelastic conductors of heat, in the same manner. The main idea is to assume a dependence upon an additional variable called thermacy whose temporal derivative is the temperature. As a result all equations obtained turn out strict conservation laws. Classical dissipative thermoelastic equations are obtained by isolation the contribution of the thermacy.

6.4.1 *Nonlinear waves in thermoelastic medium*

Below we follow Engelbrecht and Maugin (1996) where one-dimensional model is considered using the notion of thermodynamic internal variables. The evolution nonlinear equation is obtained for the observable variable (longitudinal strain $v = U_x(x,t)$) in a medium when temperature $T(x,t)$ effects are considered as internal process. The equation of motion,

$$\rho_0 U_{tt} - (\lambda+2\mu)U_{xx} - [3(\lambda+2\mu)+2l+4m]U_x U_{xx} = -(3\lambda+2\mu)\alpha_T T_x, \quad (6.61)$$

is coupled with the energy equation for the temperature,

$$\rho_0 C_v T_t + T_0(3\lambda+2\mu)\alpha_T U_{xt} = \kappa T_{xx}. \quad (6.62)$$

Single nonlinear model equation may be obtained in case of a weak coupling, $\varepsilon = (3\lambda+2\mu)\alpha_T/\rho_0$, $\varepsilon << 1$. Introducing fast and slow variables, $\xi = c_0 t - X$, $\tau = \varepsilon X$, one obtains for $w = U_t$

$$w_t + a_1\, w w_\xi + \Lambda\, w = 0, \quad (6.63)$$

where

$$a_1 = \frac{3(\lambda+2\mu)+2l+4m}{(\lambda+2\mu)\varepsilon c_0},\ \Lambda = \frac{T_0((3\lambda+2\mu)\alpha_T)^2}{2\varepsilon\rho_0 c_0 \kappa},\ c_0^2 = \frac{\lambda+2\mu}{\rho_0}.$$

Exact solution of Eq.(6.63) is known Whitham (1974), it may include shocks when the gradient of the initial excitation is large enough.

When the coupling is not weak, Eqs. (6.61), (6.62) are transformed by another way, the case was not considered in Engelbrecht and Maugin (1996). First, the temperature gradient, T_x, is expressed through the displacement using Eq.(6.61). Then it is substituted into Eq.(6.62) differentiated with respect to x, yielding nonlinear equation for U

$$(\rho_0 C_v c_0^2+\Lambda_1)U_{xxt}-\rho_0 C_v U_{ttt}+a_2(U_x^2)_{xt}+\kappa(U_{xxtt}-c_0^2 U_{xxxx}-a_2(U_x^2)_{xxx}) = 0, \tag{6.64}$$

where

$$a_2 = \frac{3(\lambda+2\mu)+2l+4m}{2\rho_0},\ \Lambda_1 = \frac{T_0((3\lambda+2\mu)\alpha_T)^2}{\rho_0}.$$

In the reference frame, $\xi = x - Vt$, the ODE reduction of Eq.(6.64) is written for the function $v = U_\xi$

$$\frac{\partial^2}{\partial\xi^2}\left(b_1 v + b_2 v^2 + b_3 v_\xi + b_4 (v^2)_\xi\right) = 0,$$

with

$$b_1 = V(\rho_0 C_v V^2 - \rho_0 C_v c_0^2 - \Lambda_1),\ b_2 = -a_2 V,$$
$$b_3 = \kappa(V^2 - c_0^2),\ b_4 = -a_2\kappa.$$

There is a similarity with the Burgers equation model if the last nonlinear term is negligibly small. The Burgers model has been developed in Engelbrecht (1983), with the relaxation tame taken into account. Comparison of the Burgers equation model and the model governed by Eq.(6.63) is done in Engelbrecht and Maugin (1996).

6.4.2 *Longitudinal waves in thermoelastic rod*

As already noted, thermal conduction weakly affects strain waves in solids. More promising looks the influence of a heat transfer through the lateral surface of a wave guide, especially caused by a laser irradiation, see Kartashov and Bartenev (1988); Mirzoev *et. al* (1996) and references therein. The influence of the external heat transfer on nonlinear longitudinal strain waves in a rod has been studied in Potapov and Semerikova (1988). Estimations done there demonstrate the dominant role of the heat transfer in comparison with the thermal conduction mechanism.

The coupled equations of thermoelasticity are used in Potapov and Semerikova (1988) with the heat transfer boundary conditions on the rod

lateral surface being taken into account:

$$U_{tt} - c_s^2 U_{xx} - \beta\, U_x U_{xx} + 0.5R^2(\nu(1-\nu)U_{ttxx} - \nu c_s^2 U_{xxxx}) = -\alpha_T c_s^2\, T_x, \tag{6.65}$$

$$\rho_0 C_v R\, T_t - \kappa R\, T_{xx} + 2h(T - T_0) = -\alpha_T E T_0 R\, U_{xt}, \tag{6.66}$$

where β is a nonlinear coefficient, $\beta = \rho_0^{-1}(3E + l(1-2\nu)^3 + 4m(1-2\nu)(1+\nu) + 6n\nu^2)$, R is a radius of the rod, T_0 is a constant temperature of an external medium, h is a heat transfer coefficient, $c_s^2 = E/\rho_0$ is a velocity of the linear waves in a rod. Note that the dispersion terms coefficient from Potapov and Semerikova (1988) are corrected here in accordance with the procedure from Chapter 3.

Let us differentiate Eq.(6.66) with respect to x and substitute T_x from Eq.(6.65). Then the governing equation for longitudinal displacements holds,

$$\frac{\partial}{\partial t}\{\rho_0 U_{tt} - E\left(1 + \frac{\alpha_T^2 E T_0}{\rho_0 C_v}\right) U_{xx} - \beta\, U_x U_{xx} + \frac{\rho_0 \nu(1-\nu)R^2}{2} U_{ttxx} -$$

$$\frac{\nu E R^2}{2} U_{xxxx}\} = \left(\frac{\kappa}{\rho_0 C_v}\frac{\partial^2}{\partial x^2} - \frac{2h}{\rho_0 C_v R}\right)\{\rho_0 U_{tt} - E U_{xx} -$$

$$\beta\, U_x U_{xx} + \frac{\rho_0 \nu(1-\nu)R^2}{2} U_{ttxx} - \frac{\nu E R^2}{2} U_{xxxx}\}. \tag{6.67}$$

We are dealing with elastic strain waves whose magnitude B is small, $B << 1$, and with long waves with typical length L, so as $R/L << 1$. As usual we consider the case of a balance between nonlinearity and dispersion introducing small parameter $\varepsilon = B = (R/L)^2$. Contribution of the terms in the r.h.s. of Eq.(6.67) is weak, they may be considered as small perturbations. Then nonlinear and dispersive terms may be omitted in the r.h.s. Obviously,

$$U_{xx} = \frac{\rho_0^2 C_v}{E(\rho_0 C_v + \alpha_T^2 E T_0)} U_{tt} + O(\varepsilon).$$

Hence the simplest equation accounting for the influence of both the heat transfer and thermal conduction on longitudinal strain waves $v = U_x$ is

$$v_{tt} - c_s^2(1 + \frac{\alpha_T^2 c_s^2 T_0}{C_v})v_{xx} - \frac{\beta}{2\rho_0}\,(v^2)_{xx} + \frac{\nu(1-\nu)R^2}{2}v_{ttxx} - \frac{\nu c_s^2 R^2}{2}v_{xxxx} =$$

$$\frac{\alpha_T^2 c_s^2 T_0}{C_v + \alpha_T^2 c_s^2 T_0}\left(\frac{\kappa}{\rho_0 C_v}v_{ttx} - \frac{2h}{\rho_0 C_v R}v_t\right). \tag{6.68}$$

Certainly Eq.(6.68) may be studied by the methods developed in Chapter 2 to account for an amplification, attenuation and selection of longitudinal thermoelastic waves.

Bibliography

Ablowitz, M. J. and Segur, H.(1981) *Solitons and the Inverse Scattering Transform*, SIAM, Philadelphia.

Akhmediev, N.N. and Ankiewicz, A. (1997) *Solitons. Nonlinear pulses and beams,* Chapman & Hall, London.

Alekseev, V.N. and Rybak S.A. (2002) "Equations of state for viscoelastic biological media", *Acoust. J.* **48**, 511.

Alexeyev, A.A.(1999) "Classical and non-classical interactions of kinks in some bubbly medium", *J. Phys. A* **32**, 4419.

Bateman, G. and Erdelyi, A. (1953-54). *Higher Transcendental Functions*, vol. 3, McGraw Hill, New York.

Belokolos, A., Bobenko, A., Enol'skij, V., Its, V. and Matveeev, V. (1994) *Algebro- Geometrical Approach to Nonlinear Integrable Equations*, Springer, Berlin.

Benilov, E.S., Grimshaw, R., Kuznetsova, E.P.(1993) " The generation of radiating waves in a singularly-perturbed KdV equation", *Physica D* **69** 270.

Berezin, Ya. A. (1987) *Modelling Non-Linear Wave Processes.* VNU Science Press, Utrecht.

Berezovski, A., Engelbrecht, J., Maugin, G.A. (2000) "Thermoelastic wave propagation in inhomogeneous media", *Arch. Appl. Mech.* **70**, 694.

Berezovski, A. and Maugin, G.A. (2001) "Simulation of Thermoelastic Wave Propagation by Means of a Composite Wave-Propagation Algorithm", *J. Compt. Phys.* **168**, 249.

Bhatnagar, P.L. (1979) *Nonlinear Waves in One-Dimensional Dispersive Systems,* Claredon Press, Oxford.

Biryukov, S.V., Gulyaev, V.V., Krylov, V.V. and Plessky, V.P. (1991) *Surface acoustic waves in inhomogeneous media*, Nauka, Moscow (in Russian).

Bland, D. R. (1960) *The Theory of Linear Viscoelasticity*, Oxford .

Bland, D.R.(1969) *Nonlinear Dynamic Elasticity*, Blaisdell, Waltham, Mass et al.

Boyd, J. P. (1991) "Weakly non-local solitons for capillary-gravity waves: the fifth-degree Korteweg-de Vries equation", *Physica D* **48**, 129.

Bridges, T. (1986) "Cnoidal standing waves and the transition to the travelling hydravlic jump", *Phys. Fluids* **29**, 2819.

Bukhanovsky, A.V. and Samsonov, A.M. (1998) "Numerical Simulation of Nonlinear Elastic waves in Inhomogeneous Wave Guides", St. Petersburg, Preprint of the Institute for High performance Computing and Data Bases No 6-98 (in Russian).

Bullough, R.K. and Caudrey, P.J. eds., (1980) *Solitons*, Springer, Berlin.

Burgers, J.M. (1948) "A Mathematical model illustrating the theory of turbulence", *Adv. Appl. Mech.* **1**, 171.

Byrd, P.F. and Friedman, M.D. (1954) *Handbook of Elliptic Integrals for Engineers and Physicists*, Springer, Berlin.

Calogero, F. and Degasperis, A. (1982) *Spectral Transform and Solitons*, North-Holland, Amsterdam.

Cariello, F. and Tabor, M.(1989) "Painlevé expansions for nonintegrable evolution equations", *Physica D* **39**, 77.

Capriz, G. (1989) Continua with microstrucure, *Springer Tracts in Nat. Phil.*, V.35, Springer, Berlin.

Cermelli, P. and Pastrone, F. (1997) "Growth and decay of waves in microstructured solids", *Proc. Estonian Acad. Sci. Phys. Math.* **46**, 32.

Chang, H.-C., Demekhin, E.A., and Kopelevich, D.I. (1995) "Stability of a Solitary Pulse against Wave Packet Disturbances in an Active Media", *Phys. Rev. Lett.* **75**, 1747.

Chow, K.W. (1995) "A class of exact, periodic solutions of nonlinear envelope equations", *J. Math. Phys.* **36**, 4125.

Christensen, R.M. (1971) *Theory of Viscoelasticity*, Academic Press, New York.

Christiansen, P.L., Eilbeck, J.C., Enolskii, V.Z., Kostov, N.A. (1995) "Quasi-periodic solutions of the coupled nonlinear Schrödinger equations", *Proc. R. Soc. Lond. A* **451**, 685.

Christou, M.A. and Christov, C.I. (2000) "Fourier-Galerkin Method for Localized Solutions of the sixth-order Generalized Boussinesq Equation", *Proc. Intern. Conf. on Dynamical Systema and Differential Equations*, May 18-21, Atlanta, USA, 121.

Christou, M.A. and Christov, C.I. (2002) "Fourier-Galerkin Method for Localized Solutions of the Equations with Cubic Nonlinearity", *J. Comp. Anal. Appl.* **4**, 63.

Christov, C.I. (1994) "Numerical Investigation of the long-time evolution and interaction of localized waves", in *Fluid Physics*, eds. Velarde, M.G. & Christov, C.I., World Scientific, Singapore, 353.

Christov, C.I. and Maugin, G.A. (1995) "An Implicit Difference Scheme for the Long-Time Evolution of Localized Solutions of a Generalized Boussinesq System", *J. Compt. Phys.* **116**, 39.

Christov, C.I., Maugin, G.A., Velarde, M.G. (1996) "Well-posed Boussinesq paradigm with purely spatial higher-order derivatives", *Phys.Rev. E* **54**, 3621.

Christov, C.I., Pontes, J., Walgraef, D., and Velarde, M.G. (1997) "Implicit time splitting for fourth-order parabolic equations", *Comput. Methods Appl. Mech. Engrg.* **148**, 209.

Christov, C.I. and Velarde, M.G. (1994) "Inelastic Interactions of Boussinesq Solitons", *Intern. J. Bif. Chaos* **4**, 1095.

Christov, C.I. and Velarde, M.G. (1995) "Dissipative solitons", *Physica D* **86**, 323.

Cole, J.D. (1968) *Perturbation Methods in Applied Mathematics*, Blaisdell, Waltham, Mass.

Conte, R. (1989) "Invariant Painlevé analysis of partial differential equations", *Phys. Lett. A* **140**, 383.

Conte, R., Fordy, A., Pickering, A. (1993) "A perturbative Painlevé approach to nonlinear differential equations", *Physica D* **69**, 33.

Crighton, D.G. (1995) "Applications of KdV", *Acta Applicandae Mathematicae* **39**, 39.

Dai, H.-H. (1998) "Model equations for nonlinear dispersive waves in a compressible Mooney-Rivlin rod", *Acta Mech.* **127**, 193.

Dodd, R.K., Eilbeck, J.C., Gibbon, J.D. and Morris, H.C. (1982) *Solitons and Nonlinear Wave Equations*, Academic Press, London et al.

Drazin, P.G. and Johnson, R.S. (1989) *Solitons: an Introduction*, Cambridge Univ. Press, Cambridge.

Dreiden, G.V., Porubov, A.V., Samsonov, A.M., Semenova, I.V., and Sokurinskaya, E.V. (1995) "Experiments in the propagation of longitudinal strain solitons in a nonlinearly elastic rod", *Tech. Phys. Lett* **21**, 415.

Dreiden, G.V. , Porubov, A.V., Samsonov, A.M., Semenova, I.V. (2001) "Reflection of a longitudinal strain solitary wave from the end face of a nonlinearly elastic rod", *Tech.Phys.* **46**, no 5, 505.

Elmer, F.-J. (1997) "Nonlinear dynamics of dry friction", *J. Phys. A: Math. Gen.*, **30**, 6057.

Engelbrecht, J. (1979) "One-Dimensional Deformation waves in Nonlinear Viscoelastic Media", *Wave Motion* **1**, 65.

Engelbrecht, J. (1983) *Nonlinear wave processes of deformation in solids*, Pitman, Boston.

Engelbrecht, J. ed. (1989) *Nonlinear Waves in Active media*, Springer-Verlag, Berlin.

Engelbrecht, J. (1997) *Nonlinear Wave Dynamics. Complexity and Simplicity,* Kluwer, The Netherlands.

Engelbrecht, J. and Braun, M. (1998) "Nonlinear waves in nonlocal media", *Appl. Mech. Rev.* **51**, No 8, 475.

Engelbrecht,J., Cermelli, P. and Pastrone, F. (1999) "Wave hierarchy in microstructured solids", In: *Geometry, Continua and Microstructure*. Ed. by G.A. Maugin, Herman Publ., Paris, 99.

Engelbrecht, J. and Khamidullin, Y. (1988) "On the possible amplification of nonlinear seismic waves", *Phys. Earth Planet. Inter.* **50**, 39.

Engelbrecht, J. and Maugin, G.A. (1996) "Deformation waves in thermoelastic media and the concept of internal variables", *Arch. Appl. Mech.* **66**, 200.

Engelbrecht, J. and Nigul, U. (1981) *Nonlinear Deformation Waves,* Nauka, Moscow (in Russian).

Erbay, S., Erbay, H.A., and Dost, S. (1991) "Nonlinear wave modulation in micropolar elastic media-I. longitudinal waves" *Int. J. Engng. Sci.* **29**, 845.

Eringen, A. C. (1968). *Theory of micropolar elasticity.* P. 622. *In: Fracture. An advanced treatise. V.2. Mathematical fundamentals.* Ed. by H. Liebowitz, Academic Press, New York.

Eringen, A.C. and Suhubi, E.S. (1964) "Nonlinear theory of micro-elastic solids", *Intern. J. Eng. Sci.* **2**, Part I, 189, Part II, 389.

Erofeev, V.I. (2002) *Wave processes in solids with microstructure*, World Scientific, Singapore.

Erofeev, V.I. and Klyueva, N.V. (2002) "Solitons and nonlinear periodic strain waves in rods, plates and shells", *Acoust. J.* **48**, 725 (in Russian).

Erofeev, V.I. and Potapov, A.I. (1993) "Longitudinal strain waves in non-linearly elastic media with couple stresses", *Int. J. Nonl. Mech.* **28**, 483.

Fares, M.E. (2000) "Generalized non-linear thermoelasticity for composite laminated structures using a mixed variational approach", *Int. J. Nonl. Mech.* **35**, 439.

Feng, B.F. and Kawahara, T. (2000) "Stationary travelling-wave solutions of an unstable KdV-Burgers equation", *Physica D* **137**, 228.

Fletcher, C.A.J. (1984) *Computational Galerkin Methods*, Springer, Berlin.

Fowler, A.C. (1997) *Mathematical Models in the Applied Sciences,* Cambridge Univ. Press, Cambridge.

Frantsevich, I.N., Voronov, F.F., and Bakuta, S.A. (1982) *Elastic Constants and Moduli of Metals and Nonmetals*, Naukova Dumka, Kiev, (in Russian).

Galin, L.A. (1980) *Contact problems of elasticity and viscoelasticity,* Nauka, Moscow (in Russian).

Garazo, A.N. and Velarde, M.G. (1991) "Dissipative Korteweg-de Vries description of Marangoni-Bénard oscillatory convection", *Phys. Fluids A* **3**, 2295.

Godunov, S.K. and Ryaben'kii, V.S. (1973) *Difference Schemes*, Nauka, Moscow, (in Russian).

Godunov, S.K. and Ryaben'kii, V.S. (1987) *Difference Schemes: introduction to the underlying theory of*, North-Holland, Amsterdam.

Godunov, S.K. (1997) *Ordinary Differential Equations with Constant Coefficients*, AMS.

Goryacheva, I.G. (1998) *Contact mechanics in tribology,* Dordrecht etc., Kluwer.

Goryacheva, I.G. (2001) *Mechanics of friction interaction*, Nauka, Moscow (in Russian).

Grimshaw, R., Malomed, B. and Benilov, E. (1994) " Solitary waves with damped oscillatory tails: an analysis of the fifth-order Korteweg-de Vries equation", *Physica D* **77**, 4783.

Grimshaw R, Pelinovsky E. and Talipova T. (1999) "Solitary wave transformation in a medium with sign-variable quadratic nonlinearity and cubic nonlinearity", *Physica D* **132**, 40.

Gulyaev, Yu.V. and Polsikova, N.I. (1978) "Shear surface acoustic waves on a cylindriucal surface of a solid body covered by a layer of a foreign material", *Sov. Phys- Acoust. R.* **24**, 287.

Gusev, A. A. (1988) Two dilatancy-based models to explain coda-wave precursors and P/S spectral ratio. *Tectonophysics* **152**, 227.

Hähner, G. and Spencer, N. (1998) "Rubbing and scrubbing", *Physics Today*, No 9, 22.

Harker, A.N. (1988) *Elastic Waves in Solids with Application to Nondestructive Testing of Pipelines*, Hilger & Bristol, Philadelphia.

Hunter, J.K. and Scheurle, J. (1988) "Existence of perturbed solitary wave solutions to a model equation for water waves", *Physica D* **32**, 253.

Ince, E. (1964) *Ordinary Differential Equations,* Dover, New York.

Jeffrey, A. and Kawahara, T. (1982) *Asymptotic Methods in Nonlinear Wave Theory*, Pitman, London.

Jeffrey, A. and Engelbrecht, J., eds. (1994) *Nonlinear Waves in Solids*, Springer, Wien.

Johnson, K.L. (1985) *Contact Mechanics*, Cambridge Univ. Press, Cambridge.

Kalker, J.J., Dekking, F.M., and Vollebregt, E.A.H. (1997) "Simulation of Rough, Elastic Contacts", *J. Appl. Mech.* **64**, 361.

Kano, K. and Nakayama, T. (1981) "An Exact Solution of the Wave Equation $u_t + u\,u_x - u_{5x} = 0$", *J. Phys. Soc. Jpn.* **50**, 361.

Karpman, V. I. (1993) "Radiation by solitons due to higher-order dispersion", *Phys.Rev. E* **47**, 2073.

Karpman, V.I. and Vanden-Broeck, J.-M. (1995) "Stationary solitons and stabilization of the collapse described by KdV-type equations with high nonlinearities and dispersion", *Phys. Lett. A* **200**, 423.

Karpman, V.I. (1998) "Evolution of radiating solitons described by the fifth order Korteweg-de Vries type equations", *Phys. Lett. A* **244**, 394.

Karpman, V.I. (2001) "Stability of solitons described by KdV-type equations with higher-order dispersion and nonlinearity (analytical results)", *Phys. Lett. A* **284**, 246.

Kartashov, E.M. and Bartenev, G.M. (1988) "Dynamic effects in solid under interactions with intensive heat fluxes", *Itogi Nauki i tekhniki, Ser.: Khimia i tekhnologia visokomolekuliarnikh soedinenii"* **25**, 3 (in Russian).

Kascheev, V.N. (1990) *Heuristic Approach to Obtain Solutions to Nonlinear Equations of Solitonics,* Zinatne, Riga (in Russian).

Kawahara, T. (1972) "Oscillatory Solitary Waves in Dispersive Media", *J. Phys. Soc. Jpn.* **33**, 260.

Kawahara, T. (1983) " Formation of saturated solitons in a nonlinear dispersive system with instability and dissipation" *Phys. Rev. Lett.* **51**, 381.

Kawahara, T. and Takaoka, M. (1988) "Chaotic Motions in an Oscillatory Soliton Lattice", *J. Phys. Soc. Jpn.* **57**, 3714.

Kerr, A.D. (1964) "Elastic and viscoelastic foundation models", *J. Appl. Mech.* **31**, 491.

Kliakhandler, I.L. (1999) http://www.math.mtu.edu/˜igor

Kliakhandler, I.L. , Porubov, A.V. and Velarde, M.G. (2000) "Localized finite-amplitude disturbances and selection of solitary waves", *Phys. Rev. E* **62**, 4959.

Kodama, J. and Ablowitz, M. (1981) "Perturbation of solitons and solitary waves", *Stud. Appl. Math.* **64**, 225.

Korpel, A. and Banerjee, P. (1984) "Heuristic guide to nonlinear dispersive wave equations and soliton-type solutions", *IEEE* **72**, 1109.

Korteweg, D.J. and de Vries, G. (1895) "On the change of the form of long waves advancing in a rectangular channel and on a new type of long stationary waves", *Phil. Mag.* **5**, 422.

Kosevich, A.M. (1981) *Physical Mechanics of Real Crystals*, Naukova Dumka, Kiev (in Russian).

Kosevich, A.M. and Savotchenko, S.E. (1999) "Features of dynamics of one-dimensional discrete systems with non-neighbouring interactions, and role of higher-order dispersion in solitary wave dynamics", *Low Temp. Phys.* **25**, 737 (in Russian).

Kostov, N.A. and Uzunov, I.M. (1992) "New kinds of periodical waves in birefringent optical fibers", *Opt. Comm.* **89**, 389.

Kozák, J. and Šilený, J. (1985) "Seismic events with non-shear component. I. Shallow earthquakes with a possible tensile source component". *PAGEOPH* **123**, 1.

Kudryashov, N.A. (1988)" Exact solitonic solutions of the generalized evolution equation of wave dynamics", *J. Appl. Math. Mech.* **52**, 361.

Landau L.D., Lifshitz E.M., Kosevich, A.M., and Pitaevsky, L.P. (1987) *Theory of Elaticity*, Pergamon Press, Oxford.

Levi, D. and Winternitz, P. , eds. (1992) *Painlevé Transcendents: Their Asymptotics and Physical Applications*, Plenum Press, New York and London.

Likov, B. Ya. (1967) *Theory of thermal conduction*, Nauka, Moscow (in Russian).

Lou, S., Huang, G. and Ruan, H. (1991) "Exact solitary waves in a convecting fluid", *J. Phys. A* **24**, L587.

Love, A.E.H. (1927) *A Treatise on the Mathematical Theory of Elasticity*, University Press, Cambridge.

Lurie, A.I. (1990) *Nonlinear Theory of elasticity*, Amsterdam, Elsevier.

Marchant, T.R. (1996) "The evolution and interaction of Marangoni-Bénard solitary waves", *Wave Motion* **23**, 307

Maugin, G.A. (1990) "Internal Variables and Dissipative Structures", *J. Non-Equilib. Thermodyn.* **15**, 173.

Maugin, G.A. (1993) *Material Inhomogeneities in Elasticity*, Chapman & Hall, London.

Maugin, G.A. (1995) "Material forces: Concepts and applications", *Appl. Mech. Rev.* **48**, 213.

Maugin, G.A. (1999) *The Thermomechanics of Nonlinear Irreversible Behaviors. An Introduction.*, World Scientific, Singapore.

Maugin, G.A. (2000) "Towards an analytical mechanics of dissipative materials" *Rendiconti del Seminario Matematico dell'Universita' e Politecnico di Torino* **58**, 171.

Maugin, G.A. and Muschik, W. (1994) "Thermodynamics with internal variables" *J.Non-Equil. Thermodyn.* **19**, 217.

Mayer, A (1990) "Thermoelastic attenuation of surface acoustic waves in coated elastic media", *J. Appl. Phys.* **68**, 5913.

Mayer, A (1995) "Surface Acoustic Waves in Nonlinear Elastic Media", *Phys. Reports* **256**, 257.

Miloserdova, I.V. and Potapov, A.I. (1983) "Nonlinear standing waves in a rod of finite length", *Sov. Phys. Acoust.*, **29**, 306.

Mindlin, R.D. (1964) "Microstructure in linear elasticity", *Arch. Rat. Mech. Anal.* No1, 51.

Mirzoev, F. Kh., Panchenko, V. Ya, Shelepin, L.A. (1996) "Laser Control of Processes in Solids", *Physics- Uspekhi* **39**, 1.

Mirzoev, F. Kh., and Shelepin, L.A. (2001) "Nonlinear Strain Waves and Densities of Defects in Metal Plates Induced by External Energy Fluxes", *Tech. Phys.* **46**, 952.

Morton, K.W. and Mayers, D.F. (1994) *Numerical Solution of Partial Differential Equations*, Cambridge University Press, Cambridge.

Murnaghan, F.D. (1951) *Finite Deformations of an Elastic Solid*, J. Wiley, New York.

Nakamura, A. (1979) "A direct method of calculating periodic wave solutions to nonlinear evolution equations. I. exact two-periodic wave solution", *J. Phys. Soc. Jpn.* **47**, 1701.

Nagashima, H. and Kuwahara, M. (1981) "Computer Simulation of Solitary Waves of the Nonlinear Wave Equation $u_t + u\,u_x - \gamma^2\,u_{5x} = 0$" *J. Phys. Soc. Jpn.* **50**, 3792.

Nayfeh, A.H. (1973) *Perturbation Methods,* J. Wiley & Sons, New York.

Nekorkin, V.I. and Velarde, M.G. (1994) "Solitary waves, soliton bound states and chaos in a dissipative Korteweg-de Vries equation", *Int. J. Bif. Chaos* **4**, 1135.

Nepomnyashchy, A.A. and Velarde, M.G. (1994) "A three-dimensional description of solitary waves and their interaction in Marangoni-Bénard layers", *Phys. Fluids A* **6**, 187.

Newell, A (1985) *Solitons in Mathematics and Physics*, SIAM, Philadelphia.

Newell, A., Tabor, M., Zeng, Y.B. (1987) "A Unified Approach to Painlevé Expansions", *Physica D* **29**, 1.

Newille, E.H. (1951) *Jacobian Elliptic Functions,* Claredon Press, Oxford.

Nikitin, L.V. (1998) *Statics and dynamics of solids with external dry friction*, Moscovskii Licei, Moscow (in Russian).

Nikolaev, A.V. (1989) "Scattering and dissipation of seismic waves in presence of nonlinearity", *PAGEOPH* **131**, 687.

Nikolova, E.G. (1977) "On the effective surface tension of solid bodies", *Sov. Phys. JETP* **45**, 285.

McNiven, H.D. and McCoy, J.J. (1974) "Vibrations and wave propagation in rods", in: G. Herrmann ed.*, R. Mindlin and Applied Mechanics*, Pergamon, New York , p. 197.

Nowacki, W. (1975) *Theory of Elasticity*, Mir, Moscow (in Russian).

Nowacki, W. (1986a) *Theory of Asymmetric Elasticity*, Pergamon, Oxford.

Nowacki, W. (1986b) *Thermoelasticity*, Pergamon, Oxford.

Oliner, A.A. ed. (1978) *Surface Acoustic Waves.* Springer-Verlag, Berlin.

Oron, A. and Rosenau, P. (1997) "Evolution and formation of dispersive-dissipative patterns", *Phys. Rev. E* **55**, R1267.

Ostrovsky, L.A. and Potapov, A.I. (1999) *Modulated waves in linear and nonlinear media*, The John Hopkins University Press, Baltimore.

Parker, D.F. (1994) "Nonlinear Surface Acoustic Waves and Waves on Stratified Media", In: A.Jeffrey and J. Engelbrecht, eds. , *Nonlinear Waves in Solids*, Springer, Berlin.

Parker, D.F. and Maugin, G.A. , eds. (1987) *Recent Developments in Surface Acoustic waves*, Springer, Berlin.

Parker, D.F. and Mayer, A. (1991) " Dissipation of Surface Acoustic Waves", In: D.Fusco and A. Jeffrey, eds., *Nonlinear Waves and Dissipative Effects*, Longman, London.

Parker, D.F. and Tsoy, E.N. (1999) "Explicit Solitary and Periodic Solutions for Optical Cascading", *J. Eng. Math.* **36**, 149.

Parkes, E.J. and Duffy, B.R. (1996) "An automated tanh-function method for finding solitary wave solutions to nonlinear evolution equations", *Computer Phys. Comm.* **98**, 288.

Pasternak, P.L. (1954) *On a New Method of Analysis of an elastic Foundation be Means of Two Foundation Constants* (in Russian), Gosudarstvennoe Izdatel'stvo Litearturi po Stroitel'stvu i Arkhitekture, Moscow, USSR (in Russian).

Porubov, A.V. (1993) "Exact travelling wave solutions of nonlinear evolution equation of surface waves in a convecting fluid", *J. Phys. A: Math. Gen.* **26**, L797.

Porubov, A.V.(1995) *Free Surface Nonlinear Waves on a viscous inhomogeneous liquid layer*. Ph.D. Thesis, State Technical University, Saint Petersburg (in Russian).

Porubov, A.V. (1996) "Periodical solution to the nonlinear dissipative equation for surface waves in a convective liquid layer", *Phys. Lett. A* **221**, 391.

Porubov, A.V. (2000) "Strain solitary waves in an elastic rod with microstructure", *Rendiconti del Seminario Matematico dell'Universita' e Politecnico di Torino* **58**, 189.

Porubov, A.V., Gursky, V.V. and Maugin, G.A. (2003) "Selection of localized nonlinear seismic waves", *Proc. Estonian Acad. Sci., Phys. Math.* **52**, No 1.

Porubov, A.V., Maugin, G.A., Krzhizhanovskaya, V.V. and Gursky, V.V. (2002) "Influence of higher- order dispersion and nonlinearity on solitary wave formation from an initial localized pulse", submitted for publication

Porubov, A.V. and Parker, D.F. (1999) "Some General Periodic Solutions to Coupled Nonlinear Schrödinger Equations", *Wave Motion* **29**, 97.

Porubov, A.V. and Parker, D.F. (2002) "Some General Periodic Solutions for Optical Cascading", *Proc. Roy. Soc. A* **458**, 2139.

Porubov, A.V. and Pastrone, F. (2001) "Influence of macro- and microdissipation on nonlinear strain solitary wave evolution". *Quaderni del Dipartimento di Matematica N. 56*, University of Turin, Turin.

Porubov, A.V. and Samsonov, A.M. (1993) "Refinement of the model for the propagation of longitudinal strain waves in a rod with nonlinear elasticity", *Tech. Phys. Lett.* **19**, 365.

Porubov, A.V. , Samsonov, A.M. , Velarde, M.G. and Bukhanovsky, A.V. (1998) "Strain solitary waves in an elastic rod embedded in another elastic external medium with sliding", *Phys.Rev. E* **58**, 3854 .

Porubov, A.V. and Velarde, M.G. (1999) "Exact Periodic Solutions of the Complex Ginzburg-Landau Equation", *J. Math. Phys.* **40**, 884.

Porubov, A.V. and Velarde, M.G. (2000) "Dispersive-dissipative solitons in nonlinear solids", *Wave Motion* **31**, 197.

Porubov, A.V. and Velarde, M.G. (2002) "Strain kinks in an elastic rod embedded in a viscoelastic medium", *Wave Motion* **35**, 189.

Pöschel, T. and Herrmann, H.J. (1993) "A simple geometrical model for solid friction", *Physica A* **198**, 441.

Potapov, A.I. and Rodyushkin, V.M. (2001) "Experimental study of strain waves in materials with microstructure", *Acoust. J.* **47**, 347.

Potapov, A.I. and Semerikova, N.P. (1988) "Nonlinear longitudinal waves in a rod taking into account the interaction between strain and temperature fields", *Sov. Appl. Mech. and Tech. Phys.*, No1, 54.

Qaisar, M. (1989) "Attenuation Properties of Viscoelastic Material" *PAGEOPH* **131**, 703.

Rayleigh Lord (J.W. Strutt) (1945) *Theory of Sound*, Vol. 1, Reprint, Dover, New York.

Rednikov, A. Ye., Velarde, M.G., Ryazantsev, Yu. S., Nepomnyashchy, A.A., and Kurdyumov V.N., (1995) "Cnoidal Wave Trains and Solitary Waves in a Dissipation Modified Korteweg- de Vries Equation", *Acta Applicandae Mathematicae* **39**, 457.

Richtmyer, R.D. and Morton, K.W. (1967) *Difference Methods for Initial-Value Problems,* Wiley & Sons, New York.

Sachdev, P.L. (1987) *Nonlinear diffusive waves*, Cambridge Univ. Press, Cambridge.

Salupere, A., Maugin, G.A., Engelbrecht, J. (1994) "Korteweg-de Vries soliton detection from a harmonic input", *Phys. Lett. A* **192**, 5.

Salupere, A. , Maugin, G.A. and Engelbrecht, J. (1997) "Solitons in systems with a quartic potential and higher-order dispersion", *Proc. Estonian Acad. Sci., Phys. Math.* **46**, 118.

Salupere, A. , Engelbrecht, J. and Maugin, G.A. (2001) "Solitonic structures in KdV-based higher-order systems", *Wave Motion* **34**, 51.

Samarskii, A.A. and Nikolaev, E.S. (1989) *Numerical Methods for Grid Equations*, Birkhäuser, Basel.

Samsonov, A.M. (1988) "On existence of longitudinal strain solitons in an infinite nonlinearly elastic rod", *Sov. Phys.-Doklady,* **33**, 298.

Samsonov, A.M. (1995) "Travelling wave solutions for nonlinear waves with dissipation", *Appl.Anal.* **57**, 85.

Samsonov, A.M. (2001) *Strain soltons in solids and how to construct them*, Chapman & Hall/CRC.

Samsonov, A.M., Dreiden, G.V., Porubov, A.V. and Semenova, I.V. (1998) "Longitudinal-strain soliton focusing in a narrowing nonlinearly elastic rod", *Phys. Rev. B* **57**, 5778.

Samsonov, A.M., Dreiden, G.V., and Semenova, I.V. (2003) "On existence of bulk solitary waves in plexiglas." *Proc. Estonian Acad. Sci., Phys. Math.* **52**, No 1.

Savin, G.N., Lukashev, A.A. and Lysko, E.M. (1973) "Elastic wave propagation in a solid with microstructure" *Soviet Appl. Mech.* **15**, 725.

Savin, G.N., Lukashev, A.A., Lysko, E.M. , Veremeeenko, S.V., and Agasiev, G.G. (1973) "Elastic wave propagation in the Cosserat continuum with constrained particle rotation", *Soviet Appl. Mech.* **15**.

Sawada, K. and Kotera, T. (1974) "A method for finding N-soliton solutions of the KdV equation and KdV-like equation", *Prog. Theor. Phys.* **51** , 1355.

Shevyakhov, N.S. (1977) "Love waves on the surface of cylinder covered by a layer", *Sov. Phys. -Acoust. R.* **23**, 86.

Sillat, T. (1999) "Wave propagation in dissipative microstructured materials". *Thesis of Master of Science.* Technical University, Tallinn.

Slyunyaev, A.V. and Pelinovsky, E. N. (1999) "Dynamics of large amplitude solitons" *JETP* **89** 173.

Soerensen, M.P., Christiansen, P.L., Lomdahl, P.S. (1984) "Solitary waves in nonlinear elastic rods, I", *J. Acoust. Soc. Amer.* **76**, 871.

Soerensen, M.P., Christiansen, P.L., Lomdahl, P.S., and Skovgaard, O. (1987) "Solitary waves in nonlinear elastic rods, II", *J. Acoust. Soc. Amer.* **81**, 6.

Spencer, A.J.M. (1971) *In* "Treatise on Continuum Physics" *(*A.C. Eringen, ed.*),* Vol. I, *Theory of invariants,* Chap.3. Academic, New York.

Sokurinskaya, E.V. (1991) "Study of nonlinear travelling strain waves in one-dimensional elastic wave guide". Ph.D. Dissertation, Technical University, St.Petersburg (in Russian).

Stefański, A., Wojewoda, J. and Wiercigroch, M. (2000) "Numerical analysis of duffing oscillator with dry friction damper", *Mech. & Mech. Ing.* **4**, No2, 127.

Svendsen, I. and Buhr-Hansen, J.B. (1978) "On the deformation of periodic waves over a gently sloping bottom", *J. Fluid Mech.* **87**, 433.

Thomas, L.H. (1949) "Elliptic problems in linear difference equations over a network", Watson Sci. Comput. Lab. Rept., Columbia University, New York.

Velarde, M.G., Nekorkin, V.I. and Maksimov, A.G. (1995) "Further results on the evolution of solitary waves and their bound states of a dissipative Korteweg-de Vries equation", *Int. J. Bif. Chaos* **5**, 831.

Vlieg-Hultsman, M. and Halford, W. (1991) "The Kotreweg-de Vries-Burgers equation: a reconstruction of exact solutions", *Wave Motion* **14**, 267.

Weiss, J. , Tabor, M. and Carnevale, G. (1983) "The Painlevé property for partial differential equations", *J. Math. Phys.* **24**, 522.

Whitham, G. B. (1974) *Linear and Nonlinear Waves*, Wiley, New York .

Whittaker, E.T. and Watson, G.N. (1927) *A Course of Modern Analysis*, Cambridge, University Press.

Winkler, E. (1867) *Die Lehre von der Elasticitaet und Festigkeit*, Prag, Dominicus.

Wolfram, S. (1999) *The Mathematica book. Fourt Edition*, Addison-Wesley.

Zhurkov, S.N. (1983) "Dilaton Mechanism of the Strength of Solids", *Sov. Phys. Solid State* **25**, 1797.

Zwillenger, D. (1989) *Handbook of Differential Equations*, Acad. Press, Boston.

Index